Monitoring Surveys at the Historical Brenton Reef Disposal Site
2007 & 2009

Disposal Area Monitoring System DAMOS

D A M O S

DISPOSAL AREA MONITORING SYSTEM

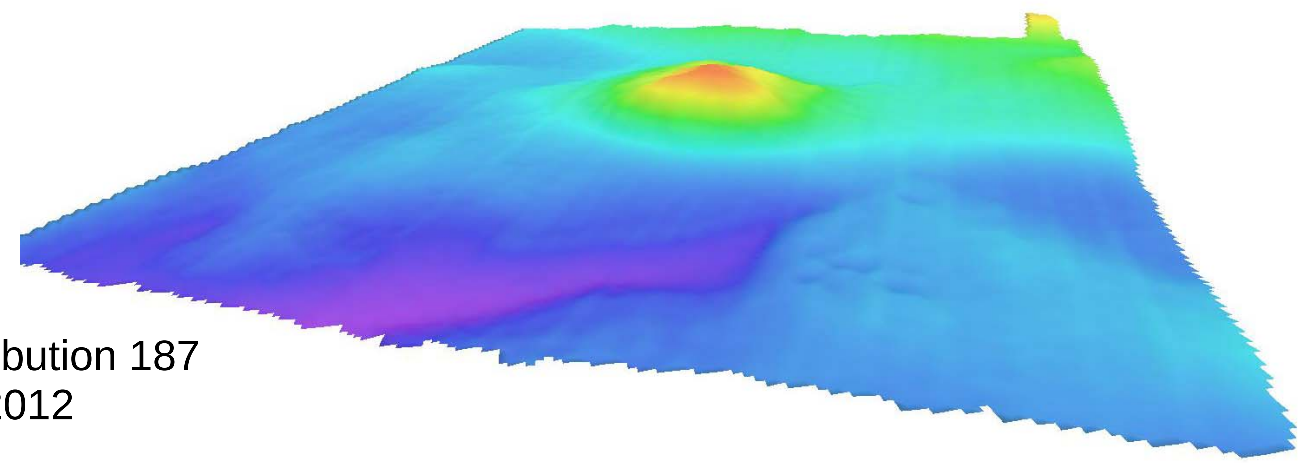

Contribution 187
May 2012

US Army Corps of Engineers ®
New England District

This report should be cited as:

Carey, D. A.; Hickey, K.; Myre, P. L.; Read, L. B.; Esten, M. E. 2012. Monitoring Surveys at the Historical Brenton Reef Disposal Site 2007 & 2009. DAMOS Contribution No. 187. U.S. Army Corps of Engineers, New England District, Concord, MA, 130 pp.

REPORT DOCUMENTATION PAGE

form approved
OMB No. 0704-0188

1. AGENCY USE ONLY (LEAVE BLANK)	2. REPORT DATE May 2012	3. REPORT TYPE AND DATES COVERED FINAL REPORT

4. TITLE AND SUBTITLE
Monitoring Surveys at the Historical Brenton Reef Disposal Site 2007 & 2009

5. FUNDING NUMBERS

6. AUTHOR(S)
Drew A. Carey, Ken Hickey, Peggy L. Myre, Lorraine B. Read, Marie Evans Esten

7. PERFORMING ORGANIZATION NAME(S) AND ADDRESS(ES)
DAMOSVision
215 Eustis Avenue
Newport, RI 02840

8. PERFORMING ORGANIZATION REPORT NUMBER
DV-2012-002

9. SPONSORING/MONITORING AGENCY NAME(S) AND ADDRESS(ES)
US Army Corps of Engineers-New England District
696 Virginia Rd
Concord, MA 01742-2751

10. SPONSORING/MONITORING AGENCY REPORT NUMBER
Contribution No. 187

11. SUPPLEMENTARY NOTES
Available from DAMOS Program Manager, Evaluation Branch
USACE-NAE, 696 Virginia Rd, Concord, MA 01742-2751

12a. DISTRIBUTION/AVAILABILITY STATEMENT
Approved for public release; distribution unlimited

12b. DISTRIBUTION CODE

13. ABSTRACT

Two surveys to evaluate the condition of the oldest capped dredged material disposal mound in New England were conducted in September 2007 and August 2009 as part of the U.S. Army Corps of Engineers New England District Disposal Area Monitoring System (DAMOS). The mound, located at the historical Brenton Reef Disposal Site (BRDS), was constructed from 1967 to 1971 as part of the Providence River Navigation Improvement Project (PRNIP) that deepened the navigation channel from 10.7 to 12.2 m (35.0 to 40.0 feet). The BRDS was the location for the first known use of sediment capping in New England; because the dredging began in the upper Providence River, Rhode Island, and proceeded down the channel, the finest sediments with the greatest concentration of contaminants were disposed first and sequentially covered with coarser and less contaminated sediments from farther down the navigation channel and from projects in Point Judith, RI and Brayton Point Channel, MA (Pratt et al. 1973). The project also provided the impetus to begin scientific monitoring of dredged material disposal activities in the northeastern United States.

In 2007, high resolution swath (multibeam) bathymetric and acoustic backscatter (side-scan sonar) data were collected over a study area that included the historical mound to determine the location of the mound, the size and shape of the mound, and the surface texture of the sediments. Sediment profile imaging and plan-view underwater camera images were collected across the mound surface and at three reference areas to assess fine-scale sediment texture and biological conditions for comparison with previous surveys.

In 2009, sediment cores were collected to assess the sediment layers within the interior of the disposal mound. Cores were collected from four locations on the main portion of the mound and from three locations within the margin of the mound, where the dredged material was expected to be thinner. Cores also were collected from two off-mound stations farther afield to provide additional information on the surrounding ambient sediments.

The historical BRDS mound has remained remarkably stable over 40 years: the size, location, and shape are virtually the same as surveyed in 1970 immediately after disposal of the majority of material. The combination of mosaicked, processed backscatter data, high resolution bathymetric data, and SPI and PUC images collected in 2007 provided a hitherto unseen characterization of the dynamic complex surface of this mound. This complex surface is consistent with previous survey results, as well as a conceptual model, and verifies that the large-scale morphology of the mound remains unchanged. It is clear that despite evidence of surface sediment modification across the surface of the mound, the mass of material placed on the seafloor from 1967 to 1971 has remained in place. A variable lag deposit composed of well-sorted sand, gravels, shells, and poorly sorted mixtures with patches of compacted silt covers the surface of the mound.

The results of chemical sampling of cores collected from the Brenton Reef Disposal Site showed that there remains a thick cap on the main portion of the mound and no evidence of contaminants in surface sediments, suggesting that the sub-surface samples containing contaminants are well isolated from the benthic environment. The shallowest elevated concentrations of metal and PAH contaminants were found at a depth of 28-38 cm (11-15 in) in a core collected on the margin of the mound. The surficial sample from this core consisted of nearly equal fractions of sand and fines and showed no evidence of contaminant migration from the lower interval. The presence of the 20+ cm (8+ in) layer above the contaminated layer is sufficient to limit biological mixing or exposure to contaminants (Rhoads and Carey 1997), and the off-peak/slope location of this core is unlikely to experience physical disturbance from periodic storms.

14. SUBJECT TERMS DAMOS, Historical Brenton Reef Disposal Site, Dredged Material

15. NUMBER OF TEXT PAGES: 130

16. PRICE CODE

17. SECURITY CLASSIFICATION OF REPORT	18. SECURITY CLASSIFICATION OF THIS PAGE	19. SECURITY CLASSIFICATION OF ABSTRACT	20. LIMITATION OF ABSTRACT
Unclassified			

Page intentionally left blank.

MONITORING SURVEYS AT THE HISTORICAL BRENTON REEF DISPOSAL SITE 2007 & 2009

May 2012

Contract No. W912WJ-09-D-0003
Report No. DV-2012-002

Submitted to:
New England District
U.S. Army Corps of Engineers
696 Virginia Road
Concord, MA 01742-2751

Prepared by:
Drew A. Carey
Ken Hickey
Peggy L. Myre
Lorraine B. Read
Marie Evans Esten

Submitted by:
DAMOSVision
215 Eustis Avenue
Newport, RI 02840
(401) 849-9236

US Army Corps of Engineers®
New England District

Frontispiece

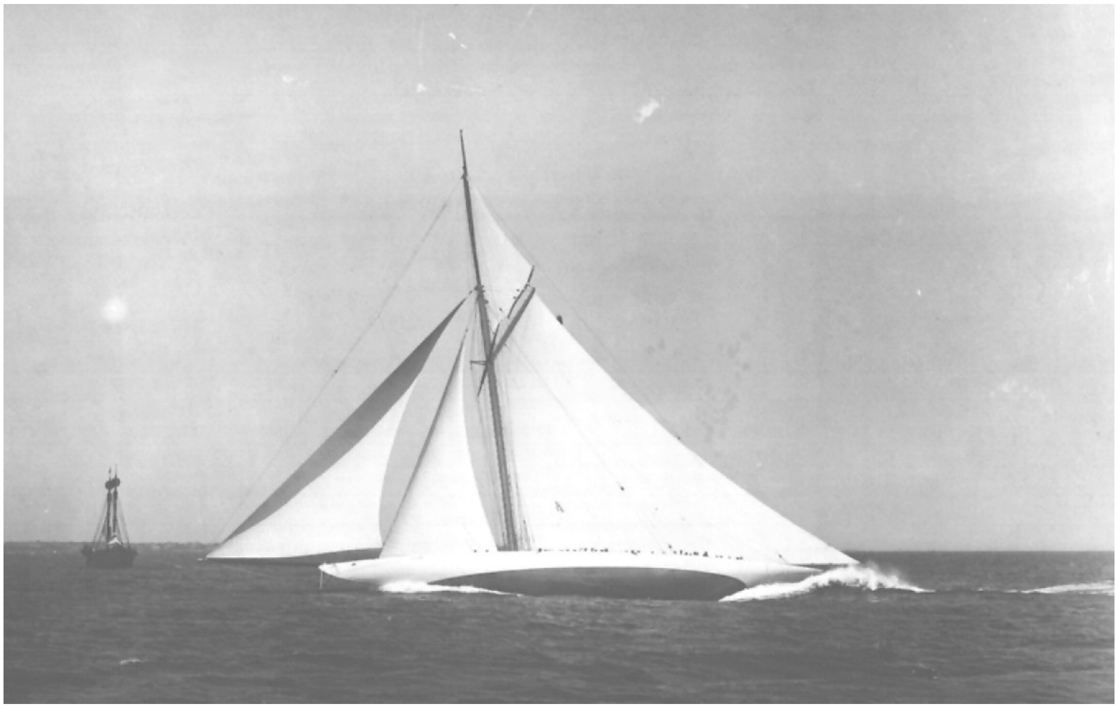

The yacht *Reliance* passing the Brenton Reef light ship at high speed, 1903.

Photograph by Nathaniel L. Stebbins.

Reliance was the 1903 America's Cup defender, the fourth America's Cup defender from the famous designer Nat Herreshoff, and reportedly the largest gaff-rigged cutter ever built. She was specially designed to have a 90-ft water line until heeled over, when the waterline and speed increased dramatically due to the long overhangs at each end. At 201 ft long with a 199-ft mast (height of a 20-story building), the ship dwarfed the Brenton Reef lightship. Her total sail area, 16157 ft^2 (1501 m^2), was the equivalent of eight 12-meter-class yachts and made her very dangerous to sail. After defeating Shamrock III in the dramatic 1903 America's Cup, the rules were changed to avoid such extreme vessels.

Note on units of this report: As a scientific contribution, information and data are presented in the metric system. However, given the prevalence of English units in the dredging industry of the United States, conversions to English units are provided for the general information in Section 1. A table of common conversions can be found in Appendix H.

TABLE OF CONTENTS

Page

LIST OF TABLES

Page

LIST OF FIGURES

Page

Page

Page

Two surveys to evaluate the condition of the oldest capped dredged material disposal mound in New England were conducted in September 2007 and August 2009 as part of the U.S. Army Corps of Engineers (USACE) New England District Disposal Area Monitoring System (DAMOS). The mound, located at the historical Brenton Reef Disposal Site (BRDS), was constructed from 1967 to 1971 as part of the Providence River Navigation Improvement Project (PRNIP) that deepened the navigation channel from 10.7 to 12.2 m (35.0 to 40.0 feet). The BRDS was the location for the first known use of sediment capping in New England; because the dredging began in the upper Providence River, Rhode Island, and proceeded down the channel, the finest sediments with the greatest concentration of contaminants were disposed first and sequentially covered with coarser and less contaminated sediments from farther down the navigation channel and from projects in Point Judith, RI and Brayton Point Channel, MA (Pratt et al. 1973). The project also provided the impetus to begin scientific monitoring of dredged material disposal activities in the northeastern United States.

Because of the legacy of this capped mound, and the location of the mound on nearshore shelf sediments exposed to open ocean conditions, the long-term status of the sediments deposited there has interest for marine environmental management programs worldwide. The objectives of the 2007 and 2009 surveys were to characterize physical, chemical, and biological conditions at BRDS sufficiently to determine the stability of the disposal mound and whether contaminated sediments were isolated from the environment by the site's intentional, but not formally engineered, cap. The monitoring investigation also sought to gather and analyze data from this 40-year-old disposal site that could potentially provide insights beneficial to current and future dredged material placement practices.

A conceptual model was developed to provide a framework for interpretation of data collected during recent surveys. This model was based on the results of earlier investigations, the history of dredged material disposal at and around Brenton Reef, as well as the long history of contaminant input into Narragansett Bay, Rhode Island and a general understanding of the processes associated with open-water placement of dredged material. The mound was expected to contain a complex sedimentary structure with a trend of finer, more organic-rich and contaminated inner harbor material at the bottom of the mound and coarser, low-organic and low-contaminant-burden outer harbor material on the top of the mound. Because the mound was not created in a rigorously engineered manner, interlayering of the fine and coarse layers within the mound was expected rather than a discrete boundary between the harbor material and a cap layer. However, given the historical volume of material placed, it was expected that a layer of less contaminated, coarser sediments covered the bathymetrically defined mound. The surface of the mound and margin was expected to have evidence of deposition and reworking of both dredged material and ambient sediments. The BRDS monitoring activities reported here were designed to gather, analyze, and interpret data and compare findings to those expected based on the conceptual site model.

In 2007, high resolution swath (multibeam) bathymetric and acoustic backscatter (side-scan sonar) data were collected over a study area that included the historical mound to determine the location of the mound, the size and shape of the mound, and the surface texture of the sediments. Sediment profile imaging (SPI) and plan-view underwater camera (PUC) images were collected across the mound surface and at three reference areas to assess fine-scale sediment texture and biological conditions for comparison with previous surveys.

In 2009, sediment cores were collected to assess the sediment layers within the interior of the disposal mound. Cores were collected from four locations on the main portion of the mound and from three locations within the margin of the mound, where the dredged material was expected to be thinner. Cores also were collected from two off-mound stations farther afield to provide additional information on the surrounding ambient sediments.

The historical BRDS mound has remained remarkably stable over 40 years: the size, location, and shape are virtually the same as surveyed in 1970 immediately after disposal of the majority of material. In 1970, the surface texture of the mound was reported as unconsolidated silts overlying coarser sands; in 1987, the surface texture was a mosaic of well-sorted sands, poorly sorted gravels, and shells. These descriptions were based on isolated samples collected over the mound surface. The combination of mosaicked, processed backscatter data, high resolution bathymetric data, and SPI and PUC images collected in 2007 provided a hitherto unseen characterization of the dynamic complex surface of this mound. This complex surface is consistent with previous survey results, as well as the conceptual model, and verifies that the large-scale morphology of the mound remains unchanged. It is clear that despite evidence of surface sediment modification across the surface of the mound, the mass of material placed on the seafloor from 1967 to 1971 has remained in place. The silts reported on the surface in 1970 likely eroded, and a variable lag deposit composed of well-sorted sand, gravels, shells, and poorly sorted mixtures with patches of compacted silt covers the surface of the mound.

The results of chemical sampling of cores collected from the Brenton Reef Disposal Site showed that there remains a thick cap on the main portion of the mound and no evidence of contaminants in surface sediments, suggesting that the sub-surface samples containing contaminants are well isolated from the benthic environment. The shallowest elevated concentrations of metal and PAH contaminants were found at a depth of 28-38 cm (11-15 in) in a core collected on the margin of the mound. The surficial sample from this core consisted of nearly equal fractions of sand and fines and showed no evidence of contaminant migration from the lower interval. The presence of the 20+ cm (8+ in) layer above the contaminated layer is sufficient to limit biological mixing or exposure to contaminants (Rhoads and Carey 1997), and the off-peak/slope location of this core is unlikely to experience physical disturbance from periodic storms.

Based on the evidence that the disposal site is subjected to periodic sediment reworking, but remains virtually the same size and shape as surveyed in 1978, it is recommended that the general oceanographic conditions of the area be monitored for storms that might exceed the storms documented here. If a storm with peak wave height of greater than 7.0 m (23 ft) is recorded at WIS Buoy #63078 with a direction within the BRDS open-water storm exposure range (110 to 190° T), a reconnaissance survey with multibeam bathymetry and acoustic backscatter collection to assess the condition of the surface of the mound is recommended. If these results indicate that the mound lost more than 1 m (3 ft) in height and changed shape (more than 20% of the 3-dimensional volume altered), a Sediment Profile Imaging (SPI) survey to confirm results is recommended. If the SPI survey records extensive exposure of fine grained material with limited biological recovery (lack of Stage 3 evidence persists in fine grained sediments more than 1 year after disturbance), sampling and testing of bulk sediment in the areas where SPI results indicate impaired recovery of fine grained sediments are recommended.

1.0 INTRODUCTION

A phased monitoring investigation was conducted at the Brenton Reef Disposal Site (BRDS) in September 2007 and August 2009, as part of the U.S. Army Corps of Engineers (USACE) New England District (NAE) Disposal Area Monitoring System (DAMOS) Program. The Brenton Reef Disposal Site is the oldest capped dredged material disposal mound in New England and was monitored to evaluate the condition of the cap and overlying materials. This report describes both phases of this monitoring activity at BRDS. After a 20-year monitoring hiatus, a reconnaissance survey was conducted in 2007 to evaluate the condition of BRDS; results provided initial information on the present physical condition of sediments on and within the mound and suggested locations where coring techniques might be most practical. In 2009, a coring survey assessed the vertical and horizontal distribution of sediment types and contaminants within the historical capped disposal mound.

DAMOS is a comprehensive monitoring and management program designed and conducted to address environmental concerns surrounding the placement of dredged material at aquatic disposal sites throughout the New England region. An introduction to the DAMOS Program, a description of the Brenton Reef Disposal Site history, and a statement of monitoring program objectives are provided below.

1.1 Overview of the DAMOS Program

For over 30 years, the DAMOS Program has conducted monitoring surveys at aquatic disposal sites throughout New England and evaluated the patterns of physical, chemical, and biological responses of seafloor environments to dredged material disposal activity. The DAMOS Program features a tiered disposal site management protocol designed to ensure that any potential adverse environmental impacts associated with dredged material disposal are promptly identified and addressed (Fredette and French 2004; Germano et al. 1994). DAMOS monitoring surveys are designed to test hypotheses related to expected physical and ecological response patterns following placement of dredged material on the seafloor at established disposal sites. The data collected and evaluated during DAMOS monitoring surveys provide input to help effectively manage the use of aquatic dredged material disposal sites.

Two primary goals of DAMOS monitoring surveys are to document the physical location of dredged material placed on the seafloor and to document the recovery of the site following dredged material placement. Sequential bathymetric measurements are performed to characterize the height and spread of discrete dredged material deposits, or mounds, created at disposal sites. Sediment-profile imaging (SPI) surveys are performed to provide additional physical characterization of the seafloor and to support evaluation of seafloor (benthic) habitat conditions and recovery over time. Acoustic backscatter surveys may be performed to characterize the sediment surface across relatively large areas, and sediment coring may be conducted to support characterization of sediment stratification, as deemed appropriate to achieve specific survey objectives. Special studies are periodically undertaken within the DAMOS Program to evaluate inactive, historical disposal sites. The Brenton Reef Disposal Site monitoring program represents a special DAMOS Program study.

1.2 Introduction to the Brenton Reef Disposal Site

The Brenton Reef Disposal Site is centered at 41° 23.470′ N, 71° 18.126′ W (NAD 1983 metric), approximately 8 km (5 mi) south of Brenton Point in Newport, Rhode Island, and covers a 3.4-km^2 area of seafloor (Figure 1-1). BRDS is named for a series of bedrock outcrops adjacent to the shore of Brenton Point at the southern tip of Aquidneck Island in Rhode Island Sound. Brenton Reef was also the name of a series of lightships moored south of the reef from 1853 to 1962. In 1962, the last lightship was replaced with a steel tower that remained until it was replaced with a lighted buoy in 1989 and dismantled in 1992 (Holmes 2008). The lightship and lighted tower were notable for providing a reference point for numerous ocean sailing races, including the oldest ocean race in America, the Brenton Reef Cup (1872 – 1885), and the America's Cup races from 1930 to 1983.

The Brenton Reef Disposal Site was created for the placement of an estimated 6.9 million m^3 (9 million yd^3) of sediments from the Providence River Navigation Improvement Project (PRNIP) that were sequentially dredged and point-dumped at the site from 1967 to 1971 (Pratt et al. 1973). BRDS was the location for the first known use of sediment capping in New England. The project dredging began in the upper Providence River and proceeded down the channel. The finest sediments with the greatest concentration of contaminants were disposed first and were sequentially covered with coarser sediments from further down the navigation channel (Saila et al. 1971). Use of less coarse and less contaminated sediments to cover the dredged material mound was intentional, but was not the result of specific engineering design and was not subject to rigorous post disposal confirmation.

The seafloor around BRDS area is generally flat with a gentle seaward slope such that water depths are approximately 30 m (98 ft) MLLW on the northern (landward) side of the site and approximately 32 m (110 ft) MLLW on the southern side. The dredged material disposed at BRDS resulted in the formation of a well-defined conical mound situated in the southwestern corner of the Site (Figure 1-2). At its peak, the mound rises approximately 5 m (16 ft) above the seafloor. The mound is broad and roughly circular, with a diameter of approximately 1600 m (5250 ft), and extends outside of the site boundary to the west and south.

1.3 Historical Dredged Material Disposal Activity

In 1967, initial disposal of dredged material from the PRNIP at BRDS was delayed because the disposal site was situated near the course for the America's Cup trials. During the initial portion of the dredging project, the dredging contractor was diverted to three temporary disposal locations situated southwest of BRDS (Figure 1-3) (Saila et al. 1971). The volume of dredged material placed at the three temporary disposal areas is not known, but is estimated to be 720,000 m^3 (940,000 yd^3) based on USACE Work History, Table 1-1. After the 1967 America's Cup race, disposal was moved northeast to the present BRDS for the remainder of the dredging project.

The Brenton Reef Disposal Site received an estimated 6.9 million m^3 (9 million yd^3) of dredged material from the PRNIP between September 1967 and June 1971 (Table 1-1). The PRNIP involved deepening the navigation channel to Providence, Rhode Island, from 10.7 to 12.2 m (35.0 to 40.0 ft), a project that was authorized by the Rivers and Harbors Act of 1965. The Project included Providence Harbor, a reach extending 8 km (5 mi) down the Providence River, and a 3.2-km (2.0-mi) approach channel in upper Narragansett Bay (Saila et al. 1971). Dredging proceeded from the upper Providence River southward and was conducted using mechanical-bucket dredges. Dredged material was barged from the PRNIP dredging locations to BRDS for disposal using split-hulled scows. Integrated with the improvement dredging was maintenance dredging from the channel (shoals in the older 35 foot channel). Later, between early 1971 and May 1973, a smaller volume of dredged material from other projects [$<$0.3 million m^3 (0.4 million yd^3)], including maintenance dredging of the federal channel in Point Judith, Rhode Island and a private channel at Brayton Point, Massachusetts (Table 1-1), was placed at BRDS. There does not appear to have been additional disposal of dredged material at BRDS after May 1973.

The USACE work history provides total volumes for dredging work sequences by project (Table 1-1), and the University of Rhode Island (URI) reports provided estimates of volumes placed at BRDS in sequences that matched monitoring events (Table 1-2). There is a discrepancy in volume between these two sources; the URI estimates are assumed to include material deposited at the three temporary areas as well as at BRDS (Table 1-1). The URI estimates are particularly useful for interpretation of sequential bathymetric survey results (see below).

1.4 Previous Monitoring Activity

The Brenton Reef Disposal Site provided the "triggering incident" for initiation of monitoring of dredged material disposal in New England (NED 1974). Prior to initiation of disposal at BRDS, the USACE asked the U.S. Fish and Wildlife Service (USFWS) to develop a monitoring program with the University of Rhode Island (URI). The program was conducted primarily in response to concerns expressed by the fishing industry "that extensive damage to fish and shellfish resources in the vicinity of the dumping may result from the discharge of dredged material." Local fishermen reported that the disposal site was situated in a "significant inshore fishery for lobsters (*Homarus americanus*), and is also utilized as a trawling ground for fin fishes" (Saila et al. 1969).

In February 1967, the monitoring program began investigating conditions at the newly defined disposal site prior to initiation of disposal activities (Saila et al. 1969). This landmark monitoring program presaged many of the activities developed further by the DAMOS Program (formally initiated in 1977) including the following:

- Sequential bathymetric profiles and depth difference analyses,
- Ambient current and turbidity measurements,
- Benthic community characterization and colonization modeling,
- Comparison of sediment chemistry and grain size of mound sediment with barge contents, and
- Diver observations following placement of material.

Extensive monitoring was conducted prior to, during, and immediately following dredged material disposal, from 1967 to 1973, resulting in a sequence of three summary reports (Saila et al. 1969, Saila et al. 1971, Pratt et al. 1973). Additional monitoring was conducted in 1978 and in 1987 (Table 1-3). No monitoring surveys of BRDS were conducted over the twenty-year period from 1988 to 2007.

In 1967–1968, URI conducted a monitoring program to assess site conditions prior to disposal, to observe disposal operations, and to assess the effects of dredged material on local fishery resources (Saila et al. 1969). The 1967–1968 program included bathymetric surveys conducted prior to disposal and while disposal was ongoing (Table 1-3). The program also included collection and analysis of ambient sediment and dredged material (for parameters including type, grain size, and % carbon), turbidity measurements, and lobster toxicity studies. The URI study found that ambient sediments consisted primarily of sand and that dredged material consisted primarily of silt with relatively high organic carbon content. The report suggested that the physical difference between ambient and dredged materials could potentially be useful for discerning sediment types in subsequent investigations. Lobster toxicity tests concluded that mature lobsters were tolerant of the dredged material placed at BRDS (Saila et al. 1969).

In 1969–1970, URI investigators (Saila et al. 1971) conducted a follow-up monitoring program designed to accomplish the following:

- Bring physical observations up to date and assess the distribution of dredged material at the site,
- Measure bottom currents and assess potential for sediment transport,
- Evaluate potential impacts to benthic invertebrates, and
- Assess the fishery present in the vicinity of the site.

The distribution of dredged material was determined by two bathymetric surveys, sediment sampling, and diver observations. The bathymetric surveys found that the volume of dredged material at the site agreed with the volume reportedly disposed, suggesting no large-scale loss of material. Much of the sediment surface was observed to consist of a layer of non-cohesive silt/clay “indicating a non-erosive hydrographic regime” (Saila et al. 1971).

Bathymetric surveys conducted on July 1, 1968; October 22, 1969; and September 25, 1970 provide a time lapse sequence of mound creation, representing estimates of completion of 21%, 58%, and 88%, respectively (Table 1-2). This sequence of dredged material disposal is useful for evaluating of the effectiveness of the intentional cap through analysis of the distribution of material at each stage (Appendix A). Specifically, it helped to determine whether potentially contaminated material placed at the beginning of the project was fully capped by material placed later.

A three-dimensional data visualization tool, (iView4D by Fledermaus), was utilized to provide an enhanced view of the historical bathymetric data. Screen-captures of the hand-drawn contour maps for each historical bathymetric survey were created and imported to ESRI ArcGIS software. Each image was geo-referenced through careful rotation and scaling using assumed common features. For most images the only common feature available was the BRDS boundary. Potential positioning errors associated with the geo-referencing process are estimated to be as great as 50 to 100 m (164 to 328 ft). Vertical uncertainty estimates associated with the original survey data were not provided in the scanned reports. However, based on the assumed survey methodology, tide modeling and sound velocity errors, vertical uncertainty for any of the surveys would likely be at least 0.5 to 1.0 m. As a result, the three-dimensional images of historical bathymetric contours (1968-1971) are useful for providing a general sense of the dredged material placement, but are not considered highly accurate representations.

To provide spatial context, a three-dimensional visualization of the BRDS mound, based on the 2007 survey, is shown without vertical exaggeration and again with fifty-times vertical exaggeration (Figure 1-4). It is useful to be aware of the visual effect that vertical scaling has as subsequent figures will represent the mound with fifty-times vertical exaggeration to better illustrate vertical gradients.

A sequence of bathymetric contours, representing stages in mound construction, provides oblique views facing northward (Figure 1-5). The initial 1.5 million m^3 (2.0 million yd^3; 21% of total dredged material volume) was placed in a broad-based low area [typical height of 0.5 to 1.5 m (1.6 to 4.9 ft) above ambient sediments] centered in the middle of the Disposal Site, as surveyed in July 1968. This initial placement was material that most likely came from the upper Providence River with the highest burden of contaminants. The remainder of dredged material was placed in the northwest and southwest portion of the BRDS and formed a well-defined conical mound centered just inside the western boundary of the disposal site with a height of approximately 5 m (16 ft) above the sea floor, as surveyed in October 1969 and September 1970. The mound margins extended 150 to 300 m (490 to 980 ft) outside the BRDS boundary to the northwest and southwest.

The 1969–1970 URI study found that high-percentage organic material from the upper Providence River had been covered by material with lower organic content over most of the disposal site, except outside the site boundary to the northwest and inside the boundary along the northeast edge (Saila et al. 1971). Surficial sediments were observed to be very heterogeneous, including fine sands, silts, silty sands, shells, pebbles, clays, and other materials. Ambient tidally dominated currents at BRDS were found to rarely exceed 0.15 meters/second (0.5 ft/sec) and were not considered sufficient to resuspend sediments. The report found that wave-induced currents associated with major storm events could potentially induce sediment erosion and recommended a detailed evaluation (Saila et al. 1971).

An analysis of fisheries resources and potential impacts of the BRDS area was conducted based on interviews with commercial fishermen (Saila et al. 1971). The analysis found trawling for finfish (including Atlantic cod [*Gadus morhua*], winter flounder [*Pseudopleuronectes americanus*], summer flounder or fluke [*Paralichthys dentatus*], butterfish [*Poronotus triacanthus*], and scup [*Stenotomus chrysops*]) was ongoing with primary trawling grounds situated in the eastern portion of the site and in adjacent areas (Figure 1-6). The winter fishery for cod and flounder was reported as successful in 1970, suggesting that the fin-fishery was not impacted in the short term by the placement of dredged material at BRDS. Fishermen reportedly expressed concerns that short dumps had resulted in placement of soft silt material that had rendered dragging equipment ineffective in primary trawling grounds outside of the site (Saila et al. 1971).

BRDS was also situated in lobstering and ocean quahog (*Arctica islandica*) grounds. Lobstermen reportedly avoided BRDS during disposal operations to avoid potentially contaminated catches or burial of traps (Saila et al. 1971). Lobstering was reported as the least affected fishery and planned to resume following cessation of disposal activity. BRDS was situated near the center of a discrete patch of ocean quahogs (Figure 1-6). This ocean quahog area had been utilized since at least 1950, and at least four boats were dredging the area for quahogs in 1970, according to fisherman interviewed (Saila et al. 1971). Quahog mortality by burial was reported along the inshore edge of the site (Figure 1-6).

In 1972–1973, URI conducted a study to continue evaluating the quality of surficial sediments, the progress of benthic recolonization, and the impacts on aquatic animals and fisheries. Surficial [0 to 6 cm (0 to 2.4 in)] sediments were collected at locations across the mound and on the margins. Sediments were characterized as highly heterogeneous with silty clay, silty sand, pebbles, and fine and medium sand observed. Sediment analyses for metals found mercury ranging from 0.06 to 0.19 mg/kg, zinc ranging from 26 to 89 mg/kg, lead ranging from 11 to 43 mg/kg, and copper ranging from 10 to 83 mg/kg.

A 1978 survey was conducted and included a bathymetric survey; collection of data on currents in the vicinity of the site; sediment sampling for bulk chemistry, tissue chemistry, and benthic community analysis; and fisheries surveys (NUSC 1979). In 1978, the mound reportedly had well-sorted sand over silt on top, silt on the sides, and high abundances of amphipod tubes at reference stations (NUSC 1979). A 1987 field survey included bathymetric, side-scan, and sub-bottom surveys; sediment-profile imaging; and sediment sampling for physical, chemical, and benthic community analyses. Surface sediment samples were archived, but no record exists of bulk sediment chemistry results from this survey. In 1987, the surface of the mound had a complex range of sediments from fine sand to cobble and shells. This basic shape, size, and depth changed very little among the 1970, 1978, and 1987 surveys.

1.5 Development of Conceptual Site Model

A conceptual model of the historical Brenton Reef Disposal Site mound was developed to provide a framework for interpretation of data collected during recent surveys. This model is based on the results of early investigations (Saila et al. 1969; Saila et al. 1971; Pratt et al. 1973; NUSC 1979; SAIC 1988, 1990) and a general understanding of the processes associated with open-water disposal of dredged material (Fredette et al, 1992).

The mound was expected to contain a complex sedimentary structure formed by placement at the site of discrete barge loads of material (sediment and water) mechanically dredged from the Providence River navigation channel and with a limited amount of material from two other projects (Table 1-1). As the dredge removed material from the navigation channel, bucket loads accumulated in the barge until it was full and transported to the site. Depending on the characteristics of the channel reach (and the depth below the channel), the bucket might have removed more recently deposited surficial fine silts with high organic content, deeper silts or clays with low organic content or coarser sediments from the channel margin or outer channel. Loading of the scow may have proceeded uniformly over its length or focused from one end to another as the dredge repositioned. For this reason, each barge load may have contained a heterogeneous mixture of fine and coarse material (sand, oyster shells, gravel) or may have been predominantly fine or coarse (based on the characteristics of the Providence River channel). After filling, each barge was transported to the site and opened, and the mix of material in the barge fell through the water column to the seafloor. As each subsequent barge load was placed at the site, layers of sediment built up, forming the mound. Each layer then was likely to have a complex signature of sediment types.

In general, as a result of this process of placement, there should be an overall trend of finer, more organic-rich and contaminated upper Providence River material at the bottom of the mound and coarser, low-organic and low-contaminant-burden outer harbor material on the top of the mound. Because the mound was not created in a rigorously engineered manner (with target coordinates for each placement and guided by interim bathymetric surveys), interlayering of the fine and coarse layers was expected within the mound rather than a discrete boundary between the harbor material and a cap layer. However, a layer of less contaminated, coarser sediments was expected to cover the bathymetrically defined mound. A further complication was that the project was a deepening project, removing as much as 1.5 m (5.0 ft) of channel bottom that may not have been dredged before. Some of these materials were likely to be pre-industrial deposits with a wide range of sediment types. As a result, the interior of the mound would be expected to have a wide range of sediment types and contaminant concentrations. The areas on the margin of this bathymetrically defined mound may contain thin layers of fine upper Providence River sediments, coarse lower Providence River sediments, and sediments from Brayton Point and Point Judith (mostly sandy silt and coarse sand respectively).

The surface of the mound and margin was expected to have evidence of deposition and reworking of both dredged materials and ambient sediments. Reworking should be most evident in the shallowest areas and deposition most evident in the deepest areas with complex results based on the wide range of sediment types placed at the site.

1.6 Project Objectives

The primary objective of the 2007/09 monitoring investigation was to characterize physical, chemical, and biological conditions at BRDS sufficiently to assess the longer term stability of this disposal mound and the isolation of contaminated sediments from the environment by the site's intentional, but not specifically engineered, cap. Early studies addressed concerns that fisheries, particularly for finfish and quahogs, would be adversely affected. There was also concern about the potential for large-scale erosion, due to the site's rising bathymetry and exposure to the open ocean to the south. The BRDS monitoring activities reported here were designed to gather, analyze, and interpret data and compare findings to those expected based on the conceptual site model. Given the age of this disposal mound (40+ years) and its exposed location, the results of this investigation will be useful in the design and evaluation of other capped mound and confined aquatic disposal cell sites.

Table 1-1.

Work History of the Federal Navigation Projects Disposed at BRDS[1]

Work Dates and Work Accomplished	Volume Placed (million m³)	Cumulative Volume at BRDS (million m³)	Cumulative Volume at BRDS (percent)
Sept 1967 – February 1967 Improvement Dredging of 40-Foot Channel (assumed to have been placed at temporary sites)	0.72	0.00	0%
February 1967 – May 1968 Improvement Dredging of 40-Foot Channel	1.15	1.15	16%
October 1968 – June 1969 Improvement Dredging of 40-Foot Channel	1.85	3.00	42%
October 1969 – June 1970 Improvement Dredging of 40-Foot Channel	1.85	4.85	68%
October 1970 – June 1971 Improvement Dredging of 40-Foot Channel	2.06	6.91	96%
May 1971– June 1971 Maintenance Dredging of 15-Foot Channel, Point Judith, RI	0.02	6.93	97%
Dredging at Brayton Point Power Plant Channel, Fall River, MA	0.25	7.18	100%

[1]Mark Habel, USACE, personal communication via Work History of Federal Navigation Projects in The New England District log, April 8, 2011 and consultation of RI Annual Reports, New England District.

Table 1-2.

Chronology of Dredged Material Disposal at BRDS

Time Period	Volume Placed (million m^3)	Cumulative Volume (million m^3)	Cumulative Volume (percent)	Reference
February to December 1967	0.069	0.069	1%	Saila et al. 1969
December 1967 to July 1968	1.4	1.5	21%	Saila et al. 1969
July 1968 to October 1969	2.7	4.2	58%	Saila et al. 1971
October 1969 to September 1970	2.1	6.3	88%	Saila et al. 1971
September 1970 to "early 1971"	0.6	6.9	96%	Pratt et al. 1973
"early 1971" to May 1973[a]	0.27	7.2	100%	Pratt et al. 1973

Notes: Dredged material originated from the PRNIP, unless otherwise noted.
[a] Material originated at the Brayton Point (MA) and Point Judith (RI) Projects

Table 1-3.

Chronology of Monitoring Activities at Brenton Reef Disposal Site since 1967

Activity	Date	Details	Reference
Bathymetry (single beam)	February 1967	12 lanes, 150 m spacing	Saila et al 1969
	15 December 1967	12 lanes, 150 m spacing	Saila et al 1969
	1 July 1968	12 lanes, 150 m spacing	Saila et al 1969
	22 October 1969	3.5 km^2	Saila et al. 1971
	25 September 1970	3.5 km^2	Saila et al. 1971
	4 August 1978	2000 m lanes, 50 m lane spacing	NUSC 1979, 1980
	5 August 1981	1800 m lanes, 50 m lane spacing	SAIC 1988
	3 September 1987	2100 m lanes, 50 m lane spacing	SAIC 1990
Current meters	July 1970	Near bottom at site	Saila et al.1969
	April 1978	Invalid data	NUSC 1979, 1980
Sediment grabs or cores	February 1967	Samples from disposal barges	Saila et al. 1969
	July 1968	17 samples cross grid	Saila et al. 1969
	August 1969	41 cores cross grid	Saila et al. 1969
	September 1970	37 Peterson grabs, 4 Smith Mac grabs	Pratt et al. 1973
	April 1978	3 grabs per site; 3 grabs per ref. area	NUSC 1979, 1980
	August 1978	3 grabs per site; 3 grabs per ref. area	NUSC 1979, 1980
	December 1978	3 grabs per site; 3 grabs per ref. area	SAIC 1988
	May 1979 & August 1981	5 grabs per site; 5 grabs per ref. area	SAIC 1988
	October 1987	10 Smith Mac grabs	SAIC 1990
Benthic analysis	September 1970	17 samples taken from 6 stations	Pratt et al. 1973
	December 1971	33 samples taken from 11 stations	Pratt et al. 1973
	December 1973	44 samples taken from 11 stations	Pratt et al. 1973
	Summer 1974	55 samples taken from 13 stations	SAIC 1988
	October 1975	12 samples taken from 4 stations	SAIC 1988
	April 1978	6 samples taken from 2 stations	NUSC 1979, 1980 SAIC 1980a, 1980b
	August 1978	6 samples taken from 2 stations	SAIC 1980a
	December 1978	6 samples taken from 2 stations	SAIC 1980a
	May 1979	10 samples taken from 2 stations	SAIC 1980a
	October 1987	12 samples taken from 12 transect stations	SAIC 1990
SPI	October 1987	68 stations and 4 reference stations	SAIC 1990
Mussel Watch	April 1978	One cage in site	NUSC 1979
	August 1981	No details	SAIC 1988
Diver observation	October 1970	Single dive: topographic features, animals, sediment texture	Saila et al. 1971
Transmissometry or turbidity	December 1967	Before and during disposal	Saila et al. 1969
	December 1971	8 stations profiled	Pratt et al. 1973
	June 1972	3 stations profiled	Pratt et al. 1973
	July 1972	3 stations profiled	Pratt et al. 1973
	November 1972	4 stations profiled	Pratt et al. 1973
Sub-bottom survey	September 1987	3-7 kHz & 12 kHz 2100 m lanes, 50 m lane spacing	SAIC 1990

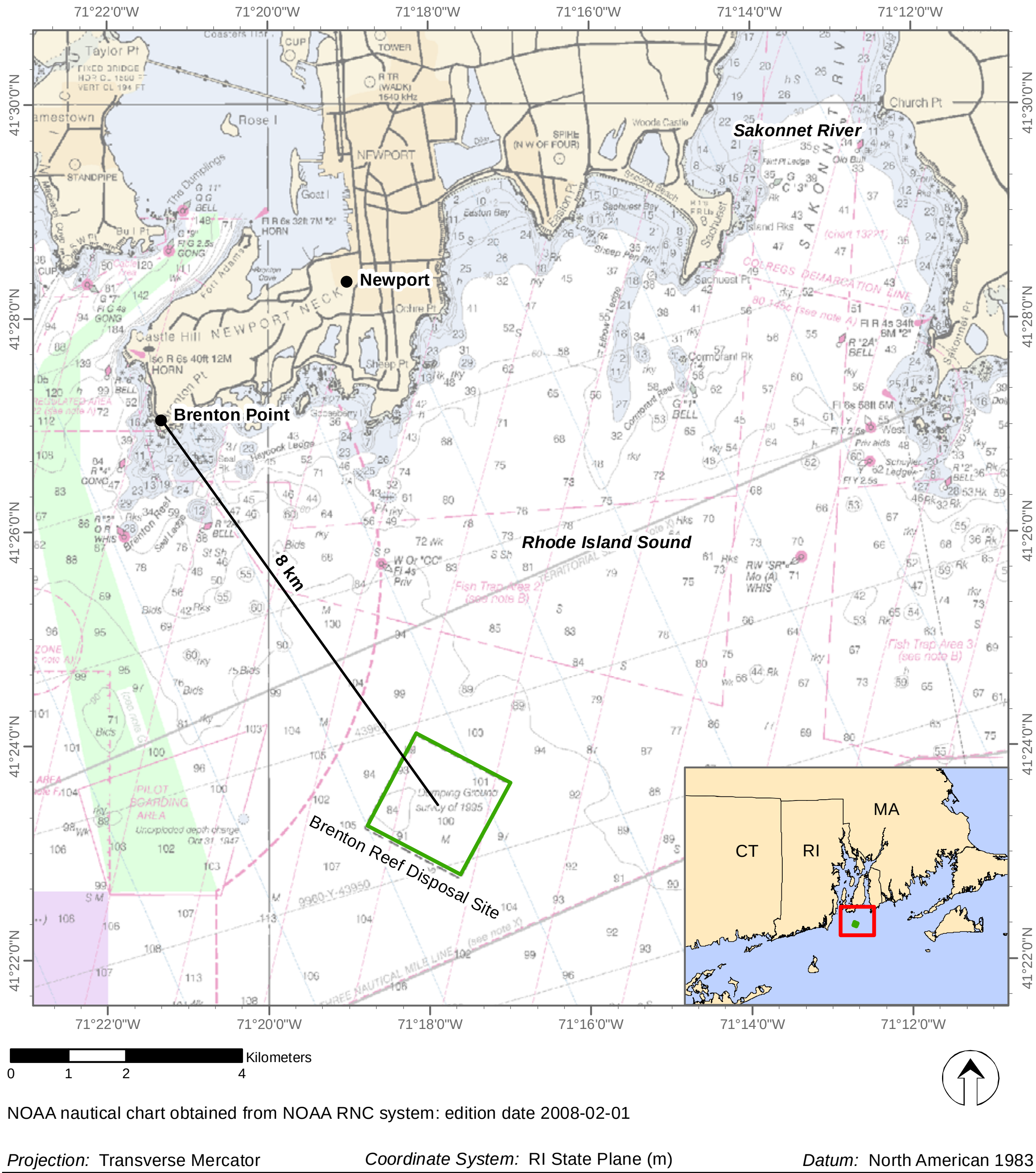

Fig1-1_BRDSLoc
August, 2011

Figure 1-1. Location of the Brenton Reef Disposal Site survey area in Rhode Island Sound

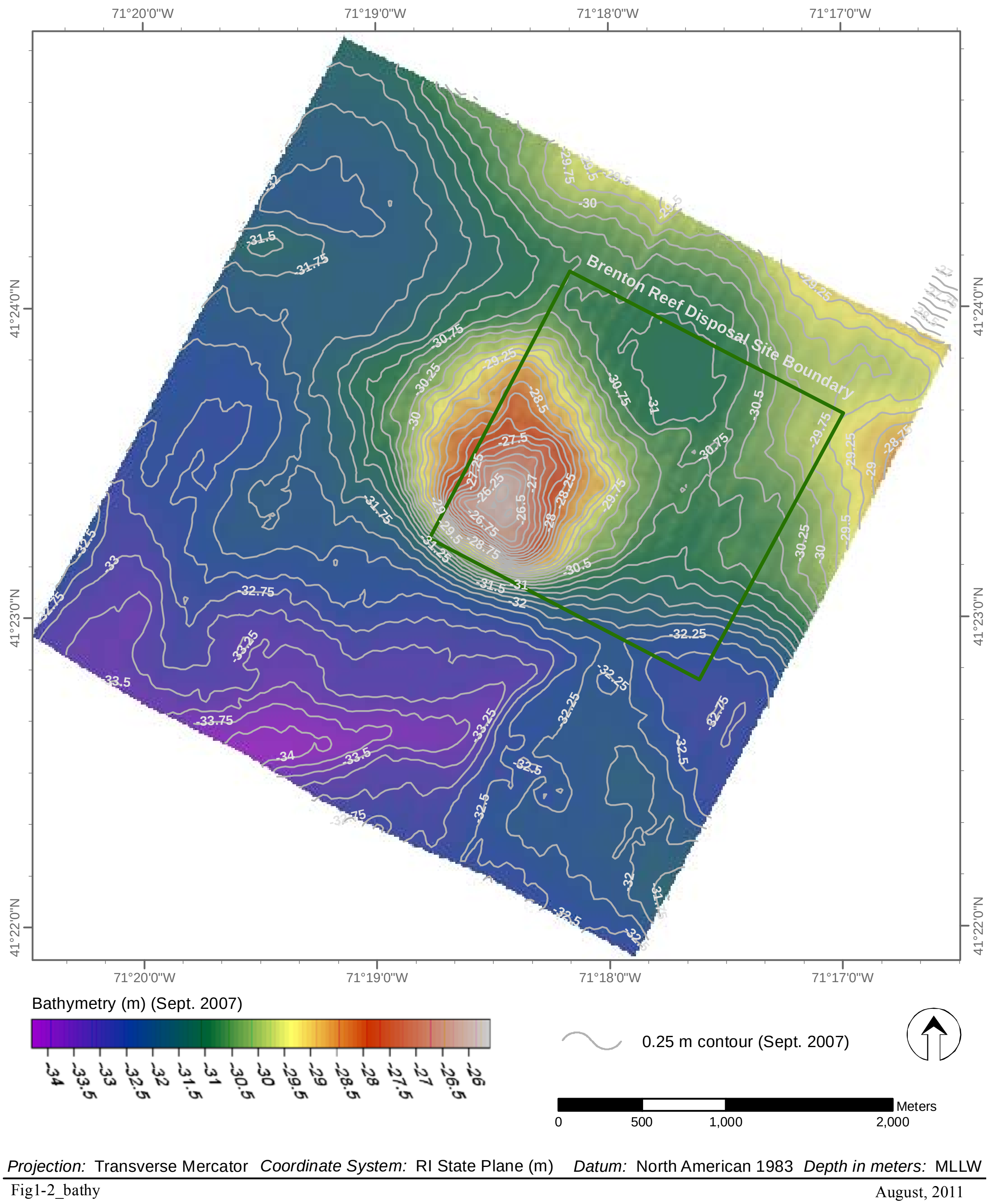

Figure 1-2. Bathymetry of the Brenton Reef Disposal Site survey area

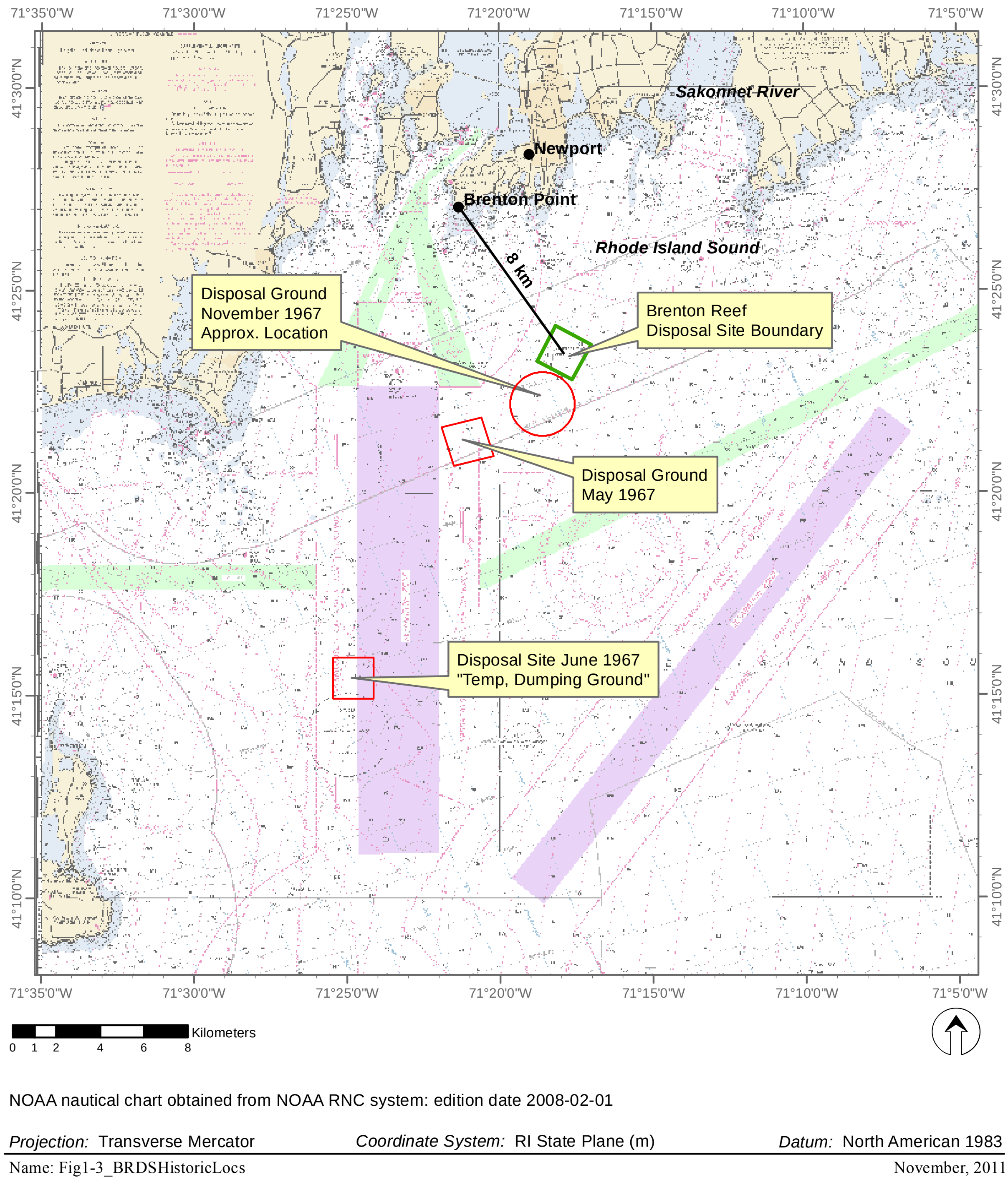

Figure 1-3. Location of the historical disposal areas and the Brenton Reef Disposal Site

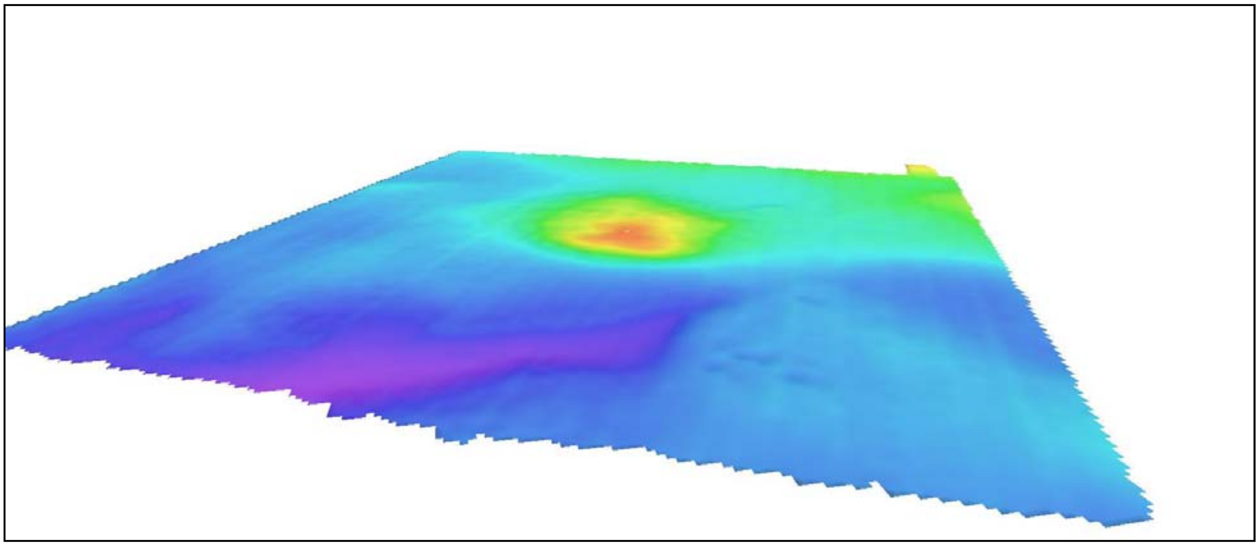

Vertical exaggeration scale at zero

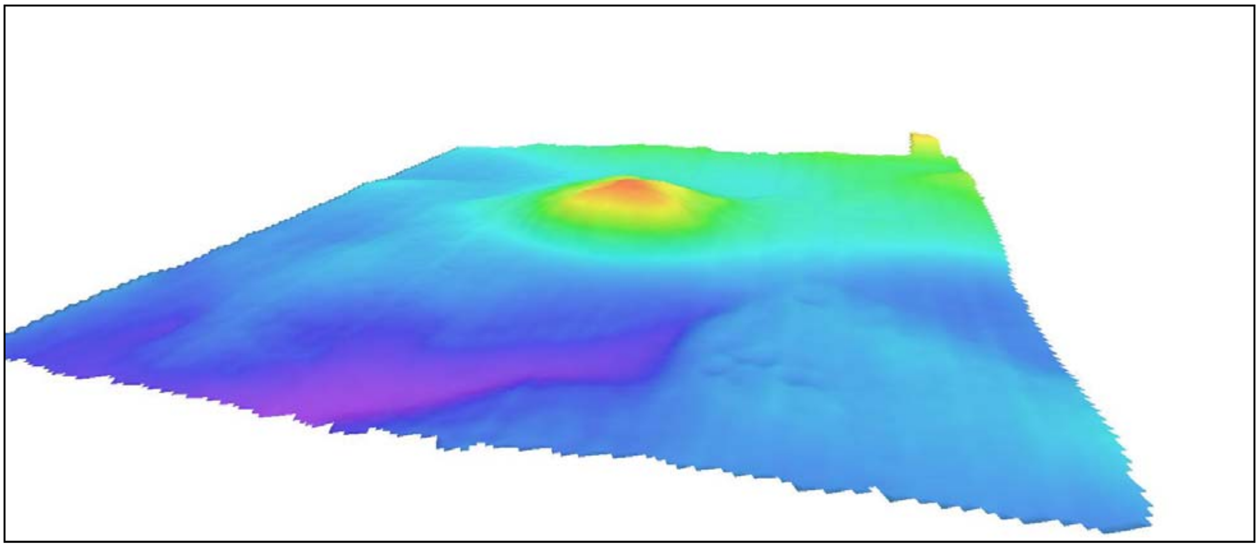

Vertical exaggeration scale at 50x

Figure 1-4. Three-dimensional bathymetric contour of BRDS with vertical exaggeration scale at zero and at 50 times

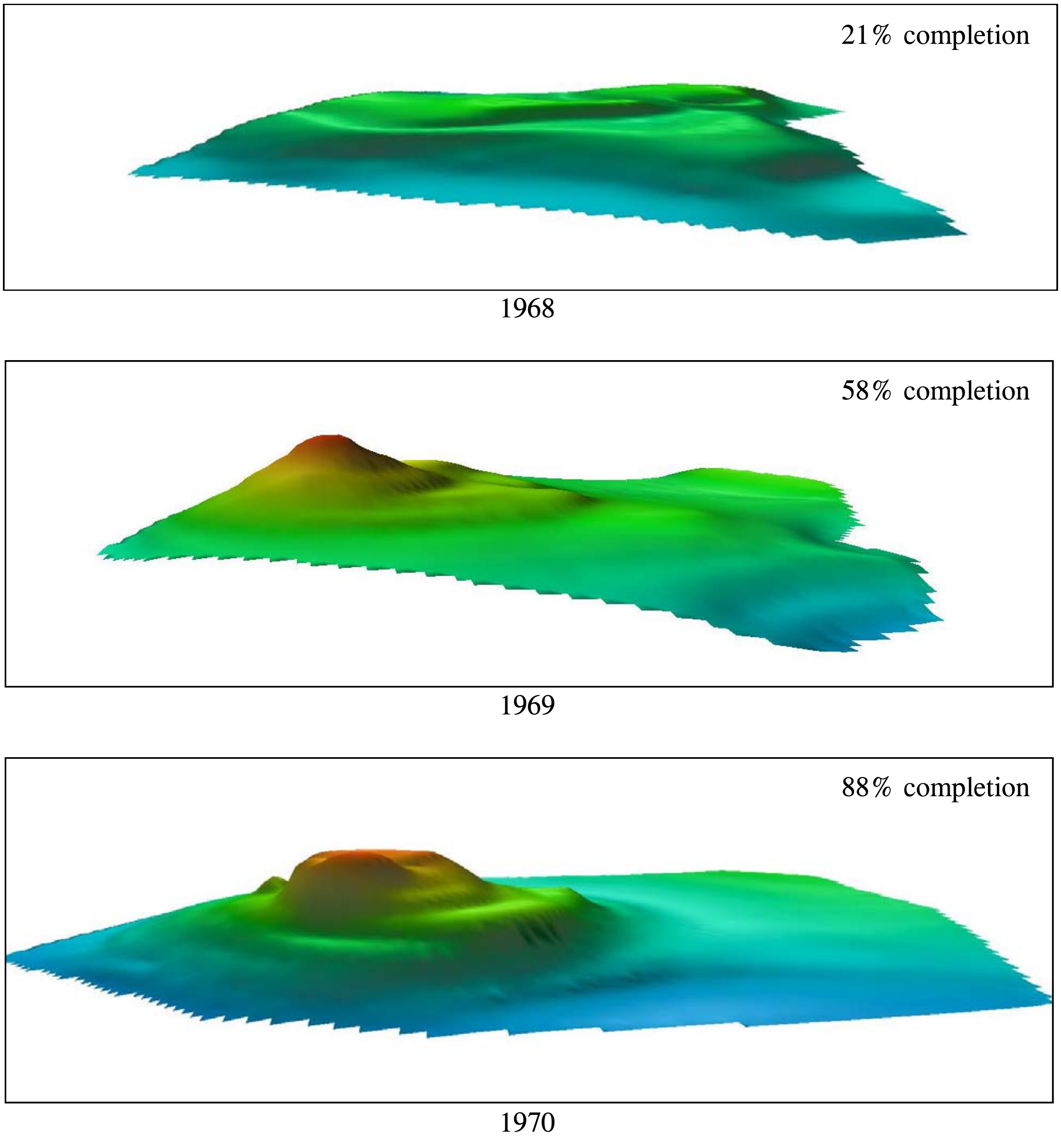

Figure 1-5. Three-dimensional contours of BRDS from 1968, 1969, and 1970, representing approximately 21%, 58% and 88% complete (vertical exaggeration 50x)

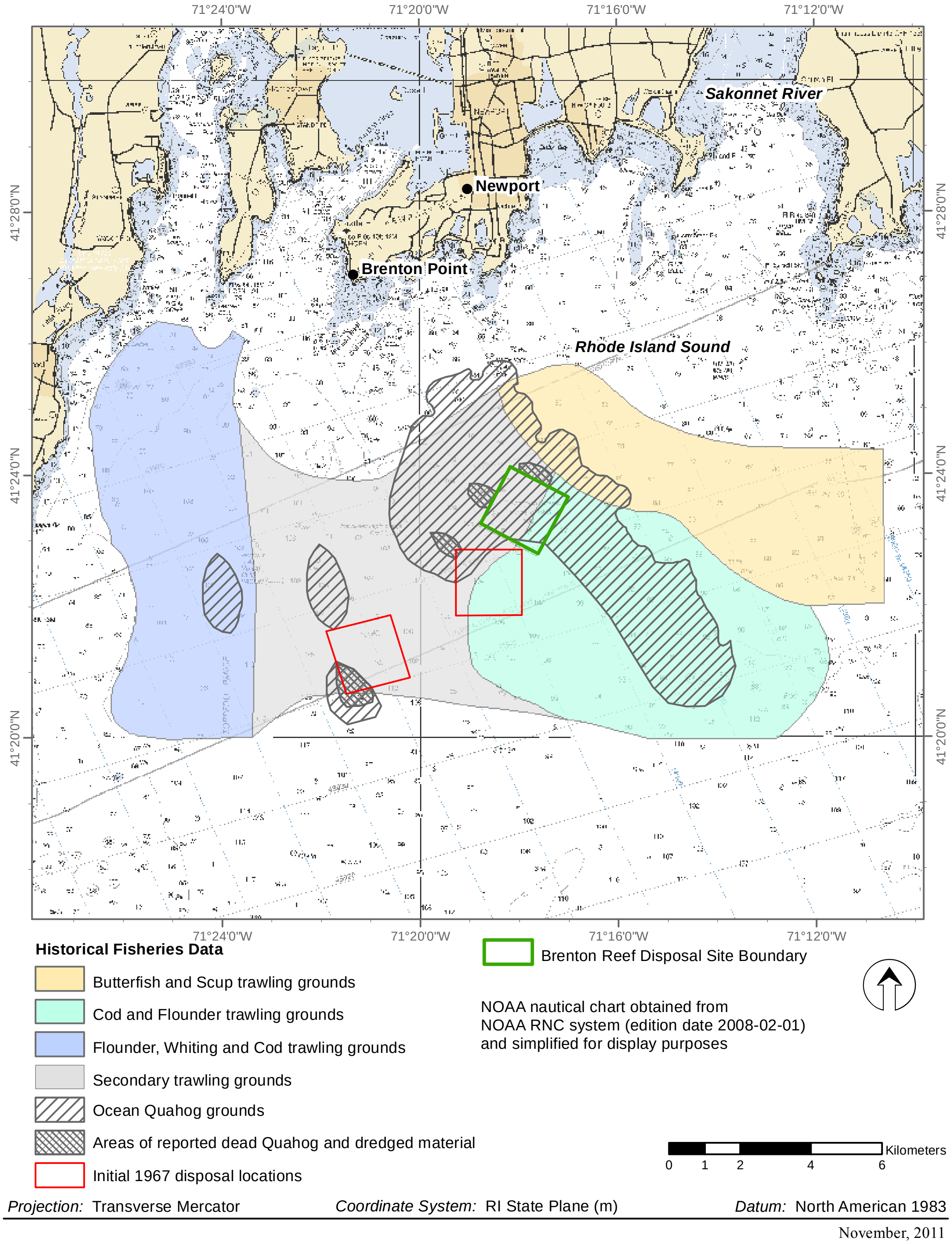

Figure 1-6. Location of historical fisheries areas in the Brenton Reef Disposal Site region

2.0 METHODS

A phased monitoring program was conducted to support characterization of physical, chemical, and biological conditions at the Brenton Reef Disposal Site with two surveys performed in September 2007 and one performed in August 2009. The monitoring program was conducted by CoastalVision, CR Environmental, Germano & Associates, and Ocean Surveys, Inc.; and featured bathymetric, acoustic backscatter, sediment profile imaging, plan-view photography, and sediment coring activities. A description of the phased monitoring approach is provided below, followed by an overview of the methods used to collect the survey data. Detailed descriptions of methodology and the related terminology are available in previous DAMOS contributions (e.g., ENSR 2004).

2.1 Overall Survey Planning

The monitoring program was conducted following a phased approach whereby the information obtained from each of three surveys was evaluated and applied to guide the next survey. Field activities are summarized in Table 2-1. The survey area included BRDS and three reference areas (Figure 2-1). The reference areas were situated southeast of the disposal site (Ref-SE), south of the disposal site (Ref-S), and west of the disposal site (Ref-W) and were designed to provide a basis of comparison between BRDS sediment conditions and the ambient sediment conditions in Rhode Island Sound.

Initially, a multibeam bathymetric survey was conducted from 10–17 September 2007 by CR Environmental aboard the R/V *Shanna Rose*. Data acquired during the multibeam survey included bathymetry and acoustic sonar backscatter and covered the entire Brenton Reef Disposal Site and some surrounding areas. Multibeam bathymetric survey data were applied to support characterization of site-wide surficial sediment conditions and to guide specification of sediment-profile imaging sites.

A sediment-profile imaging survey was conducted from 24–27 September 2007 aboard the R/V *Shanna Rose* by CR Environmental and Germano & Associates. Sediment Profile Imaging (SPI) and plan-view underwater camera (PUC) photographs were collected at a total of 89 stations, with 75 stations situated at the site and 14 situated in reference areas. Stations were preferentially targeted toward areas that appeared to be relatively free of hard surface materials and that were concentrated on the acoustically detectible footprint of the mound as identified in previous surveys. Acoustic backscatter data provided high-quality characterization of the mound and were used to improve the preliminary SPI survey design. Specifically, the SPI survey design was modified to enhance characterization of the margins of the mound by extending stations to the east, west, northeast, and northwest.

The findings of the 2007 surveys were applied to guide specification of sediment coring locations to characterize sediment stratigraphy at the site. The sediment coring survey was conducted from 27–29 August 2009 aboard the R/V *West Cove III* by Ocean Surveys, Inc. Sediment cores were collected at nine locations, with seven situated at BRDS and two in reference areas. The sediment coring locations were selected to represent a range of mound locations (near the mound peak and toward the margins) in an attempt to capture a range of site conditions while avoiding obstacles such as large rocks. Of the two reference area sampling locations, one was expected to have no dredged material present and the second was expected to have some dredged material present.

The phased monitoring approach was developed in coordination with NAE, and individual survey plans were approved by NAE. Together, the September 2007 and August 2009 surveys were designed to characterize the physical, chemical, and biological conditions at the Brenton Reef Disposal Site in support of project objectives.

2.2 Navigation and On-Board Data Acquisition

Navigation for the surveys was accomplished using a Trimble AgGPS 132, 12-channel Differential Global Positioning System (DGPS) system capable of receiving the U.S. Coast Guard (USCG) beacon corrections as well as OmniStar® subscription-based satellite differential corrections. The system is capable of submeter (i.e., less than one meter) horizontal position accuracy. The DGPS receiver installed on the survey vessel was interfaced to the onboard navigation computer running HYPACK® software; this provided the field team with the ability to precisely navigate the vessel throughout the survey area, along the preselected survey tracklines for the multibeam bathymetry survey, and to the target stations for the SPI, plan-view imaging, and sediment coring survey. HYPACK® MAX hydrographic survey software, developed by HYPACK, Inc. (formerly Coastal Oceanographics, Inc.) was used to acquire, integrate, and store all positional data from the DGPS as well as bathymetric, acoustic backscatter, and station data. HYPACK® continually recorded vessel position and DGPS satellite quality and provided a steering display for the vessel captain.

2.3 Bathymetry

2.3.1 Bathymetric Data Acquisition

A total of 41 survey lines, each 100 m apart and oriented in a northeast to southwest direction were occupied as part of the survey (Figure 2-2). It is noteworthy that rough sea states were experienced during some periods of data acquisition, and the conditions had an impact on data quality. On 15 September sea states included approximately 1- to 2-m breaking waves amongst irregular swells. The survey was aborted at 1400 h due to suspected impaired data quality associated with severe pitch and roll. Sea states on 17 September were less severe, and wave heights ranged from approximately 0.3 to 1.5 m, with lesser but substantial swells. Rough sea states introduce artifacts into bathymetric data that must be carefully processed after collection (see Section 3).

The bathymetric data were collected using a Reson 8101 Multibeam Echo Sounder (MBES) outfitted with a 1.5°, 240-kHz transducer. The MBES transducer was mounted to the amidships port rail of the survey vessel using a high-strength adjustable boom. The DGPS antenna was attached to the top of the transducer boom. The transducer depth below the water surface was checked and recorded at the start and end of each day.

The MBES topside processor was equipped with components necessary to transmit depth solutions and side-scan sonar signals to the HYPACK® acquisition computer via Ethernet communications. HYPACK® also received and recorded navigation data from the DGPS, motion data from a serially interfaced Ixsea Hydrins motion reference unit (MRU), and heading data from a TSS Meridian gyro compass. Patch tests were conducted at the start and end of each survey day to allow computation of angular offsets between the MBES system components. The system was calibrated for local water mass speed of sound by performing conductivity-temperature-depth (CTD) casts at frequent intervals throughout each survey day with a Seabird SBE-19 Seacat CTD profiler. Additional confirmation of proper calibration was obtained using the "bar check" method, in which a metal plate was lowered beneath the echo sounder's transducer to several known distances (e.g., 5.0 and 10.0 m) below the water surface. Bar-check calibrations were consistently accurate to within 0.05 m throughout the survey.

2.3.2 Bathymetric Data Processing and Analysis

Bathymetric data were processed using the HYSWEEP Processor Module. Major components of processing included the following:

- Calculation and application of MRU and heading sensor offsets relative to the MBES transducer and the vessel center of motion using patch test data;
- Removal of outlying soundings associated with water column interference (e.g., fish or midwater column debris);
- Conversion of soundings to mean lower low water (MLLW) elevations based on water level data recorded at National Oceanographic and Atmospheric Administration (NOAA) Station 8452660 (Newport, RI); and
- Adjustment of data for water column stratification and associated ray bending (refraction) using profiles of water column temperature and salinity. Sound velocity profiles were calculated using the Chen equation (Chen and Millero 1977). Profile data were entered into HYPACK® and used to adjust raw soundings.

After performing these adjustments and corrections, HYPACK®'s implementation of the Combined Uncertainty and Bathymetry Estimator (CUBE) developed at the NOAA/University of New Hampshire (UNH) Center for Coastal and Ocean Mapping (CCOM) was used to statistically estimate the depth solution with the least uncertainty for a network grid of 5 x 5 m over the entire survey area. The CUBE data were exported in a single comma-delimited ASCII text file including fields for northing, easting, and elevation. This file was then imported to Golden Software, Inc., Surfer® v.8.1 Surface Modeling Software, and a grid of the seabed elevations was replicated using Kriging interpolation methods and a 5-m node interval. Artifacts in the grid associated with a combination of rough sea state and thermocline variations were minimized using Gaussian low-pass filtering. Contour maps depicting bottom elevations using 0.25-m and 0.5-m contour intervals were created from the filtered grid, and the layers were exported in SHP and DXF formats. Additional layers were created using conventional hydrographic spectrum shading and 2-times vertically exaggerated relief. These layers were exported as georeferenced TIF image files. All data were projected to the Rhode Island State Plane grid, NAD83 (metric).

2.3.3 Acoustic Backscatter Data Processing and Analysis

Backscatter data collected during the surveys consisted of the side-scan sonar signal from the MBES recorded in HSX format. Sonar data were processed using a combination of four software tools:

- SonarWeb, from Chesapeake Technology, Inc., was used to create preliminary sonar mosaics, HTML-navigable data files, and GIS-formatted navigation shapefiles.

- GeoCoder was developed by scientists at NOAA's CCOM Joint Hydrographic Center and implemented in HYPACK® and was used to create mosaics best suited for substrate characterization through the use of innovative beam-angle correction algorithms.
- Sideview, from Quester Tangent Corporation, was used to statistically analyze data and classify areas with similar acoustic signatures.
- IDRISI GIS, from Clark Laboratories, was used to calculate and display clusters of similar mosaic raster values using a K-means algorithm which assigned pixels to clusters based on Euclidean distance analysis.

Sonar resolution is defined as the ability of the sonar system to discriminate between two adjacent objects of particular sizes and separation. This resolution decreases with increasing range from the sensor due to signal spreading. The theoretical resolution of the side-scan sonar data is determined by swath width (range setting), frequency, beam width, ping duration, and vessel speed. Data collected for this survey using a 240-kHz signal and assumed 25- to 40-m slant range has a resolution (beam footprint) of approximately 0.5 to 1.0 m. The resolution of georeferenced side-scan imagery was therefore set to 1.0 m/pixel.

Side-scan sonar data processed in SonarWeb were produced in several forms including georeferenced JPG files, high-resolution annotated "waterfall" imagery of each survey lane, and GIS shapefiles (polygons) of transect navigation data with the width of the polygons corresponding to sonar range settings. Also, a set of HTML files for the project was created, allowing Web-browser (i.e., Internet Explorer or Firefox) access to all survey data and imagery. Georeferenced sonar data were incorporated in a GIS database for comparison with other data. Because of the degree of overlap between navigation polygons, the navigation shapefiles are best queried and analyzed in ESRI ArcMAP 9.0 (or later). It is also important to note that while the mosaics produced for this report included all projected sonar files, users of ArcMAP can create customized mosaics of areas of specific interest by selectively adding data for individual transects and adjusting image transparency and contrast. In some instances, selective removal of the extensively overlapped sonar data may result in a "clearer" image. Files produced using SonarWeb are projected (when applicable) to the Rhode Island State Plane Grid, NAD83 (metric).

Side-scan data were next processed using HYPACK, Inc.'s implementation of GeoCoder software. GeoCoder was used to create a mosaic best suited for substrate characterization through the use of innovative beam-angle correction algorithms. GeoCoder was also used to export sonar backscatter values in an ASCII-delimited format with fields for northing, easting and backscatter (dB). Surfer® was used to create grids and contour maps of seafloor backscatter using these files. Data and imagery created using GeoCoder have been projected to the Rhode Island State Plane Grid, NAD83 (metric).

Data were acquired using Reson MBES settings selected to optimize bathymetric data quality in rough seas. Among the settings used was an automatic gain function which dynamically adjusted signal gains to maximize the signal-noise ratio in bathymetric data. These frequent minor adjustments are visible in side-scan sonar backscatter data, particularly near the transition zones between different substrate textures. The automatic gain adjustments thus had the effect of reducing the magnitude of backscatter variations between sediment types.

2.4 Seafloor Imaging

2.4.1 SPI and PUC Data Collection

A total of 89 target camera stations were selected for the SPI and PUC photograph survey, with 75 stations at the disposal site and 14 stations in reference areas (Table 2-2, Figure 2-3). At each station, the vessel was positioned at the target coordinates, and the camera frame was lowered to the seafloor within a defined station tolerance of 10 m. The SPI and plan-view cameras were deployed simultaneously. Three replicate SPI images were collected at each of the 89 stations (Table 2-2). Station 6 had six replicate SPI images collected due to a change in the trigger wire for the PUC system (between replicate C and D) three replicates (B,C,F) were chosen for analysis based on quality of the SPI images.

2.4.2 Sediment Profile Imaging

Sediment-profile imaging was used to provide data on the physical characteristics of the seafloor as well as the status of the benthic biological community. The technique involves deploying an underwater camera system to photograph a cross section of the sediment-water interface. Acquisition of high-resolution SPI images was accomplished using a Nikon D200 digital single-lens reflex camera mounted inside an Ocean Imaging Systems Model 3731 pressure housing system. The pressure housing sits atop a wedge-shaped prism with a front faceplate and a back mirror. The mirror is mounted at a 45° angle to reflect the profile of the sediment-water interface. As the prism penetrates the seafloor, a trigger activates a time-delay circuit that fires an internal strobe to obtain a cross-sectional image of the upper 15 to 20 cm of the sediment column (Figure 2-4). The camera remains on the seafloor for approximately 20 seconds to ensure that a successful image has been obtained.

Test exposures of the Kodak® Color Separation Guide (Publication No. Q-13) were made on deck at the beginning and end of each survey to verify that all internal electronic systems were working to design specifications and to provide a color standard against which final images could be checked for proper color balance. After deployment of the camera at each station, the frame counter was checked to ensure that the requisite number of replicates had been obtained. In addition, a prism penetration depth indicator on the camera frame was checked to verify that the optical prism had actually penetrated the bottom to a sufficient depth. If images were missed or the penetration depth was insufficient, the camera frame stop collars were adjusted and/or weights were added or removed, and additional replicate images were taken. Changes in prism weight amounts, the presence or absence of mud doors, and frame stop collar positions were recorded for each replicate image.

Each image was assigned a unique time stamp in the digital file attributes by the camera's data logger and cross-checked with the time stamp in the navigational system's computer data file. In addition, the field crew kept redundant written sample logs. Images were downloaded periodically to verify successful sample acquisition and/or to assess what type of sediment/depositional layer was present at a particular station. Digital image files were renamed with the appropriate station name immediately after downloading as a further quality assurance step.

Computer-aided analysis of the resulting images provided a set of standard measurements that enabled comparison between different locations and different surveys. The DAMOS Program has successfully used this technique for over 20 years to map the distribution of disposed dredged material and to monitor benthic recolonization at disposal sites. For a detailed discussion of SPI methodology, see DAMOS Contribution No. 156 (ENSR 2004).

2.4.3 Plan-View Imaging

Plan-view underwater images were also collected at each station using a second camera mounted on the sediment-profile camera frame. An Ocean Imaging Systems Model DSC6000 plan-view underwater camera (PUC) system was attached to the Model 3731 camera frame and used to collect plan-view photographs of the seafloor surface (Figure 2-4). The PUC system consisted of a Nikon D-70 camera encased in a titanium housing, a 24 VDC autonomous power pack, a 500W strobe, and a bounce trigger. As the camera apparatus was lowered to the seafloor, the weight attached to the bounce trigger contacted the seafloor prior to the camera frame hitting the bottom and triggered the camera. The length of the stainless steel trigger cable was adjusted for changing conditions in water clarity within the site. The field of view for the plan-view images ranged from approximately 0.6 m^2 to 3.1 m^2, depending on the length of the trigger wire.

All PUC images were collected as 6-megapixel raw Nikon Exchange Format (*.nef) files and converted to JPG files after the survey.

2.4.4 SPI and PUC Data Analysis

SPI Data Analysis

Each station is represented by three replicates; when stations have been over-sampled due to equipment or weather conditions, three replicates are chosen with the best quality images (e.g. Station 6 had six replicates due to change in the PUC trigger wire, and replicates B, C, and F were analyzed). Computer-aided analysis of each SPI image was performed to provide measurement of the following standard set of parameters:

Sediment Type. The sediment grain size major mode and range were estimated visually from the images using a grain size comparator at a similar scale. Results were reported using the phi scale. Conversion to other grain size scales is provided in Appendix B. The presence and thickness of disposed dredged material were also assessed by inspection of the images.

Penetration Depth. The depth to which the camera penetrated into the seafloor was measured to provide an indication of the sediment density or bearing capacity. The penetration depth can range from a minimum of 0 cm (i.e., no penetration on hard substrates) to a maximum of 20 cm (full penetration on very soft substrates).

Surface Boundary Roughness. Surface boundary roughness is a measure of the vertical relief of features at the sediment-water interface in the sediment-profile image. Surface boundary roughness was determined by measuring the vertical distance between the highest and lowest points of the sediment-water interface. The surface boundary roughness (sediment surface relief) measured over the width of sediment-profile images typically ranges from 0 to 4 cm, and may be related to physical structures (e.g., ripples, rip-up structures, mud clasts) or biogenic features (e.g., burrow openings, fecal mounds, foraging depressions). Biogenic roughness typically changes seasonally and is related to the interaction of bottom turbulence and bioturbational activities.

Apparent RPD Depth. Redox potential discontinuity (RPD) provides a measure of the integrated history of the balance between near-surface oxygen conditions and biological reworking of sediments. Sediment particles exposed to oxygenated waters oxidize and lighten in color to brown or light grey. As the particles are moved downwards by biological activity or buried, they are exposed to reduced oxygen concentrations in subsurface pore waters and their oxic coating slowly reduces, changing color to dark grey or black. When biological activity is high, the RPD depth increases;

when it is low or absent, the RPD depth decreases. The apparent RPD (aRPD) depth was measured by assessing color and reflectance boundaries within the images.

Infaunal Successional Stage. Infaunal successional stage is a measure of the biological community inhabiting the seafloor. Current theory holds that organism-sediment interactions in fine-grained sediments follow a predictable sequence of development after a major disturbance (such as dredged material disposal), and this sequence has been divided subjectively into four stages: Stage 0, indicative of a sediment column that is largely devoid of macrofauna, occurs immediately following a physical disturbance or in close proximity to an organic enrichment source; Stage 1 is the initial community of tiny, densely populated polychaete assemblages; Stage 2 is the start of the transition to head-down deposit feeders; and Stage 3 is the mature, equilibrium community of deep-dwelling, head-down deposit feeders (Rhoads and Germano 1982, 1986). Successional stage was assigned by assessing which types of species or organism-related activities were apparent in the images.

Additional components of the SPI analysis included calculation of means and ranges for the parameters listed above and mapping of station-averaged values.

PUC Image Data Analysis

Computer-aided analysis of each PUC image was performed to provide additional information about large-scale sedimentary features, density and patch size of surface fauna, density of infaunal burrowers, and occurrences and density of epifaunal foraging patterns on the seafloor of the disposal site and reference areas.

2.5 Sediment Core Collection and Processing

Nine sediment cores were collected: seven cores were collected from BRDS, and two cores were collected from nearby reference areas (Table 2-3, Figure 2-5). Cores were collected using vibracoring equipment and were subsequently split, imaged, and subsampled at the University of Rhode Island (URI) Marine Geomechanics Laboratory (MGL).

2.5.1 Coring Survey

The sediment coring survey was conducted using an OSI model 1500 pneumatic vibratory corer and coring stand. The OSI 1500 was equipped with a 3-meter-long steel core barrel (10 cm I.D.) that accepted 8 cm (I.D.) Lexan (polycarbonate) core liners. The corer was also fitted with a nose cone or "cutter" and a core retainer to improve core retention and sample retrieval. The system was mobilized with a three-point mooring system and a handling framework for managing the vibratory corer.

Fourteen attempts were made to collect long cores from mound and reference areas; seven successful core recoveries were made. Core refusal was attributed to packed sand, cobbles and equipment malfunction. Core samples were successfully collected on the first attempt at 5 locations (denoted “a” in Table 2-3), on the second attempt at three locations (denoted “b”) and on the third attempt at reference location BR70 (denoted "c"). Core lengths varied from 0.59 to 2.87 m (Table 2-3). Survey operations were based out of Jamestown, Rhode Island, and cores were transferred to the URI MGL for processing at the end of each field day.

2.5.2 Core Processing

Core processing was performed at MGL. Cores were split in half lengthwise using a splitting device that consisted of two opposing router bits designed to travel the length of the core tube in parallel until it was severed from top to bottom on opposite sides. After the plastic core tube was severed, a wire was pulled through the sediment from the top of the core to the bottom to complete the splitting process. Next, the two sediment halves were separated and sealed with plastic film for short-term storage. After each core was split lengthwise, one half was transferred to the imaging laboratory for high-resolution imaging and analysis. The other half of the core was described by examining the open surface, labeled, and subsampled for chemical analysis.

2.5.3 Core Description

Each core was examined, and observations of surface texture, odor, color, stratigraphic changes, and potential presence of contaminants were documented on log forms. Visual core observations were described by sample interval and were transcribed into Microsoft Excel® spreadsheets to enable graphical presentation of core descriptions along with core imaging results. Core descriptive information was applied to support selection of subsampling locations within each core. Stratigraphic intervals identified in the core descriptions were used to guide selection of sampling locations for physical and chemical analyses. Each subsample was homogenized before containerization and transfer to the analytical laboratory.

Samples were collected near the surface of each core to establish whether contaminants were present in the surficial cap sediments, at specific lithologic intervals that suggested the presence of contaminants (generally black, organic-rich sediments), and to provide down-core profiles characterizing any potential contaminant profile gradients that might suggest transport of contaminants into the overlying sediment or water column.

2.5.4 Core Imaging

Core imaging was performed using a GeoTek™ multisensor core logger with a digital camera. Each core was logged at 2-cm intervals. The sediment cores were first prepared for digital scanning by scraping the exposed sediment along the horizontal to provide a fresh, unaltered sediment surface. High-resolution digital photographs were taken of the full length of each core. Next, the GeoTek™ logger nondestructively collected data along the full length of each core for a suite of physical parameters, including bulk density, magnetic susceptibility, resistivity, and P-wave velocity.

2.6 Laboratory Methods

Forty samples were collected for grain size, TOC, and metals analyses (Table 2-4). The target metals list included aluminum (Al), arsenic (As), beryllium (Be), cadmium (Cd), chromium (Cr), copper (Cu), iron (Fe), lead (Pb), nickel (Ni), selenium (Se), silver (Ag), vanadium (V), and zinc (Zn). Of the 40 samples, 20 were also analyzed for PAHs. The target PAH list included the 16 original priority PAH pollutants plus 2-methylnaphthalene. Grain size samples were analyzed by Geotesting Express in Boxborough, Massachusetts. Chemistry samples were analyzed by Mitkem Laboratories in Warwick, Rhode Island. All data were provided by the laboratories in electronic format for direct transfer into the project database.

2.6.1 Grain Size Measurements

Sediment grain size was determined using an ASTM sieve/hydrometer methodology (ASTM D422; ASTM 2009). Seven sieves were used to classify the coarse sediment fraction (Sieve # 4, 10, 20, 40, 60, 100, and 200). Sediments finer than 75 µm were classified (silt/clay) by their settling properties (hydrometer).

2.6.2 Chemical Analyses

Sediments were prepared for PAH analysis according to EPA SW-846 Method 3550B and analyzed using method 8270D modified to utilize selected ion mass spectrometer (SIM) mode (USEPA 1997). TOC was analyzed using the Lloyd Kahn combustion method (USEPA 1988). Samples collected for metals analysis were extracted by acid digestion according to EPA SW-846 Method 3050B and analyzed using Method 6010 by inductively coupled plasma-optical emission spectrometry (ICP-IES; Table 2-4).

2.6.3 Data Analysis

The data were processed and summarized in preparation for data analysis. Data reported as below detection were evaluated using the reporting limit for that sample and chemical. If both results from duplicate samples were reported as above detection, the values were averaged. If only one sample was reported above detection, then that value was used. If both results were reported as below detection, then the maximum reporting limit was used for the analysis. An exception was made when two samples were reported both as a first run and as a diluted sample: after verification that the dilution results were adjusted for the dilution ratio, the results from the dilution run were used in data analyses.

Total high and low molecular weight PAHs were calculated using the reporting limit for data below detection as described above. Low molecular weight PAHs (LPAHs) included 2-methylnaphthalene, acenaphthene, acenaphthylene, anthracene, fluorene, naphthalene, and phenanthrene. High molecular weight PAHs (HPAHs) included benzo[a]anthracene, benzo[a]pyrene, benzo[b]fluoranthene, benzo[g,h,i]perylene, benzo[k]fluoranthene, chrysene, dibenzo[a,h]anthracene, fluoranthene, indeno[1,2,3-cd]pyrene, and pyrene. Total PAHs were calculated as LPAH+HPAH.

2.6.4 Data Quality Assurance and Quality Control Review

The chemistry quality control samples indicated that the chemical samples were analyzed with sufficient accuracy and precision to meet the project objectives. Chemical measurements were reported in two batches. Method blank, matrix spike, and laboratory control sample (LCS) data were used to evaluate chemical data accuracy; matrix duplicates, matrix spike duplicates (MS/MSD), or control sample duplicates (LCS/LCSD) were used to evaluate precision. The reporting limits and method detection limits for each parameter are provided in Table 2-5.

The method blanks associated with the project sample set indicated that the samples were processed and analyzed without significant contamination. None of the PAH compounds were detected in the blank samples; only a few metals (Cu, Fe, Zn) were detected, and these were at levels below laboratory reporting limits. Laboratory control sample (LCS) measurements used to determine accuracy of PAH compounds were largely all within laboratory-defined control limits of 45%–145%. Naphthalene and 2-methylnapthalene were measured with a small negative bias (at 35% and 36% recovery, respectively). Precision was satisfactory for all measured compounds and consistently better than the laboratory control limit of 40% relative percent difference (RPD).

The measured quality control sample accuracy associated with all metal analytes was excellent and within 80%–120% of the target (true) value. Precision indicators (as matrix replicates) were also within the laboratory target (20% RPD) with the exception of arsenic. In the case of arsenic, one of the two matrix pairs was measured with a calculated RPD of 55%.

The quality of TOC data was monitored with LCS samples and all related TOC measurements were within accuracy targets of 80%–120%. As noted by the laboratory, samples BR32-181-192, BR03-231-246, and BR78-42-57 contained TOC at concentrations exceeding the upper calibration limit, and those measurements were qualified with "E."

To measure precision of the group of 40 grain size sample analyses, three grain size samples were prepared for duplicate analysis. Precision of grain size measurements was satisfactory relative to project objectives with relative percent differences (RPD) for the duplicate pairs ranging from 1% to 21%.

Table 2-1.

Brenton Reef Disposal Site Field Activity Summary

Survey Type	Date	Summary
Bathymetry and Acoustic Backscatter	10-17 September 2007	Area: 4000 x 4000 m Lines: 41 Spacing: 100 m Orientation: NE to SW
Sediment-Profile and Plan-View Imaging	24-27 September 2007	Stations: 89 Brenton Reef Disposal Site: 75 Reference Areas: 14
Sediment Coring	27-29 August 2009	Stations: 9 Brenton Reef Disposal Site: 7 Reference Areas: 2

Table 2-2.

Brenton Reef Disposal Site Sediment-Profile and Plan-View Image Sampling Locations (Reference Stations 63–72, 94–97 are highlighted in bold text)

Station	Latitude (N)	Longitude (W)	Station	Latitude (N)	Longitude (W)
BRDS-01-A	41° 23.370'	71° 18.387'	BRDS-25-A	41° 24.020'	71° 18.363'
BRDS-01-B	41° 23.373'	71° 18.389'	BRDS-25-B	41° 24.021'	71° 18.363'
BRDS-01-C	41° 23.374'	71° 18.391'	BRDS-25-C	41° 24.022'	71° 18.364'
BRDS-02-A	41° 23.504'	71° 18.492'	BRDS-26-A	41° 23.830'	71° 18.984'
BRDS-02-B	41° 23.504'	71° 18.496'	BRDS-26-B	41° 23.832'	71° 18.984'
BRDS-02-C	41° 23.507'	71° 18.495'	BRDS-26-C	41° 23.832'	71° 18.982'
BRDS-03-A	41° 23.542'	71° 18.371'	BRDS-27-A	41° 23.821'	71° 18.826'
BRDS-03-B	41° 23.538'	71° 18.365'	BRDS-27-B	41° 23.826'	71° 18.822'
BRDS-03-C	41° 23.540'	71° 18.366'	BRDS-27-C	41° 23.827'	71° 18.821'
BRDS-04-A	41° 23.414'	71° 18.445'	BRDS-28-A	41° 23.790'	71° 18.922'
BRDS-04-B	41° 23.417'	71° 18.443'	BRDS-28-B	41° 23.786'	71° 18.919'
BRDS-04-C	41° 23.421'	71° 18.443'	BRDS-28-C	41° 23.789'	71° 18.916'
BRDS-05-A	41° 23.356'	71° 18.497'	BRDS-30-A	41° 23.892'	71° 18.710'
BRDS-05-B	41° 23.353'	71° 18.489'	BRDS-30-B	41° 23.894'	71° 18.705'
BRDS-05-C	41° 23.356'	71° 18.497'	BRDS-30-C	41° 23.893'	71° 18.705'
BRDS-06-A	41° 23.318'	71° 18.408'	BRDS-31-A	41° 23.600'	71° 18.778'
BRDS-06-B	41° 23.317'	71° 18.412'	BRDS-31-B	41° 23.598'	71° 18.779'
BRDS-06-C	41° 23.316'	71° 18.416'	BRDS-31-C	41° 23.599'	71° 18.778'
BRDS-06-D	41° 23.326'	71° 18.402'	BRDS-32-A	41° 23.527'	71° 18.700'
BRDS-06-E	41° 23.324'	71° 18.399'	BRDS-32-B	41° 23.525'	71° 18.697'
BRDS-06-F	41° 23.319'	71° 18.401'	BRDS-32-C	41° 23.525'	71° 18.700'
BRDS-07-A	41° 23.427'	71° 18.327'	BRDS-33-A	41° 23.678'	71° 18.828'
BRDS-07-B	41° 23.428'	71° 18.326'	BRDS-33-B	41° 23.680'	71° 18.826'
BRDS-07-C	41° 23.430'	71° 18.326'	BRDS-33-C	41° 23.685'	71° 18.826'
BRDS-08-A	41° 23.241'	71° 18.381'	BRDS-34-A	41° 23.644'	71° 18.421'
BRDS-08-B	41° 23.244'	71° 18.375'	BRDS-34-B	41° 23.647'	71° 18.419'
BRDS-08-C	41° 23.248'	71° 18.366'	BRDS-34-C	41° 23.648'	71° 18.418'
BRDS-09-A	41° 23.300'	71° 18.542'	BRDS-35-A	41° 23.778'	71° 18.357'
BRDS-09-B	41° 23.298'	71° 18.544'	BRDS-35-B	41° 23.779'	71° 18.354'
BRDS-09-C	41° 23.297'	71° 18.542'	BRDS-35-C	41° 23.778'	71° 18.356'
BRDS-10-A	41° 23.392'	71° 18.634'	BRDS-36-A	41° 23.703'	71° 18.612'
BRDS-10-B	41° 23.392'	71° 18.636'	BRDS-36-B	41° 23.706'	71° 18.609'
BRDS-10-C	41° 23.393'	71° 18.639'	BRDS-36-C	41° 23.706'	71° 18.606'
BRDS-19-A	41° 23.944'	71° 19.067'	BRDS-37-A	41° 23.822'	71° 18.527'
BRDS-19-B	41° 23.942'	71° 19.066'	BRDS-37-B	41° 23.820'	71° 18.529'
BRDS-19-C	41° 23.943'	71° 19.064'	BRDS-37-C	41° 23.820'	71° 18.532'
BRDS-21-A	41° 23.972'	71° 18.865'	BRDS-38-A	41° 23.893'	71° 18.381'
BRDS-21-B	41° 23.974'	71° 18.864'	BRDS-38-B	41° 23.897'	71° 18.384'
BRDS-21-C	41° 23.975'	71° 18.866'	BRDS-38-C	41° 23.901'	71° 18.385'
BRDS-24-A	41° 24.084'	71° 18.484'	BRDS-39-A	41° 23.868'	71° 18.142'
BRDS-24-B	41° 24.086'	71° 18.485'	BRDS-39-B	41° 23.869'	71° 18.143'
BRDS-24-C	41° 24.086'	71° 18.490'	BRDS-39-C	41° 23.868'	71° 18.141'

Table 2-2., continued

Brenton Reef Disposal Site Sediment-Profile and Plan-View Image Sampling Locations (Reference Stations 63–72, 94–97 are highlighted in bold text)

Station	Latitude (N)	Longitude (W)	Station	Latitude (N)	Longitude (W)
BRDS-40-A	41° 23.804'	71° 18.062'	BRDS-54-A	41° 23.038'	71° 18.477'
BRDS-40-B	41° 23.803'	71° 18.065'	BRDS-54-B	41° 23.038'	71° 18.475'
BRDS-40-C	41° 23.802'	71° 18.060'	BRDS-54-C	41° 23.039'	71° 18.474'
BRDS-41-A	41° 23.731'	71° 18.001'	BRDS-55-A	41° 23.059'	71° 18.298'
BRDS-41-B	41° 23.734'	71° 18.002'	BRDS-55-B	41° 23.059'	71° 18.299'
BRDS-41-C	41° 23.735'	71° 18.008'	BRDS-55-C	41° 23.061'	71° 18.300'
BRDS-42-A	41° 23.602'	71° 17.959'	BRDS-56-A	41° 23.138'	71° 18.201'
BRDS-42-B	41° 23.605'	71° 17.962'	BRDS-56-B	41° 23.141'	71° 18.207'
BRDS-42-C	41° 23.605'	71° 17.961'	BRDS-56-C	41° 23.138'	71° 18.202'
BRDS-43-A	41° 23.677'	71° 18.095'	BRDS-57-A	41° 23.182'	71° 18.312'
BRDS-43-B	41° 23.676'	71° 18.102'	BRDS-57-B	41° 23.180'	71° 18.313'
BRDS-43-C	41° 23.679'	71° 18.102'	BRDS-57-C	41° 23.185'	71° 18.312'
BRDS-44-A	41° 23.740'	71° 18.220'	BRDS-58-A	41° 23.477'	71° 17.908'
BRDS-44-B	41° 23.743'	71° 18.212'	BRDS-58-B	41° 23.479'	71° 17.903'
BRDS-44-C	41° 23.745'	71° 18.219'	BRDS-58-C	41° 23.476'	71° 17.905'
BRDS-45-A	41° 23.594'	71° 18.179'	BRDS-59-A	41° 23.462'	71° 18.143'
BRDS-45-B	41° 23.595'	71° 18.174'	BRDS-59-B	41° 23.461'	71° 18.141'
BRDS-45-C	41° 23.594'	71° 18.174'	BRDS-59-C	41° 23.465'	71° 18.140'
BRDS-46-A	41° 23.639'	71° 18.298'	BRDS-60-A	41° 23.287'	71° 18.183'
BRDS-46-B	41° 23.641'	71° 18.297'	BRDS-60-B	41° 23.290'	71° 18.188'
BRDS-46-C	41° 23.644'	71° 18.295'	BRDS-60-C	41° 23.288'	71° 18.188'
BRDS-47-A	41° 23.737'	71° 18.722'	BRDS-61-A	41° 23.311'	71° 18.017'
BRDS-47-B	41° 23.736'	71° 18.715'	BRDS-61-B	41° 23.312'	71° 18.024'
BRDS-47-C	41° 23.733'	71° 18.714'	BRDS-61-C	41° 23.315'	71° 18.016'
BRDS-48-A	41° 23.261'	71° 18.832'	BRDS-62-A	41° 23.533'	71° 18.201'
BRDS-48-B	41° 23.258'	71° 18.833'	BRDS-62-B	41° 23.533'	71° 18.203'
BRDS-48-C	41° 23.258'	71° 18.836'	BRDS-62-C	41° 23.534'	71° 18.204'
BRDS-49-A	41° 23.286'	71° 18.701'			
BRDS-49-B	41° 23.287'	71° 18.702'	**BRDS-63-A**	**41° 22.622'**	**71° 17.270'**
BRDS-49-C	41° 23.290'	71° 18.700'	**BRDS-63-B**	**41° 22.625'**	**71° 17.269'**
BRDS-50-A	41° 23.228'	71° 18.637'	**BRDS-63-C**	**41° 22.626'**	**71° 17.269'**
BRDS-50-B	41° 23.229'	71° 18.634'	**BRDS-64-A**	**41° 22.565'**	**71° 17.176'**
BRDS-50-C	41° 23.227'	71° 18.634'	**BRDS-64-B**	**41° 22.569'**	**71° 17.175'**
BRDS-51-A	41° 23.150'	71° 18.767'	**BRDS-64-C**	**41° 22.569'**	**71° 17.175'**
BRDS-51-B	41° 23.675'	71° 18.789'	**BRDS-65-A**	**41° 22.478'**	**71° 17.149'**
BRDS-51-C	41° 23.150'	71° 18.763'	**BRDS-65-B**	**41° 22.479'**	**71° 17.149'**
BRDS-52-A	41° 23.150'	71° 18.608'	**BRDS-65-C**	**41° 22.480'**	**71° 17.148'**
BRDS-52-B	41° 23.148'	71° 18.604'	**BRDS-66-A**	**41° 22.550'**	**71° 17.359'**
BRDS-52-C	41° 23.146'	71° 18.608'	**BRDS-66-B**	**41° 22.551'**	**71° 17.359'**
BRDS-53-A	41° 23.157'	71° 18.445'	**BRDS-66-C**	**41° 22.554'**	**71° 17.364'**
BRDS-53-B	41° 23.159'	71° 18.441'	**BRDS-67-A**	**41° 22.464'**	**71° 17.328'**
BRDS-53-C	41° 23.155'	71° 18.443'	**BRDS-67-B**	**41° 22.464'**	**71° 17.330'**
			BRDS-67-C	**41° 22.466'**	**71° 17.332'**

Table 2-2., continued

Brenton Reef Disposal Site Sediment-Profile and Plan-View Image Sampling Locations
(Reference Stations 63–72, 94–97 are highlighted in bold text)

Station	Latitude (N)	Longitude (W)
BRDS-68-A	**41° 22.325'**	**71° 18.201'**
BRDS-68-B	**41° 22.327'**	**71° 18.201'**
BRDS-68-C	**41° 22.327'**	**71° 18.199'**
BRDS-69-A	**41° 22.325'**	**71° 18.365'**
BRDS-69-B	**41° 22.328'**	**71° 18.37'**
BRDS-69-C	**41° 22.329'**	**71° 18.367'**
BRDS-70-A	**41° 22.251'**	**71° 18.345'**
BRDS-70-B	**41° 22.252'**	**71° 18.345'**
BRDS-70-C	**41° 22.256'**	**71° 18.346'**
BRDS-71-A	**41° 22.209'**	**71° 18.232'**
BRDS-71-B	**41° 22.21'**	**71° 18.232'**
BRDS-71-C	**41° 22.211'**	**71° 18.232'**
BRDS-72-A	**41° 22.269'**	**71° 18.208'**
BRDS-72-B	**41° 22.27'**	**71° 18.211'**
BRDS-72-C	**41° 22.267'**	**71° 18.204'**
BRDS-73-A	41° 23.301'	71° 19.383'
BRDS-73-B	41° 23.3'	71° 19.378'
BRDS-73-C	41° 23.299'	71° 19.372'
BRDS-74-A	41° 23.323'	71° 19.144'
BRDS-74-B	41° 23.325'	71° 19.147'
BRDS-74-C	41° 23.321'	71° 19.148'
BRDS-75-A	41° 23.341'	71° 18.927'
BRDS-75-B	41° 23.338'	71° 18.93'
BRDS-75-C	41° 23.341'	71° 18.93'
BRDS-76-A	41° 23.36'	71° 18.713'
BRDS-76-B	41° 23.361'	71° 18.713'
BRDS-76-C	41° 23.36'	71° 18.711'
BRDS-77-A	41° 23.361'	71° 18.267'
BRDS-77-B	41° 23.364'	71° 18.267'
BRDS-77-C	41° 23.361'	71° 18.27'
BRDS-78-A	41° 23.376'	71° 18.053'
BRDS-78-B	41° 23.371'	71° 18.055'
BRDS-78-C	41° 23.377'	71° 18.049'
BRDS-79-A	41° 23.403'	71° 17.835'
BRDS-79-B	41° 23.406'	71° 17.831'
BRDS-79-C	41° 23.404'	71° 17.83'
BRDS-80-A	41° 23.441'	71° 17.583'
BRDS-80-B	41° 23.439'	71° 17.585'
BRDS-80-C	41° 23.439'	71° 17.583'
BRDS-81-A	41° 23.454'	71° 17.407'
BRDS-81-B	41° 23.459'	71° 17.414'
BRDS-81-C	41° 23.46'	71° 17.403'
BRDS-82-A	41° 23.453'	71° 17.168'
BRDS-82-B	41° 23.452'	71° 17.166'
BRDS-82-C	41° 23.451'	71° 17.164'
BRDS-83-A	41° 23.499'	71° 16.902'
BRDS-83-B	41° 23.495'	71° 16.902'
BRDS-83-C	41° 23.492'	71° 16.902'
BRDS-91-A	41° 23.782'	71° 17.923'
BRDS-91-B	41° 23.783'	71° 17.925'
BRDS-91-C	41° 23.782'	71° 17.928'
BRDS-92-A	41° 23.823'	71° 17.814'
BRDS-92-B	41° 23.823'	71° 17.817'
BRDS-92-C	41° 23.825'	71° 17.814'
BRDS-93-A	41° 23.869'	71° 17.695'
BRDS-93-B	41° 23.87'	71° 17.693'
BRDS-93-C	41° 23.871'	71° 17.695'
BRDS-94-A	**41° 23.039'**	**71° 20.099'**
BRDS-94-B	**41° 23.043'**	**71° 20.1'**
BRDS-94-C	**41° 23.044'**	**71° 20.1'**
BRDS-95-A	**41° 23.064'**	**71° 20.039'**
BRDS-95-B	**41° 23.064'**	**71° 20.033'**
BRDS-95-C	**41° 23.065'**	**71° 20.033'**
BRDS-96-A	**41° 23.125'**	**71° 19.995'**
BRDS-96-B	**41° 23.125'**	**71° 19.994'**
BRDS-96-C	**41° 23.127'**	**71° 19.996'**
BRDS-97-A	**41° 23.185'**	**71° 20.043'**
BRDS-97-B	**41° 23.189'**	**71° 20.044'**
BRDS-97-C	**41° 23.191'**	**71° 20.043'**

Note: Coordinate system NAD 83

Table 2-3.

Sediment Core Collection Summary

Core ID	Location Type	Latitude	Longitude	Core Length (m)	Core Penetration (m)	Core Recovery (m)
BR03a	Mound Area	41° 23.544'	-71° 18.374'	2.87	3.0	2.9
BR08a	Mound Area	41° 23.243'	-71° 18.383'	2.23	2.7	2.4
BR28b	Mound Area	41° 23.788'	-71° 18.925'	0.59	2.4	0.67
BR32a	Mound Area	41° 23.530'	-71° 18.699'	2.75	3.0	2.8
BR42b	Mound Area	41° 23.607'	-71° 17.957'	0.93	3.0	0.76
BR44a	Mound Area	41° 23.748'	-71° 18.215'	0.59	1.5	0.64
BR78a	Mound Area	41° 23.379'	-71° 18.058'	2.23	2.7	2.4
BR70c	Reference	41° 22.254'	-71° 18.343'	1.36	2.9	1.6
BR94b	Reference	41° 23.038'	-71° 20.099'	2.62	3.0	2.7

Note: Coordinate System NAD83

Table 2-4.

Samples Submitted for Chemical and Physical Analyses

Core	Location	Sample	Lab Sample ID	Depth Interval* (cm)
BR03a	Mound area	BR03-1	H1718-13A	6–19
		BR03-2	H1718-14A	41–56
		BR03-3	H1718-15A	88–103
		BR03-4	H1718-16A	159–170
		BR03-5	H1718-17A	187–202
		BR03-6	H1718-18A	231–246
		BR03-7	H1718-19A	246–261
BR08a	Mound area	BR08-1	H1717-07	7–20
		BR08-2	H1717-08	40–55
		BR08-3	H1717-09	114–129
		BR08-4	H1717-10	165–180
		BR08-5	H1717-11	185–200
BR28b	Mound area	BR28-1	H1717-14	7–20
		BR28-2	H1717-15	28–38
		BR28-3	H1717-16	38–46
		BR28-4	H1717-17	54–59
BR32a	Mound area	BR32-1	H1718-03A	15–28
		BR32-2	H1718-04A	50–65
		BR32-3	H1718-05A	139–154
		BR32-4	H1718-06A	181–192
		BR32-5	H1718-07A	231–246
BR42b	Mound area	BR42-1	H1717-18	7–20
		BR42-2	H1717-19	33–48
		BR42-3	H1717-20	61–71
BR44a	Mound area	BR44-1	H1717-12	7–20
		BR44-2	H1717-13	44–59
BR70c	Reference area	BR70-1	H1718-01A	7–20
		BR70-2	H1718-02A	40–55

* Depth intervals measured from top of core downward

Table 2-4., continued

Samples Submitted for Chemical and Physical Analyses

Core	Location	Sample	Lab Sample ID	Depth Interval* (cm)
BR78a	Mound area	BR78-1	H1717-01	6–20
		BR78-2	H1718-20A	42–57
		BR78-3	H1717-02	90–110
		BR78-4	H1717-03	110–125
		BR78-5	H1717-04	140–155
		BR78-6	H1717-05	180–195
		BR78-7	H1717-06	218–224
BR94b	Reference area	BR94-1	H1718-08A	7–20
		BR94-2	H1718-09A	40–55
		BR94-3	H1718-10A	114–129
		BR94-4	H1718-11A	174–189
		BR94-5	H1718-12A	247–262

* Depth intervals measured from top of core downward

Table 2-5.

Sediment Chemistry Laboratory Methods and Limits of Detection

Analyte Group	Parameter	Analytical Method[1]	Reporting Limit Range	Method Detection Limit Range
Conventionals				
	Total organic carbon (mg/kg)	Lloyd Kahn	23–91	23–81
	Grain size (%)	ASTM D-422	NA	NA
Metals (mg/kg)				
	Aluminum	SW-846 6010	1.2–24	1.2–2.8
	Arsenic	SW-846 6010	0.16–2.4	0.16–0.38
	Beryllium	SW-846 6010	0.0020–0.59	0.0020–0.0047
	Cadmium	SW-846 6010	0.013–0.59	0.013–0.031
	Chromium	SW-846 6010	0.055–2.4	0.053–0.13
	Copper	SW-846 6010	0.43–3.5	0.41–0.99
	Iron	SW-846 6010	10.0–310	2.2–69
	Lead	SW-846 6010	0.14–1.2	0.14–0.33
	Nickel	SW-846 6010	0.067–5.9	0.064–0.16
	Selenium	SW-846 6010	0.80–3.5	0.76–1.8
	Silver	SW-846 6010	0.081–3.5	0.077–0.19
	Vanadium	SW-846 6010	0.039–5.9	0.037–0.90
	Zinc	SW-846 6010	0.28–5.9	0.26–0.64

[1]See text for description.

Table 2-5, continued

Sediment Chemistry Laboratory Methods and Limits of Detection

Analyte Group	Parameter	Analytical Method[1]	Reporting Limit Range	Method Detection Limit Range
PAHs (µg/kg)				
	2-Methylnaphthalene	SW-846 8270D	3.9–7.8	0.30–0.59
	Acenaphthene	SW-846 8270D	3.9–7.8	0.34–0.69
	Acenaphthylene	SW-846 8270D	3.9–7.8	0.28–0.57
	Anthracene	SW-846 8270D	3.9–7.8	3.0–5.9
	Benzo[a]anthracene	SW-846 8270D	3.9–7.8	1.4–2.8
	Benzo[a]pyrene	SW-846 8270D	3.9–7.8	0.91–1.8
	Benzo[b]fluoranthene	SW-846 8270D	3.9–7.8	2.1–4.3
	Benzo[g,h,i]perylene	SW-846 8270D	3.9–7.8	1.0–2.0
	Benzo[k]fluoranthene	SW-846 8270D	3.9–7.8	1.3–2.6
	Chrysene	SW-846 8270D	3.9–7.8	1.1–2.2
	Dibenzo[a,h]anthracene	SW-846 8270D	3.9–7.8	0.82–1.6
	Fluoranthene	SW-846 8270D	3.9–7.8	2.4–4.7
	Fluorene	SW-846 8270D	3.9–7.8	0.68–1.3
	Indeno[1,2,3-cd]pyrene	SW-846 8270D	3.9–7.8	0.85–1.7
	Naphthalene	SW-846 8270D	3.9–7.8	0.83–1.7
	Phenanthrene	SW-846 8270D	3.9–7.8	3.1–6.1
	Pyrene	SW-846 8270D	3.9–7.8	2.0–4.0

[1]See text for description.

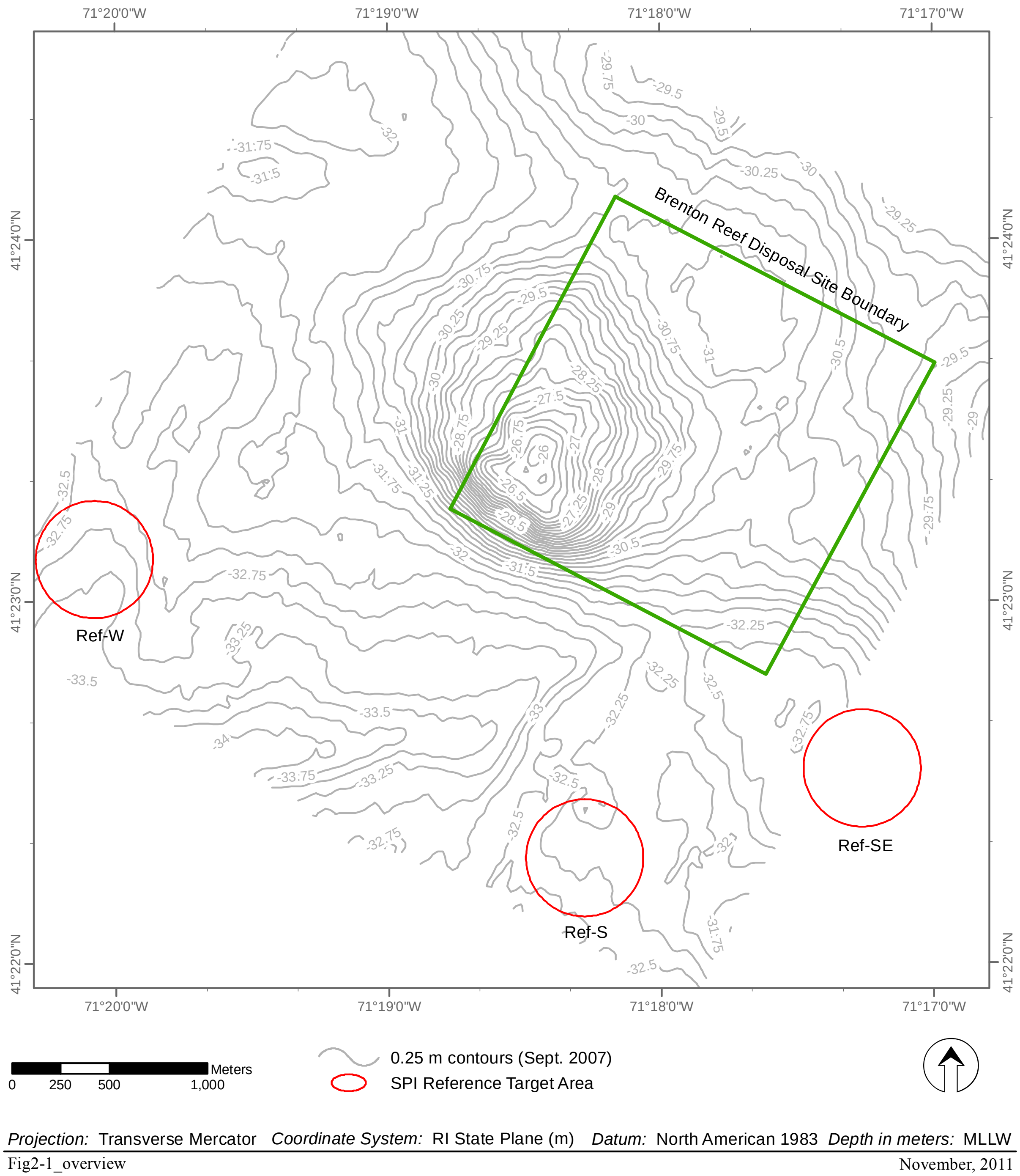

Figure 2-1. Brenton Reef Disposal Site and reference areas

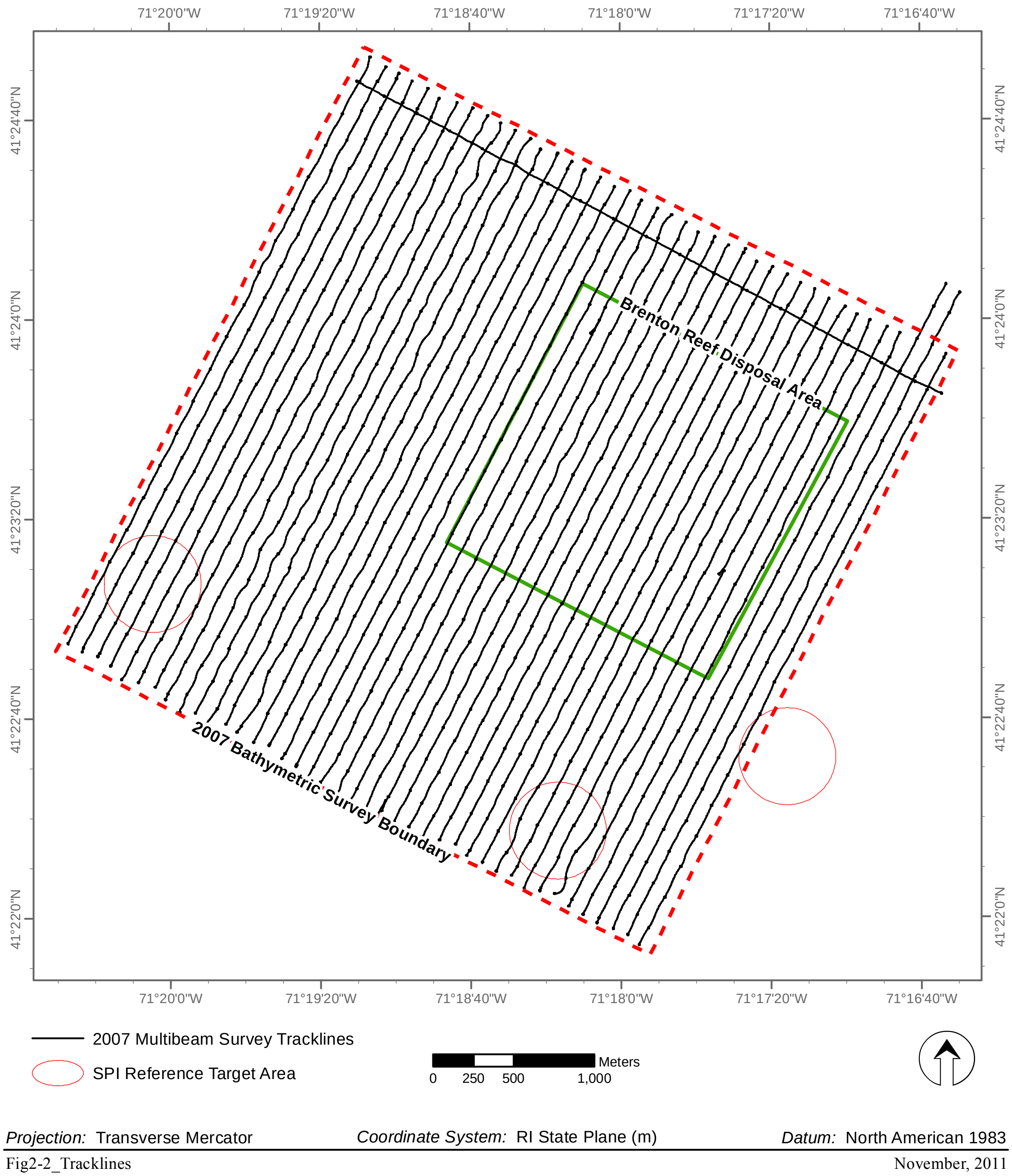

Figure 2-2. Bathymetric survey boundary and survey lines indicated

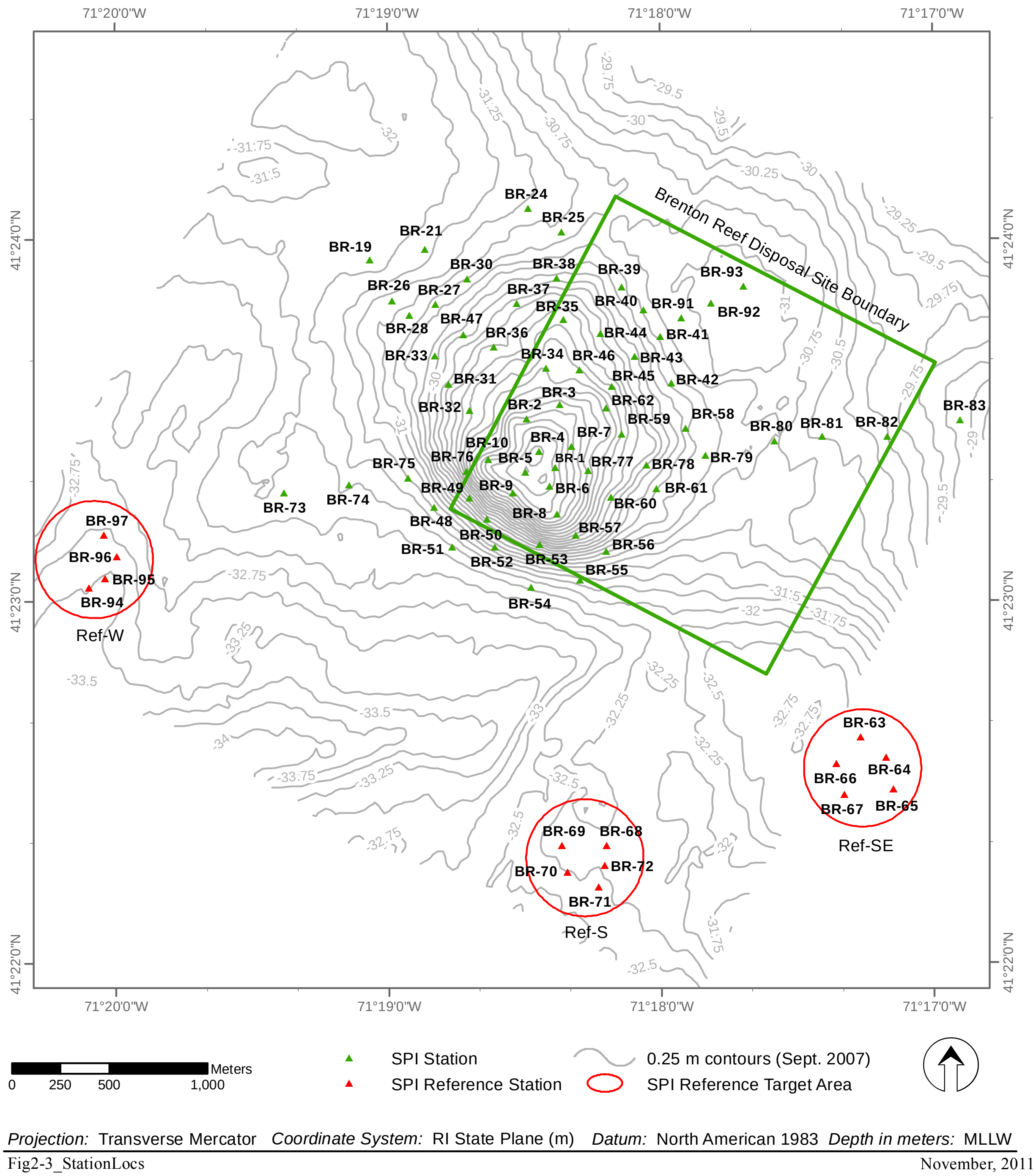

Figure 2-3. Sediment-profile and plan-view image station locations

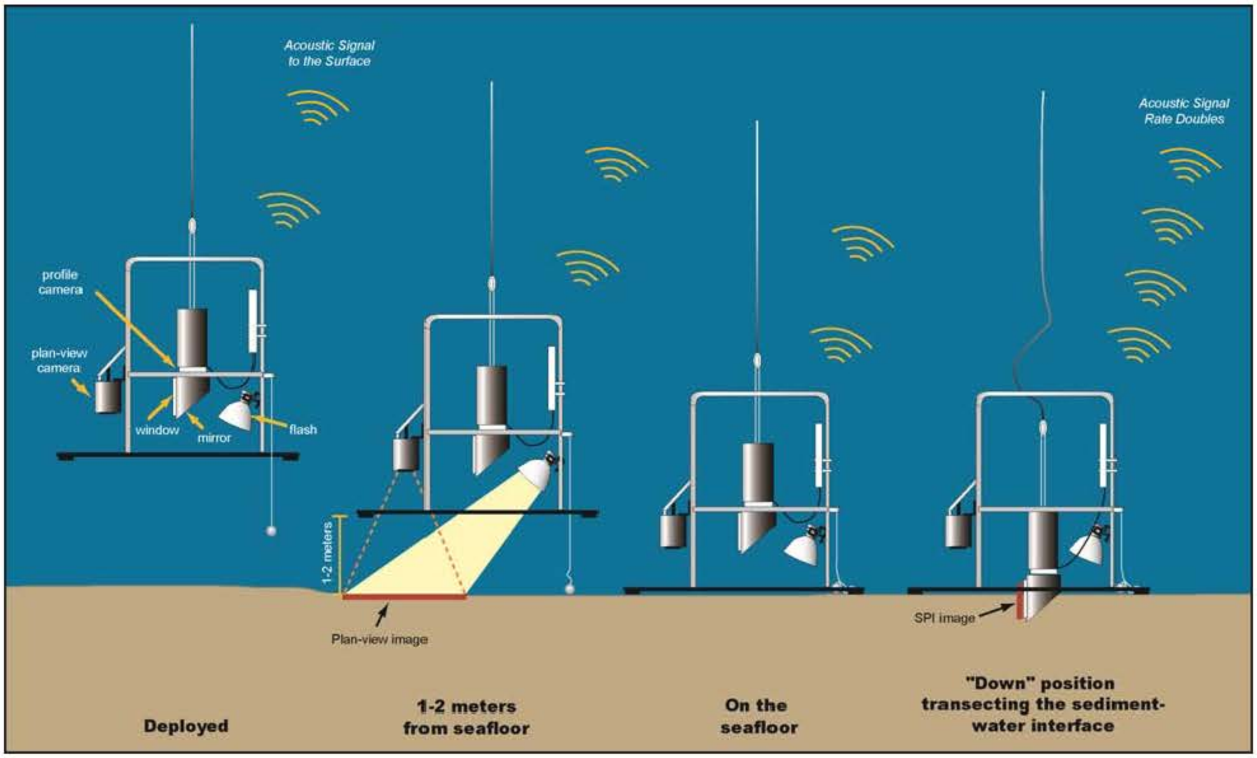

Figure 2-4. Operation of the combined Ocean Imaging Model 3731 Sediment-Profile and Model DSC-6000 Plan-View cameras

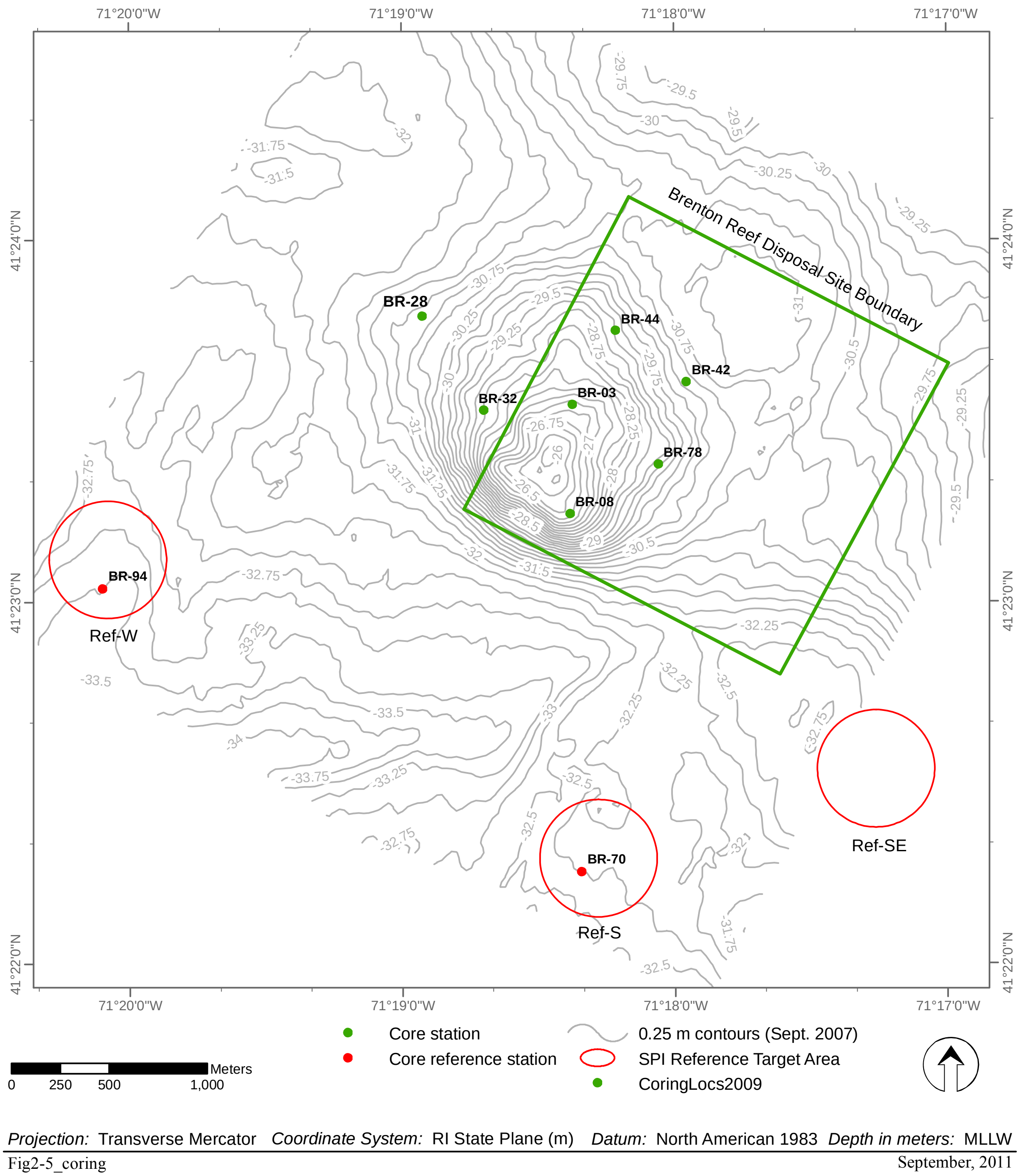

Figure 2-5. Sediment coring station locations

3.0 RESULTS

3.1 Bathymetry

The area surveyed around the historical Brenton Reef Disposal Site has depths that range from 26 to 34 m, MLLW, but it is generally a nearly flat platform with a very gentle seaward slope to the south. There is some topographic variation, a shallow edge of a ridge to the northeast, and a ramp with a narrow neck between two depressions to the south (Figure 3-1).

The mound has a relatively steep face on the seaward side oriented in a northwest to southeast direction (15% slope), a flat square top, and a shallow slope (4% slope) extending shoreward (Figure 3-1). Along the margin of the mound, there are shallow ramps to the northwest and east.

On the seaward side, the mound lies right on the edge of an increase in slope of the platform into the depression to the southwest. As a result, the relatively steep southwest slope of the mound represents the first shallow point for waves coming from the southerly direction. The placement of the mound in the general topography of the site is best displayed in a hillshaded image where depths are displayed by color gradation and the topography is rendered in a "sun-illuminated" three-dimensional image (Figure 3-2).

A more detailed view of the mound reveals that it is composed of four distinct levels: a triangular apex (depth of 25.5–26.5 m, MLLW), a square top (26.5–28.0 m), an ovoid central mound (28.0–29.5 m) and an irregular margin (29.5–30.5 m). The triangular apex and square top are oriented north-northeast, while the ovoid mound is oriented more north to south. There are very distinct contours at the transition from the top to the central mound and mound to margin, but the apex and margin edges are less distinct (Figure 3-3). The edge of the mound and margin are displaced from the ovoid shape about 125 m and 225 m (respectively) to the east in line with the tip of the triangular apex. There is a slight displacement in both the mound and margin in the northwest quadrant just north of the margin of the square.

As noted in Section 2, the 2007 bathymetric survey was conducted during rough sea conditions. Low-magnitude artifacts associated with vessel motion are apparent throughout the bathymetric data set, largely because of the low relief present in the survey area. The magnitude of these artifacts generally ranges from approximately 2 cm to 10 cm. In order to ensure that bathymetric data quality complied with applicable hydrographic performance standards, data quality metrics were compared to Standards promulgated by the International Hydrographic Organization (IHO) and adopted by NOAA's National Ocean Service (NOS, NOAA 2011). Bathymetric data quality was also assessed using performance standards recommended by USACE for civil works projects conducted in waters shallower than 24 m. Note that the entirety of this survey area was deeper than this USACE depth constraint. Using classification criteria specified by the IHO, this bathymetric survey would be classified as Order 1b, shallower than 100 m (IHO, S-44, February 2008). Using USACE Guidance, the survey would be classified under the category "Other General Surveys & Studies," because the project objectives do not involve dredging or identification of navigational hazards.

Data quality (accuracy) criteria established by both agencies are depth and substrate dependent, with higher accuracy standards set for shallow waters and rocky or "hard" seafloors. IHO Order 1b survey accuracy specifications for the depths of approximately 26 m to 36 m observed at the site would be 0.60 and 0.68 m (95% confidence interval or C.I.), respectively. USACE Performance Standards for soft-bottom dredging projects in depths greater than 12 m specify 95% C.I. accuracy of +/- 0.61 m (USACE 2002).

In order to assess data quality across the MBES swath, within-cell depth variations were mapped and statistically evaluated. The average uncertainty within bathymetric grid cells was 0.21 m (95% C.I.), substantially lower than either IHO/NOAA or USACE accuracy performance standards. Less than 0.3 percent of individual map cells were not compliant with performance standards. Thus, taken in its entirety, the bathymetric data collected for this survey were compliant with these specifications.

3.2 Acoustic Backscatter

The acoustic backscatter data (i.e., side-scan sonar results from a multibeam sensor) revealed a high level of detail throughout the survey area (Figure 3-4). Backscatter intensity (generally displayed as a grey scale, in this case as a reversed image with black as hard returns and white as shadow) is related to a wide range of seafloor properties but can generally provide a map of relative hardness of the seafloor. Patterns in sediment distribution, corresponding to differences in sound reflectance, can be readily distinguished from the image, but the specific grain size and composition of the sediments cannot easily be correlated from the backscatter signal alone.

The mound surface is characterized by a broad area of moderately high backscatter across the entire surface of the mound. Near the apex of the mound, there is smooth area (about 250 m^2) and within it there are waveforms parallel to the front edge of the mound with slight variation in backscatter (Figure 3-5). North of the apex, the moderate backscatter pattern is interspersed with elongated forms of very low backscatter and smaller areas of high backscatter. The patches of varying backscatter form a complex pattern with braided, arcuate, dendritic, and flame-shaped elements indicative of surficial sediment transport (Figure 3-5). Most of the elements are oriented north to south (perpendicular to the front of the mound) and are grouped into larger elements oriented in the same direction. The largest of the groupings are about 300 m long and 50–100 m wide, while the smallest elements are up to 300 m long and 5 m wide. Within the complex of these linear elements there are several irregularly shaped patches of moderate backscatter that look similar to the mound apex. The largest of these areas is about 50 m^2.

At the margins of the mound the patterns diverge from the north to south orientation and radiate slightly to the west and east, again separated by large patches of moderate backscatter. At the very edges of the bathymetric expression of the mound, the patterns thin out into individual elements of moderate to high backscatter extending into a background of moderately low backscatter. The mound margin can most easily be distinguished by the boundary between the moderately high backscatter and the moderately low backscatter (Figure 3-5). Some of the subcircular patches around the margins of the mound have evidence of reworking (Figure 3-5). The features are most evident to the northwest and east of the mound margin but can also be seen in isolated clusters and strings to the southwest and north (Figure 3-4).

Specific sediment features are diagnostic of dredged material disposal (ENSR 2007) while others are representative of sediment transport conditions. The surface of the mound is dominated by sediment transport features, but the margins and areas to the west and east have relatively unmodified impact craters from individual barge disposal events (Figures 3-4 and 3-6).

Surrounding the margin of the mound in two distinct groups are rounded features that are consistent with impact scars from dredged material disposal (ENSR 2007). The features are visible in backscatter images as subcircular patches of high intensity backscatter return interspersed with low intensity backscatter return (Figure 3-6). To the east of the mound just past one group of craters is the edge of a small rise (29.5 m, Figure 3-1) with elongated sand ribbons indicating sediment transport (Figure 3-6).

3.3 SPI

3.3.1 Reference Areas

Physical Sediment Characteristics

Sediment at all stations in the three reference areas (including replicate samples) consisted of silt or very fine sand with no physical sorting of surface material (Appendix C). The station-averaged grain size major mode of all stations was >4 phi (silt). There was no evidence of low dissolved oxygen or sedimentary methane at any of the reference area stations (Appendix C). Three stations in Ref-W (94, 95, and 96) showed some evidence of layering in the sediment column with bands of very pale brown to gray to olive silt 3–5 cm thick (Figure 3-7). This layering may be from older dredged material, but there was no apparent composition change between the layers other than color.

Average prism penetration among all stations at the three reference areas ranged from 10.1 to 15.4 cm. The number of weights and camera penetration settings were kept constant during sampling at the reference areas, so the variation in prism penetration among the stations was an indication of the relative bearing strength of the sediment. Station-averaged small-scale boundary roughness ranged from 0.7 to 3.6 cm and was dominated by biological features (pits, mounds, tubes; Figure 3-8).

Biological Conditions

In the SPI survey of September 2007, all of the images from the reference area showed the presence of Stage 3 infauna, indicating an advanced successional status (Appendix B). Average aRPD depths at the reference area stations ranged from 0.9 to 3.3 cm, with an overall average of 2.0 cm (Table 3-1). Such aRPD depths suggest a moderate to high degree of biologically-mediated sediment reworking in muddy coastal sediments (Figure 3-9).

3.3.2 Historical Mound Study Area

Physical Sediment Characteristics

The sediment distribution within the study area was quite complex (Figure 3-10). Outside of the margin of the mound (>30.5 m depth) the station-averaged grain size major mode was >4 phi (silt) and quite uniform in character, except for several stations to the east of the mound in the area with distinctive disposal features (see above; Appendix C). Inside the margin of the mound (<30.5 m depth) sediment size and texture varied widely from station to station and within stations (Appendix C). Three broad types of sediment were identified from SPI images (Figure 3-11):

- Uniform silt similar to the seafloor outside the mound margin with some physical sorting of the surface layer;
- Thin layers of coarse material overlying silt; and
- Relatively thick layers of coarse sand, shell, and gravel.

The areas of silt identified at the surface were confined to the margins of the mound, and many had some enrichment of fine sand in the upper layers (e.g., Station

61). The thin layers of coarse material over silt occurred in a band around the southern edge of the mound and extended to the northwest and north-northeast (Figure 3-10). The coarse horizons were distributed over the top of the mound and onto the northern margin. However, the types of sediment observed in SPI images could vary considerably from replicate to replicate, indicating small-scale variability of sediment texture across the surface of the mound. Within these broad types, there were many specific variations that were described in conjunction with the plan-view images and backscatter patterns (see Section 4).

Although there was some evidence of dredged material in SPI images, in most cases the sediment was sufficiently reworked physically and biologically that the dredged material was not easily distinguished from natural sediment. As discussed below, the presence of the coarse fractions mixed with silt is distinct from the conditions at the reference areas and is the most diagnostic characteristic for the presence of dredged material.

Average prism penetration ranged widely from 2.7 to 16.9 cm (Figure 3-12). Although the weights and stop settings were varied slightly (from 3 to 5 weights per carriage and 14 to 15 on the stop setting, Appendix C), these camera-setting changes are not sufficiently large to account for this variation in prism penetration. Prism penetration was similar to sediment distribution with deeper penetration outside the mound margin (apart from one broad area east of the mound) and highly variable results within the margin (Figure 3-12). The shallowest penetration occurred at those stations with coarse and well-sorted sediments at the surface (compare Figures 3-10 and 3-12).

Station-averaged boundary roughness varied from 0.7 to 3.1 cm (average 1.6 cm). The highest boundary roughness occurred over the apex of the mound (Figure 3-13) with features that were largely physical (ripples, windrows; Appendix C). The lowest boundary roughness values occurred off and within the mound margin with a mix of physical and biological features (burrows, pits, mounds).

Biological Conditions

Most stations had at least one replicate with evidence of Stage 3 infauna (Figure 3-14). The eight stations with no evidence of Stage 3 infauna were either well-sorted sands or compact coarse sediments with shallow prism penetration (Appendix C). Evidence of Stage 3 activities are best observed in finer grained or poorly sorted sediments where feeding and burrowing activities are well-preserved.

Average aRPD depths at the mound stations ranged from 0.6 to 3.8 cm, with an overall average of 1.7 cm (Table 3-1). The aRPD could not be measured (indeterminate) at 26% of the mound stations, particularly those near the apex, due to the presence of homogenous sand lacking an aRPD contrast and/or poor camera penetration in sand or gravel (Table 3-1 and Figure 3-15).

3.4 Plan-View Images

3.4.1 Reference Areas

The plan-view images from the reference areas showed that the sediment surface was highly uniform with evidence of Stage 3 infauna and epifauna (Figure 3-16, Appendix C).

3.4.2 Historical Mound Study Area

Plan-view images from the mound revealed highly variable sediment surfaces, and patterns of surface texture and composition that were easier to discern than in the SPI images. Distinctive features included apparent lag deposits of gravel, cobbles, boulders, bricks, and large oyster shells; linear windrows of gravel, oyster and clam shells, and muddy sand waves; and alternating bands of silt and poorly sorted sand (Figure 3-17). Variations in surface texture and composition occurred over relatively short scales, even within replicates of a single station (Figure 3-18).

A transect across the surface of the historical mound provided some indication of the distribution of sediment textures visible in plan-view images (Figure 3-19). Outside the western margin of the mound (Station 75, 31.5 m depth) the seafloor resembled that of the reference areas (burrowed silt, epifaunal tracks). At the steepest contour interval on the side of the mound (Station 76, 28 m depth), the seafloor was covered with large encrusted cobbles (epifauna and oxidized iron crusts), gravel (pebbles), and well-sorted sand. Across the top of the mound, the surface varied from coarse sand to gravel with cobbles, large cobbles, and shells (Stations 10, 5, 4, 1, 7, 77; 26 to 27.5 m depth). There was no clear gradation in texture across the surface. On the eastern margin (Station 78, 29.25 m depth), the seafloor was again covered in large cobbles and gravel. Inside the edge of the eastern margin (Station 79, 30.5 m depth) the seafloor resembled the reference areas.

To fully describe the complex variations in sediment texture and transport features on this historical mound, it was necessary to examine both the plan-view surface images and the vertical cross-sections provided by the SPI images. Hence, the results of plan-view images were combined with the SPI image physical descriptions to develop a synthesis of the three-dimensional sediment texture and transport characteristics of the mound surface (see Section 4).

3.5 Sediment Cores

3.5.1 Core Data Summaries

Sediment cores were collected at nine locations (Table 2-3 and Figure 2-5), and samples were collected for laboratory analysis at a variety of depths from the individual cores (Table 3-2). In most cores a near-surface horizon (7-20 cm) and a subsurface horizon (ca. 40-55 cm) were sampled with some adjustments for the visual lithology of the core. In each case the near-surface horizon was analyzed for physical properties (grain size and TOC) metals and PAHs (except for BR70) and the subsurface horizon only for metals and physical properties unless there was an obvious black silt or petroleum odor at that horizon (BR28, 42, 44). Photographs and descriptions of each core were used for interpretation of sediment horizons encountered in the cores (Figures 3-20a-i). The top one meter of each core is described below with a summary of physical and chemical analytical results; the near-surface conditions of the mound and margin has the greatest relevance for management decisions. Additional horizons were sampled based on visual lithology to characterize distinct horizons below 55 cm. Full-length core photographs and descriptions were compiled (Appendix D) and considered along with extensive assessment of the distribution of contaminants and core properties in the overall assessment of the condition of the mound and ambient sediments (Appendices E and F).

3.5.2 Physical-Chemical Characteristics and Observations

The two cores collected from reference areas BR70 and BR94 contained relatively consistent olive gray to light gray-brown silty sand with several distinct layers of shells and sands. BR70 contained fine silty sand near the surface with a transition to medium sand at about 60 cm with a burrow halo and increasing amounts of broken shells including a large ocean quahog (*Arctica islandica*) shell near 1 m depth (Figure 3-20a). BR94 contained a relatively homogeneous profile of greenish gray to light gray fine silty sand with some lenses of fine sand, large broken shells, and oxidized burrows at depth (Figure 3-20b). The top meter of the two reference cores had low TOC values (0.1- 0.4 %) and very low levels of metals (Figures 3-20 a, b and Table 3-2). Only one horizon (BR94-1) in the top meter of the reference cores had PAHs measured with a TPAH level of 102 μg/kg.

The seven cores collected from the historical mound area had more heterogeneous sediment composition than the reference cores with complex layers of fine silty sand, olive gray silt, well-sorted medium sand, poorly-sorted coarse sand, gravel, black silt, silty clay, peat and estuarine shells (Figures 3-20a-i). Surficial sediments were primarily sands with only two cores (BR32 and BR03) containing light gray silt at the surface.

Mound area cores typically contained several distinct interbedded layers of gray to brown sandy silts, black silts, well-sorted sands, and silty sands with shell hash and large oyster (*Crassostrea* sp.) and quahog (*Mercenaria* sp.) shells. In some cases, layers of black or gray silt near the top of the core were found to contain relatively high PAH and metals concentrations (e.g., BR28-2, BR42-3, BR44-2, BR78-3,4). Measured mound core horizons near the top of the core also had relatively low TOC content (0.018 - 1.6%, Table 3-2).

Core BR28, situated in the western margin of the mound, had a distinctive black silt layer below silty sand and brown sandy silt layers; this black silt layer (28-38 cm) corresponded with relatively high copper and total PAH (TPAH) concentrations and had a sharp interface with underlying dark well-sorted medium fine sand with moderate TPAH concentrations (Figure 3-20c).

Core BR44, situated in the northern margin of the mound, contained distinct layers of fine sand, dark silt, and coarse sand. Towards the bottom of the core (43-59 cm), an olive gray silt layer was observed that corresponded with elevated TPAH concentrations (Figure 3-20d).

Core BR42, situated in the northeastern margin of the mound, featured numerous layers of well-sorted sands, gray silts, shells, poorly sorted sand and dark sandy silt. Elevated TPAH concentrations were observed in several layers. In one dark sandy silt layer (61-71 cm), elevated copper and TPAH concentrations were observed (Figure 3-20e).

The upper portion of Core BR32, situated west of the mound apex, was relatively uniform and consisted primarily of light gray sandy silt with shells and discrete coarse sand layers. A silt horizon at 50-65 cm had elevated TPAH but no visible distinction from other horizons (Figure 3-20f).

Core BR03, situated north of the mound apex, contained numerous layers of silts, clayey silt and fine to coarse sands with shells (Figure 3-20g). The top horizon had interbedded sands and silts with a moderate TPAH level. The lower horizons of this core had increased amounts of clay with some elevation in copper and TPAH particularly at the lowest measured horizon (246-261 cm, Table 3-2).

Core BR78, situated northeast of the mound apex, contained numerous layers of silts and sands. One horizon with clayey silt (42-57 cm) had the highest TOC measured (1.6%) but no elevation in arsenic or copper (PAH not measured). A lower horizon (90-100 cm) contained a layer of black silt with distinct interbeds of fine sand that corresponded to elevated TPAH and copper concentrations (Figure 3-20h).

BR08, situated on the mound apex, had a thin layer (7 cm) of silty medium sand with shell hash on top of relatively uniform gray silt in the top 55 cm. The silt graded from sandy clayey silt to sandy silty clay with gravel and elevated TPAH at the bottom (Table 3-2). Below the thick silt layer a peat clast lay on top of several varied layers of silts, sands, and coarse gravels, shell pieces and clay clasts (Figure 3-20i).

3.5.3 Sediment Chemistry Summary

A statistical summary of chemical and physical core sample results is provided in Table 3-3. Grain size of the measured samples varied widely, as was expected based on visual observations of the cores. The total fine-grained size fraction (silt and clay, or fines) ranged from 6.4% to 95.9%. Reference samples generally had less fine-grained content (median value 41.2%) than mound area samples (median value 61.8%), although large ranges of grain sizes were observed in both areas. The two coarsest samples were from BR28, located in the western mound margin, with >93% sand and gravel in the 38–46 and 54–59 cm intervals (Table 3-2 and Figure 3-20c). The two finest samples were from BR03, located north of the mound apex, with >93% fines in the 187–202 and 246–261 cm intervals (Table 3-2 and Appendix D). Total fines in the reference core BR94 increased gradually down-core from 40% to 55% fines, and then to 92% in the lowermost 247–262 cm interval (Table 3-2 and Appendix D). Total organic carbon (TOC) ranged from below detection (0.018%) to 1.6% (Table 3-3). The reference samples had an average TOC of approximately 0.4%.

Many of the metals covaried within the metals group and also with grain size, based on Principal Component Analysis (PCA) results (see below and Appendix E). Metals results discussed below are reported as dry weight. Only selenium and silver had detection frequencies less than 50%; the remaining metals were detected in 88% to 100% of the samples (Table 3-3). Metals concentrations in the mound area stations were often similar to or slightly greater than those in reference area samples (Al, As, Be, Fe, Se, V; Table 3-2). Arsenic, however, was highest in the lowermost sample of the reference core BR94 (Table 3-2 and Appendix D). Down-core profiles showed that the second sample from BR28 (28–38 cm) had the highest concentrations detected for several metals.

Polycyclic aromatic hydrocarbons (PAHs) were found to covary strongly within the PAH group and also with grain size, based on PCA results (see below and Appendix E). PAH results discussed below are reported in dry weight. Concentrations of low molecular weight PAHs (LPAHs) were always less than concentrations of the high molecular weight PAHs (HPAHs), with an LPAH:HPAH concentration ratio ranging from 0.13 to 0.74 (Table 3-2). The median concentration of LPAHs among the mound area samples was 37 µg/kg, with a maximum of 1,100 µg/kg at core BR28 (the second sample, or 28–38 cm). The same mound area samples had a median HPAH concentration of 190 µg/kg and a maximum concentration of 5,900 µg/kg (also in the 28–38 cm sample from BR28). The range of measured PAHs from mound area samples was higher than the range measured in the reference cores (Table 3-3).

Boxplots (a.k.a. box-and-whisker plots) were used to illustrate the location, spread, and skewness of the data. Each boxplot has a shaded rectangle that shows the spread of values between the first and third quartiles (i.e., the 25th and 75th percentiles). The height of this box is the interquartile range (IQR) which is the value of the 3rd quartile minus the value of the 1st quartile. The line inside the box indicates the median; the outer brackets (the "whiskers") represent the minimum and maximum values or 1.5 times the IQR from the median, whichever is less. Values outside the whiskers are possible extreme values and are shown as single lines. The value of 1.5 times the IQR is a somewhat arbitrary but reasonable boundary for what is expected from a normal (Gaussian) distribution. Concentrations of metals and PAHs tended to be slightly higher and more variable for the BRDS mound area locations than at reference areas, with consistently higher concentrations in the samples from the lower sections of the cores with the exception of silver (Appendix F, Figures 3-21 and 3-22).

3.5.4 Principal Components Analysis

A Principal Components Analysis (PCA) was applied to illustrate relationships among individual samples (all groups, all depths) on patterns of contamination. It provided useful insights by summarizing the multivariate data sets. The PCA on PAHs found that the total PAH covaried very closely with individual PAHs. Based on the PCA findings for the individual PAHs, PAH results can be accurately represented in a summary format, such as total PAH (TPAH), low (LPAH) and high (HPAH).

In the metals PCA, the first principal component (Comp. 1) represents an average of all the individual metals, and explains 68% of the total variation. This kind of "average" and moderate variance PC indicates that the original data set is fairly strongly correlated, but that some samples have a different metals contamination pattern. This could be indicative of different source materials. Some samples appear to have metals concentrations that are more like "native" sediment (i.e., dominated by aluminum, beryllium, vanadium, and iron), while other samples have contaminant patterns more similar to Narragansett Bay sediments (i.e., dominated by cadmium, chromium, copper, lead, and zinc) even if their concentrations are low. A more detailed discussion of PCA results is covered in Appendix E.

Table 3-1.

Station Averaged aRPD Results

MOUND STATIONS				REFERENCE STATIONS		
Station	Mean aRPD Depth (cm)	Station	Mean aRPD Depth (cm)	Reference Area	Station	Mean aRPD Depth (cm)
BR_01	IND	BR_43	IND	Ref-E	BR_63	2.1
BR_02	IND	BR_44	0.9		BR_64	3.0
BR_03	2.3	BR_45	1.4		BR_65	3.3
BR_04	IND	BR_46	1.0		BR_66	2.5
BR_05	IND	BR_47	1.3		BR_67	2.7
BR_06	IND	BR_48	0.9	Ref-SE	BR_68	2.1
BR_07	IND	BR_49	2.1		BR_69	2.5
BR_08	1.9	BR_50	1.8		BR_70	2.7
BR_09	1.6	BR_51	1.3		BR_71	1.6
BR_10	2.1	BR_52	0.7		BR_72	1.3
BR_19	1.2	BR_53	1.2	Ref-SW	BR_94	0.9
BR_21	1.1	BR_54	1.5		BR_95	1.1
BR_24	0.8	BR_55	2.6		BR_96	1.8
BR_25	2.2	BR_56	3.8		BR_97	0.9
BR_26	1.2	BR_57	2.9			
BR_27	1.4	BR_60	IND		Average	2.0
BR_28	1.0	BR_61	1.5		Std. Dev.	0.8
BR_30	1.8	BR_62	IND		Min.	0.9
BR_31	1.0	BR_73	1.9		Max	3.3
BR_32	1.5	BR_74	1.9			
BR_33	1.2	BR_75	1.1			
BR_34	IND	BR_76	IND			
BR_35	IND	BR_77	IND			
BR_36	IND	BR_78	IND			
BR_37	IND	BR_79	3.0			
BR_38	0.6	BR_80	3.4			
BR_39	1.6	BR_81	1.2			
BR_40	2.6	BR_82	1.9			
BR_41	2.6	BR_83	2.6			
BR_42	2.2	BR_91	2.6			
		BR_92	1.4			
	Average	1.7				
	Std. Dev.	0.7				
	Min	0.6				
	Max	3.8				

IND=Indeterminate

Table 3-2.

Chemical and Physical Core Data Summary

Analysis	Site Type Station Sample ID Start Depth (cm) End Depth (cm)	Mound BR-03 BR03-1 6 19	Mound BR-03 BR03-2 41 56	Mound BR-03 BR03-3 88 103	Mound BR-03 BR03-4 159 170	Mound BR-03 BR03-5 187 202	Mound BR-03 BR03-6 231 246	Mound BR-03 BR03-7 246 261	Mound BR-08 BR08-1 7 20	Mound BR-08 BR08-2 40 55
Conventionals	**Units**									
Gravel	percent	5.2	2.5	0.0	7.8	0.0	0.0	0.0	2.3	16.3
Sand	percent	68.5	74.1	16.6	27.8	7.00	22.4	4.10	32.1	19.0
Silt	percent	19.3	17.4	65.4	49.4	65.0	62.6	74.9	41.6	39.7
Clay	percent	7.0	6.0	18	15	28	15	21	24	25
Fines (silt+clay)	percent	26.3	23.4	83.4	64.4	93.0	77.6	95.9	65.6	64.7
Total Organic Carbon	percent	0.38	0.40	0.65	1.0	1.2	1.5 E	0.006 U	0.34	0.65
Metals	**Units**									
Aluminum	mg/kg	4,760	4,560	10,100	8,900	12,200	8,700	10,600	10,600	13,300
Arsenic	mg/kg	4.4	3.9	8.0	7.5	9.3	9.2	10.4	6.8	8.4
Beryllium	mg/kg	0.37	0.32	0.85	0.77	1.1	0.72	0.76	0.66	0.86
Cadmium	mg/kg	0.051 B	0.04 B	0.18 B	0.26 B	0.22 B	0.65	0.81	0.06 B	0.065 B
Chromium	mg/kg	12.4	12.5	26.9	40.7	31.6	51.0	63.9	23.3	30.4
Copper	mg/kg	10.8	9.0	17.4	38.2	20.1	88.2	128	7.3	9.3
Iron	mg/kg	11,000 E	9,880 E	21,900 E	20,200 E	33,900 E	20,600 E	29,200 E	20,100	30,200
Lead	mg/kg	8.7 E	6.6 E	11.9 E	20.2 E	12.0 E	34.7 E	44.4 E	7.1	9.0
Nickel	mg/kg	6.8 E	6.6 E	13.5 E	13.2 E	17.0 E	14.7 E	18.1 E	14.8	18.6
Selenium	mg/kg	1.2 B	0.92 U	1.3 B	1.1 B	2.3 B	1.6 B	2.2 B	1.1 U	0.1 U
Silver	mg/kg	0.096 U	0.093 U	0.12 U	0.44 B	0.13 U	1.1 B	1.5 B	0.1 U	1.2 U
Vanadium	mg/kg	13.5	11.8	25.7	22.6	30.6	25.8	30.2	26.0	33.5
Zinc	mg/kg	26.5 E	24.6 E	53.4 E	66.3 E	63.1 E	91.2 E	112 E	47.8	60.1
PAHs	**Units**									
Total HPAH	µg/kg	150		106				720	56	
Total LPAH	µg/kg	10		33				102	31	
Total PAH	µg/kg	190		140				820	87	
LPAH:HPAH	ratio	0.27		0.32				0.14	0.55	

U indicates that the parameter is not detected. E indicates that the value is estimated due to the presence of interferences, as determined by serial dilution analysis.
B indicates the presence of a 'trace' concentration below the reporting limit and equal to or above the detection limit.

Table 3-2., continued.

Chemical and Physical Core Data Summary

Analysis	Site Type / Station / Sample ID / Start Depth (cm) / End Depth (cm)	Mound BR-08 BR08-3 114 129	Mound BR-08 BR08-4 165 180	Mound BR-08 BR08-5 185 200	Mound BR-28 BR28-1 7 20	Mound BR-28 BR28-2 28 38	Mound BR-28 BR28-3 38 46	Mound BR-28 BR28-4 54 59	Mound BR-32 BR32-1 15 28	Mound BR-32 BR32-2 50 65
Conventionals	**Units**									
Gravel	percent	0.0	0.1	0.3	1.5	0.0	0.0	2.5	0.0	0.0
Sand	percent	36.9	73.3	17.2	44.4	15.9	93.6	89.7	33.6	28.6
Silt	percent	48.1	23.6	64.5	40.1	66.1	5.4	5.8	49.4	52.4
Clay	percent	15	3.0	18	14	18	1.0	2.0	17	19
Fines (silt+clay)	percent	63.1	26.6	82.5	54.1	84.1	6.40	7.80	66.4	71.4
Total Organic Carbon	percent	0.51 E	0.13	0.30	0.21	0.65	0.072	0.018	0.92	0.54
Metals	**Units**									
Aluminum	mg/kg	8,690	3,500	13,900	7,770	11,700	1,490	1,750	9,070	9,830
Arsenic	mg/kg	7.3	3.5	6.7	7.0	21.3	4.0	3.6	8.0	7.9
Beryllium	mg/kg	0.52	0.22 B	0.41	0.51	0.86	0.14 B	0.16 B	0.75	0.78
Cadmium	mg/kg	0.25 B	0.069 B	0.018 B	0.21 B	15.0	0.11 B	0.01 U	0.25 B	0.25 B
Chromium	mg/kg	31.5	10.4	31.2	26.5	395	10.3	7.8	31.2	32.5
Copper	mg/kg	40.4	11.6	11.9	28.1	1,260	15.3	3.6	31.9	36.6
Iron	mg/kg	17,500 E	7,720 E	23,900 E	15,900 E	28,500 E	7,060 E	7,190 E	24,900	26,300
Lead	mg/kg	16.7	5.0	8.8	14.6	305	11.2	5.1	15.8 E	16.8 E
Nickel	mg/kg	12.7	4.8	15.5	11.3	37.9	2.7	2.9	12.9 E	13.8 E
Selenium	mg/kg	1.0 U	1.0 B	1.0 U	1.1 U	1.8 U	0.8 U	0.8 U	1.6 B	1.8 B
Silver	mg/kg	0.35 B	0.1 U	0.1 U	0.22 B	29.5	0.19 B	0.1 U	0.17 B	0.21 B
Vanadium	mg/kg	22.9	10.1	38.2	22.4	42.2	16.0	16.2	23.5	24.3
Zinc	mg/kg	59.2	23.3	53.9	51.4	696	23.7	14.2	59.7 E	61.4 E
PAHs	**Units**									
Total HPAH	µg/kg	230			150	5,900	150			220
Total LPAH	µg/kg	36			35	1,100	27			38
Total PAH	µg/kg	270			180	7,000	180			260
LPAH:HPAH	ratio	0.16			0.24	0.19	0.18			0.18

U indicates that the parameter is not detected. E indicates that the value is estimated due to the presence of interferences, as determined by serial dilution analysis.
B indicates the presence of a 'trace' concentration below the reporting limit and equal to or above the detection limit.

Table 3-2., continued.

Chemical and Physical Core Data Summary

Analysis	Site Type Station Sample ID Start Depth (cm) End Depth (cm)	Mound BR-32 BR32-3 139 154	Mound BR-32 BR32-4 181 192	Mound BR-32 BR32-5 231 246	Mound BR-42 BR42-1 7 20	Mound BR-42 BR42-2 33 48	Mound BR-42 BR42-3 61 71	Mound BR-44 BR44-1 7 20	Mound BR-44 BR44-2 44 59
Conventionals	**Units**								
Gravel	percent	6.3	2.4	2.7	0.0	1.5	0.2	3.3	0.0
Sand	percent	28.7	30.4	80.7	68.7	48.4	38.0	65.5	30.1
Silt	percent	51.0	54.2	11.6	23.3	39.1	48.8	24.2	55.9
Clay	percent	14	13	5.0	8.0	11	13	7.0	14
Fines (silt+clay)	percent	65	67.2	16.6	31.3	50.1	61.8	31.2	69.9
Total Organic Carbon	percent	0.0065 U	0.96 E	0.23	0.16	0.21	0.32	0.23	0.51
Metals	**Units**								
Aluminum	mg/kg	9,300	9,110	2,970	5,860	6,500	8,520	4,450	11,400
Arsenic	mg/kg	5.2	5.4	2.7	5.8	6.2	11.7	3.8	8.9
Beryllium	mg/kg	0.53	0.56	0.24 B	0.33	0.38	0.69	0.23 B	0.75
Cadmium	mg/kg	0.16 B	0.14 B	0.013 U	0.065 B	0.26 B	2.6	0.062 B	0.34 B
Chromium	mg/kg	23.0	22.5	9.6	18.4	30.5	120	14.3	43.9
Copper	mg/kg	25.3	25.7	4.8	14.8	42.7	310	13.4	49.9
Iron	mg/kg	23,200 E	18,100 E	7,680 E	12,200 E	13,600 E	19,400	9,210 E	22,900
Lead	mg/kg	11.8 E	11.7 E	6.7 E	10.7	20.2	101	10.1	24.0
Nickel	mg/kg	14.3 E	13.6 E	4.8 E	8.8	10.4	18.3	6.8	16.6
Selenium	mg/kg	0.85 U	1.6 B	0.8 U	0.4 U	1.0 U	1.3 U	1.0 U	1.4 B
Silver	mg/kg	0.086 U	0.096 U	0.081 U	1.0 U	0.39 B	4.2	0.1 U	0.33 B
Vanadium	mg/kg	21.4	19.8	11.0	17.6	18.0	29.3	12.2	28.3
Zinc	mg/kg	49.0 E	47.9 E	20.2 E	36.8	58.2	219	30.1	81.0
PAHs	**Units**								
Total HPAH	µg/kg				140	320	1,800	140	370
Total LPAH	µg/kg				33	48	300	32	55
Total PAH	µg/kg				180	370	2,100	170	420
LPAH:HPAH	ratio				0.24	0.15	0.16	0.23	0.15

U indicates that the parameter is not detected. E indicates that the value is estimated due to the presence of interferences, as determined by serial dilution analysis.
B indicates the presence of a 'trace' concentration below the reporting limit and equal to or above the detection limit.

Table 3-2., continued.

Chemical and Physical Core Data Summary

Analysis	Site Type Station Sample ID Start Depth (cm) End Depth (cm)	Reference BR-70 BR70-1 7 20	Reference BR-70 BR70-2 40 55	Mound BR-78 BR78-1 6 20	Mound BR-78 BR78-2 42 57	Mound BR-78 BR78-3 90 110	Mound BR-78 BR78-4 110 125	Mound BR-78 BR78-5 140 155	Mound BR-78 BR78-6 180 195	Mound BR-78 BR78-7 218 224
Conventionals	**Units**									
Gravel	percent	8.0	0.3	9.0	0.0	1.0	13.5	1.3	2.1	0.4
Sand	percent	63.1	66.1	62.0	9.5	38.8	48.8	83.6	78.3	37.8
Silt	percent	23.9	21.6	25.0	69.5	51.2	32.7	11.1	14.6	58.8
Clay	percent	5.0	12	4.0	21	9.0	5.0	4.0	5.0	3.0
Fines (silt+clay)	percent	28.9	33.6	29.0	90.5	60.2	37.7	15.1	19.6	61.8
Total Organic Carbon	percent	0.11	0.28	0.29	1.6 E	0.74	0.24	0.22	0.52	0.1
Metals	**Units**									
Aluminum	mg/kg	4,150	3,661	6,650	11,700	7,360	6,576	3,370	3,580	2,580
Arsenic	mg/kg	3.8	4.5	5.5	10.2	7.7	7.3	2.7	4.9	1.9
Beryllium	mg/kg	0.27 B	0.28	0.30	1.0	0.42	0.36	0.22 B	0.21 B	0.17 B
Cadmium	mg/kg	0.014 U	0.014 U	0.059 B	0.11 B	2.1	0.86	0.038 B	0.051 B	0.021
Chromium	mg/kg	11.4	10.6	18.8	26.3	85.2	44.6	11.9	10.4	6.7
Copper	mg/kg	4.6	4.4	9.1	10.1	243	114.5	10.7	6.0	4.3
Iron	mg/kg	10,100 E	8,660 E	12,800 E	34,900 E	15,100 E	14,679 E	8,200 E	8,610 E	4,950
Lead	mg/kg	7.7 E	6.6 E	7.2	9.2 E	84.5	38.0	10.2	5.6	3.6
Nickel	mg/kg	7.3 E	5.8 E	10.0	15.8 E	19.0	14.1	5.6	5.6	3.6
Selenium	mg/kg	0.88 B	1.03 B	0.8 U	2.0 B	1.0 U	0.9 U	1.0 U	0.8 U	0.8 U
Silver	mg/kg	0.086 U	0.085 U	0.8 U	0.13 U	3.4	1.269 B	0.1 U	0.08 U	0.08 U
Vanadium	mg/kg	13.1	13.6	17.2	31.5	21.0	17.3	12.3	12.6	7.9
Zinc	mg/kg	26.8 E	21.2 E	31.8	53.2 E	183	96.3	30.8	21.9	12.4
PAHs	**Units**									
Total HPAH	µg/kg			70		3,700	1,400			33
Total LPAH	µg/kg			26		630	180			25
Total PAH	µg/kg			96		4,300	1,600			58
LPAH:HPAH	ratio			0.37		0.17	0.13			0.74

U indicates that the parameter is not detected. E indicates that the value is estimated due to the presence of interferences, as determined by serial dilution analysis.
B indicates the presence of a 'trace' concentration below the reporting limit and equal to or above the detection limit.

Table 3-2., continued.

Chemical and Physical Core Data Summary

Analysis	Site Type Station Sample ID Start Depth (cm) End Depth (cm)	Reference BR-94 BR94-1 7 20	Reference BR-94 BR94-2 40 55	Reference BR-94 BR94-3 114 129	Reference BR-94 BR94-4 174 189	Reference BR-94 BR94-5 247 262
Conventionals	**Units**					
Gravel	percent	0.4	0.0	0.0	0.0	0.0
Sand	percent	58.4	59.8	57.0	47.0	8.50
Silt	percent	31.7	30.2	32.0	41.0	69.5
Clay	percent	9.5	10	11	12	22
Fines (silt+clay)	percent	41.2	40.2	43.0	53.0	91.5
Total Organic Carbon	percent	0.30	0.41	0.45	0.50	0.70
Metals	**Units**					
Aluminum	mg/kg	4,420	4,680	4,960	5,610	12,700
Arsenic	mg/kg	4.6	4.1	5.9	9.7	27.3
Beryllium	mg/kg	0.35	0.36	0.37	0.41	0.71
Cadmium	mg/kg	0.023 B	0.017 U	0.021 B	0.042 B	0.170 B
Chromium	mg/kg	14	13.7	13.3	14.5	24.6
Copper	mg/kg	7.8	4.5	3.9	5.3	14.7
Iron	mg/kg	10,700 E	11,600 E	13,000 E	14,500 E	47,900 E
Lead	mg/kg	11.8 E	5.7 E	4.6 E	5.1 E	9.1 E
Nickel	mg/kg	6.5 E	7.4 E	7.8 E	9.4 E	21.5 E
Selenium	mg/kg	1.1 B	1.0 U	1.7 B	1.5 B	2.8
Silver	mg/kg	0.092 U	0.1 U	0.1 U	0.099 U	0.11 U
Vanadium	mg/kg	15.9	16.7	17.5	19.7	34.0
Zinc	mg/kg	30.5 E	25.2 E	24.2 E	27.7 E	58.3 E
PAHs	**Units**					
Total HPAH	µg/kg	74				53
Total LPAH	µg/kg	28				29
Total PAH	µg/kg	102				82
LPAH:HPAH	ratio	0.38				0.55

U indicates that the parameter is not detected. E indicates that the value is estimated due to the presence of interferences, as determined by serial dilution analysis.
B indicates the presence of a 'trace' concentration below the reporting limit and equal to or above the detection limit.

Table 3-3.

Chemical and Physical Core Statistical Summary

Analyte Group	Parameter	Mound Area Samples						Reference Samples					
		N	N-Det	Min	Max	Mean	Median	N	N-Det	Min	Max	Mean	Median
Conventionals													
	Total Organic Carbon (%)	33	31	0.018	1.6	0.51	0.38	7	7	0.11	0.7	0.39	0.41
	Fine-grained content (clay + silt, %)	33	33	6.4	95.9	53.7	61.8	7	7	28.9	91.5	47.3	41.2
Metals (mg/kg)													
	Aluminum	33	33	1,490	13,900	7,617	8,520	7	7	3,661	12,700	5,740	4,680
	Arsenic	33	33	1.9	21.3	6.9	6.8	7	7	3.8	27.3	8.6	4.6
	Beryllium	33	33	0.1	1.1	0.5	0.5	7	7	0.3	0.7	0.4	0.4
	Cadmium	33	31	0.0	15.0	0.8	0.2	7	4	0.0	0.2	0.1	0.0
	Chromium	33	33	6.7	395	41.1	26.5	7	7	10.6	24.6	14.6	13.7
	Copper	33	33	3.6	1260	80.4	17.4	7	7	3.9	14.7	6.5	4.6
	Iron	33	33	4,950	34,900	17,621	17,500	7	7	8,660	47,900	16,637	11,600
	Lead	33	33	3.6	305	27.5	11.7	7	7	4.6	11.8	7.2	6.6
	Nickel	33	33	2.7	37.9	12.3	13.2	7	7	5.8	21.5	9.4	7.4
	Selenium	33	13	0.9	2.3	1.5	1.6	7	6	0.9	2.8	1.5	1.3
	Silver	33	14	0.2	29.5	3.1	0.4	7	1	0.1	0.1	0.1	0.1
	Vanadium	33	33	7.9	42.2	21.6	21.4	7	7	13.1	34.0	18.6	16.7
	Zinc	33	33	12.4	696	77.6	53.2	7	7	21.2	58.3	30.6	26.8
PAHs (µg/kg)													
	Total LPAHs	18	18	25	1,100	150	37	2	2	28	29	29	29
	Total HPAHs	18	18	33	5,900	870	190	2	2	53	74	64	64
	Total PAHs	18	18	58	7,000	1,000	220	2	2	82	102	92	92

N-Det= Number of Samples with Detectable Levels

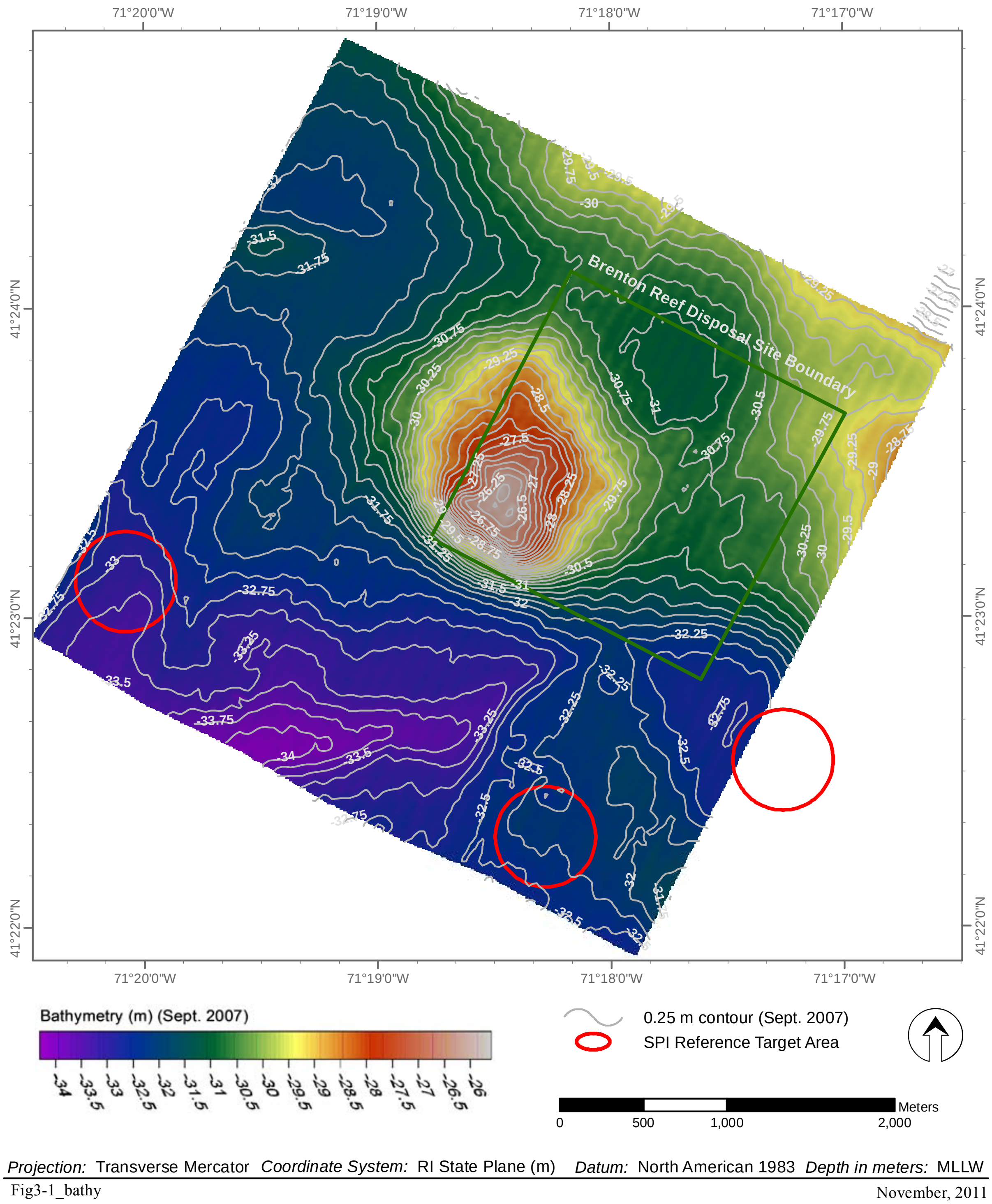

Figure 3-1. Bathymetry of the Brenton Reef Disposal Site survey area

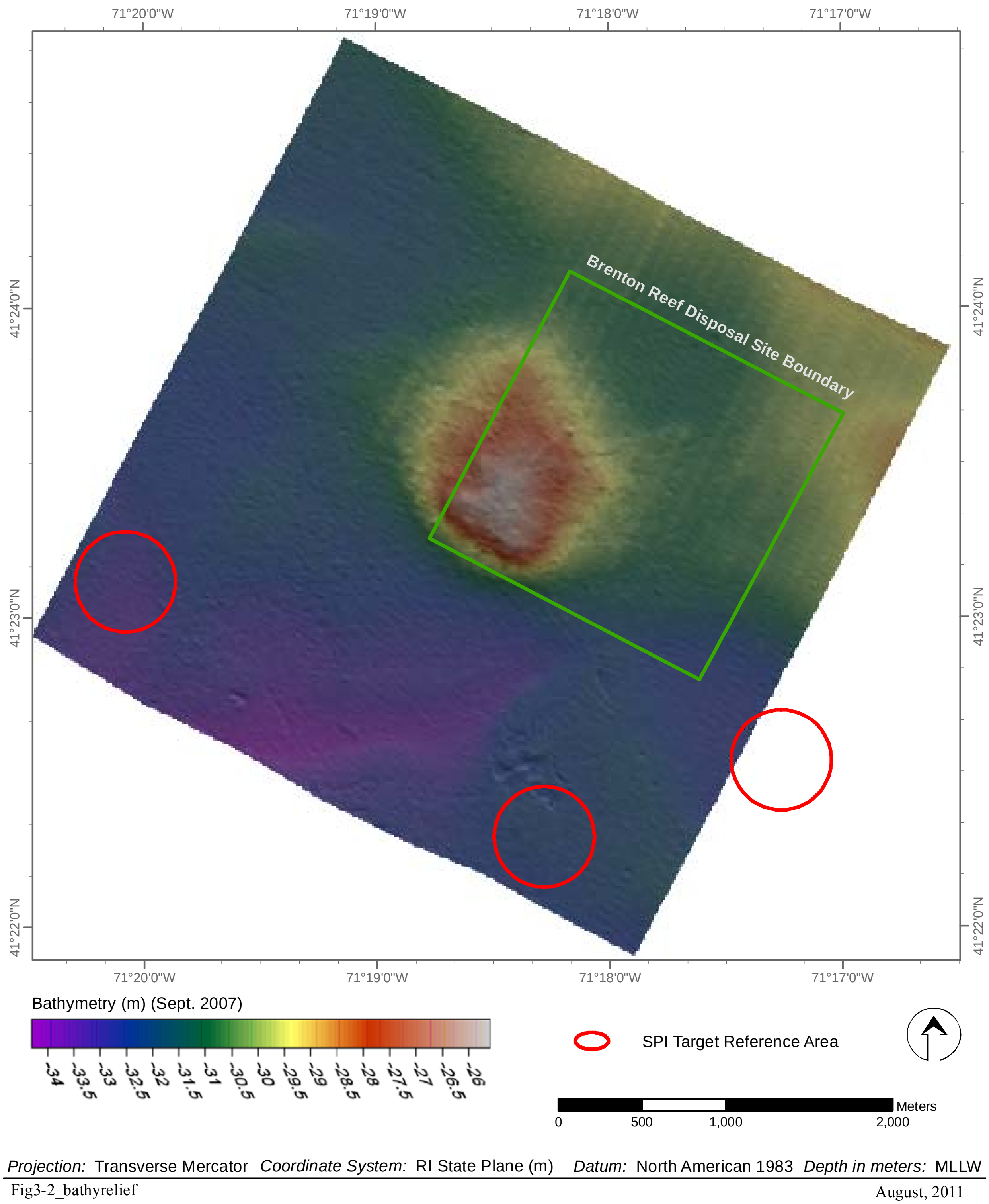

Figure 3-2. Hillshaded bathymetry of the Brenton Reef Disposal Site survey area

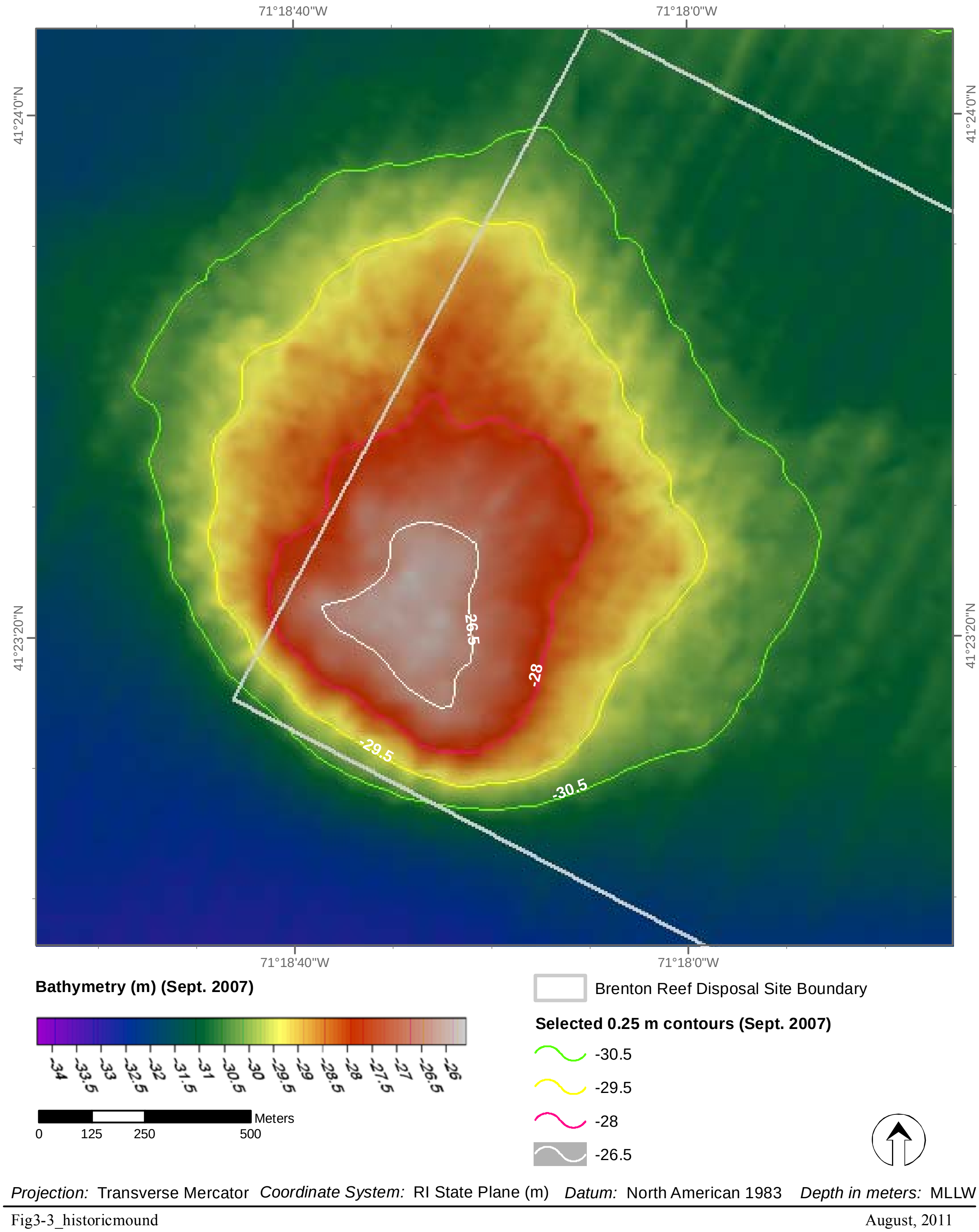

Figure 3-3. Historical Brenton Reef Disposal Site mound bathymetry (mound with selected contours)

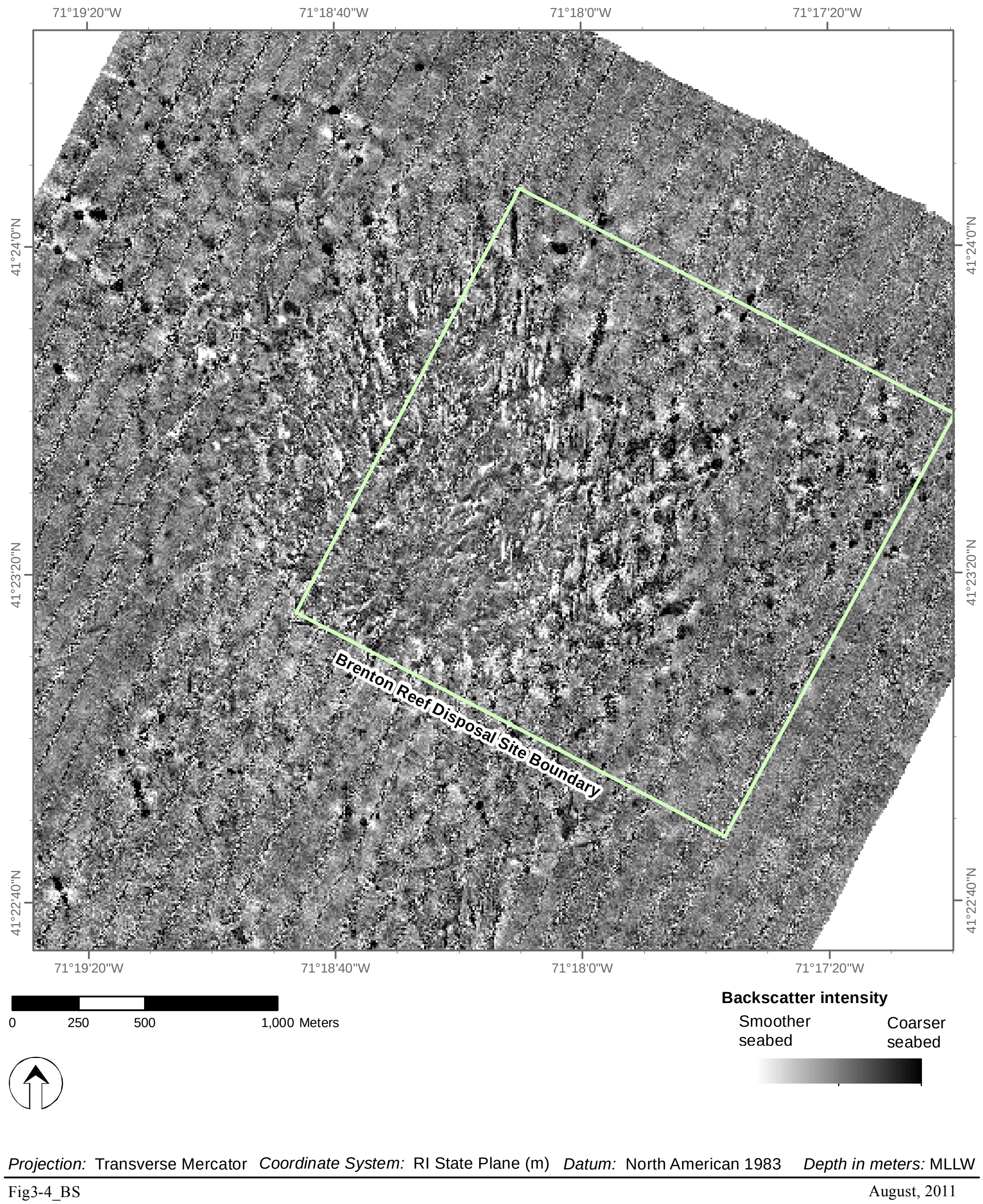

Figure 3-4. Backscatter image of historical Brenton Reef Disposal Site mound and surrounding disposal features

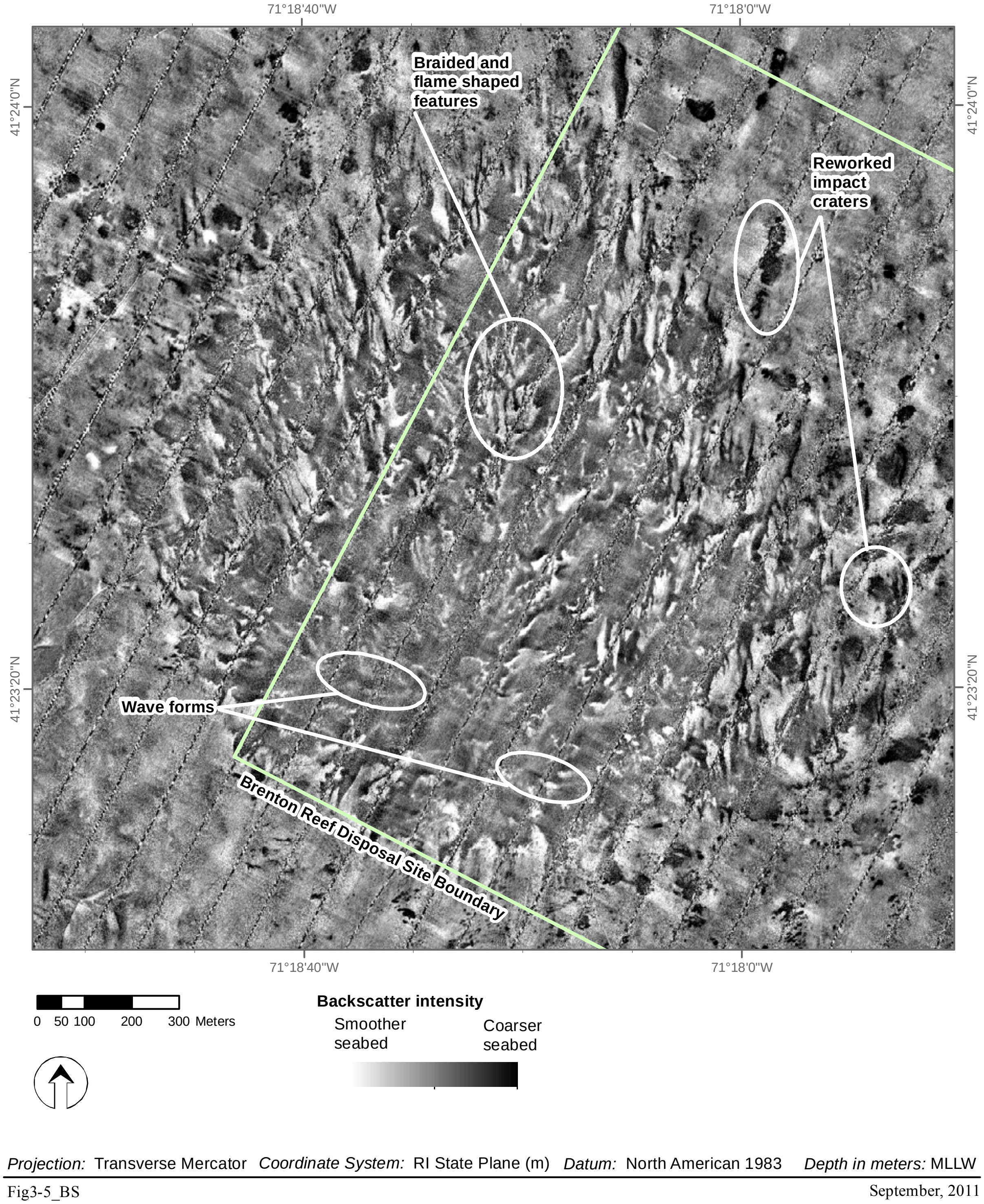

Figure 3-5. Backscatter image of historical Brenton Reef Disposal Site mound, near the apex

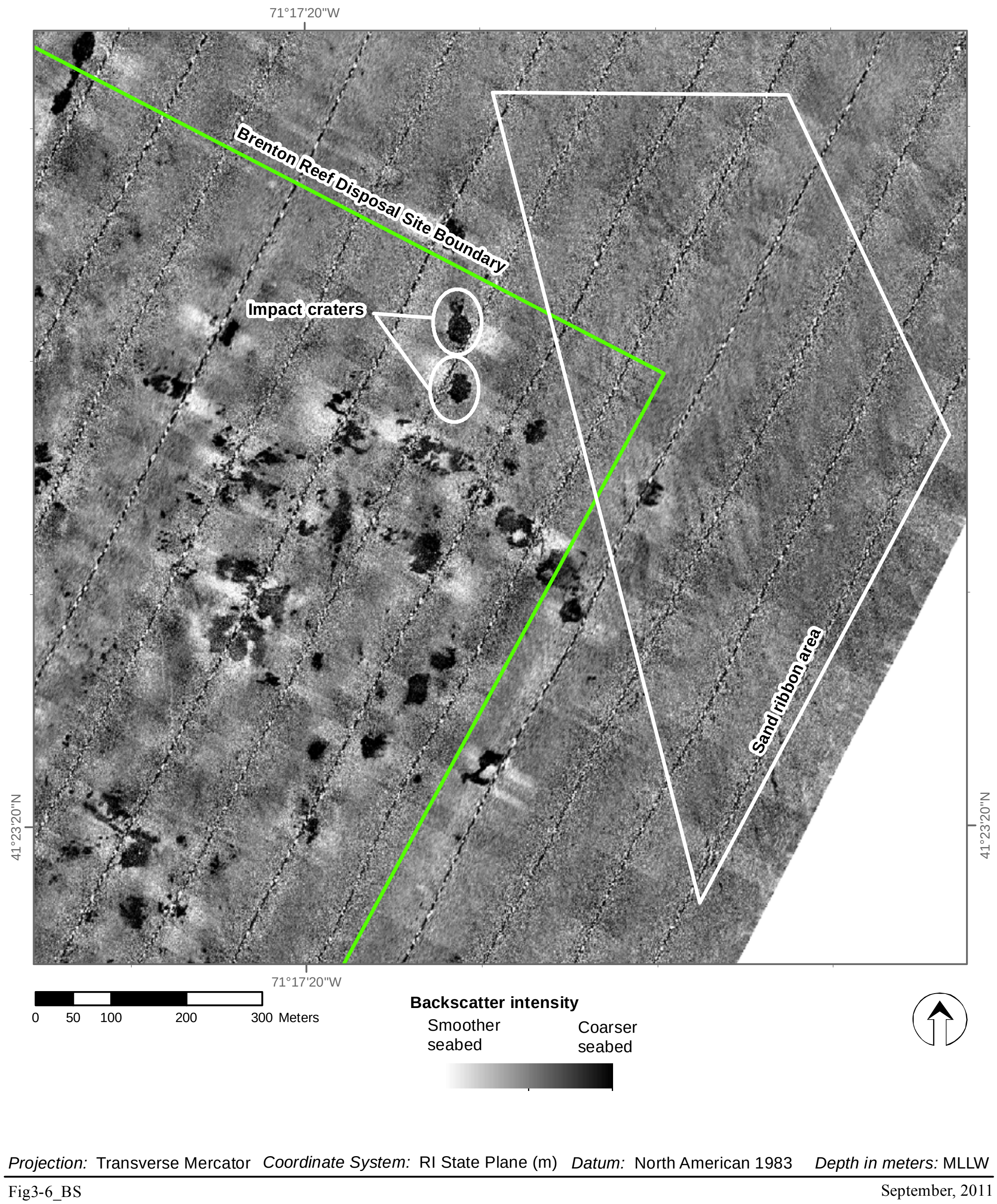

Figure 3-6. Backscatter image of apparent disposal and sediment transport features east of the historical Brenton Reef Disposal Site mound

Figure 3-7. The layering in this sediment-profile image from reference Station 95 may be from older dredged material but may also represent episodic disturbance of the surface. The surface has been recently disturbed.

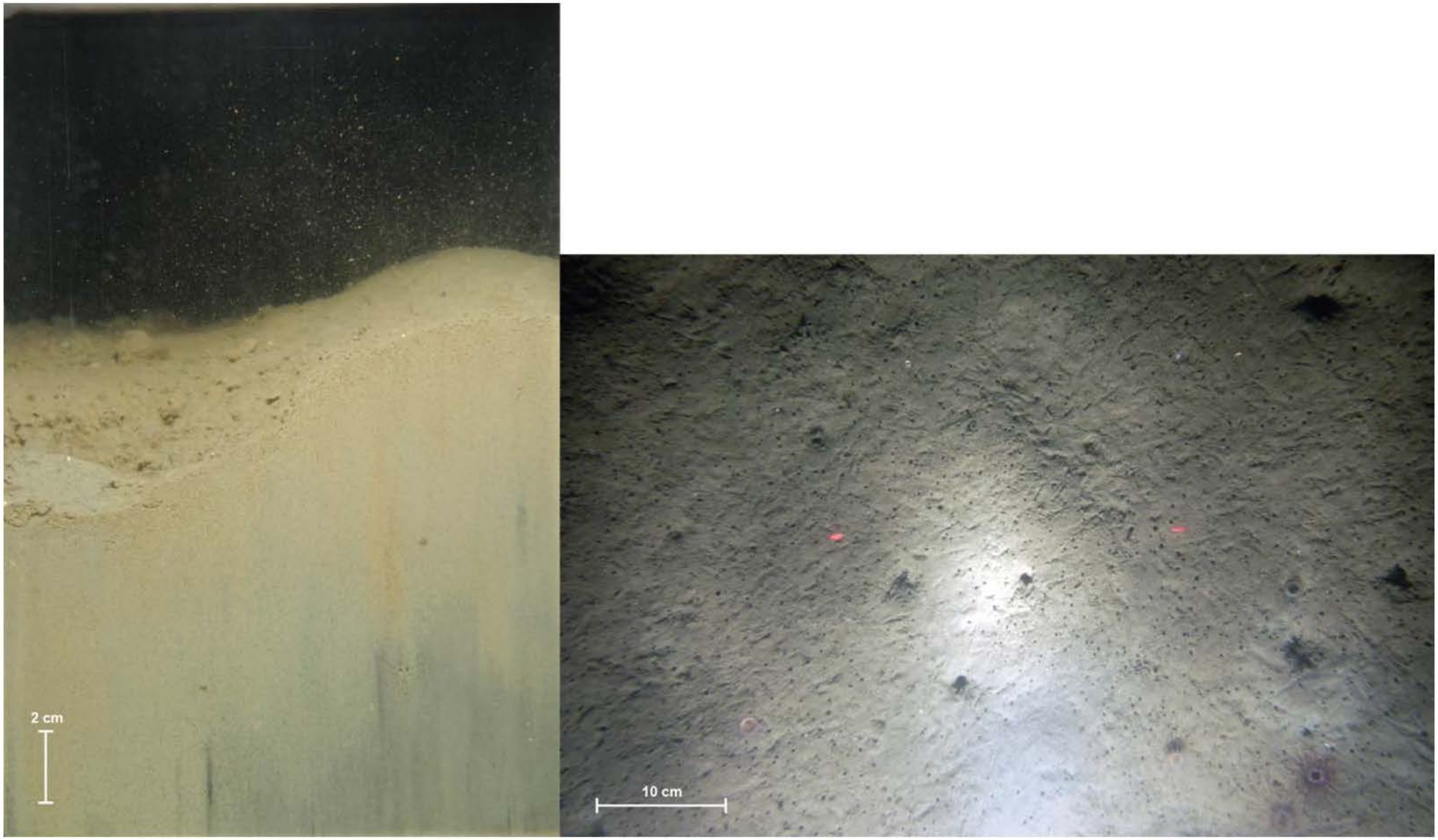

Figure 3-8. The small-scale surface boundary roughness in these SPI and plan-view images from reference Station 67 are from burrowing activities and foraging of epibenthic animals.

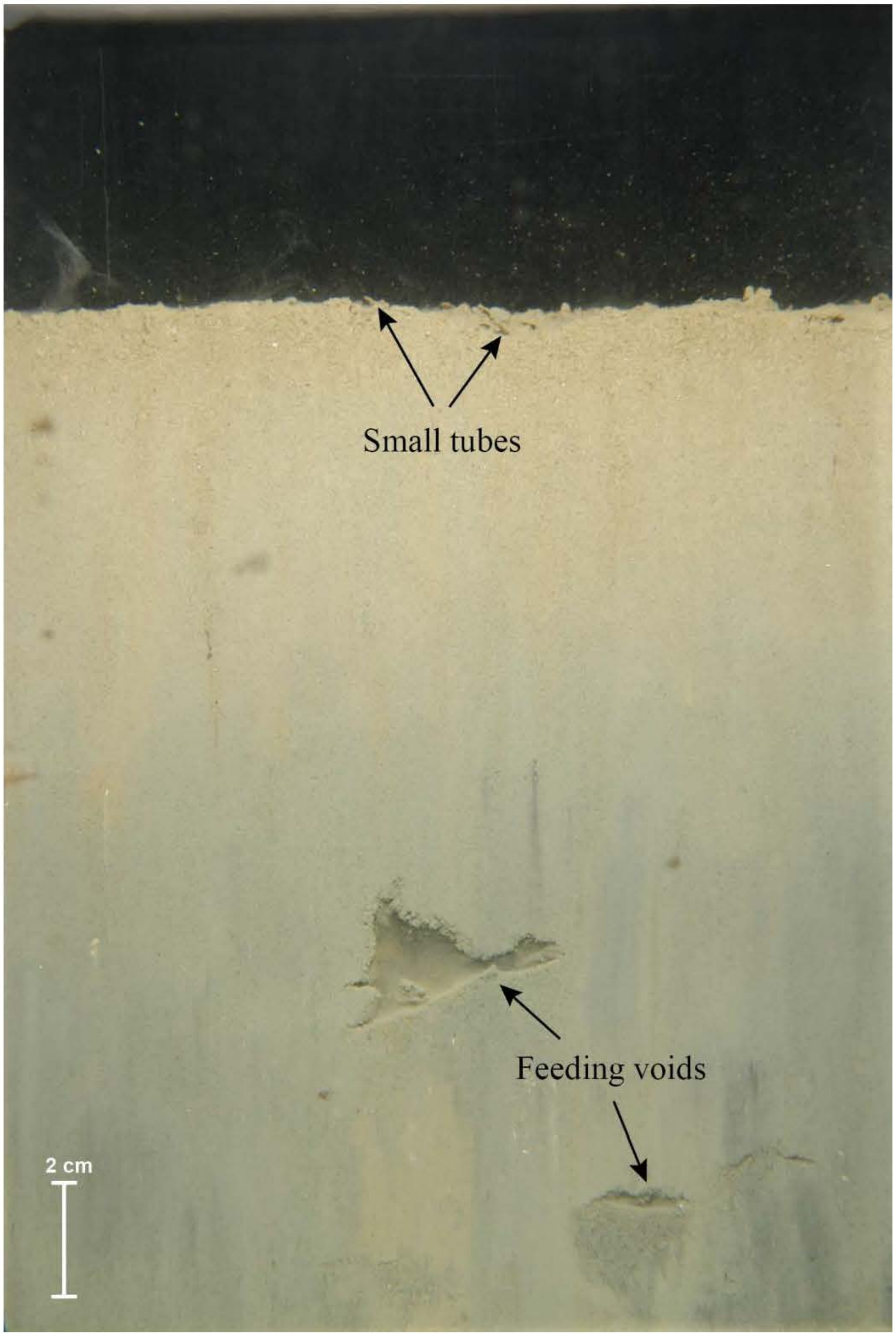

Figure 3-9. The infaunal successional stage (Stage 1 on 3) in this SPI image from Station 65 is representative of conditions in all of the reference areas. The small tubes are Stage 1 animals, and the feeding voids are diagnostic of Stage 3 animals.

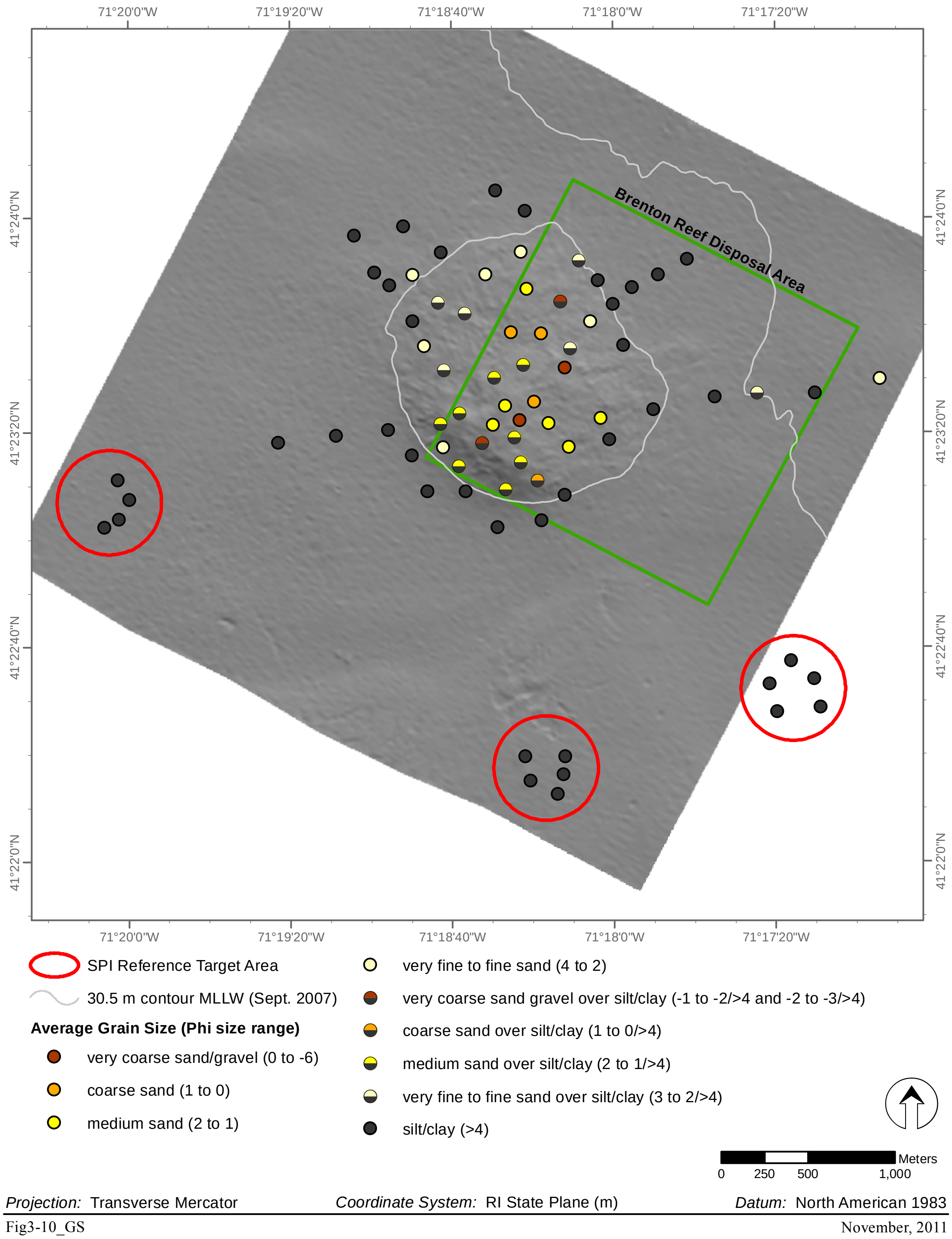

Figure 3-10. Sediment grain size distribution across the Brenton Reef Disposal Site study area

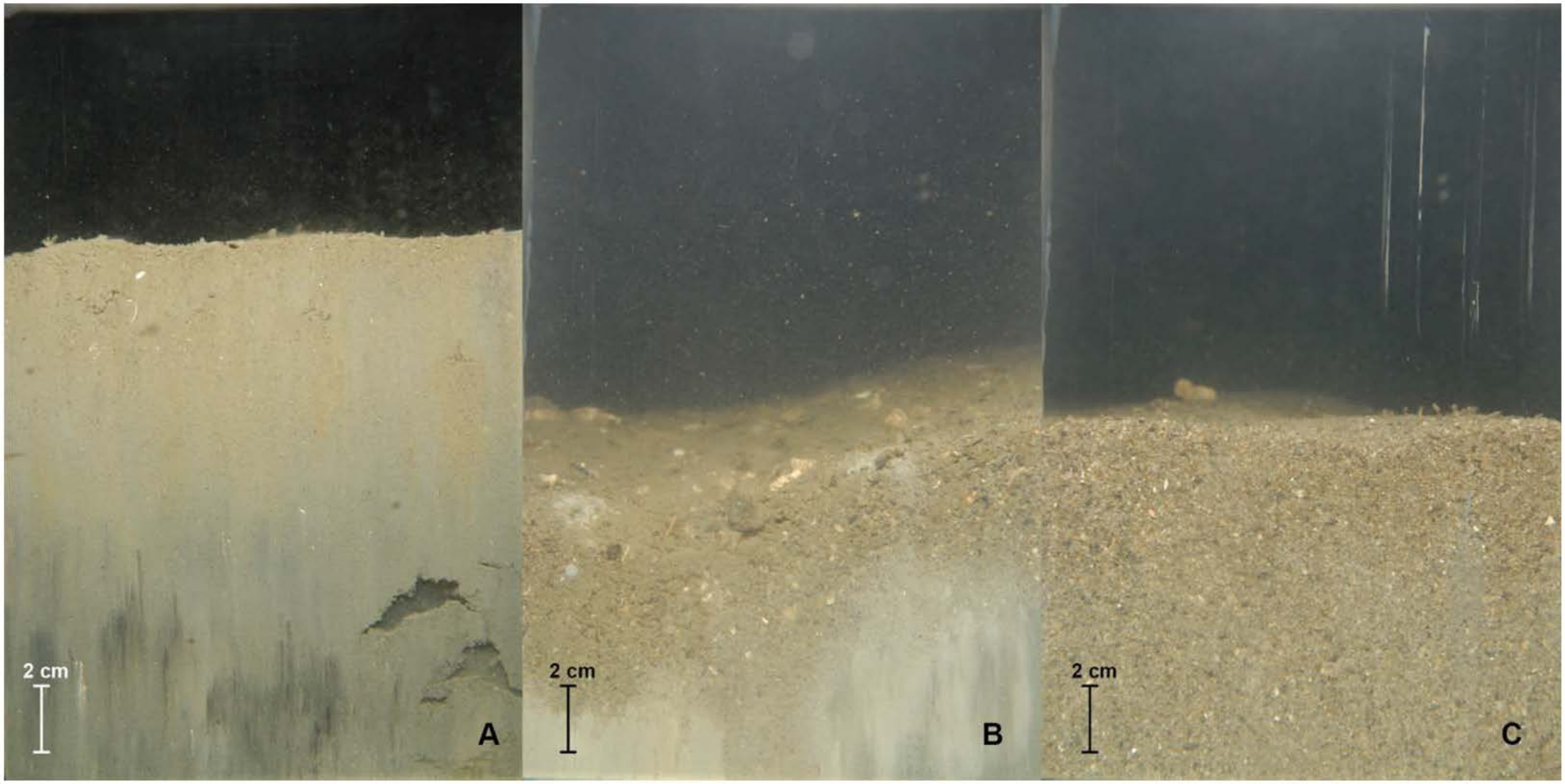

Figure 3-11. Three sediment types from the historical mound at the Brenton Reef Disposal Site. A. Silt from Station 79 on the margin of the mound. B. Thin layer of coarse sand over silt from Station 4 on mound top. C. Relatively thick layers of well-sorted medium sand and gravel from Station 4 on mound top.

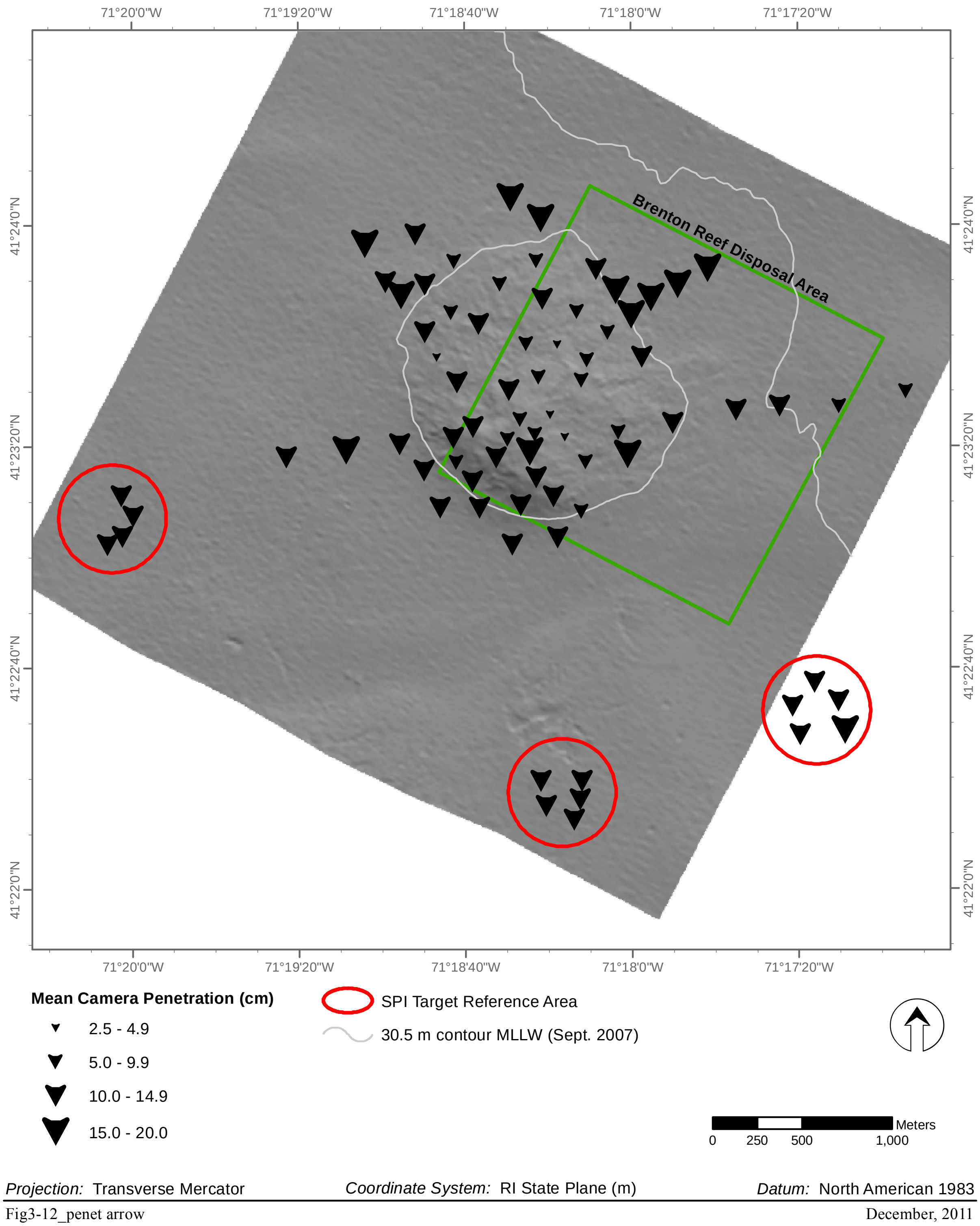

Figure 3-12. Station-averaged camera penetration at the Brenton Reef Disposal Site study area

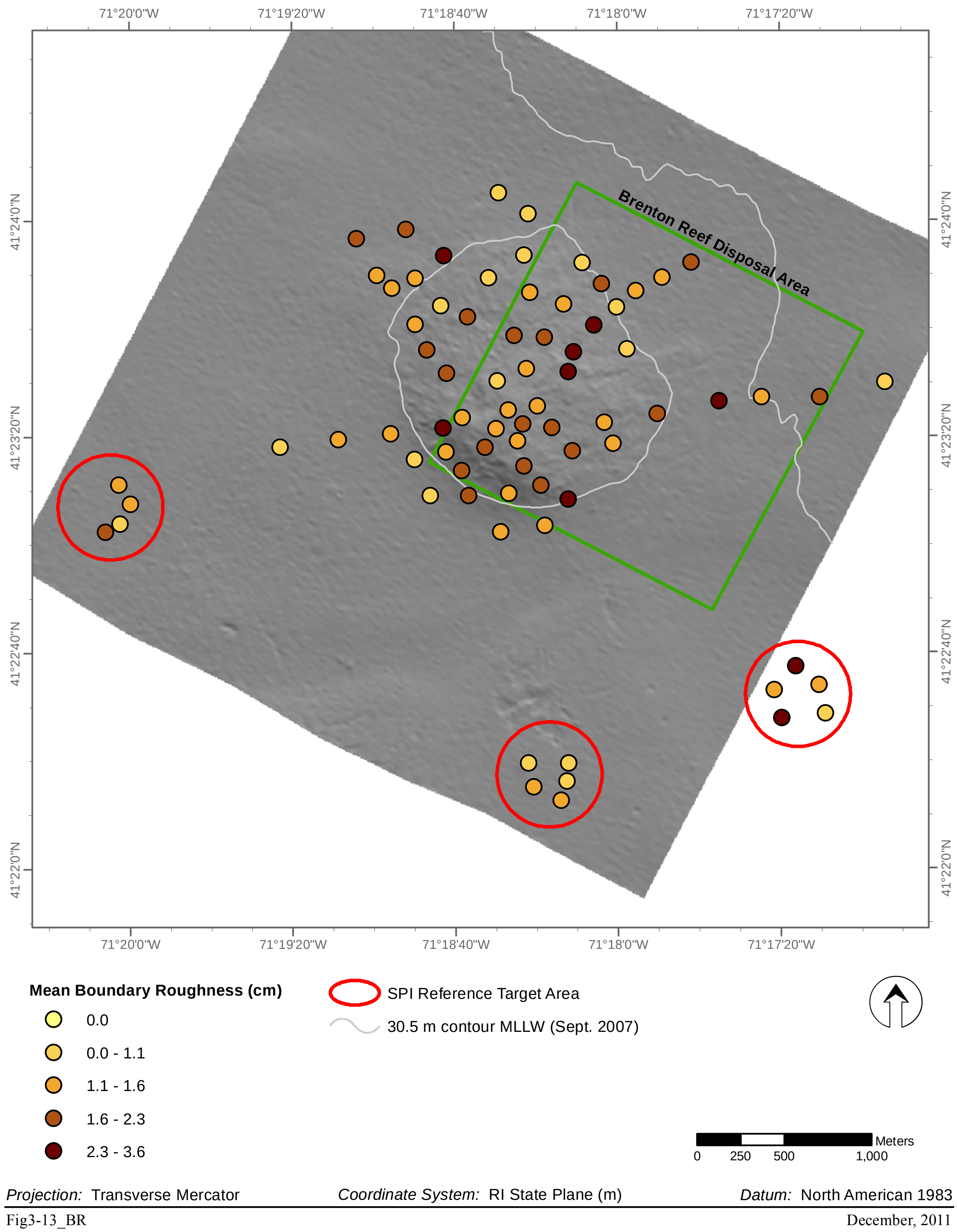

Figure 3-13. Station-averaged boundary roughness at the Brenton Reef Disposal Site study area

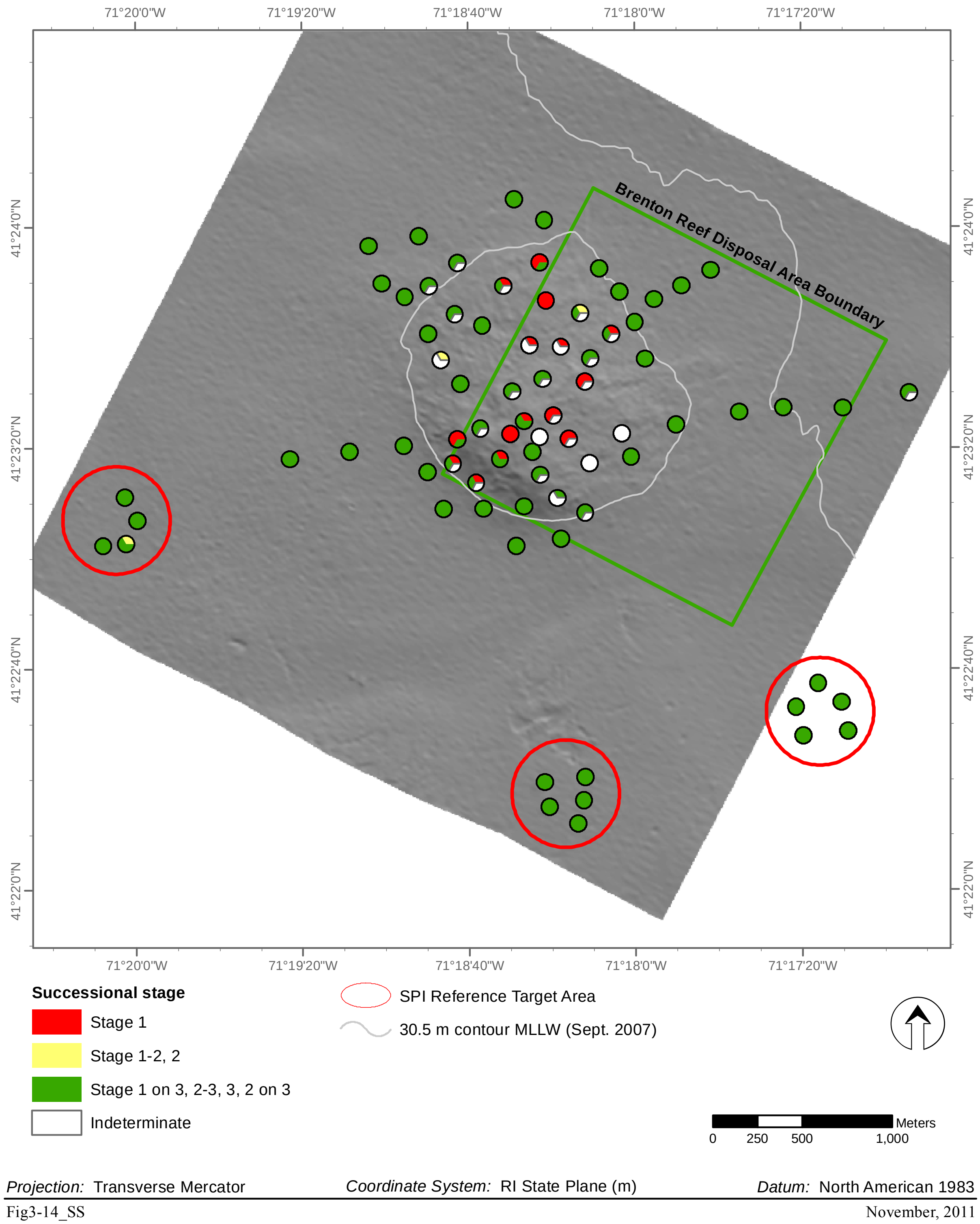

Figure 3-14. Successional stage at the Brenton Reef Disposal Site study area

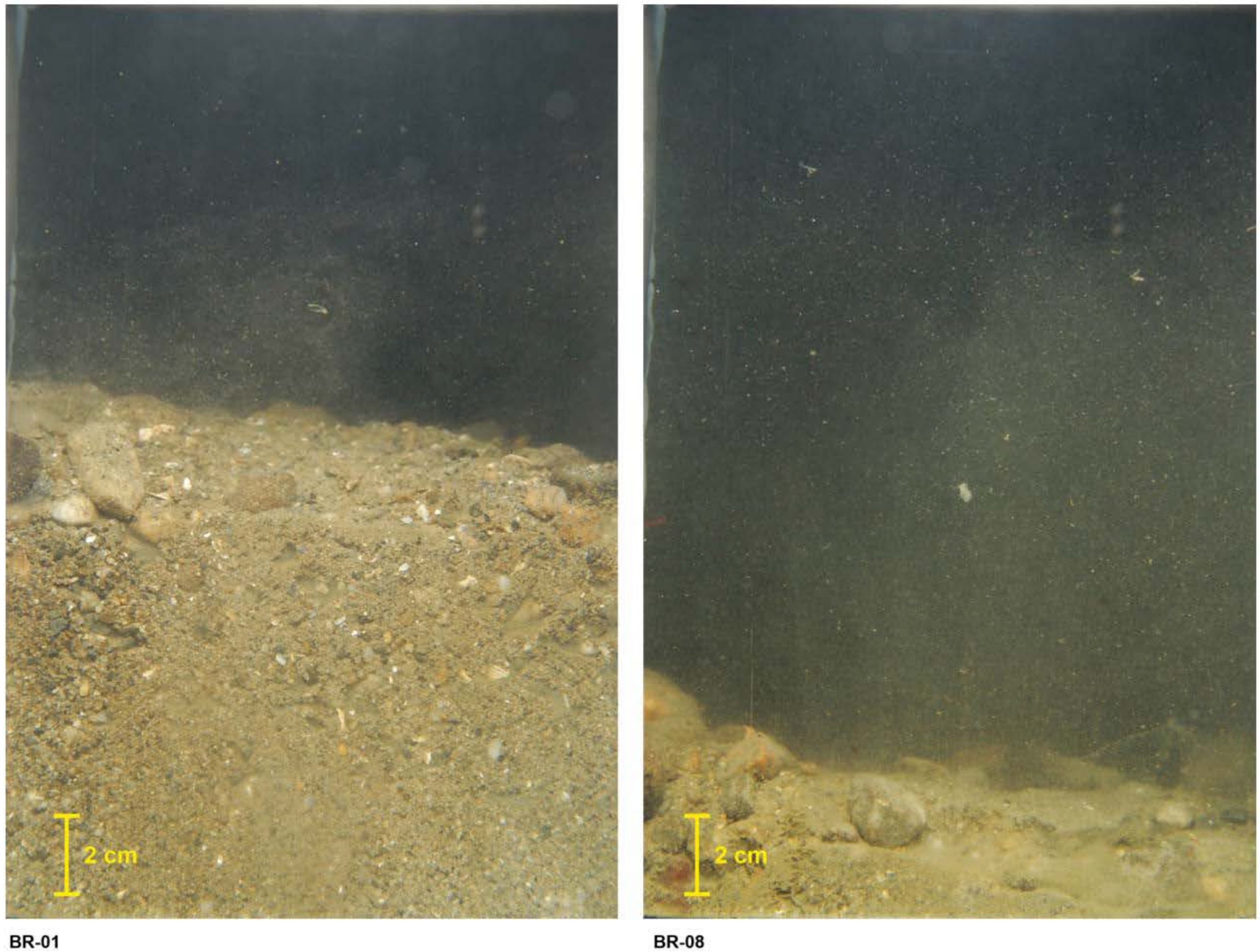

Figure 3-15. Profile image from Station BR-01 (left) illustrating coarse sand that lacks any vertical color changes associated with an aRPD. The aRPD likewise could not be measured in the right image from Station BR-08 due to low penetration of the camera prism in the gravel sediment.

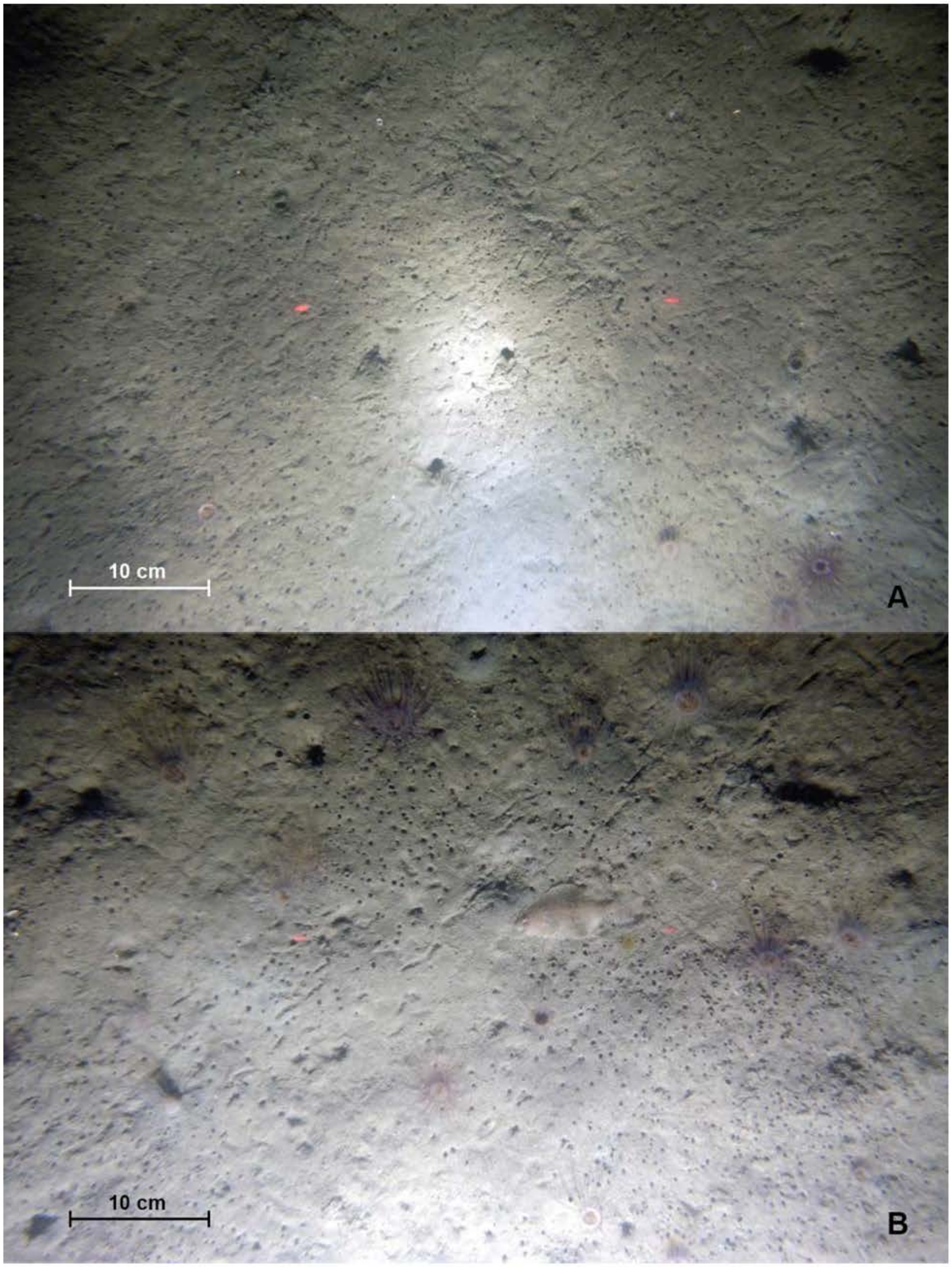

Figure 3-16. A. Plan-view image of typical sediment surface at reference areas (Station 67) with burrows and tubes of large and small infauna (including numerous cerianthid anemones) and tracks and trails of epifauna. B. Plan-view image of sediment surface at silt stations off mound (Station 73) with burrows and tubes of large and small infauna and tracks and trails of epifauna.

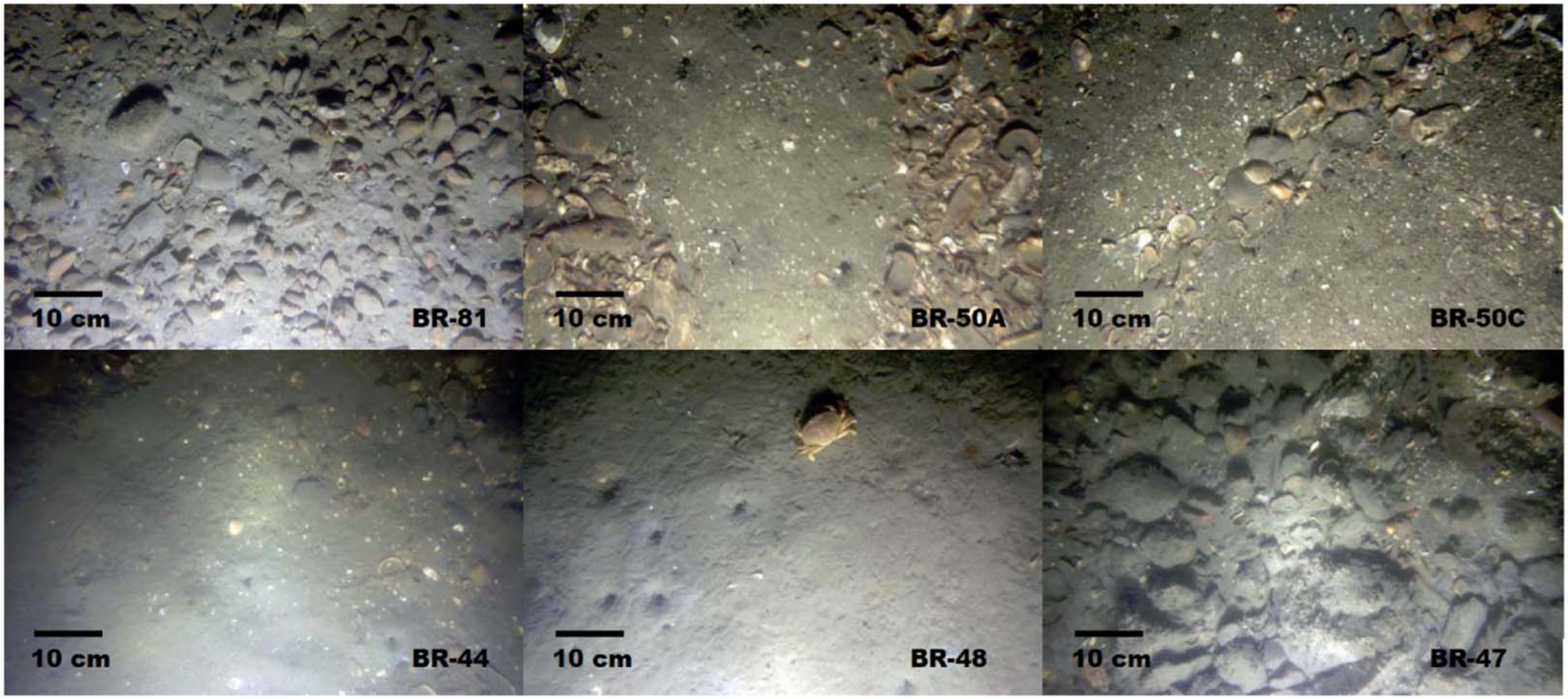

Figure 3-17. Range of sediment features visible in plan-view images taken across the mound. Station 81 - gravel lag with pebbles and cobbles; Station 50A - shell windrows separated by 30 cm of muddy sand; Station 50C - shell windrow; Station 44 - muddy sand wave (wavelength about 25 cm); Station 48 - burrowed silt with tracks; Station 47 - medium to large cobbles.

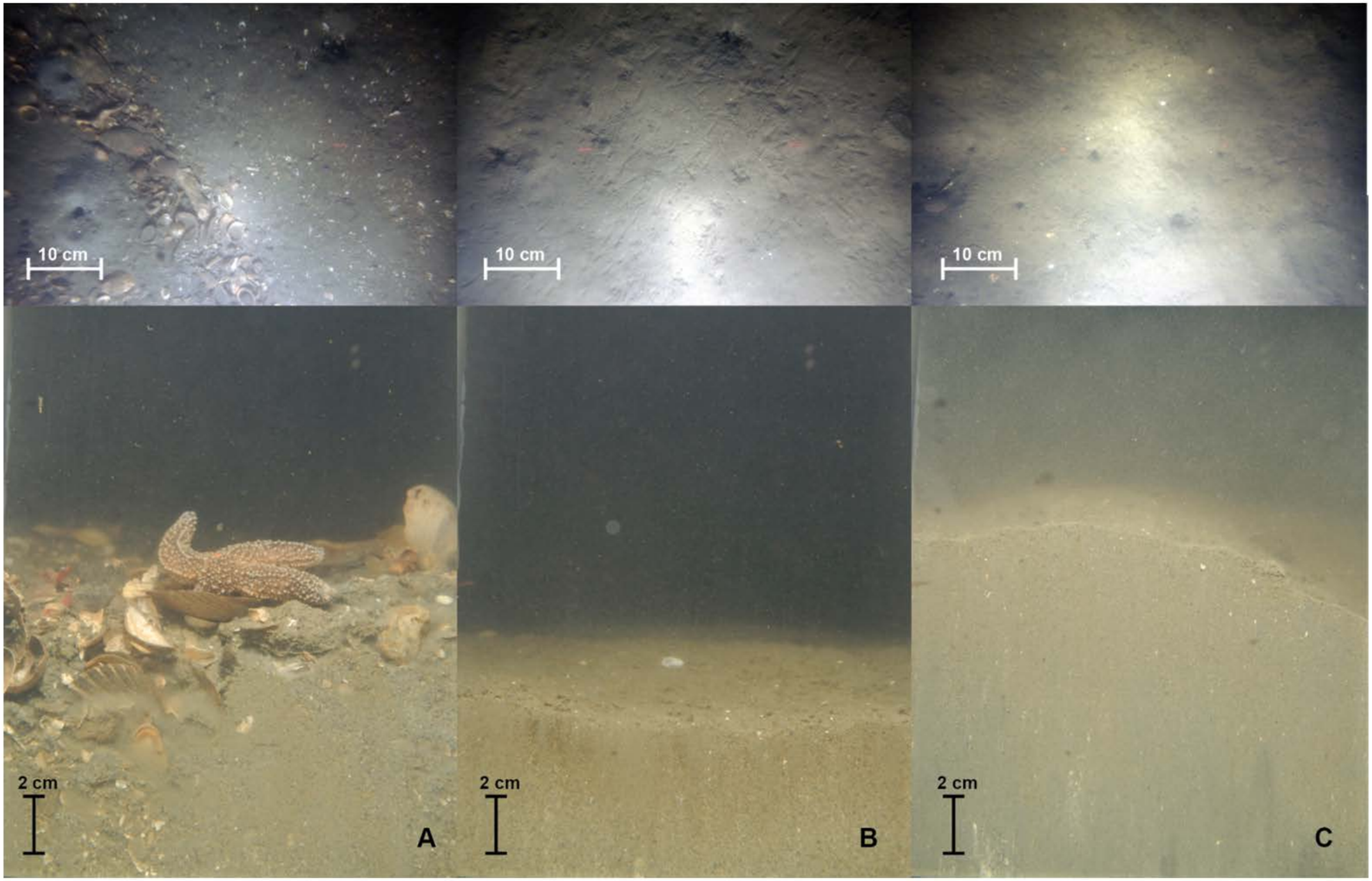

Figure 3-18. Plan-view images (top) and SPI images (bottom) from three replicates of Station 43 on the historical Brenton Reef Disposal Site mound

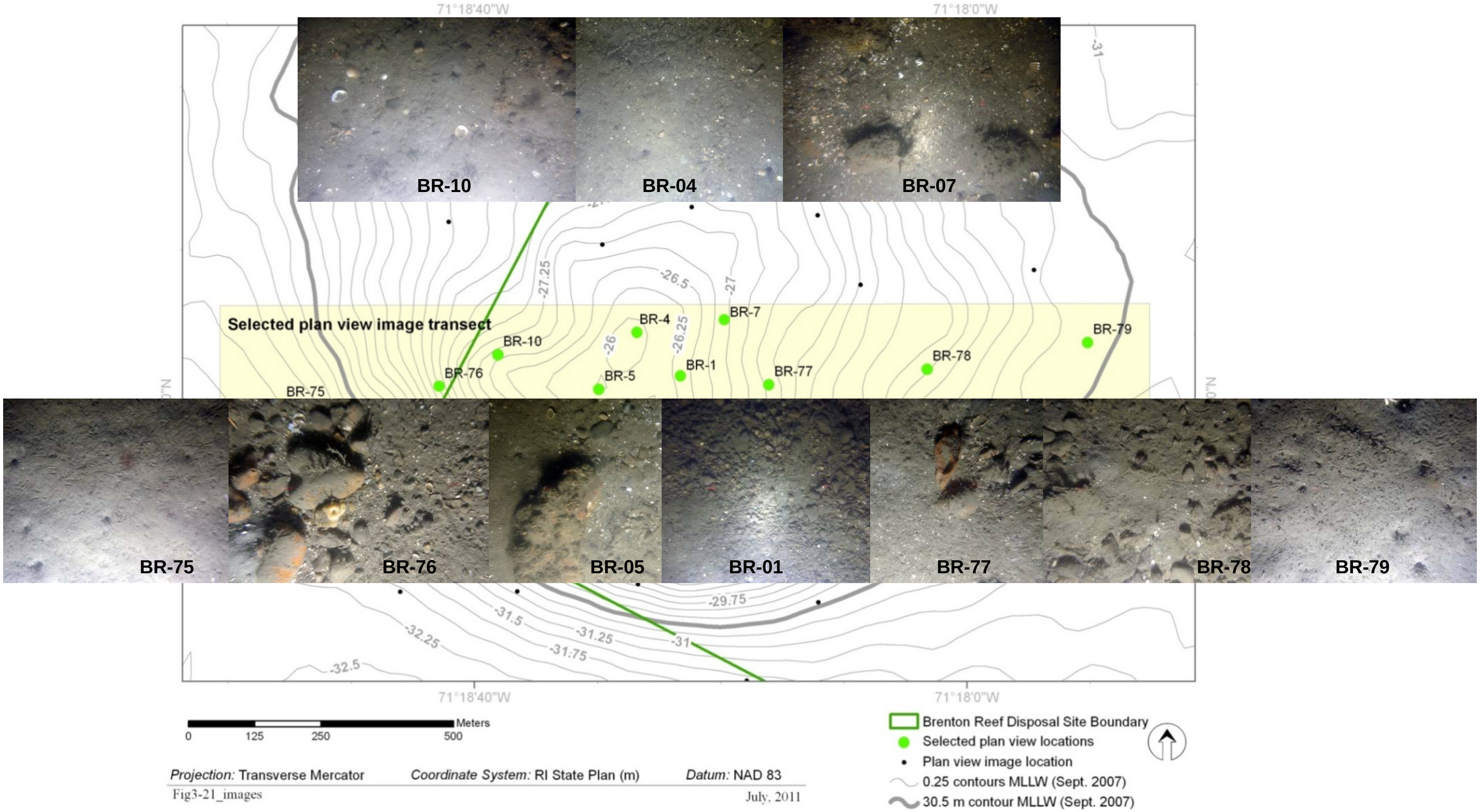

Figure 3-19. Representative plan-view images from a transect across the top of the Brenton Reef Disposal Site mound

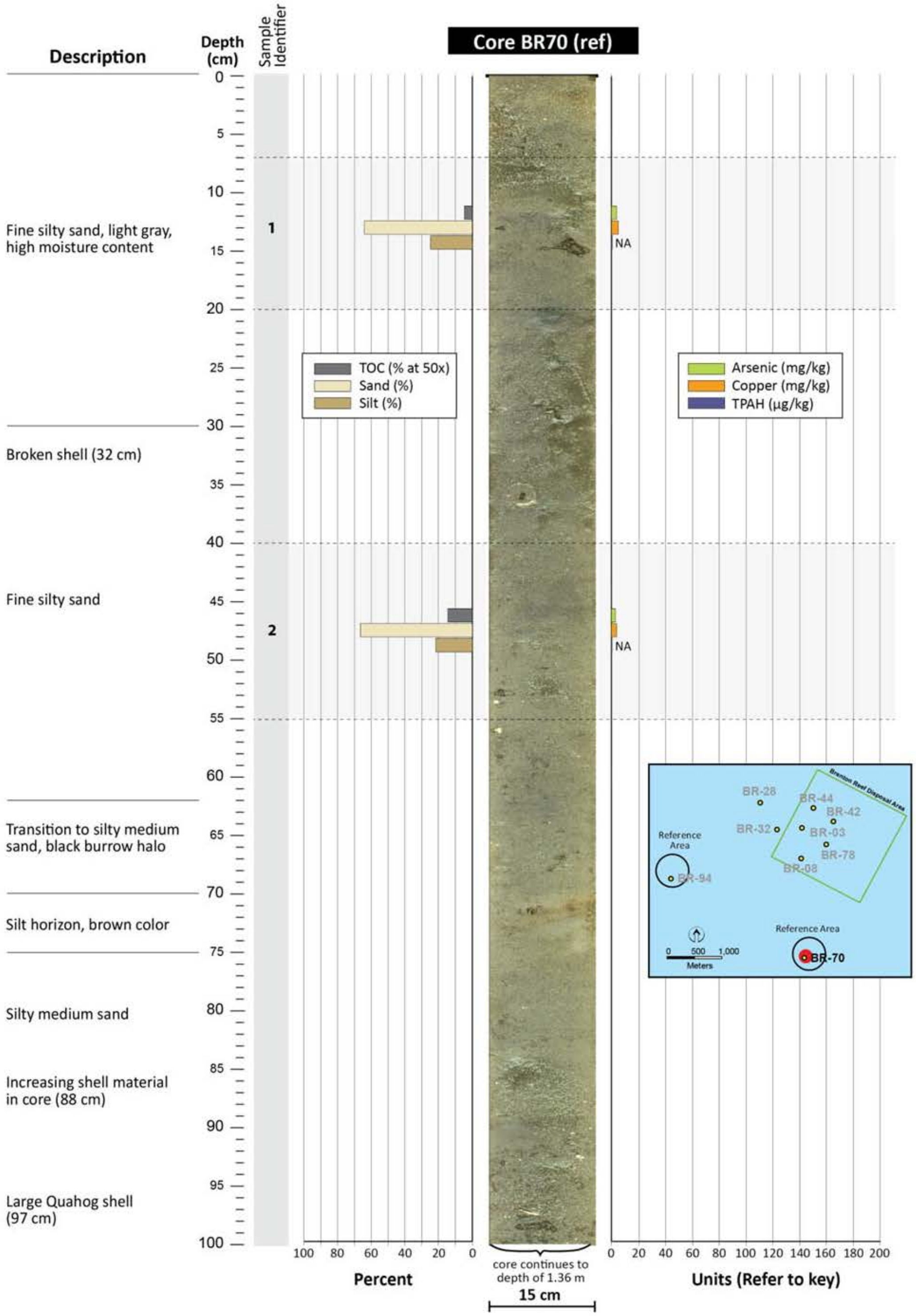

Figure 3-20a. Core BR70 characteristics, horizon descriptions and selected analyte values (0 to 1 meter)

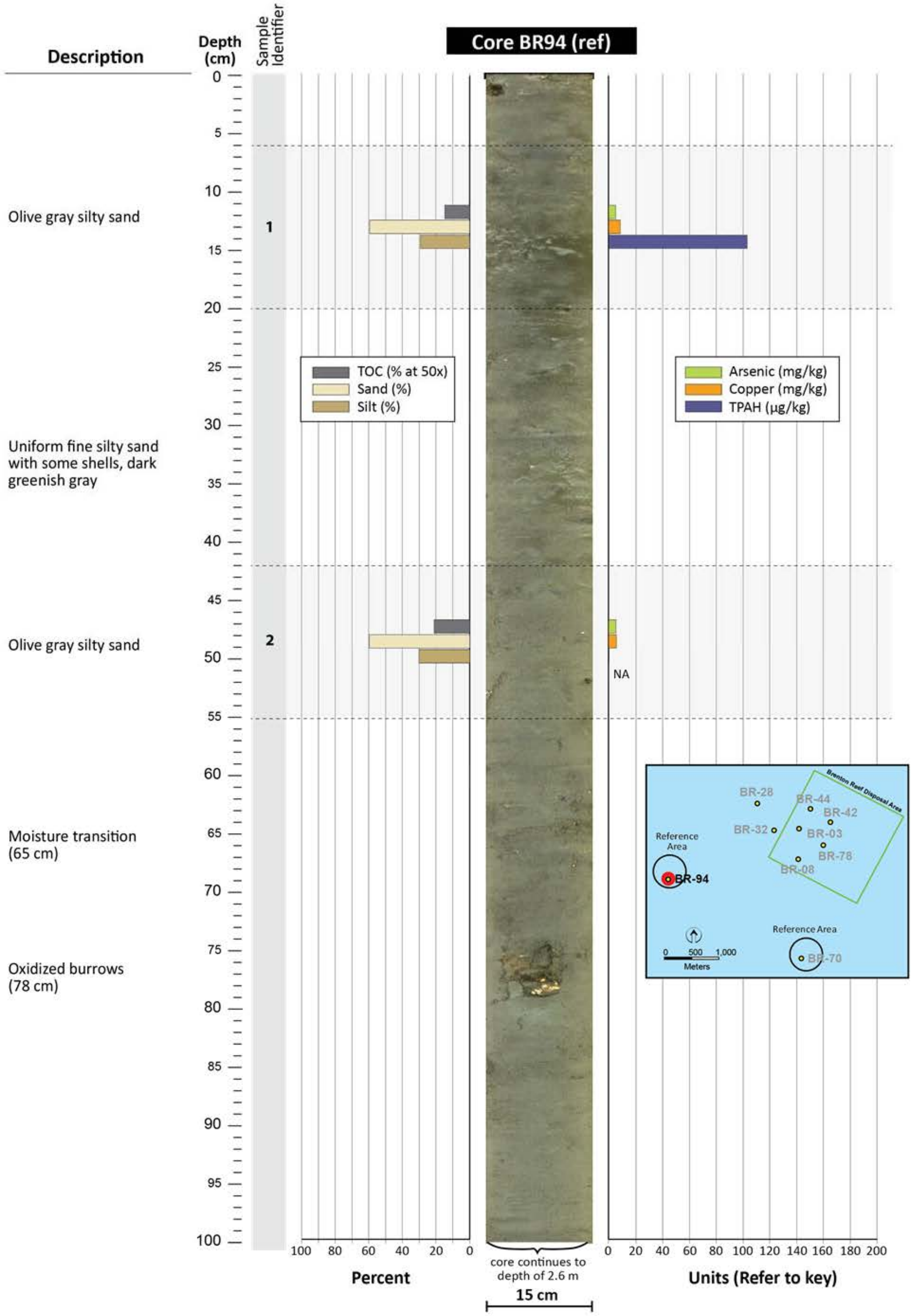

Figure 3-20b. Core BR94 characteristics, horizon descriptions and selected analyte values (0 to 1 meter)

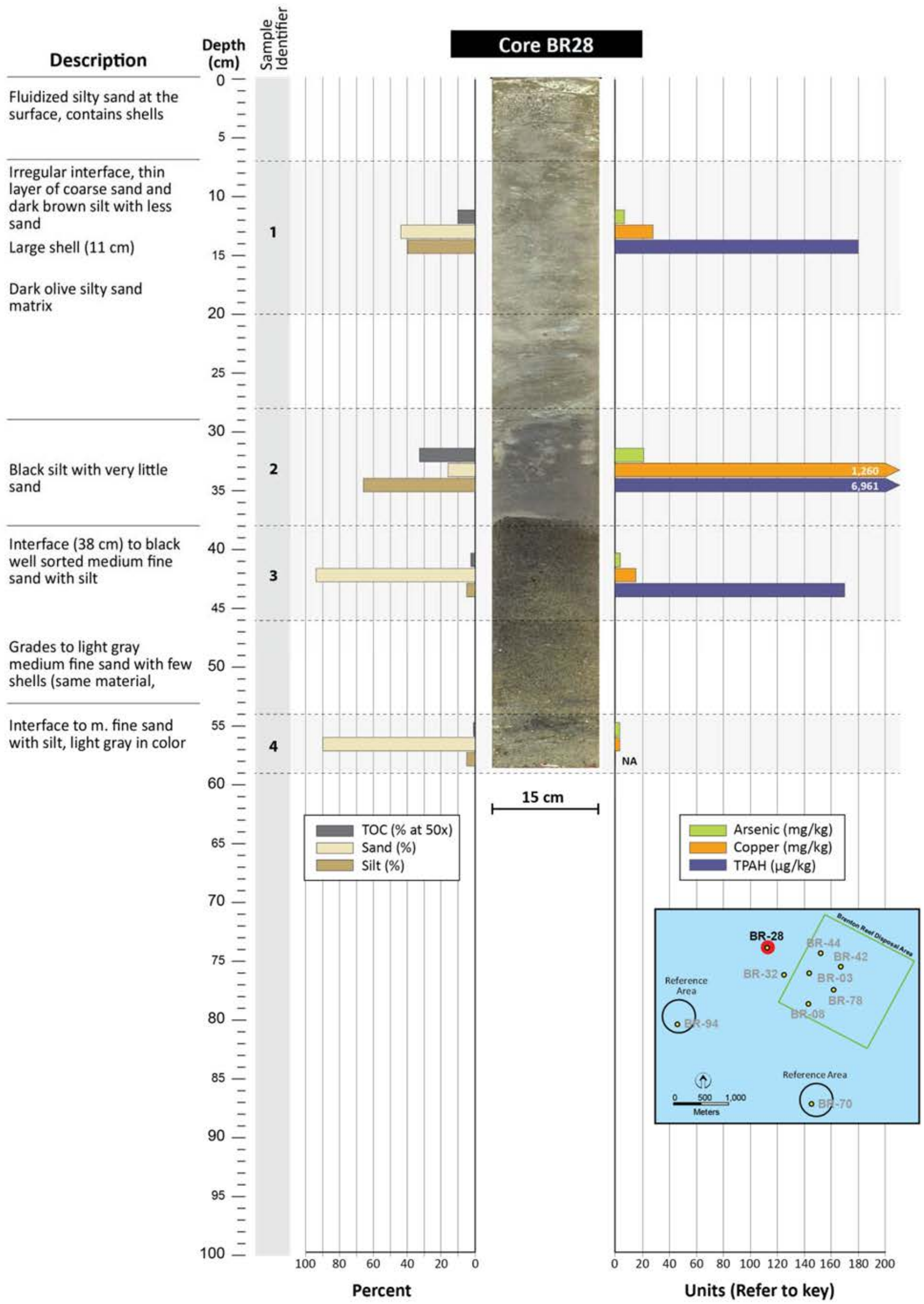

Figure 3-20c. Core BR28 characteristics, horizon descriptions and selected analyte values (0 to 60 cm)

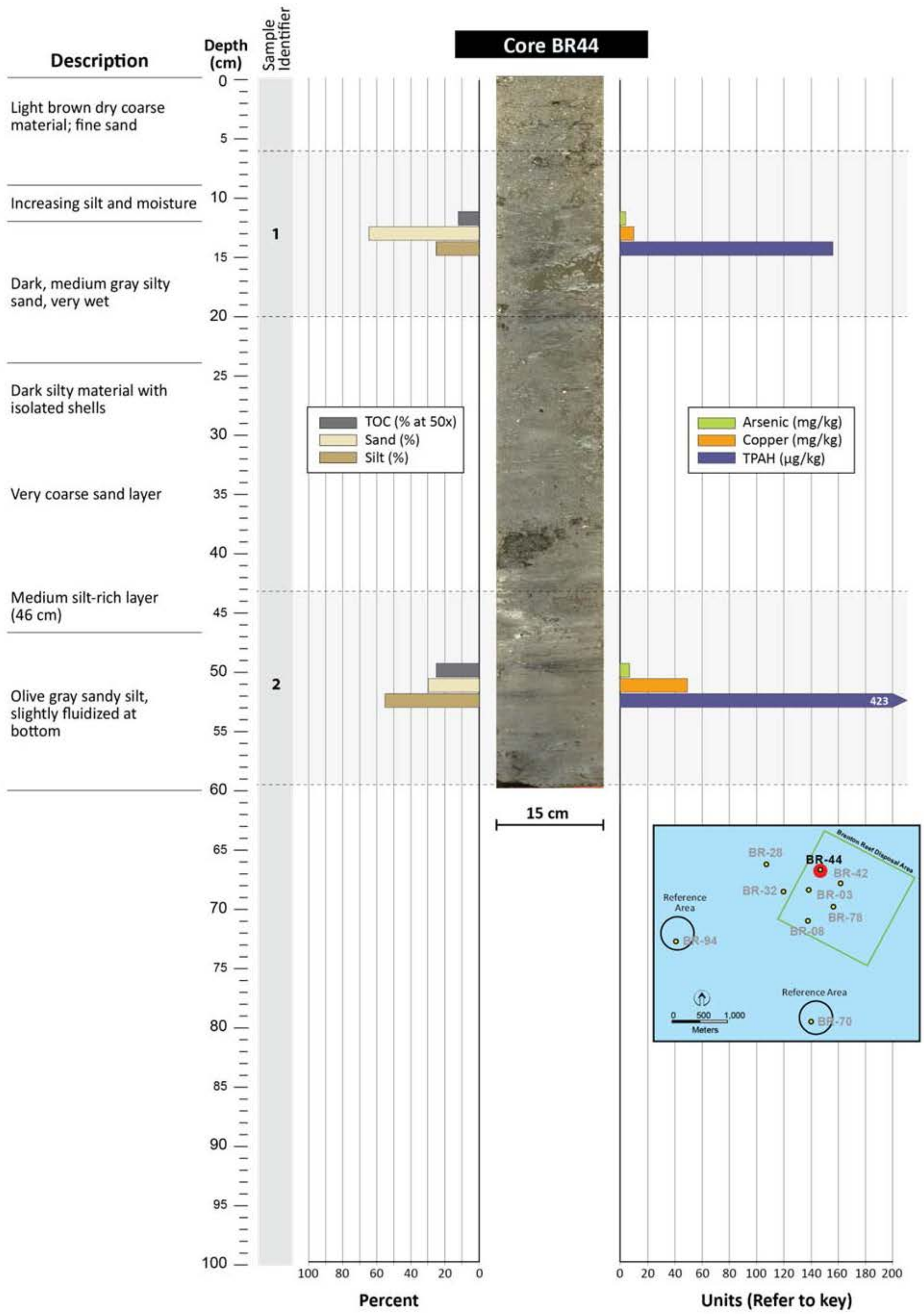

Figure 3-20d. Core BR44 characteristics, horizon descriptions and selected analyte values (0 to 60 cm)

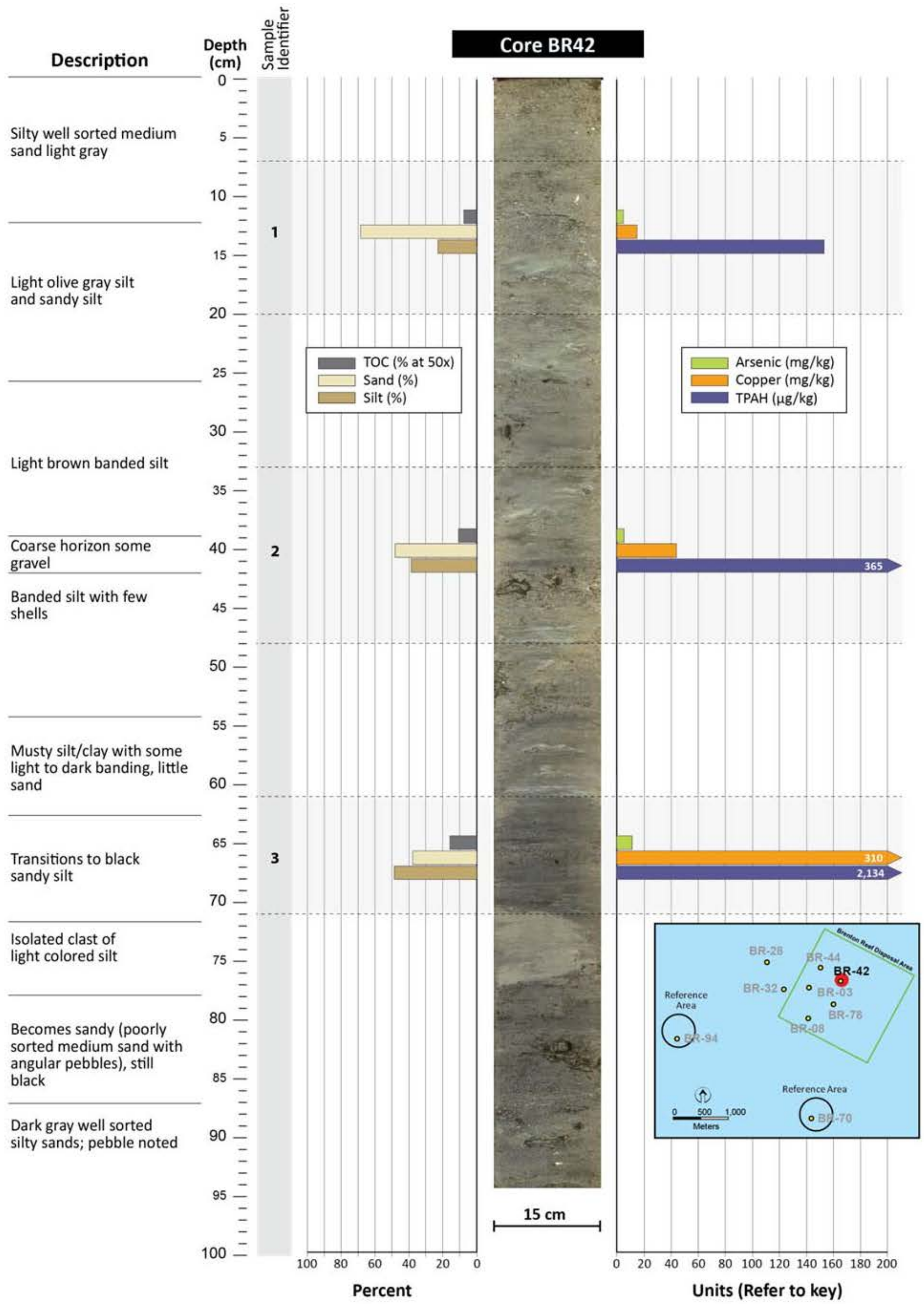

Figure 3-20e. Core BR42 characteristics, horizon descriptions and selected analyte values (0 to 1 meter)

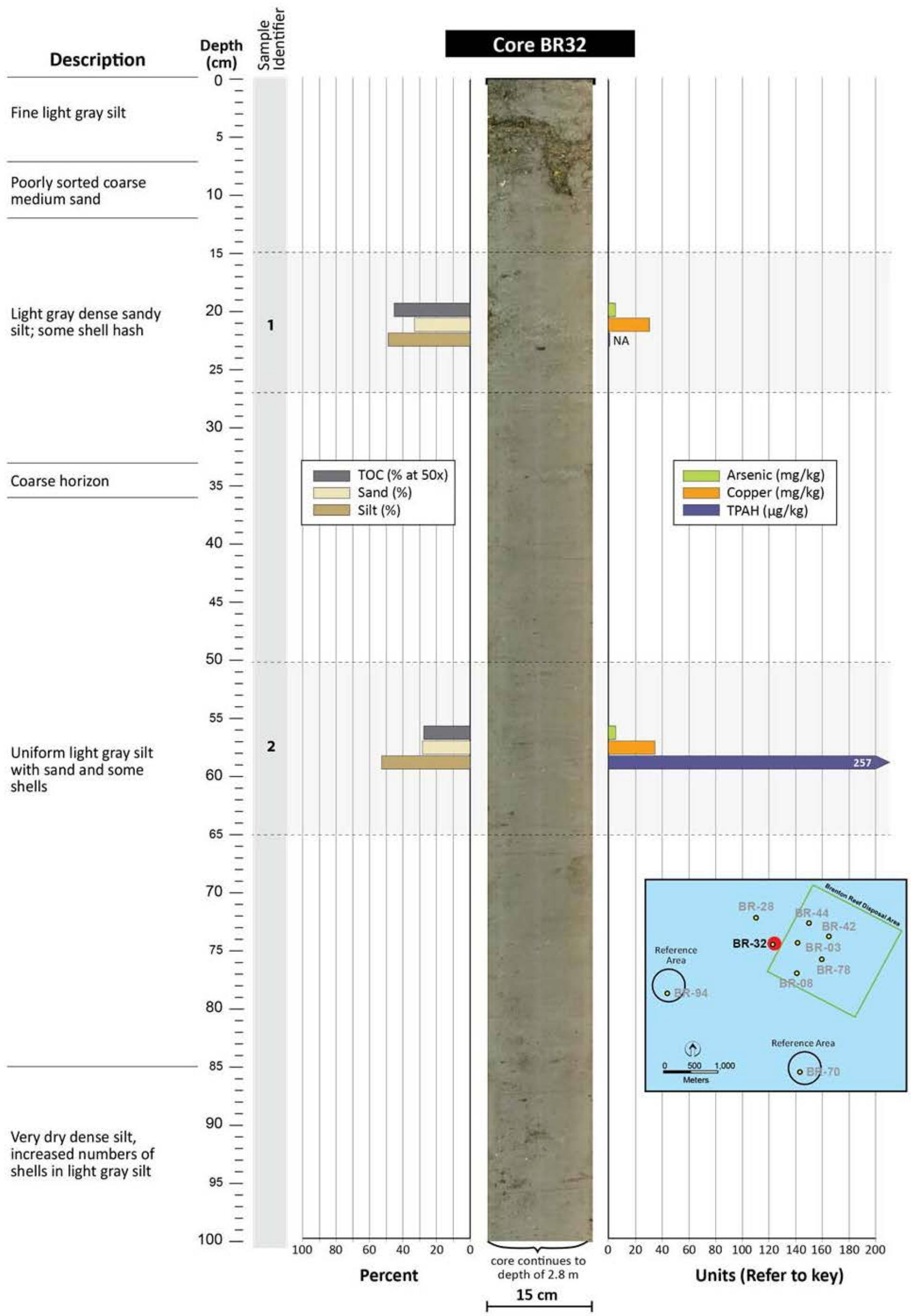

Figure 3-20f. Core BR32 characteristics, horizon descriptions and selected analyte values (0 to 1 meter)

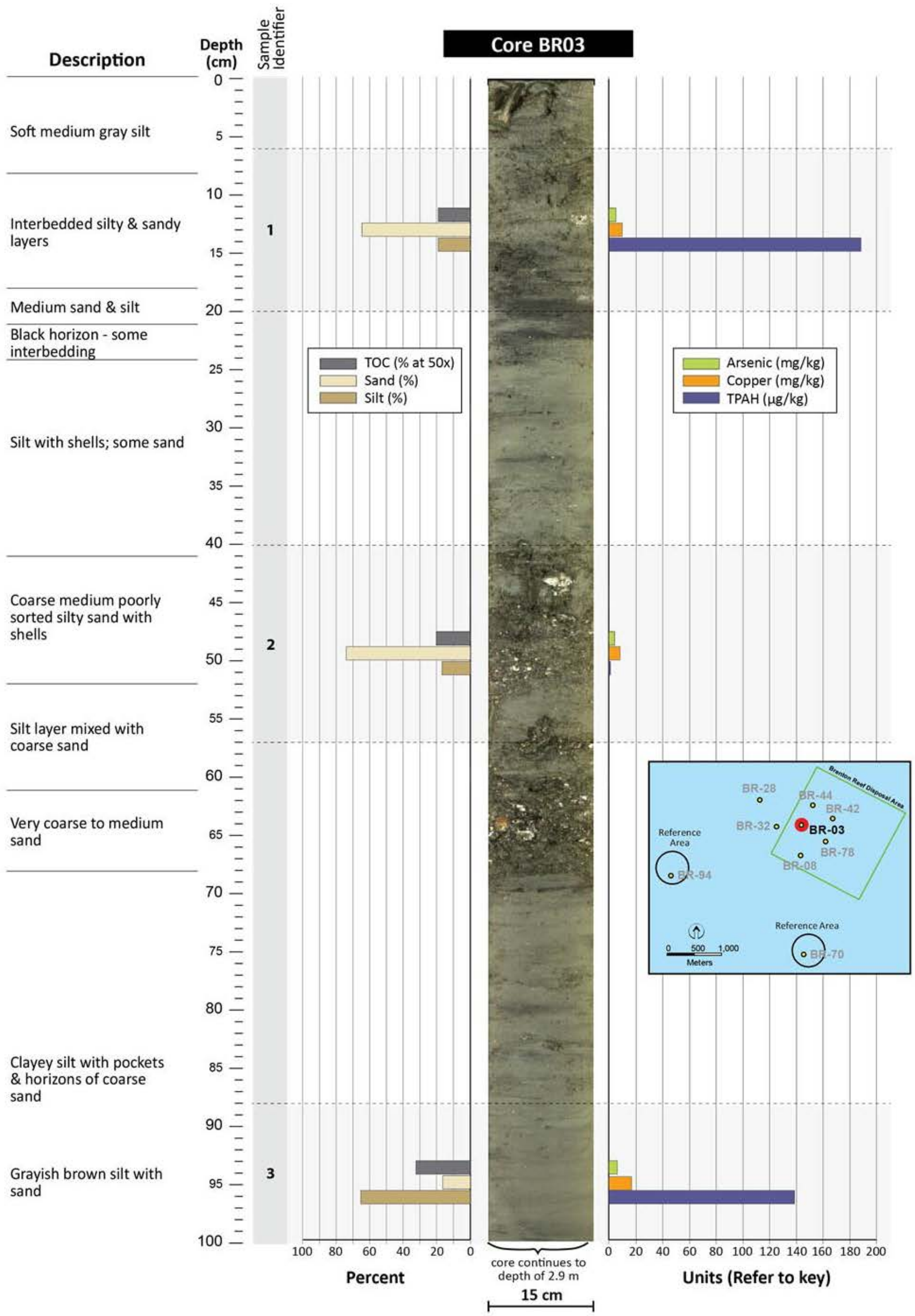

Figure 3-20g. Core BR03 characteristics, horizon descriptions and selected analyte values (0 to 1 meter)

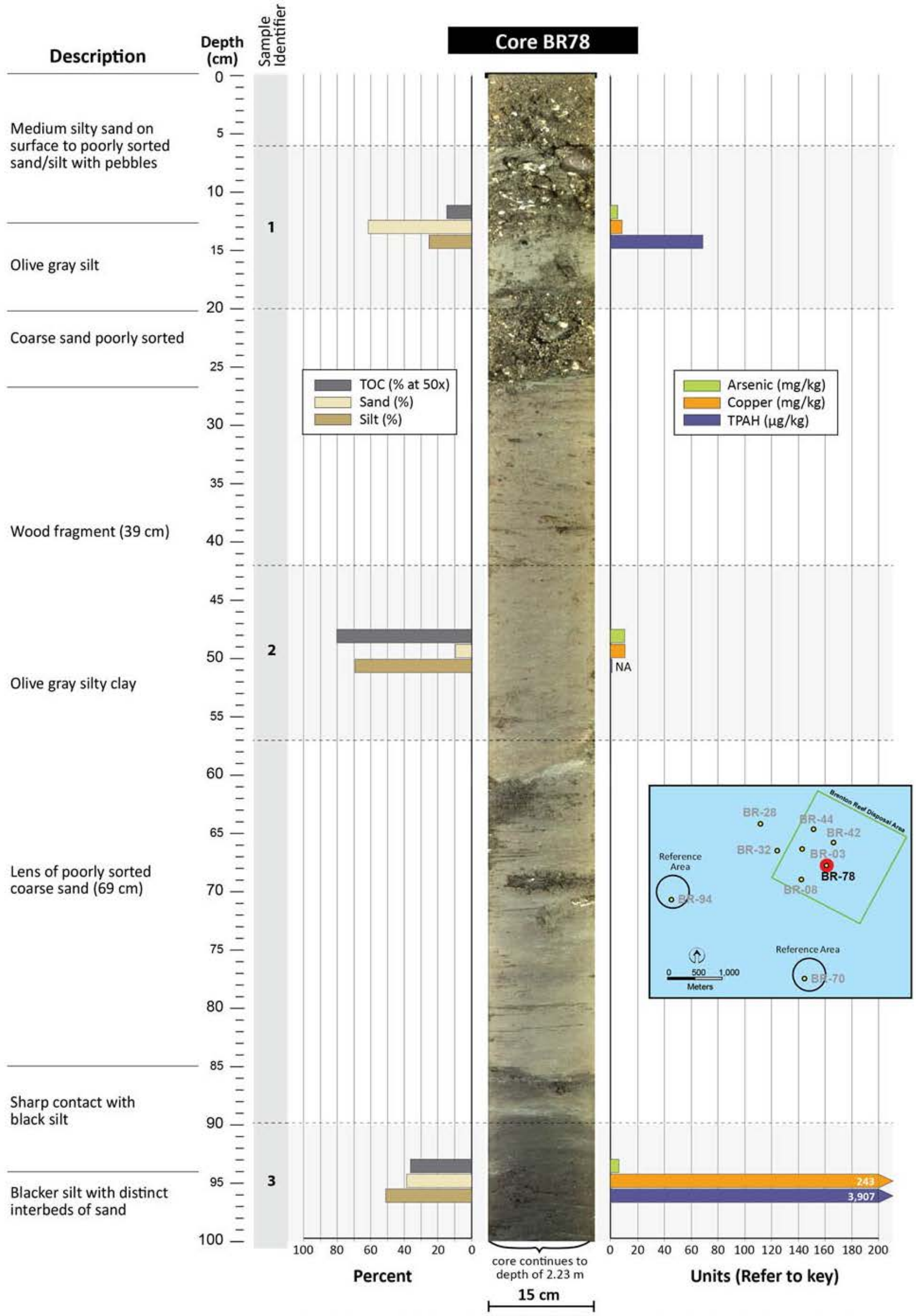

Figure 3-20h. Core BR78 characteristics, horizon descriptions and selected analyte values (0 to 1 meter)

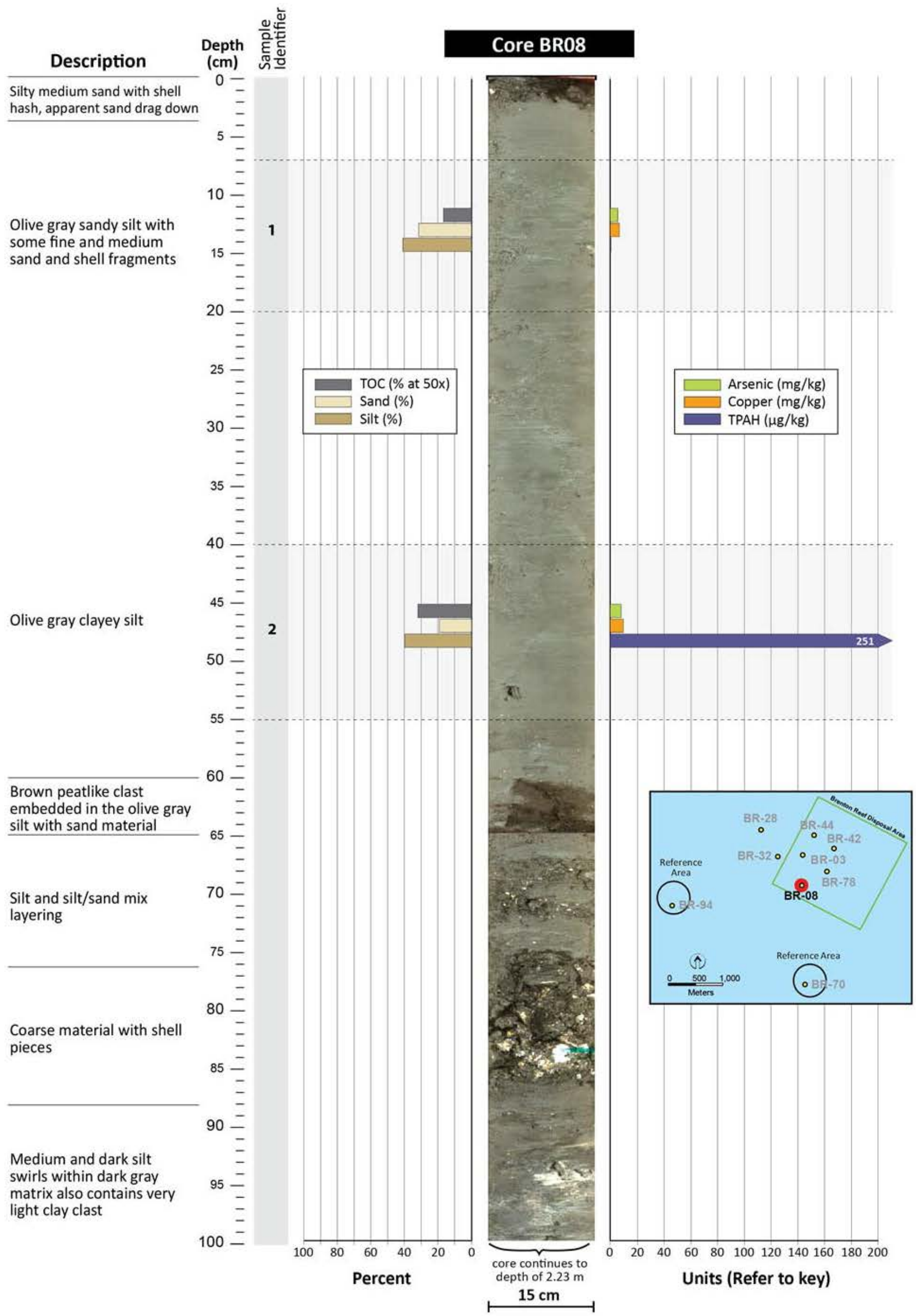

Figure 3-20i. Core BR08 characteristics, horizon descriptions and selected analyte values (0 to 1 meter)

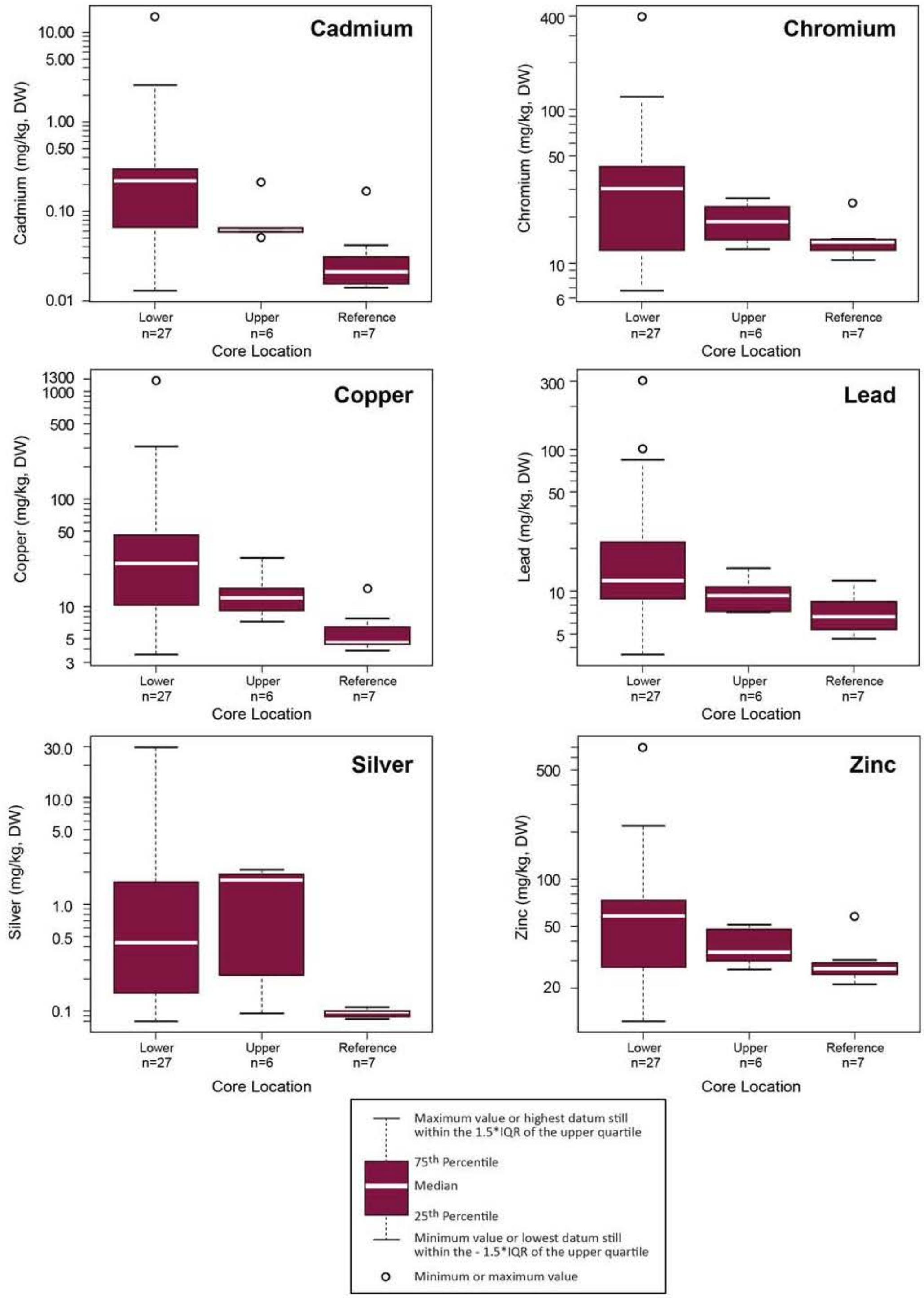

Figure 3-21. Boxplots showing distribution of metals concentrations in mound area and reference area samples

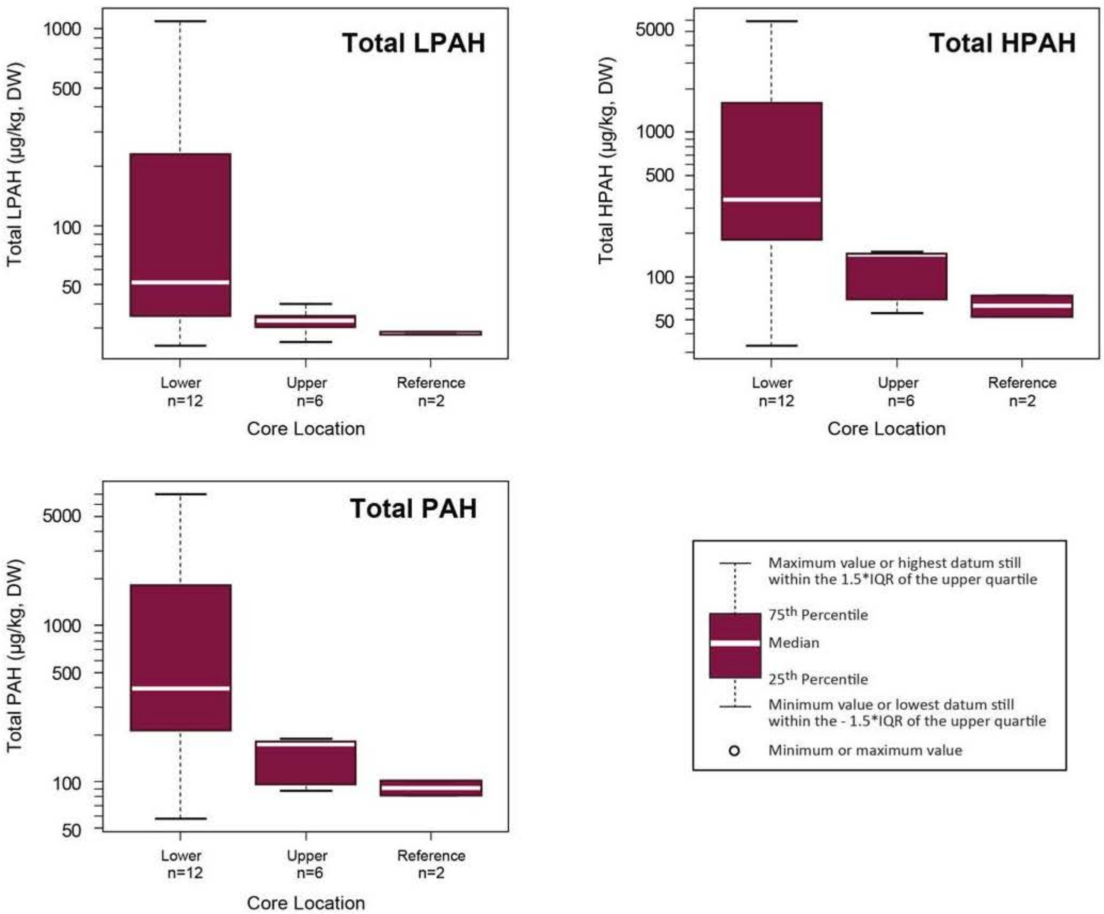

Figure 3-22. Boxplots showing distribution of low (LPAH), high (HPAH), and all PAH (LPAH + HPAH) concentrations in mound area and reference area samples

4.0 DISCUSSION

The presence of a dredged material placement mound on a shallow, nearshore sediment platform exposed to open ocean waves and currents provides a natural experiment in the long-term stability of mixed sediment deposits placed on the seafloor. From 1967 to 1971, silty dredged material from the upper Providence River was deliberately placed beneath coarser channel sediments dredged from the lower Providence River. The total volume of dredged material placed at BRDS from the Providence River Navigation Improvement Project (PRNIP) was approximately 6.9 million m^3. Additional coarse maintenance material from the Point Judith federal channel and sandy silt from the Brayton Point Power Plant channel was added between 1971 and 1973 (totaling approximately 0.27 million m^3). In September 2007, the mound still stood some 5 m above the surrounding seafloor in a broad, rounded shape that peaked at 25.5 m depth above a seafloor with average depths of 31 m. The mound represents a slight shoal on a broad sediment platform and would be expected to experience greater modification of surface textures from storm waves and currents than the surrounding seafloor.

The BRDS mound has been in place on this shallow platform for forty years with exposure to numerous storms. Because the material from the upper Providence River is known to have contained elevated levels of metals and PAHs, this special monitoring study was designed to assess the physical and biological condition of the mound's surface, and physical and chemical composition of the subsurface layers. Characterizing the sediments on and within this historical mound was expected to be useful for helping to evaluate the long-term prospects for success of more recent capped mounds and confined aquatic disposal cells.

Conditions at the historical BRDS mound were evaluated based on the review of the results of previous surveys and the phased monitoring surveys in 2007 and 2009. A reconnaissance survey was conducted in 2007 to evaluate the surficial characteristics of the mound and surrounding area. Data were collected using bathymetric, acoustic backscatter, SPI, and PUC techniques in support of the 2007 site-wide characterization. In 2009, a coring survey, guided by the 2007 survey findings, was conducted to assess the vertical distribution of sediment types and contaminants within the historical capped placement mound.

A conceptual model of the site was developed based on the results of early investigations and on a general understanding of the processes associated with open-water placement of dredged material. The mound was expected to contain a complex sedimentary structure formed by placement at the site of discrete barge loads of material (sediment and water) mechanically dredged from the Providence River. A wide range of sediment was transported to the site with high variability of texture, grain size and organic content both between, and within, barge loads. Some sediment consisted of fine silts with high organic content, while other sediment consisted of silts or clays with low organic content. As each subsequent barge load was placed at the site, layers of sediment built up, forming the mound. As a result, each mound layer is likely to have a complex signature of sediment types.

Dredging proceeded from the upper Providence River southward followed by 0.27 million m^3 of material from Point Judith and Brayton Point). In general, as a result of this process of placement, a deposit of finer, more organic-rich and contaminated upper Providence River material was expected at the bottom of the mound and coarser, low-contaminant-burden outer harbor material was expected on the top of the mound. Because the mound was not created in a rigorously engineered manner, and because of the additional placement of material at the end of the project, interlaying of the fine and coarse layers were expected within the mound, rather than a discrete boundary between the harbor material and a cap layer. However, a layer of less contaminated, coarser sediments was expected to be found covering the mound surface.

The surface of the mound and margin was expected to have evidence of deposition and reworking of both dredged materials and ambient sediments. Reworking should be most evident in the shallowest areas where ambient currents are relatively stronger and deposition most evident in the deepest areas where currents are relatively weaker with complex results based on the wide range of sediment types placed at the site. Early studies described concerns expressed regarding potential for adverse impact to fisheries. There was also concern about the potential for large-scale erosion, due to the site's relatively shallow depth and exposure to the open ocean to the south.

The conceptual model provided a framework for interpreting data collected during the 2007 and 2009 surveys. A discussion of the characterization of the physical, chemical, and biological conditions at BRDS mound is provided below along with discussion of findings in comparison to the conceptual model.

4.1 Physical Structure and Stability of the BRDS Mound

A general description of physical processes that can alter dredged material placement mounds and specific evidence of sediment transport and a discussion of the overall stability of the mound at the site are provided below.

4.1.1 General Sediment Dynamic Processes

Physical processes that can alter a dredged material mound in the seafloor environment include consolidation, anthropogenic activities, and natural processes. Consolidation, also known as sedimentary compaction, occurs in mounds as water introduced into the sediment during dredging and placement is compressed out of the pore waters by the weight of the overlying sediment (Silva et al. 1994, Poindexter-Rollings 1990). The consolidation process typically results in some reduction in the height and profile of the mound within the first several years after placement. Anthropogenic disturbances are activities, such as bottom fishing (trawling) and anchoring, that also result in alteration of the seafloor.

Natural processes that can alter sediments on the seafloor include physical processes associated with currents and biological processes associated with benthic organisms. Natural sediment transport processes locally remove finer sediments (which once suspended can travel farther before deposition) and leave behind coarser "lag" deposits that are too large to resuspend, or are moved a shorter distance through selective transport. Episodic storms may modify the surface, and during quiescent periods finer sediments may be deposited on the surface and be reworked deeper into the sediment by benthic organisms. Benthic organisms are typically active in the top 10 to 20 cm of seafloor sediment and mix surficial sediments through a variety of activities including feeding and burrowing. On the New England inner continental shelf, most current-driven resuspension and reworking activity occurs during about 5 percent of the year (Manning et al. 1994, Vincent et al. 1981). Closer to shore in shallower depths, current-driven reworking occurs more frequently (McMullen et al. 2007, 2008, 2009, Knebel et al. 1982), but the time-scales and degree of reworking have not been clearly established.

Over long periods of time (e.g., 100 years for processes controlled by very large storms) and broad areas, sediment textures often reach equilibrium with the time-averaged sediment transport characteristics of the location, which are dependent on sediment supply, water depth, current speed, and wave properties. The dredged material mound represents a juxtaposition of mixed layers of sediments with a wide range of sizes and a large-scale feature that is exposed to wave-induced currents during periodic storms. The introduced material has a sufficient supply of coarser grains (both sediment and shells) to potentially create a lag deposit that may "armor" the surface of the mound during most storms. If this is the case, the mound may be in a form of equilibrium with sediment transport conditions, but in a different equilibrium state than the surrounding seafloor.

4.1.2 Wave and Current Conditions

An analysis of worst-case storm events was conducted to evaluate the nature and extent of storm-driven near-bottom currents that the historical BRDS mound has experienced. The analysis was conducted using data collected by the USACE Wave Information System (WIS) and followed an approach similar to that of recent evaluations of storm-driven sediment transport in Massachusetts Bay (Butman et al. 2008, Warner et al. 2008).

The US Army Corps of Engineers has continuously collected wave data at buoy #63078 situated 15 km south of BRDS in 34 m of water (USACE 2010). These data are available from 1980 to 1999 and include dates, duration, significant wave height, wave period, and direction of extreme events. The ten most extreme storm events, as measured by wave height at buoy #63078 (Table 4-1) were analyzed to support characterization of worst-case storm events experienced at BRDS.

The largest or most extreme storm events in terms of potential to impact the BRDS mound are storms that result in the largest near-bottom currents. Storm recurrence intervals (e.g., a 100-year storm event) are typically calculated based on different factors, such as maximum storm surge along the coastline. As a result, recurrence intervals for storms potentially affecting the BRDS mound are not readily available. The largest storms of the past 20 years were evaluated (Table 4-1) and represent the largest storms occurring during one-half of the 40-year time span of the BRDS mound.

Major storms from the south and southeast are likely to generate worst-case wave and associated orbital near-bottom water velocities at BRDS and were the focus of this analysis. The BRDS is exposed to large, open-ocean fetches to the southeast and south, over a compass range of approximately 80º, from 20º south of east to 10º west of south (i.e., approximately 110 – 190 ºT). The BRDS is protected from long, open-water fetches to the east by Martha's Vineyard and to the west-southwest by Block Island and Long Island (Figure 1-1, inset).

The five largest storms measured at buoy #63078 between 1980 and 1999 were associated with Nor'easters. A Nor'easter is a type of macro-scale east coast storm traveling to the northeast from the south with leading winds coming from the northeast. Five of these ten storms came from the south or southeast and appear to be appropriate selections as worst-case BRDS storm events (Table 4-1). Near-bottom orbital water velocities associated with surface waves were estimated using a set of simplifying assumptions (Komar 1976; Hunt 1979). The United States Geological Survey (USGS) provides a linear wave calculation applet online for estimating near-bottom orbital velocity based on surface wave height, wave period, and water depth (USGS 2007). The

USGS estimation tool was utilized to obtain rough estimates of near-bottom velocities that were likely associated with the worst-case storm events.

A near-bottom orbital velocity of 1.3 meters/second was calculated as associated with the peak wave height (6.75 m) at the WIS buoy (at 34 m depth) during the Downslope Nor'easter of 1992. Four other storm events in Table 4-1 had waves from the southeast or south. Near-bottom orbital velocities associated with the peak wave height of the other four storm events were estimated to range from 0.8 to 1.1 m/s (Table 4-1). Concurrent surface wave and near-bottom velocities at the BRDS site, situated 15 km north of the WIS buoy, during these storm events are not known. However, based on bathymetry and orientation, it appears likely that, during storms from the south and southeast, the conditions at BRDS and at the WIS buoy would have been roughly similar. The water depths at the WIS buoy and at 1 km south of BRDS are the same (34 m MLLW; Figure 1-2). Water depths within BRDS range from 31 m (101.7 ft) adjacent to the mound to 25.5 m (83.7 ft) at the mound apex. Incoming surface waves driving from the south would have induced increasingly higher near-bottom velocities as water depths become shallower with distance northward and across the BRDS mound. In summary, near-bottom velocities at BRDS during worst-case storm events are not known, but may have reached peaks of approximately 1 m/s during several major storms occurring during the 1980 to 1999 time period.

In a related analysis, modeling studies were conducted on Rhode Island Sound using the historical wind field and the Grant-Madsen model of sediment transport (Battelle 2004). The model was applied to evaluate sediment erodibility in the BRDS area and predicted the distribution of sediment erodibility for 1.0-mm grain size sediments. According to the model, the BRDS lies in an area of high wave and current energy where erosion of fine sediments is expected. The Battelle 2004 model results suggested a relatively steep increase in erodibility between 33- and 25-m water depths. Within the BRDS area, sediments of 1.0-mm size (coarse sand) and smaller would be expected to be erodible according the modeling analysis.

4.1.3 Evidence of Sediment Transport

The surface of the mound does show substantial evidence of sediment reworking. The surface of the mound is marked by small-scale (1-20 m) heterogeneity in surface sediment type, bedform patterns, topography, and subsurface sediment type. This heterogeneity is apparent in the patterns of backscatter returns and the results from PUC and SPI images. This heterogeneity is unusually complex and appears to mark the confluence of direct deposition of heterogeneous materials from dredged material (cobbles, gravels, sand, and silt) and subsequent episodic reworking. Because the "source" sediment is not uniform, the patterns of deposition may influence the sediment transport patterns. For example, large patches of shell, gravel, sand, and silt may reflect the original pattern of deposition with minor reworking or may be the product of a more extensive reworking process.

The sediments surrounding the mound show some evidence of reworking (some fine sand in the surface layers, sediment transport patterns on the edge of the eastern shoal visible in Figure 3-6), but are not representative of a surface exposed to frequent high wave and current energy as demonstrated by the decades-long persistence of distinct disposal features.

Sediment transport processes in the area surrounding BRDS have been previously investigated. The mapped results of McMullen et al. (2007, 2008, 2009) identified areas of sorting and reworking at water depths of 33.5 – 39.3 m and areas of coarse bedload transport at depths ranging from 21.3 – 36.3 m (Figure 4-1). The areas of sorting and reworking in McMullen's map are deeper than the area adjacent to the mound described above (30.5 - 33 m; Figures 3-1 and 3-10). This suggests that wave and current activity is stronger or more frequent in the areas mapped by McMullen et al. at the same water depth, as compared to the BRDS mound-adjacent areas.

There is a broad ridge from 27.4 to 30.5 m depth that extends southwest from the broad platform east of the mound that may provide some protection for the area around BRDS from southerly swell (Figure 4-1). This ridge has been characterized by McMullen et al. (2008) as an area with coarse bedload transport which may correspond to the fine sand ribbons observed in the northeast corner of the survey area at a similar depth (Figure 3-6). Driscoll (1996) demonstrated in Block Island Sound that passage of five major storms between 1991 and 1994 had little effect on large-scale features of the seafloor, but they did observe changes in medium-scale features (sand waves with wavelengths of about 100 m).

Although much of the mound surface is modified from waves and currents, there is still clear evidence of individual barge disposal events around the margin of the mound and some distance away from the mound (Figures 3-4, 3-5, and 3-6). McMullen et al. (2009) also noted the visible presence of dredged material in the area identified as the June 1967 disposal area (Figure 4-1).

The steep seaward face of the mound is marked by short (50-150 m) linear features that appear to be interfingered fine and coarse sediment transport features. The coarse sediments extend down the slope as ribbon-shaped features, and the fine sediments extend up the slope in softer less well-defined features. The sand ribbons are 10-25 m wide tapering to fine tips pointing downslope south-southwest (SSW). The eastern margins of the sand ribbons are very well defined in most cases, and resemble small-scale sediment gravity flow features. The sand ribbons have distinctive windrows of large shells (weathered oyster and quahog shells likely derived from dredged material) and gravel. Along this face, it is difficult to determine the larger scale superposition of textures (i.e., whether coarse sediments have been transported over silts or silt features represent consolidated silt areas stripped of coarse cover materials). These linear features are consistent with episodic sediment transport along the seaward face of the mound from storm-generated bottom currents oriented N-S.

4.1.4 Scales of Identified Features

The complexity of features identified in the acoustic, PUC and SPI data was unusual for a dredged material placement mound. Because the BRDS mound showed evidence of specific sediment transport patterns in the larger context of variation in depth and source materials, it was helpful to group the identified features by scale into a sedimentary process classification model (facies model). This type of model gathers data and observations collected at different scales into groups organized by presumed processes (Reading 1996). The results of the model can be mapped to provide insights into the importance of the distribution of source materials (dredged material or ambient) and depth variations in the scale and frequency of sediment transport. This section provides an overview of the development and analysis of the facies model which is discussed in more detail in Appendix G.

The largest scale feature (1 km) identified in this survey represented the entire mound which is about 1600 m in diameter with a longer axis shoreward. This scale represents that portion of the study area with clear evidence of sediment transport and appeared to be depth controlled (sediments shallower than 30.5 m). The next largest scale (20-100 m) included groups of sediment features within the zone of transport, discontinuous transgressive sand sheets (a thin sheet of surficial sand that is transported over other sediments), lag (winnowed) deposits, shell windrows, and reverse-graded gravel beds. The next largest scale (1-20 m) included sediment transport features such as individual sand ribbons, lag windrows, and gravel beds. The smallest visible scale (10-100 cm) consisted of graded beds within sand and gravel sheets, and thin sand layers on mud.

In order to resolve some of the complexity of the sediment features and provide a descriptive sediment process framework for the study area, nine ‘facies’ were defined (Table 4-2) based on analysis of PUC and SPI images. Facies are generally used to describe the sum of characteristics of a sedimentary unit at a small (cm-m) scale (Reading 1996). In this study, facies is simply a descriptive classification of imaging results into process classes (a small sedimentary unit formed by specific processes and source material, such as transgressive sands).

The distribution of the facies demonstrated that the sediment transport activities were most pronounced over the south slope and top of the mound (Figure 4-2). Lag deposits, shell windrows, and gravel dominated the southern edge of the mound while transgressive sands and gravels were clustered on the top of the mound and between shell windrows and reverse-graded gravels along the northern margin of the mound. These facies were characterized by shallow penetration depths of the SPI camera indicating firm, consolidated sediments (Figure 3-12). They exhibited mixed boundary roughness with lower values in the transgressive sands and higher values in most of the lag and gravel deposits (Figure 3-13, but see Appendix G Figures G-2, G-3, and G-4).

Burrowed silts and sandy silts surrounded the mound and mound margins and were intermixed with thin lag deposits on silt and thin sand layers. The burrowed and sandy silts were characterized by deeper penetration depths indicating less consolidation due to bioturbation activities (Figure 3-12). They also exhibited mixed boundary roughness, with most texture coming from biological features (Figure 3-13 and Appendix C). The distributions of these facies are consistent with the conceptual model, descriptive results from 1987 (SAIC 1990), and results of wave modeling that suggested the slight elevation of the mound above the surrounding seafloor might be sufficient to trigger sediment reworking of coarse sediment during episodic storms. These results are also consistent with additional quantitative analysis of acoustic backscatter data performed to support characterization of surficial features (Appendix G).

4.1.5 Overall Mound Stability and Internal Structure

The height and shape of the mound were virtually unchanged over the past 40 years (compare Figure 1-2 from 2007 survey with Figure 1-5c and Appendix A, from historical surveys). The persistence of the mound and its presence at a water depth of 31 m suggests that the sediment transport patterns on the mound surface may represent a form of dynamic armoring. The consistency of the size and shape of the mound over the years indicates that very little material has been completely eroded from the mound despite clear evidence of surface sediment modification through periodic sediment transport. Although the time span of the mound (40 years) is short compared to the cycle time of 100-year storm events, nor'easters and hurricanes have done little to modify the large-scale morphology of the mound.

Further, the region surrounding the BRDS has been remarkably stable for many decades. The bathymetric surface created from multibeam acoustic data collected in 2007 (Section 3) was compared to a bathymetric surface created from lead-line survey data collected in 1939. The 1939 survey was conducted by the National Ocean Service and was corrected by -13 cm to account for NOAA's published regional sea level increase and to adjust to the MLLW from the original Mean Low Water datum. Multibeam data collected in 2007 at a substantial distance from the mound were compared to lead line data collected in 1939 that had been adjusted for sea level rise and tidal datum differences. This comparison found an average depth reduction (shoaling) of 28 cm, or an approximately 0.4 cm per year sediment deposition rate over the 68-year period from 1939 to 2007. It is important to note that uncertainties associated with data acquisition, tidal adjustments and sea level rise may contribute significantly to this depth difference estimate.

The interpretation of the internal structure of the historical BRDS mound was based on analysis of the sequential bathymetric profiles and cores collected from the mound. The sequence of bathymetric surveys from 1968, 1969, and 1970 capture two critical phases in the development of the mound (Figure 1-5). After the first phase of dredging in May 1968, the bathymetric survey in July 1968 captured a flat deposit typical of less consolidated upper Providence River material (Tables 1-2 and 1-3). Survey reports identified high-organic, fine-grained material at the site (Saila et al. 1969). After the second phase of dredging in October 1969, the bathymetric survey captured a conical mound typical of coarse grained material from the lower Providence River (Figure 1-5 and Table 1-2). Survey reports identified coarse-grained material covering the high organic fine-grained material (Saila et al. 1969). After further deposition, the September 1970 bathymetric survey showed evidence of coverage of the initial deposit with a much broader distribution than in October 1969 (Figure 1-5 and Table 1-2). Subsequent to the 1970 survey, additional material was deposited and then presumably covered with material from Point Judith and Brayton Point. Some of this material was investigated in 1972-1973 by URI and found to be very heterogeneous. Later, in 1978, the mound was found to be covered with well-sorted sand over silt with silt on the mound margins. All subsequent surveys have confirmed evidence of armoring of the mound surface with lag deposits of coarse shells, gravel, and sand (Figures 3-10 and 4-3, SAIC 1990). These results broadly support the conceptual model of a consolidated mound with a coarse layer covering horizons of interbedded silts and sands; the finer structure was investigated with vibracores.

One of the objectives of the study was to sample each part of the complete sequence of the mound (cap material from the lower reaches of the Providence River and Brayton Point, Upper Providence River material, and ambient material). Although it is clear that the study was able to collect samples from each of the elements, it does not appear that any one core sampled the entire horizon of the mound into ambient material. Because of the compact coarse sediment on the surface of the mound, only three of the cores (BR28, BR42, and BR78) were long enough to potentially sample the ambient sediment below the mound based on estimated dredged material thickness calculated from the change in depth from 1939 to 2007 (Table 4-3). However, it was necessary to use multiple lines of evidence to determine the provenance of sediment layers within the cores due to the complexity of sediments from core to core.

The presence of estuarine shells (oysters, slipper shells, quahogs), poor sorting, very well-sorted sands, interbedded silt and sand, layering of silts, pebbles, rocks, peat, clay and enriched PAH or metal profiles was indicative of dredged material. The presence of ocean quahogs, thick sequences of silty sand and burrow halos was indicative of ambient material. The lithological and chemical evidence supports a conclusion that none of the mound cores sampled ambient material (Appendix D).

The presence of large oyster shells at the bottom of core BR78 and the distinct fine well-sorted sandy silt beneath it; the presence of quahogs (*Mercenaria* sp.) oyster shells (*Crassostrea* sp.) at the bottom of core BR32; the black silty clay, silt clast, and poorly sorted sand at the bottom of BR42; the alternating layers of dark, light gray, and black silty clay at the bottom of BR03; and the silty clay at the bottom of BR08 all suggested dredged materials (Figure 4-3). BR44 was too short to have sampled ambient material, and the lowest horizon had elevated TPAH and metals (Table 4-3 and Figure 3-20d). As short as BR28 was, it still might have encountered ambient material based on uncertainties in the depth difference map (Figure 4-4). The deepest horizon in this core (BR28-4, 54-59 cm) was analyzed for sediment properties and metal concentrations (Figure 3-20c and Table 3-2). Metal concentrations were low in medium to fine well-sorted sand with traces of silt and shells, with a very distinctive interface to the contaminated black silt above (Figure 4-5). This well-sorted fine sand was not present in the reference core samples but might have been similar to an unsampled sand horizon near the bottom of BR70 (Figure 3-20a).

Further analysis of lithology and chemistry supported the conclusion that the mound cores sampled dredged material and reference cores sampled ambient material (Appendices E and F). The mound cores were not long enough to reach what are likely more highly contaminated sediments deep within the mound. Only unequivocal sampling of ambient sediment at the base of one of the mound cores would verify sampling of the full sequence including all phases of upper Providence River dredged material placement. The details collected on the fine structure of the inner layers of the mound are incomplete, but they are consistent with the conceptual model of a stable mound with a coarse layer covering complex horizons of interbedded silts and sands. This model does not predict a clear 'stratigraphy' with marker horizons to distinguish UDM from CDM, but predicts interbedding of horizons with the finest, most highly contaminated sediments near the bottom of the mound just above ambient material.

4.1.6 Comparison with Sediment Texture from Previous Surveys

The SPI results of sediment texture from 2007 are consistent with SPI results collected in October 1987 (SAIC 1990). Reference SPI stations in 1987 were located west, east, and southeast of the historical BRDS mound, and a grid of stations was sampled over the mound extending well beyond any apparent dredged material. Dredged material (cobbles, and shell lag) was detected along the eastern margin of the site at one reference station and one grid station, both in the vicinity of 2007 station BR-81 (classified as lag with cobbles) and the disposal impact features observed in the backscatter data (Figures 3-6 and 4-2). Coarse dredged material, evidence of winnowing, lag deposits, coarse shells, cobbles, and sand over mud stratigraphy were observed over the mound area in 1987 in a distribution very similar to that observed in 2007 (compare Figure 3-4, SAIC 1990 with Figure 4-2).

The reference areas in 2007 were located west, south, and southeast of the BRDS in different locations from 1987. Historical records consulted after the survey indicated that an unknown volume of dredged material from the upper Providence River was placed south of BRDS in November, 1967 (Figure 1-3). Potential evidence of this disposal is visible in the backscatter image in the form of disposal impact features (Figure 4-2). Disposal features are not evident in the backscatter at any of the 2007 reference areas, but the SPI results from Ref-W did reveal layers of sandy silt that might be consistent with older fine-grained dredged material (Figure 3-7).

4.2 Biological Recovery

The sequence and pace of recovery of benthic communities after dredged material placement is well-documented, particularly in New England waters (Germano et al. 2011). The coarse condition of much of the sediments and apparent episodic sediment reworking on the surface of the mound would tend to favor benthic communities that adapt quickly to disturbance and lower organic content in the sediments. These communities may not be exactly the same as those adjacent to the mound, but likely reflect communities found in sediments at similar water depths further inshore. Based on extensive evidence from other dredged material placement mounds, the benthic communities on the surface of the mound should have long since recovered from the disturbance of mound creation (Germano et al. 1994). Because the mound is shallower and covered in relatively coarse sediments, it might also be expected to differ from the benthic conditions in the softer, fine-grained sediments adjacent to the mound, including the stations used as reference areas in this study.

In the results from the SPI survey of September 2007, all of the replicate images from the reference areas showed the presence of Stage 3 infauna, indicating a uniformly advanced successional status. At the mound stations, a lower percentage of replicate images had evidence of Stage 3 infauna, although most of the stations had at least one replicate image with Stage 3 (Figure 3-14). The results suggested a lower density of Stage 3 infauna over the mound compared to the reference area, which is attributed to the coarser sediment (sand and gravel) at the mound. Stations with coarser sediment at, and immediately around, the mound apex therefore appear to have experienced somewhat lower rates of biologically-mediated sediment reworking compared to stations with soft muddy sediment on the margins of the mound and at the nearby reference areas. The results for successional stage were consistent with the results from 1987, with Stage 1 and indeterminate results over the apex of the mound and Stage 1 on 3 or Stage 3 over most of the mound margin and reference areas (SAIC 1990).

The aRPD depth provides a time-integrated measure of the balance between bottom oxygen levels and the degree to which sediments are reworked by infaunal organisms. When biological activity is high, the aRPD depth generally increases; when it is low or absent, the aRPD depth decreases. On a comparative basis, the mound and reference area stations did not differ markedly in average aRPD values (1.7 versus 2.0 cm). The 0.3 cm difference is very slight, and the two station groups had similar variability as reflected in their standard deviations and ranges (Table 3-1).

All of the reference area stations were characterized by relatively soft, muddy sediments. In contrast, sand and gravel occurred at almost half of the mound stations, particularly those located near the apex. Due to the presence of fine to coarse sand lacking any vertical color contrast typically associated with the redox layer, the aRPD depth could not be measured (indeterminate) at 26% of the mound stations (Table 3-1, Figure 3-15).

In summary, the presence of Stage 1 fauna and frequent indeterminate classification of successional stage and aRPD depth at mound stations is consistent with the conceptual model of a mound with coarse sediments and episodic reworking. The presence of Stage 3 fauna throughout the study area and at apparent higher densities at the mound margin and at reference areas stations was consistent with the conceptual model and patterns of benthic recovery from dredged material placement observed throughout New England (Germano et al. 2011).

4.3 Isolation of Mound Sediments

Once a deposit of dredged UDM, such as that from the PRNIP, has been placed on the seafloor, covered with sufficient additional sediment to limit disturbance by bioturbation, and consolidated, the pathways for contaminant exposure to organisms or release of contaminants to the overlying water column are limited. Most metals and PAH compounds typically found in harbor UDM are tightly bound to organic-mineral aggregates; the primary diagenetic (chemical and physical change in sediments after deposition) processes affecting dissolved contaminants are molecular diffusion and chemical reactions (Murray et al. 1994). Although a variety of chemical reactions (oxygen consumption, metal oxide reduction, sulfate reduction) can affect concentrations of contaminants in sediment pore water, only molecular diffusion or physical disturbance can move these dissolved chemicals to the sediment surface at a site such as CLDS. This is because sediments outside of the influence of terrestrial hydrogeologic systems are saturated with seawater under a uniform hydraulic pressure, i.e., there is no driving force for advection of pore water through the sediment layers.

Molecular diffusion rates are slow; worst case models suggest greater than 500 years for a 50 cm cap to reach breakthrough flux (5% of steady-state flux at the surface of the cap, Murray et al. 1994). These model results and reports from a wide range of capped mounds provide evidence that a relatively thin, stable layer of suitable cap material can effectively isolate UDM from the marine environment (Fredette et al. 1992, ENSR 2005, Carey et al. 2006).

Although the capping of the more contaminated material from the Upper Providence River at the BRDS was not specifically engineered (i.e., with documented placement and clear demarcation between the UDM and overlying cap; SAIC 1995 and Palermo et al. 1998), based on the volume of material placed at the site and the relative proportion of the material from the lower reaches of Providence Harbor, the surficial material was expected to be effective in isolating Upper Providence River UDM at BRDS. Previous surveys at BRDS indicated that this was the case (Pratt et al. 1973, SAIC 1990). The 2009 coring survey at the site was intended to assess the upper structure of the mound and isolation of contaminants nearly 40 years after the creation of the mound.

The conceptual model of the historical BRDS mound included the consideration that the combination of maintenance and improvement dredging that was part of the PRNIP would have removed unconsolidated industrial-era sediment along with both unconsolidated and consolidated pre-industrial sediments. For such sites, the simple image of a capped placement mound with ambient sediment covered by a homogeneous layer of UDM and a distinct, homogeneous layer of cap material is not realistic (Myre and Germano 2007). Rather, the mechanical dredging and scow transport-disposal operations of the PRNIP were expected to result in highly heterogeneous UDM and capping sequences at the BRDS mound (Fredette et al. 1992 and ENSR 2005).

With this conceptual model of BRDS mound structure, it was expected that each core of the 2009 survey would intersect a different sequence of placement and depositional history of the site, but it was also expected that a general assessment of structure and isolation of UDM could be made. Cores collected near the apex of the BRDS mound were expected to have sequences of coarse sediments at the surface and a very thick, complex lithology deeper in the core (BR32, BR03, and BR08 in Figure 3-20). Cores collected near the margin of the mound were expected to have a mix of coarse and fine sediments at the surface and variable thicknesses of complex lithology that might include PRNIP as well as Brayton Point and Point Judith sediments (BR28, BR42, BR44, and BR78 in Figure 3-20). The assessment of mound structure and isolation involved examination of core chemical concentrations compared to ambient sediment concentrations from Providence Harbor and Narragansett Bay. To place the results in context, the results were compared to accepted sediment quality guidelines, and an evaluation of the potential for chemical exposure to the benthic environment was made, as discussed below.

4.3.1 Comparison to Regional Sediment Concentrations and Guidelines

Ideally, the chemical concentrations from the 2009 cores would be evaluated in the context of the range of sediment concentrations from the original PRNIP. As detailed chemistry data from that project were not available, data from two other sources were used, historical deposition in Narragansett Bay and a later Providence Harbor dredging project. Cores collected in depositional areas of Narragansett Bay and reported by Nixon (1995) show spikes of metal concentrations peaking in subsurface sediments (e.g. Pb and Cu in Figure 4-6) assumed deposited from the late nineteenth through mid-twentieth century when industrial inputs into the Bay were unregulated. These contaminants were biologically mixed into the upper sediment layer through deposition, which served to flatten the curve of the contaminant profiles. Moving down these cores, concentrations diminished to pre-anthropogenic conditions. As the PRNIP included both maintenance and improvement dredging, the material removed was expected to span the full profile of concentrations shown in Figure 4-6, contributing to the expected heterogeneity over very small scales.

As the name implies, the Providence River and Harbor Maintenance Dredging Project (PRHMDP) was a maintenance project required by the active deposition of sediments into the channel areas in the decades following the PRNIP. As part of the planning for the PRHMDP, sediment samples were collected in 1992 and 1993 from the same reaches dredged in the PRNIP. Sediment testing data from these samples were compiled and classified according to the final suitability determination for the Providence River reach where the samples originated (USACE NAE 2001). Although surficial sediments were undoubtedly much less contaminated than those removed during the PRNIP, samples from some reaches in the inner portions of the harbor (Upper Providence River) were classified as unsuitable for open water placement (UDM). All other PRHMDP samples were classified as suitable for open water placement. The

PRHMDP sediment data were compiled into suitable and unsuitable subsets and compared with the BRDS 2009 mound and reference area core data (Figure 4-7).

Concentrations in the upper core samples (6-20 cm) from BRDS were consistently below the range of suitable PRHMDP samples and overlapped the concentration range of reference area samples for all metals (except silver which was not evaluated in the PRHMDP testing) and total PAHs (Figure 4-7). Concentrations in the lower core samples (below 20 cm) from BRDS were below the concentration range of unsuitable PRHMDP samples and overlapped the range of suitable PRHMDP samples for metals and total PAH with the exception of one sample, BR28-2, collected from below the surficial level at a depth of 28-38 cm. For this sample, a gradient in concentration was not apparent above or below the peak concentration (Figure 3-20c), suggesting an isolated layer in the heterogeneous mix of material at the site.

Sediment chemistry measurements were compared to existing sediment quality guidelines (SQGs) to see if core samples would be identified in a screening level assessment for the presence of contaminants of concern (USACE/USEPA 1991). Because there are no applicable regional guidelines, two sets of established, relatively conservative national guidelines were selected and applied (Berry et al. 2002). Two "upper end" SQGs: the ERM (Effects-Range Median, Long and MacDonald 1992) and the PELSW (Probable Effects Level-Saltwater, MacDonald et al. 1996) were selected (Table 4-4).

Sediment chemistry data from the seven BRDS mound cores and two reference area cores were compared to the SQG data provided in Table 4-4. Any sediment chemistry concentrations greater than the reference SQG concentrations were identified and tabulated with a calculated exceedance factor (Table 4-5). Silver concentrations were reported at or slightly above SQGs in a number of samples, but there were no other exceedances of the national sediment quality guidelines for the surficial samples. Of the deeper samples, only BR28-2 noted above consistently exceeded the SQGs.

4.3.2 Potential for Contaminated Sediment Exposure to the Benthic Environment

The process of bioturbation is the most rapid diagenetic process occurring at a site like BRDS and, hence, the mechanism most likely to result in transport of deeper contaminants into the upper sediment layer with potential exposure to the benthos. The maximum anticipated thickness of the active biological layer is a common consideration in cap design for sequestering contaminated sediments (Rhoads and Carey 1997). Planned cap thicknesses can be 0.5-1 m to provide a safety factor at sites where physical disturbance is a concern, but the active biological layer is much thinner, 10-20 cm at most, and even thinner in coarse-grained settings (Rhoads and Carey 1997). The relatively low chemical concentrations identified in the surficial layer (< 20 cm) of the

BRDS cores collected 40 years after mound formation indicate that bioturbation is not been sufficient to mobilize contaminants from deeper within the mound.

Table 4-1.

Ten Largest Storm Events Measured at WIS Buoy #63078 from 1980 - 1999

Rank	Storm Event Type or Name	Date	Peak Wave Height (meters)	Peak Wave Period (seconds)	Direction From (degrees True)	Within BRDS SE exposure Range?[1]	Near-Bottom Velocity (m/s)
1	Downslope Nor'easter	December 11, 1992	6.75	12.85	162	Yes	1.3
2	Superstorm of 1993	March 14, 1993	6.35	11.80	77	No	NA[2]
3	Nor’easter	December 30, 1997	6.24	11.28	71	No	NA[2]
4	Nor'easter	November 12, 1995	5.97	10.68	132	Yes	1.0
5	Nor'easter	October 20, 1996	5.83	12.24	173	Yes	1.1
6	Hurricane Gloria	September 27, 1985	5.79	10.01	99	No	NA[2]
7		December 3, 1986	5.78	10.80	131	Yes	0.9
8		December 7, 1983	5.76	11.21	56	No	NA[2]
9		October 26, 1980	5.65	10.82	103	No	NA[2]
10		February 12, 1981	5.61	10.15	112	Yes	0.8

[1]The BRDS open-water storm exposure range is approximately 110 to 190 °T.
Sources: USACE 2010 (storm event data); USGS 2007 (near-bottom velocity estimate)
[2]NA indicates that near-bottom velocity was not estimated because the storm event was not within the BRDS open water exposure range.

Table 4-2.

Summary Sediment Data Based on Analysis of Sediment Profile (SPI) and Plan-view Underwater Camera (PUC) Images

Sedimentary Environment	Facies	Surface Sediment	Bedforms	Sediment texture	Camera Penetration	Example Station	Frequency (# Observations)
Depositional	Burrowed silt	Very pale brown to gray fine sandy silt to very pale brown to olive gray silt/clay	Burrows, mounds tubes	Highly bioturbated, some fine sand mixed in surface layer	Good penetration by SPI camera	97-B	65
Reworking	Sandy silt	Fine sandy silt with slight concentration of fine sand at sediment water interface	Burrows, mounds, tubes, ripples, protruding tubes	Increased proportion of sand in upper sediment column, not sorted or layered	Good penetration by SPI camera	33-C	50
Reworking	Hard mixed sand silt	Very pale brown to light gray silty sand shell fragments	Burrows, mounds, tubes, ripples, no gravel visible	Bioturbated silty sand overlying silt no defined layer	Poor penetration by SPI camera	44-B	8
Reworking or bedload transport	Transgressive sand	Very pale brown, well-sorted, medium to coarse sand	Sand ripples, burrows, tracks	Well-defined layer of well-sorted sand over silt	Poor to moderate penetration by SPI camera	02-A	17
Reworking or bedload transport	Transgressive sand and gravel	Very pale brown, well-sorted, medium to coarse sand with gravel and shells	Sand ripples, burrows, tracks, gravel ribbons	Well-defined layer of gravel and sorted sand over silt	Poor penetration by SPI camera	04-B	16

Table 4-2., continued.

Summary Sediment Data Based on Analysis of Sediment Profile (SPI) and Plan-view Underwater Camera (PUC) Images

Sedimentary Environment	Facies	Surface Sediment	Bedforms	Sediment texture	Camera Penetration	Example Station	Frequency (# Observations)
Erosion or nondeposition	Lag on silt	Very pale brown to light gray gravelly shelly sandy silt	Gravel, burrows, ripples	Lag deposit (gravel and shell) over silt	Poor to moderate penetration by SPI camera	30-A	12
Erosion or non-deposition	Lag	Very pale brown medium to coarse gravelly sand	Gravel pavement, scattered gravel, and shells	Lag deposit; not enough penetration to see substrate	Poor penetration by SPI camera	46-A (SPI) 47-A (PUC)	19
Erosion or nondeposition	Reverse graded gravel	Very pale brown, firm, reverse-graded, gravelly very coarse sand	Gravel pavement, scattered gravel, and coarse sand	Reverse-graded gravel to fine gravel to coarse sand to medium sand	Poor penetration by SPI camera	60-C (SPI) 9-A (PUC)	13
Erosion or nondeposition	Shell windrow	Shells and Very pale brown poorly sorted medium to coarse sand	Large weathered oysters and quahogs in lines or rows separated by burrowed sand or silt	Poorly sorted to well-sorted coarse sand and shell hash over gray silt	Poor to moderate penetration by SPI camera	50-A 50-C	5
Erosion or nondeposition	Shell windrow and gravel	Shells and Very pale brown poorly sorted medium to coarse sand	Large weathered oysters, quahogs, and gravel in lines or rows separated by burrowed sand or silt	Poorly sorted to well-sorted coarse gravelly sand and shell hash over gray silt	Poor to moderate penetration by SPI camera	36-A	15

Table 4-3.

Summary of Core Length and Estimated Dredged Material Thickness

Core ID	Location Type	Core Length (m)	Dredged Material Thickness[1] (m)
BR03	Mound Area	2.87	5.0
BR08	Mound Area	2.23	4.0
BR28	Mound Area	0.59	1.0
BR32	Mound Area	2.75	4.5
BR42	Mound Area	0.93	1.0
BR44	Mound Area	0.59	3.5
BR78	Mound Area	2.23	2.5
BR70	Reference	1.36	0
BR94	Reference	2.62	0

[1]Dredged material thickness estimated from depth difference calculated from 1939 surface compared to 2007 surface of Figure 4-4.

Table 4-4.

Selected National Sediment Quality Guidelines for Metals and PAHs

Chemical	Units	ERM92	PELSW
Metals			
Arsenic	mg/kg dw	70	41.6
Cadmium	mg/kg dw	9.6	4.21
Copper	mg/kg dw	270	108
Lead	mg/kg dw	218	112
Nickel	mg/kg dw	51.6	42.8
Silver	mg/kg dw	3.7	1.77
Zinc	mg/kg dw	410	271
PAH			
2-Methylnaphthalene	ug/kg dw	670	201
Acenaphthene	ug/kg dw	500	88.9
Acenaphthylene	ug/kg dw	640	128
Anthracene	ug/kg dw	1,100	245
Benzo(a)anthracene	ug/kg dw	1,600	693
Benzo(a)pyrene	ug/kg dw	1,600	763
Chrysene	ug/kg dw	2,800	846
Dibenzo(a,h)anthracene	ug/kg dw	260	135
Fluoranthene	ug/kg dw	5,100	1,494
Fluorene	ug/kg dw	540	144
Naphthalene	ug/kg dw	2,100	391
Phenanthrene	ug/kg dw	1,500	543.5
Pyrene	ug/kg dw	2,600	1,398
PAHs, total	ug/kg dw	44,792	16,770
Total HPAH	ug/kg dw	9,600	6,676
Total LPAH	ug/kg dw	3,160	1,442

ERM92: Effects Range-Median (Long et al., 1995)
PELSW: Probable Effect Level, saltwater (MacDonald et al. 1996)

Table 4-5.

Summary of Sediment Chemistry Samples that Exceeded Selected National Sediment Quality Guidelines

Analyte Group	Parameter	Core Sample	Interval	Value	Exceedance Factor	
					ERM92[1]	PELSW[2]
Metals (mg/kg)	Cadmium	BR28-2	28–38 cm	15	1.6	3.6
	Chromium	BR28-2	28–38 cm	395	1.1	2.5
	Copper	BR28-2	28–38 cm	1260	8.0	11.7
	Copper	BR42-3	61–71 cm	310	1.1	2.9
	Lead	BR28-2	28–38 cm	305	1.4	2.7
	Silver	BR28-2	28–38 cm	29.5	8.0	16.7
	Silver	BR42-3	61–71 cm	4.2	1.1	2.4
	Silver	BR42-1	7–20 cm	1.8		1.0
	Silver	BR78-3	90–110 cm	3.4		1.9
	Silver	BR08-2	40–55 cm	2.4		1.4
	Silver	BR08-1	7–20 cm	2.1		1.2
	Silver	BR44-1	7–20 cm	1.9		1.1
	Silver	BR08-5	185–200 cm	1.8		1.0
	Silver	BR78-5	140–155 cm	1.8		1.0
	Zinc	BR28-2	28–38 cm	696	1.7	2.6
PAHs (µg/kg)	Acenaphthene	BR28-2	28–38 cm	260		2.0
	Anthracene	BR28-2	28–38 cm	270		1.1
	Fluorene	BR28-2	28–38 cm	200		1.4

[1]Effects Range-Median (Long and MacDonald 1992)
[2]Probable Effect Level, Saltwater (MacDonald et al.1996)

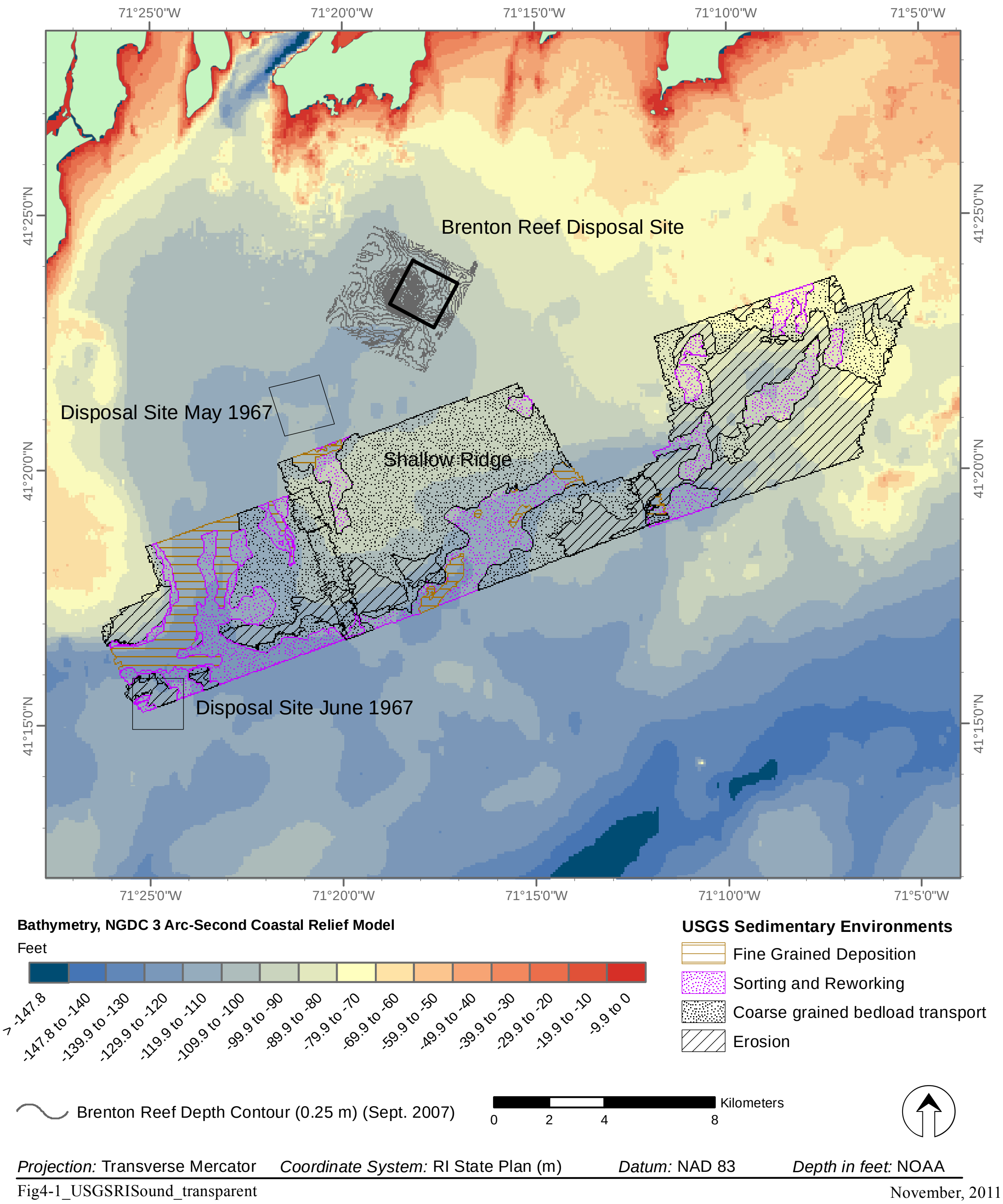

Figure 4-1. Sedimentary processes mapped in the vicinity of Brenton Reef Disposal Site based on NOAA side-scan and bathymetry (after McMullen et al. 2007, 2008, 2009).

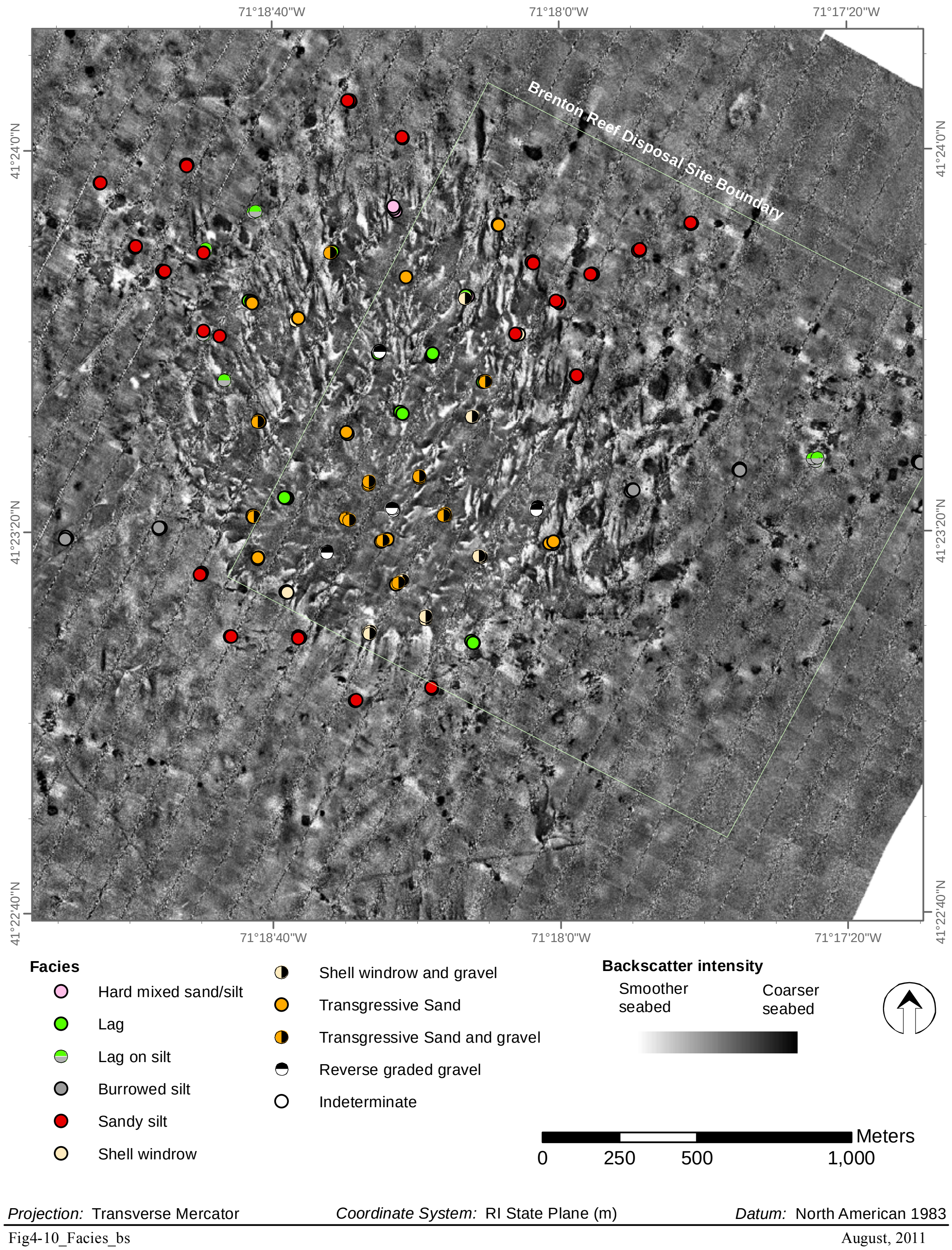

Figure 4-2. Sediment facies distribution across the backscatter image of the Brenton Reef Disposal Site

Figure 4-3. a. Large oyster shells (*Crassostrea* sp.) from bottom of core BR78 (200-215 cm depth). b. Silty clay with quahog (*Mercenaria* sp.) from bottom of core BR08 (200-215).

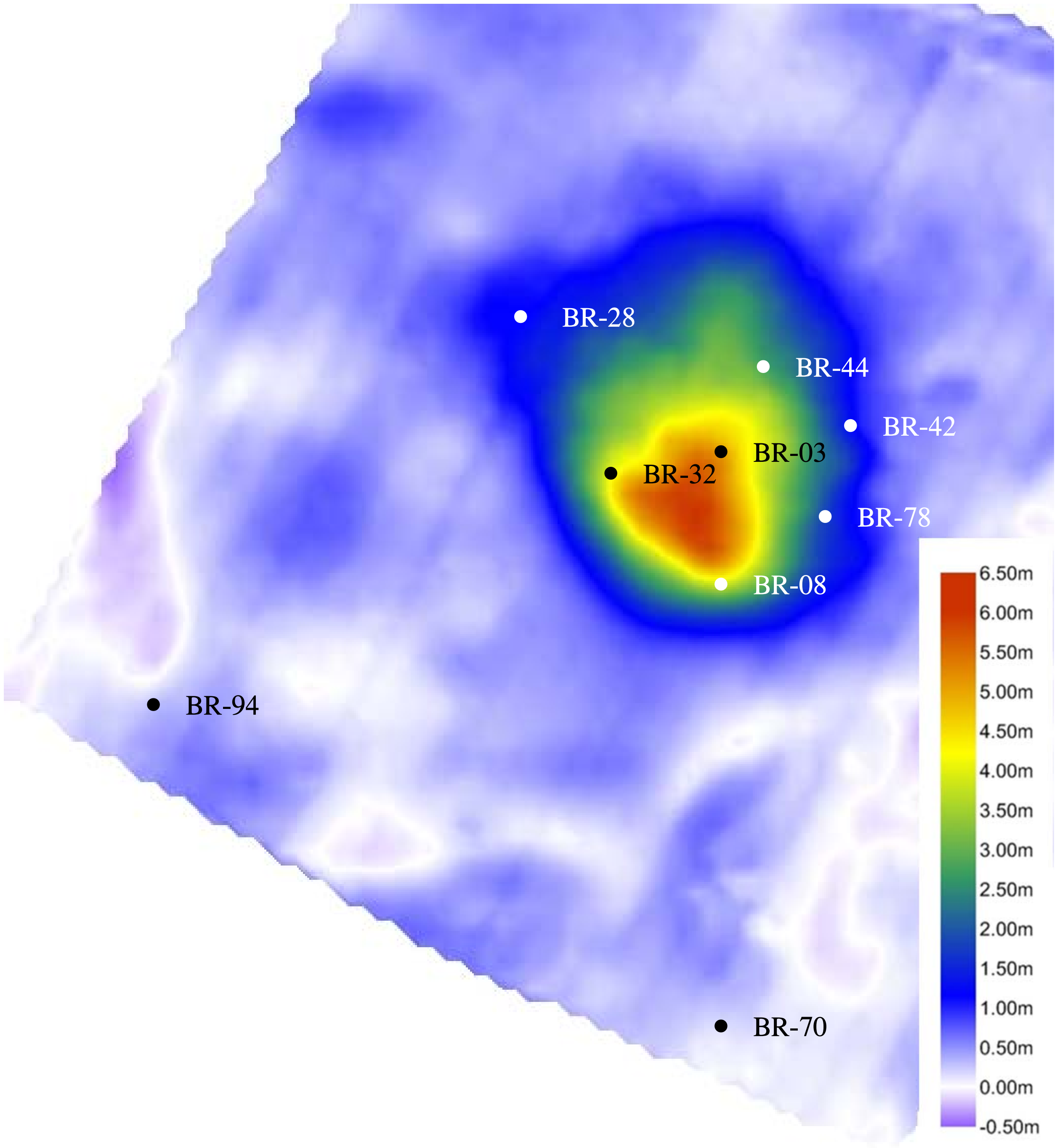

Figure 4-4. Core locations shown with depth difference calculated between 1939 and 2007

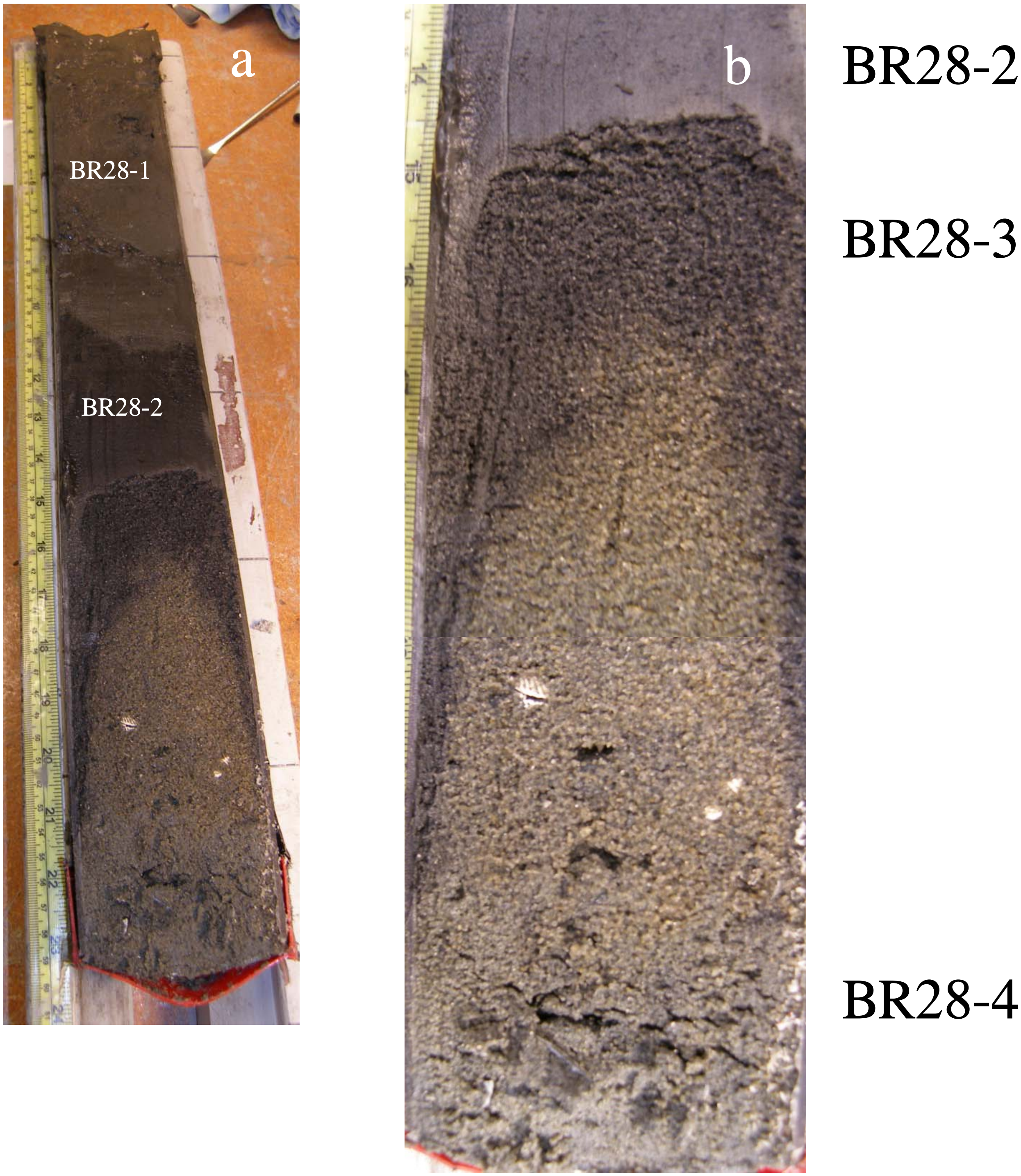

Figure 4-5. Core BR28. a. Dark horizon in center is BR28-2 horizon with elevated metal and PAH concentration below sandy silt cap. b. Interfaces between black silt (BR28-2), black well-sorted sand (BR28-3) and light gray well-sorted fine sand (BR28-4).

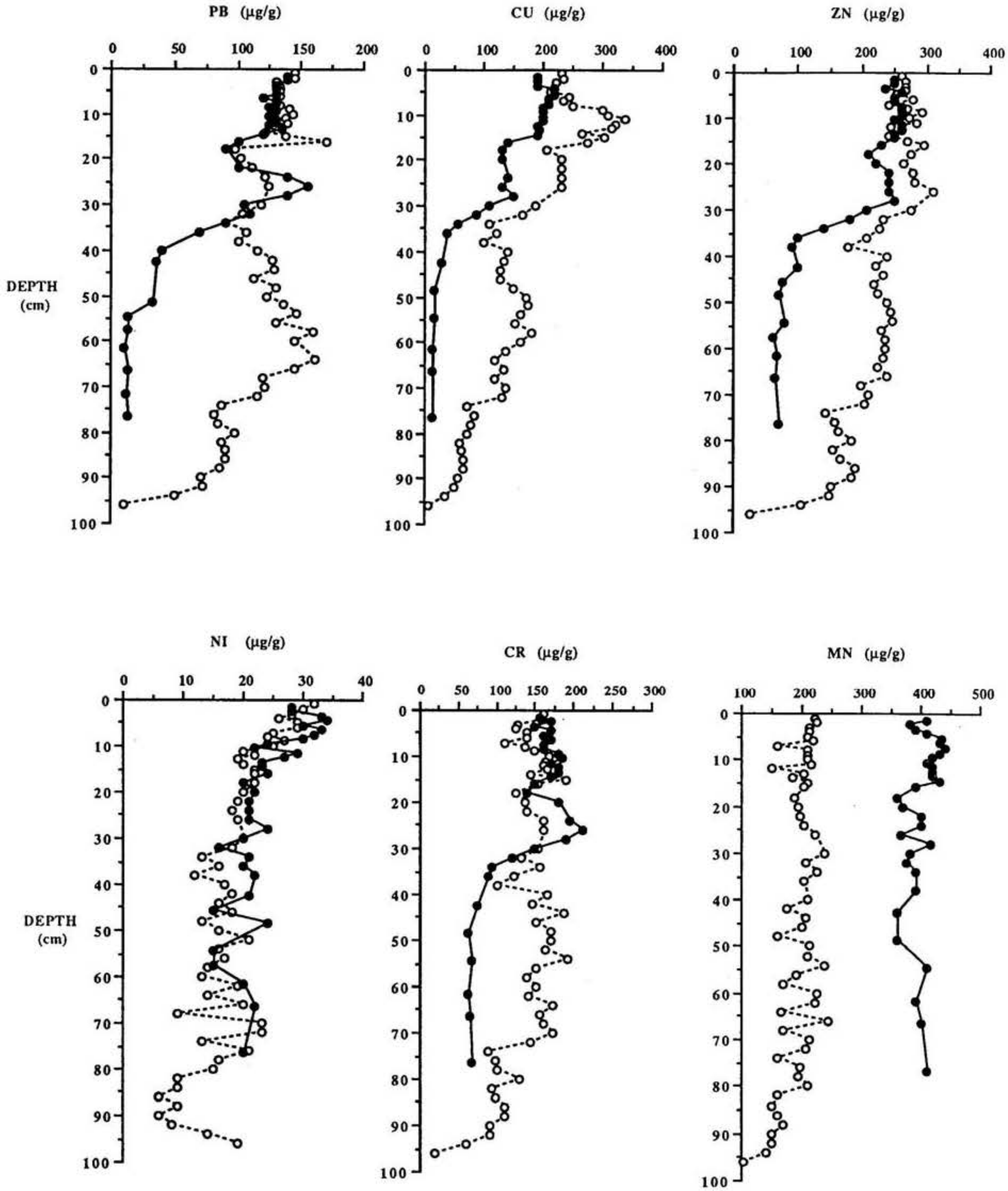

Figure 4-6. Concentrations of metals with depth in sediments from cores collected from upper Narragansett Bay, near Ohio Ledge (and the Rumstick Neck Reach), analyzed by Goldberg et al. (1977; solid line) and Santschi et al. (1984; dashed line), adopted from Nixon 1995.

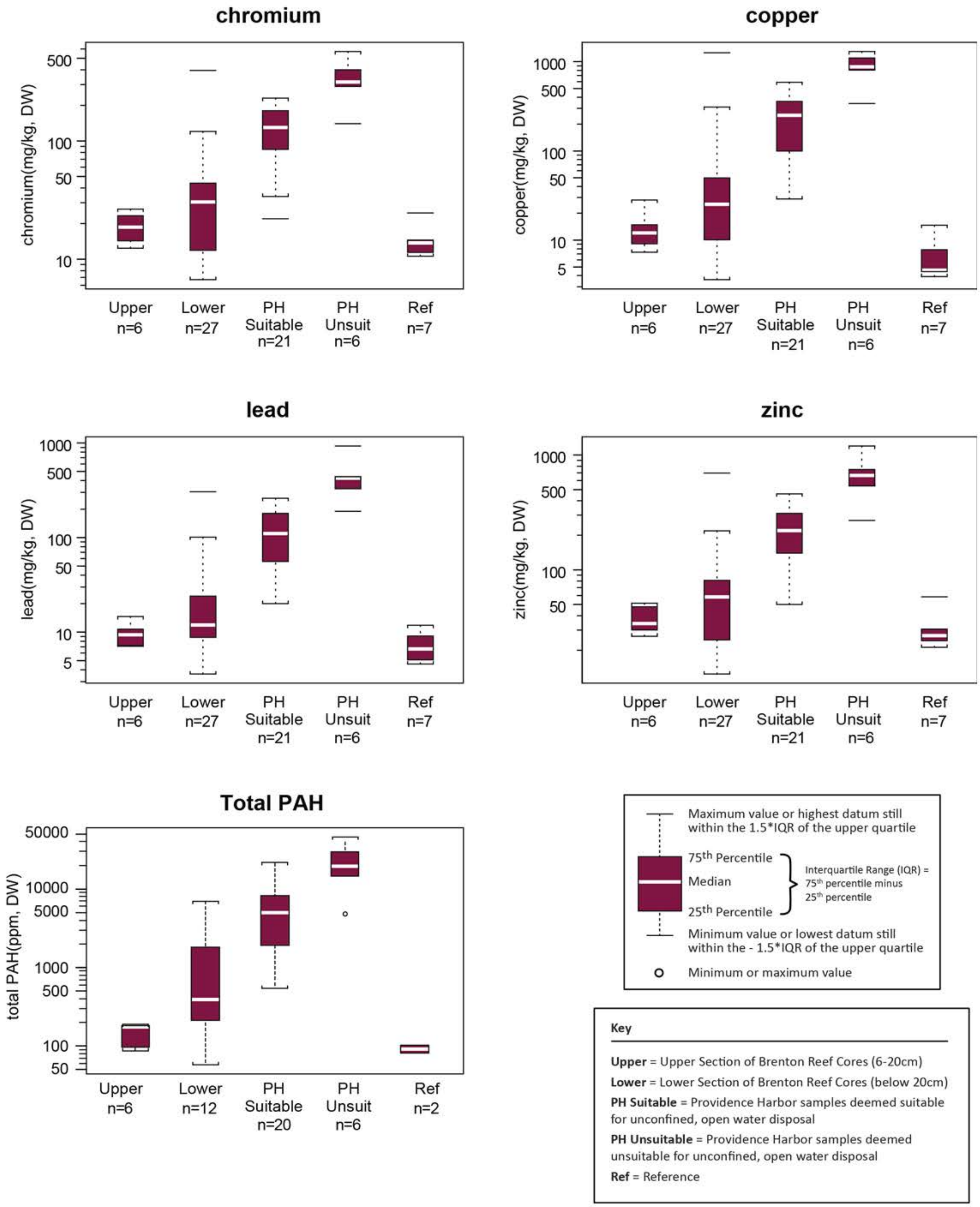

Figure 4-7. Boxplots showing concentrations of metals and PAHs from the lower and upper portion of BRDS cores compared to reference cores, and to samples designated as suitable or unsuitable from the PRHMDP.

5.0 CONCLUSIONS AND RECOMMENDATIONS

The historical Brenton Reef Disposal Site (BRDS) mound has persisted as a stable feature on the seafloor for over four decades. It is clear that despite evidence of surface sediment modification from sediment transport across the surface of the mound, the mass of material placed on the seafloor from 1968 to 1973 has remained in place. The silts reported on the surface in 1970 may have been covered by Brayton Point material or eroded; variable lag deposits composed of well-sorted sand, gravels, shells, and poorly sorted mixtures with patches of compacted silt now cover the surface of the mound. These lag deposits apparently become mobile during extreme storm events but appear to protect the mass of the mound from large-scale erosion. The complex patterns of sediment types appear related to the episodic nature of the movement with deposition of silt and biological reworking between storm events. The biological community on the mound surface has developed in response to the episodic reworking and mixture of coarse and fine sediments. The concentrations of metals and PAHs in the surface of the mound are similar to reference area concentrations.

The investigation reported here, consisting of a bathymetric and SPI survey performed in 2007 and coring with chemical analysis performed in 2009, supports a conceptual model of inner mound sediments (dredged from the Upper Providence River and likely to be deemed unsuitable for unconfined open water placement) effectively sequestered from the overlying water column based on the following three lines of evidence:

Physical – The mound has remained virtually the same size and shape as surveyed in 1978 and the surface of the mound is armored with coarse sands and shells that resist strong erosive forces.

Biological – The biological community on the surface of the mound and surrounding area is in equilibrium with the sediment grain size and dynamics of the benthic habitats. There is no evidence of adverse impact on biological resources from contact with unsuitable sediments.

Chemical – The bulk sediment chemistry results from the surface of the mound (0-20 cm) were similar to the results from off mound reference areas. The results from most sediment samples collected below the surface of the mound (> 20 cm depth) were similar to results from dredged material that would be deemed suitable for open water placement. Cores were unlikely long enough to reach and document the higher concentrations of contaminants that likely exist within the mound.

Some variability in results was found, which was expected based on the conceptual model of highly heterogeneous distribution of dredged material. One sample collected from 28–38 cm from station BR28 contained elevated concentrations of selected metals and PAHs relative to surrounding sediments. The presence of this single horizon of elevated metal and PAH concentrations is considered to be a product of the heterogeneity of the dredged material placed at the site rather than from erosion of the top of the mound or transport of contaminants from inner layers of the mound. The uppermost sample in this core, collected from the 7–20 cm interval and consisting of almost equal fractions of sand and fines, showed no evidence of migration of metals or PAHs from the underlying sediments. The presence of the 20 cm (minimum) layer above the contaminated layer is sufficient to limit biological mixing or exposure to the contaminants (Rhoads and Carey 1997). The location of this core is off the mound and far less likely to experience reworking from periodic storms.

Based on the above findings, it is recommended that BRDS be monitored using bathymetry and depth differencing to assess stability on a 10-year cycle or following a significant storm event exceeding those reported in Table 4-1. Should the depth-differencing reveal significant reworking of the mound (loss of 1 m or more in height over more than 5% of the mound footprint), the site should return to standard DAMOS tiered monitoring protocol.

6.0 REFERENCES

Andrews, J. T.; Stravers, J. A. 1995. Magnetic susceptibility of late quaternary marine sediments, Frobisher Bay, N.W.T.: An indicator of changes in provenance and processes. Quat. Sci. Reviews 12:157–167.

ASTM. 2009. Standard Test Method for Particle-Size Analysis of Soils. ASTM Standard Method No. D422-63(2007). In: 2009 Annual Book of ASTM Standards, volume 04.08, Soil and rock (I): D420–D5876. West Conshohocken, PA: ASTM International.

Battelle. 2004. Analysis of dredged material transport potential at two disposal alternatives in Rhode Island Sound. Prepared for the U.S. Army Corps of Engineers under Contract No. DACW33-01-D-0004, Delivery Order No. 2.

Berry, W. J.; Bridges, T. S.; Ellis, S. J.; Gries, T. H.; Ireland, D. S.; Maher, E. M.; Menzie, C. A.; Porebski, L. M.; Stronkhorst, J. 2002. Use of sediment quality guidelines in existing assessment frameworks. In: Wenning, R. J.; Bailey, B. E.; Ingersoll, C. G.; Moore, D. W., editors. Use of sediment quality guidelines and related tools for the assessment of contaminated sediments. Proceedings from the Pellston Workshop; 18–22 August 2002; Fairmont, MT. Pensacola, FL: SETAC Press. p. 383–428.

Butman, B.; Sherwood, C. R.; Dalyander, P. S. 2008. Northeast storms ranked by wind stress and wave-generated bottom stress observed in Massachusetts Bay, 1990–2006. Continent. Shelf. Res.28: 1231–1245.

Carey, D. A.; Lewis, D.; Wolf, S.; Greenblatt, N.; Fredette, T. J. 2006. Long term stability of capped dredged material disposal mounds: Stamford New Haven North and Cap Site 2 in Long Island Sound. Proceedings of the Western Dredging Association Twenty-Sixth Technical Conference and Thirty-Eighth Texas A&M Dredging Seminar, 26-28 June 2006, San Diego, CA. Center for Dredging Studies, Ocean Engineering Program, Civil Engineering Department, Texas A&M University, College Station, TX. pp. 389-409.

Chen, C-T.; Millero, F. J. 1977. Speed of sound in seawater at high pressure. J. Acoust. Soc. Am. 62(5): 1129–1135.

Corbin, J. M. 1989. Recent and historical accumulation of trace metal contaminants in the sediment of Narragansett Bay, Rhode Island [master’s thesis]. Kingston, RI: University of Rhode Island, 289 pp.

Currie, R. G.; Bornhold, B. D. 1983. The magnetic susceptibility of continental-shelf sediments, west coast Vancouver Island, Canada. Mar. Geol. 51:115–127.

Driscoll, N. W. 1996. Side-scan sonar investigation of shallow-water depositional processes in and around Block Island Sound: Before and after the Nor'easter of 1992. Lamont-Doherty Geological Observatory Report No. A488813 to Office of Naval Research, Arlington, VA, 24 pp.

ENSR. 2004. Monitoring survey at the Rockland Disposal Site, September 2003. DAMOS Contribution No. 156. U.S. Army Corps of Engineers, New England District, Concord, MA, 68 pp.

ENSR. 2005. Stamford-New Haven North/Cap Site 2 Investigation May 2004. DAMOS Contribution No. 165. U.S. Army Corps of Engineers, New England District, Concord, MA, 97 pp.

ENSR. 2007. Baseline bathymetric surveys at the Central and Western Long Island Sound Disposal Sites, July 2005. DAMOS Contribution No. 177. U.S. Army Corps of Engineers, New England District, Concord, MA, 85 pp.

ENSR. 2008. Providence River and Harbor Maintenance Dredging Project Synthesis Report. DAMOS Contribution No. 178. U.S. Army Corps of Engineers, New England District, Concord, MA, 133 pp.

Fredette, T. J.; Germano, J. D.; Kullberg, P. G.; Carey, D. A.; Murray, P. 1992. Chemical stability of capped dredged material disposal mounds in Long Island Sound, USA. Chem. Ecol. 7:173–194.

Fredette, T. J.; French, G. T. 2004. Understanding the physical and environmental consequences of dredged material disposal: history in New England and current perspectives. Mar. Pollut. Bull.49: 93–102.

Germano, J. D.; Rhoads, D. C.; Lunz, J. D. 1994. An integrated, tiered approach to monitoring and management of dredged material sites in the New England region. DAMOS Contribution No. 87 (SAIC Report No. 90/7575&234). U.S. Army Corps of Engineers, New England Division, Waltham, MA.

Germano, J. D.; Rhoads, D. C.; Valente, R. M.; Carey, D. A.; Solan, M. 2011. The use of sediment profile imaging (SPI) for environmental impact assessments and monitoring studies: Lessons learned from the past four decades. Oceanography and Marine Biology: An Annual Review. 49:235-285.

Goldberg, E. D.; Gamble, E.; Griffin, T. T.; Koide, M. 1977. Pollution history of Narragansett Bay as recorded in its sediments. Estuar. Coast. Mar. Sci. 5:549–561.

Holmes, R. 2008. Rhode Island lighthouses: A pictorial history. Fall River, MA: Rhodeislandlighthousehistory.info Publishing.

Hunt, J. N. 1979. Direct solution of wave dispersion equation. J. Waterways, Ports, Coastal Ocean Div., ASCE 105(WW4):457-459.

[IHO] International Hydrographic Organization. 2008. IHO Standards for hydrographic surveys. 5th Edition, February 2008. Special Publication No. 44. Monaco: International Hydrographic Bureau. http://www.iho-ohi.net/iho_pubs/standard/S-44_5E.pdf (4 September 2011).

Knebel, H. J.; Needell, S. W.; O'Hara, C. J. 1982. Modern sedimentary environments on the Rhode Island Inner Shelf, off the eastern United States: Mar. Geol. 49: 241–256.

Komar, P. D. 1976. Beach Processes and Sedimentation. Prentice-Hall, Inc., Englewood Cliffs. 429 p.

Long, E. R.; MacDonald, D. D. 1992. National Status and Trends Program Approach. In: Sediment Classification Methods Compendium. EPA 823-R-92-006. EPA Office of Water (WH-556). Washington, DC.: U.S. Environmental Protection Agency.

Long, E. R.; MacDonald, D. D.; Smith, S. L.; Calder, F. D. 1995. Incidence of adverse biological effects within ranges of chemical concentrations in marine and estuarine sediments. Environmental Management 19:81-97.

MacDonald, D. D.; Carr, R. S.; Calder, F. D.; Long, E. R.; Ingersoll, C. G. 1996. Development and evaluation of sediment quality guidelines for Florida coastal waters. Ecotoxicology 5:253–278.

Manning, J. P.; Oey, L. Y.; Packer, D.; Vitaliano, J.; Finneran, T. W.; You, K. W.; Fromm, S. 1994. Observations of bottom currents and estimates of resuspended sediment transport at the New York Bight 12-mile dumpsite. J. Geophys. Res.99(C5):10211–10239.

MathSoft. 1999. S-Plus 2000 Professional Release 1. Seattle, WA: MathSoft, Inc.

McMullen, K. Y.; Poppe, L. J.; Twomey, E. R.; Danforth, W. W.; Haupt, T. A.; Crocker, J. M. 2007. Sidescan-sonar imagery, multibeam bathymetry, and surficial geologic interpretations of the sea floor in Rhode Island Sound, off Sakonnet Point, Rhode Island: U.S. Geological Survey Open-File Report 2007-1150, DVD-ROM, also available online at http://woodshole.er.usgs.gov/pubs/of2007-1150/ [Accessed 13 May 2009]. [Accessed 13 May 2009].

McMullen, K. Y.; Poppe, L. J.; Dennym H, F.; Haupt, T. A.; Crocker, J. M. 2008. Sidescan-sonar imagery and surficial geologic interpretations of the sea floor in central Rhode Island Sound: U.S. Geological Survey Open-File Report 2007-1366, DVD-ROM, also available online at http://woodshole.er.usgs.gov/pubs/of2007-1366/ [Accessed 13 May 2009]. [Accessed 13 May 2009].

McMullen, K. Y.; Poppe, L. J.; Haupt, T. A.; Crocker, J. M. 2009. Sidescan-sonar imagery and surficial geologic interpretations of the sea floor in western Rhode Island Sound: U.S. Geological Survey Open-File Report 2008-1181, DVD-ROM, also available online at http://woodshole.er.usgs.gov/pubs/of2008-1181/ [Accessed 13 May 2009].

Myre, P. L.; Germano, J. D. 2007. Field Verification Program (FVP) Disposal Mound Monitoring Survey 2005. DAMOS Contribution No. 175. U.S. Army Corps of Engineers, New England District, Concord, MA, 71 pp.

NED. 1974. A compendium of Corps of Engineers studies and reports from 1970 to 1974 relating to dredging an ocean disposal: New England Division, Waltham, MA, 20 pp.

Needell, S. W.; O'Hara, C. J.; Knebel, H. J. 1983. Maps showing geology and shallow structure of western Rhode Island Sound, Rhode Island: U.S. Geological Survey miscellaneous field studies map MF-1537, scale 1:125,000.

Nixon, S. W. 1995. Metal inputs to Narragansett Bay: A history and assessment of recent conditions. Narragansett, RI: Rhode Island Sea Grant.

[NOAA] National Oceanographic and Atmospheric Administration. 2011. NOS hydrographic surveys specifications and deliverables. U.S. Department of Commerce. http://www.nauticalcharts.noaa.gov/hsd/specs/SPECS_2011.pdf (4 September 2011).

[NUSC] Naval Underwater Systems Center. 1979. DAMOS Disposal Area Monitoring System – Annual Data Report – 1978. Supplement E Brenton Reef Disposal Site.

Submitted to the New England Division, U.S. Army Corps of Engineers, May 1979. 34 pp.

[NUSC] Naval Underwater Systems Center. 1980. DAMOS Disposal Area Monitoring System – Annual Data Report – 1980. DAMOS Contribution No. 17. U.S. Army Corps of Engineers, New England Division, Waltham, MA.

O'Hara, C. J.; Oldale, R. N. 1980. Maps showing geology and shallow structure of eastern Rhode Island Sound and Vineyard Sound, Massachusetts: U.S. Geological Survey miscellaneous field studies map MF-1186, Scale 1:125,000.

Pace, N. G.; Gao, H. 1988. Swath Seabed Classification, IEEE J. Oc. Eng., 13: 83-90,

Palermo, M. R.; Clausner, J. E.; Rollings, M. E.; Williams, G. L.; Myers, T. E.; Fredette, T. J.; Randall, R. E. 1998. Guidance for subaqueous dredged material capping. Technical Report DOER-1, US Army Engineer Waterways Experiment Station, Vicksburg, MS. 302 pp.

Poindexter-Rollings, M. E. 1990. Methodology for analysis of subaqueous sediment mounds. Technical Report D-90-2, U.S. Army Engineer Waterways Experiment Station Vicksburg, MS.

Pratt, S. D.; Saila, S. B.; Sissenwine, M. P. 1973. Study and report on environmental effects of dredged material, Rhode Island Sound – Phase III. SR Report SR-3. U.S. Army Corps of Engineers, New England Division, Waltham, MA.

Reading, H. G. (Editor). 1996. *Sedimentary Environments. Processes, Facies and Stratigraphy.* Blackwell, Oxford, 688 pp.

Reynolds, R.; Bothner, M.; Crusius, J. 2010. Magnetic properties as proxies for metal contamination in coastal sediments of Massachusetts [abstract]. In: GSA Abstracts with Programs, Geological Society of America Annual Meeting, Denver, CO.

Rhoads, D. C.; Carey, D. A. 1997. Capping dredged materials in the New York Bight: Evaluation of the effects of bioturbation. Science Applications International Corporation Report 374 and Report #39 of the New York Mud Dump Site Studies. Prepared for the U.S. Army Corps of Engineers, New York District, New York, NY, 30 pp.

Rhoads, D. C.; Germano, J. D. 1982. Characterization of organism-sediment relations using sediment profile imaging: an efficient method of remote ecological monitoring of the seafloor (REMOTS System). Mar. Ecol. Prog. Ser. 8:115–128.

Rhoads, D. C.; Germano, J. D. 1986. Interpreting long-term changes in benthic community structure: a new protocol. Hydrobiologia 142:291–308.

SAIC. 1980a. Disposal Area Monitoring System progress report March 15–May 15, 1980. DAMOS Contribution No. 13. U.S. Army Corps of Engineers, New England Division, Waltham, MA.

SAIC. 1980b. Disposal Area Monitoring System progress report May 15–July 30, 1980. DAMOS Contribution No. 14. U.S. Army Corps of Engineers, New England Division, Waltham, MA.

SAIC. 1988. A summary of DAMOS physical monitoring of dredged material disposal activities. Report No. SAIC-88 submitted to U.S. Army Engineer Waterways Experiment Station, Vicksburg, MS.

SAIC. 1990. Preliminary field operations in support of disposal site designation in the Rhode Island Sound region. DAMOS Contribution No. 79. U.S. Army Corps of Engineers, New England Division, Waltham, MA, 92 pp.

SAIC. 1995. Sediment Capping of subaqueous Dredged Material Disposal Mounds: An Overview of the New England Experience, 1979 - 1993. DAMOS Contribution No. 95. Special Technical Report. U.S. Army Corps of Engineers, New England Division, Waltham, MA, 101 pp.

Saila, S. B.; Polgar, T. T.; Rogers, B. A. 1969. Results of studies related to dredged sediment dumping in Rhode Island Sound - Phase I. SR Report SR-1. U.S. Army Corps of Engineers, New England Division, Waltham, MA.

Saila, S. B.; Pratt, S. D.; Polgar, T. T. 1971. Providence Harbor - Improvement spoil disposal site evaluation study – Phase II. SR Report SR-2. U.S. Army Corps of Engineers, New England Division, Waltham, MA.

Santschi, P. H.; Nixon, S. W.; Pilson, M.; Hunt, C. 1984. Accumulation of sediments, trace metals (Pb, Cu) and total hydrocarbons in Narragansett Bay, Rhode Island. Estuar. Coast. Shelf Sci. 19(4):427–449.

Silva, A. J.; Brandes, H. G.; Uchytil, C. J.; Fredette T. J.; Carey, D. 1994. Geotechnical analysis of capped dredged material mounds. Proceedings of the Conference, Dredging '94, Orlando, Florida, pp. 410–419.

[USACE] U.S. Army Corps of Engineers. 2002. Engineering and design - hydrographic surveying. EM1110-2-1003. Change 1. April 1, 2004. http://140.194.76.129/publications/eng-manuals/em1110-2-1003/toc.htm (4 September 2011).

[USACE] U.S. Army Corps of Engineers. 2010. Wave Information Studies Project Documentation. December 2010. Coastal and Hydraulics Laboratory, Engineering Resource and Development Center. Project Manager: Dr. Robert Jensen. Online at: http://frf.usace.army.mil/wis2010

[USACE/USEPA] United States Army Corps of Engineers/United States Environmental Protection Agency. 1991. Evaluation of dredged material proposed for ocean disposal: Testing manual. EPA 503/8-91/001. Washington, DC: U.S. EPA.

[USACE NAE] U.S. Army Corps of Engineers, New England District. 2001. Providence River and Harbor Maintenance Dredging Project Final Environmental Impact Statement. U.S. Army Corps of Engineers, New England District, Concord, MA.

[USEPA] United States Environmental Protection Agency. 1997. Test methods for evaluating solid waste, physical/chemical methods, SW-846. 3rd edition. Washington, DC: U.S. EPA, Office of Solid Waste.

[USEPA] United States Environmental Protection Agency. 1988. Determination of total organic carbon in sediment (Lloyd Kahn method). Edison, NJ: U.S. EPA Region II, Environmental Services Division, Monitoring Management Branch.

US Geological Survey 2007. Demonstration Sediment Transport Applets. Online at: http://woodshole.er.usgs.gov/staffpages/csherwood/sedx_equations/sedxinfo.html

Vincent, C. E.; Swift, D. J. P.; Hillard, B. 1981. Sediment transport in the New York Bight, North American Atlantic Shelf. Mar. Geol. 32: 369–398.

Warner, J. C.; Butman, B.; Dalyander, P. S. 2008. Storm-driven sediment transport in Massachusetts Bay. Continent. Shelf Res. 28: 257–282.

Weber, M. E.; Niessen, F.; Kuin, G.; Wiedicke, M. 1997. Calibration and application of marine sedimentary physical properties using a multi-sensor core logger. Mar. Geol. 136:151-172.

INDEX

APPENDIX A

BATHYMETRIC CONTOUR MAPS OF BRDS 1967 - 1987

APPENDIX A
BATHYMETRIC CONTOUR MAPS OF BRDS 1967 – 1987

LIST OF FIGURES

APPENDIX A

Bathymetric Contour Maps of BRDS 1967 - 1987

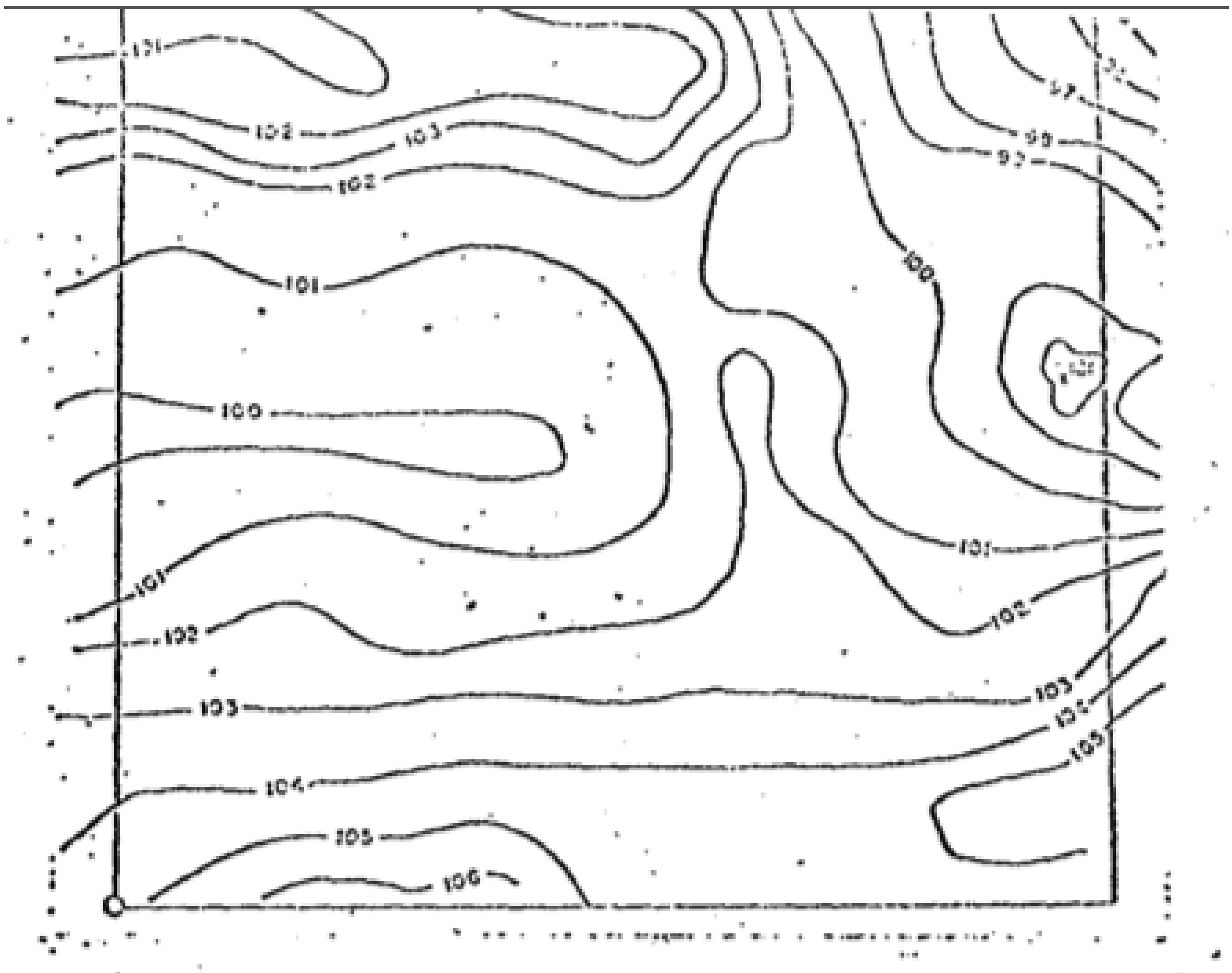

Figure A-1. Baseline bathymetric contour map. Data collected prior to December 15, 1967. Dredged material placed to date: 0.069 million m³ (Saila et al. 1969).

Bathymetric Contour Maps of BRDS 1967 - 1987

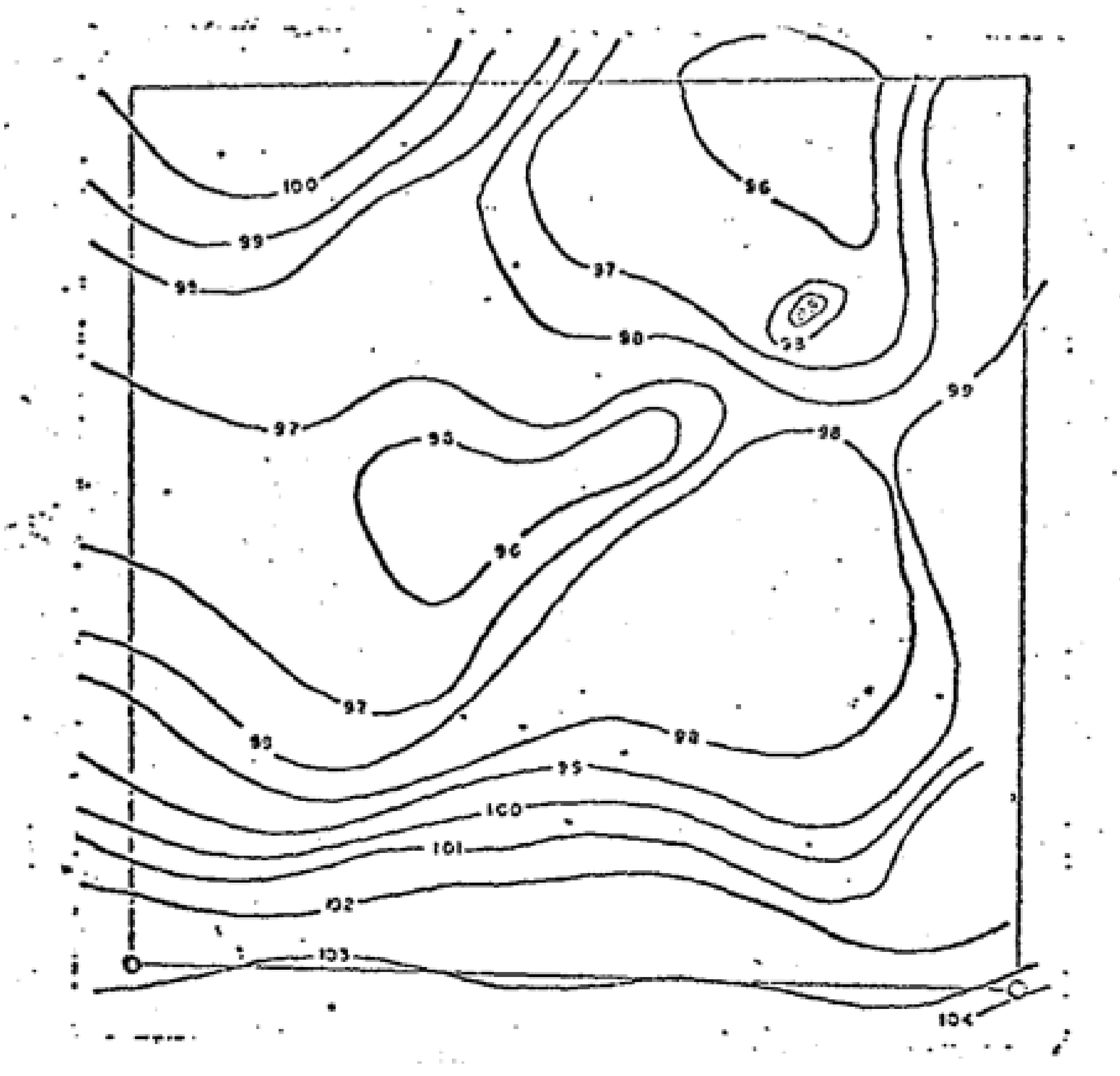

Figure A-2. Bathymetric contour map. Data collected on July 1, 1968. Dredged material placed between December 15, 1967 and July 1, 1968:1.4 million m³. Cumulative dredged material: 1.5 million m³ (Saila et al. 1969).

Bathymetric Contour Maps of BRDS 1967 - 1987

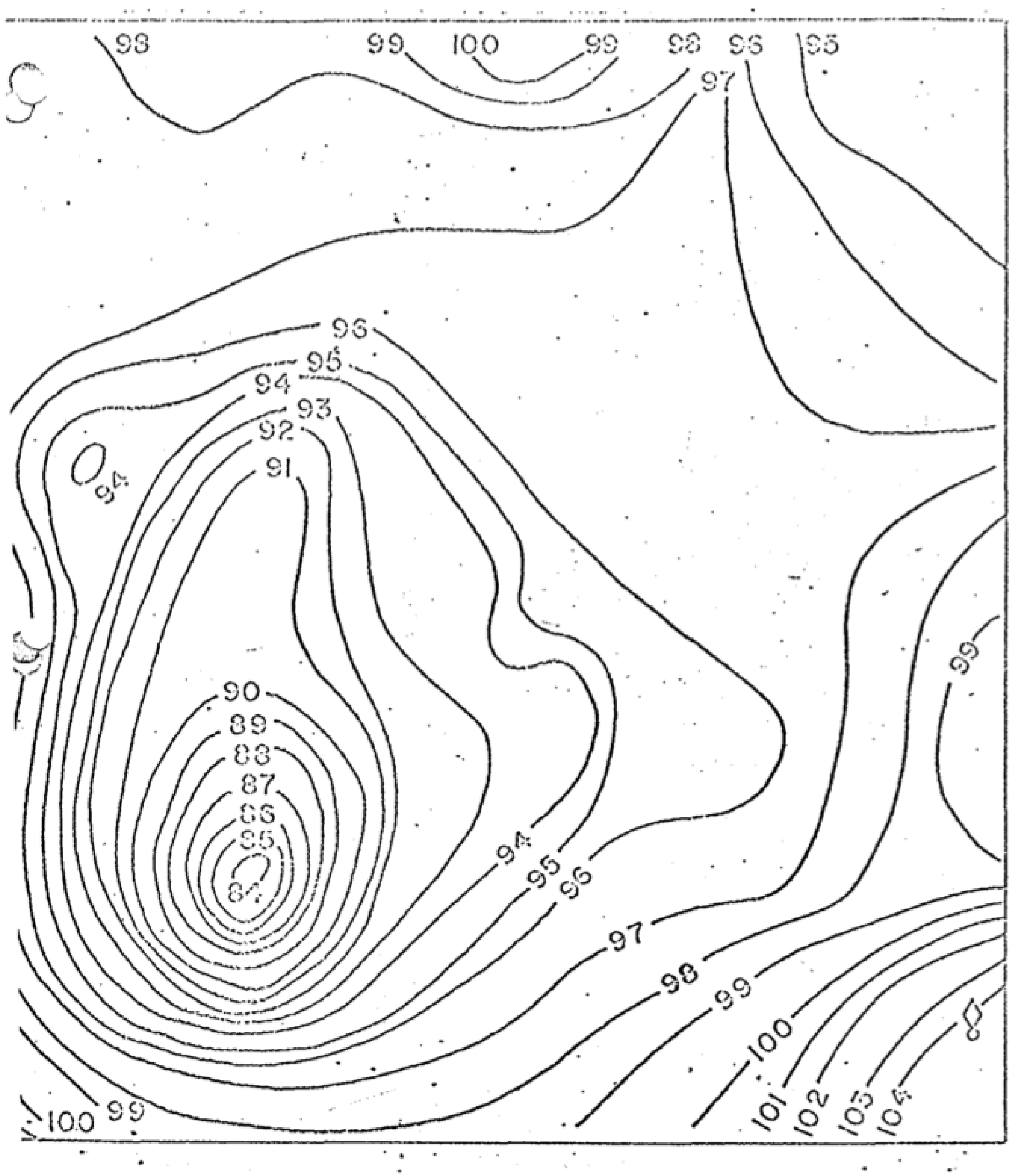

Figure A-3. Bathymetric contour map. Data collected on October 22, 1969. Dredged material placed between July 1, 1968 and October 22, 1969: 2.7 million m³. Cumulative dredged material: 4.2 million m³ (Saila et al. 1971).

Bathymetric Contour Maps of BRDS 1967 - 1987

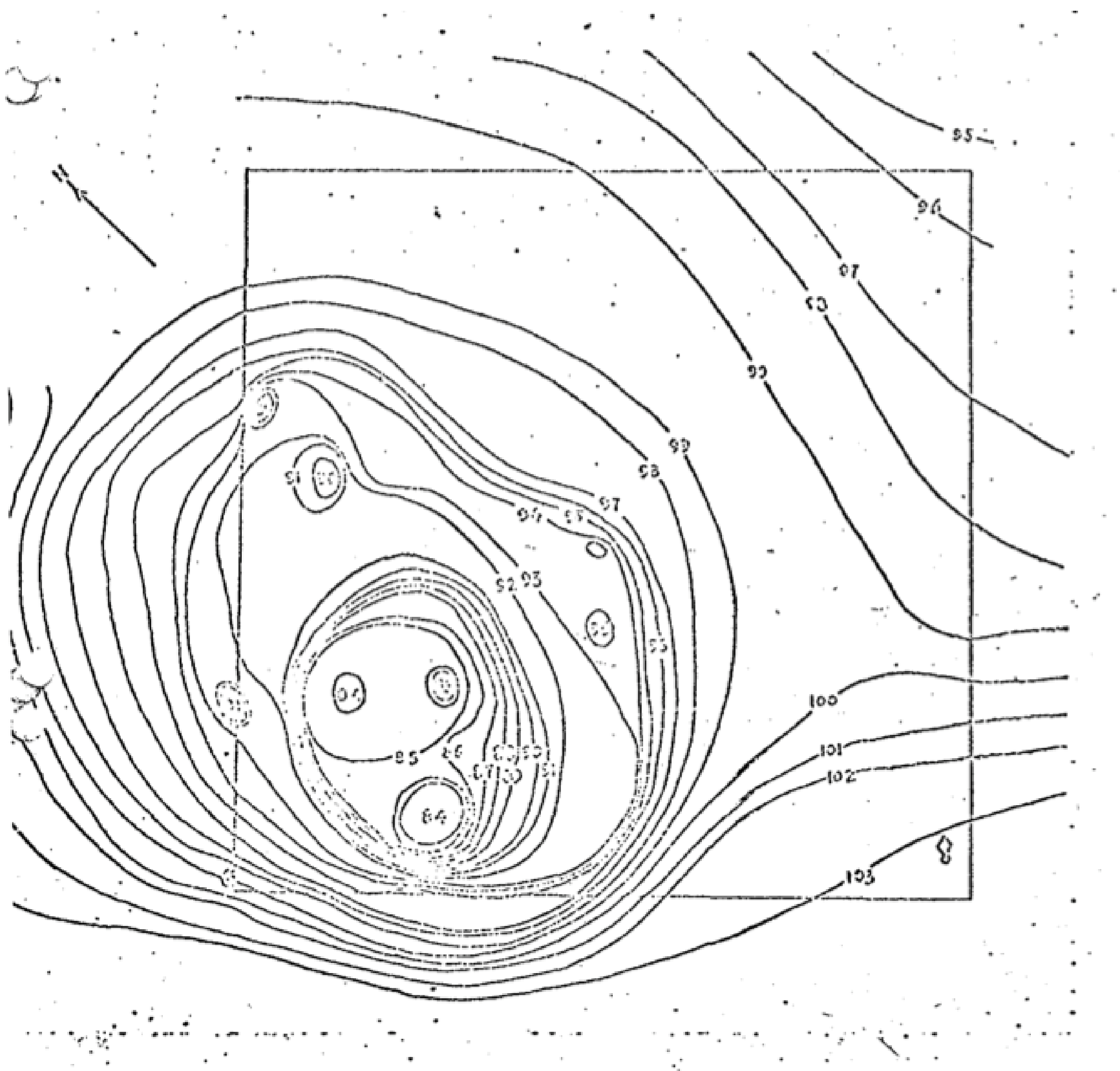

Figure A-4. Bathymetric contour map. Data collected on September 25, 1970. Dredged material placed between October 22, 1969 and September 25, 1970: 2.1 million m³. Cumulative dredged material: 6.3 million m³ (Saila et al. 1971).

Bathymetric Contour Maps of BRDS 1967 - 1987

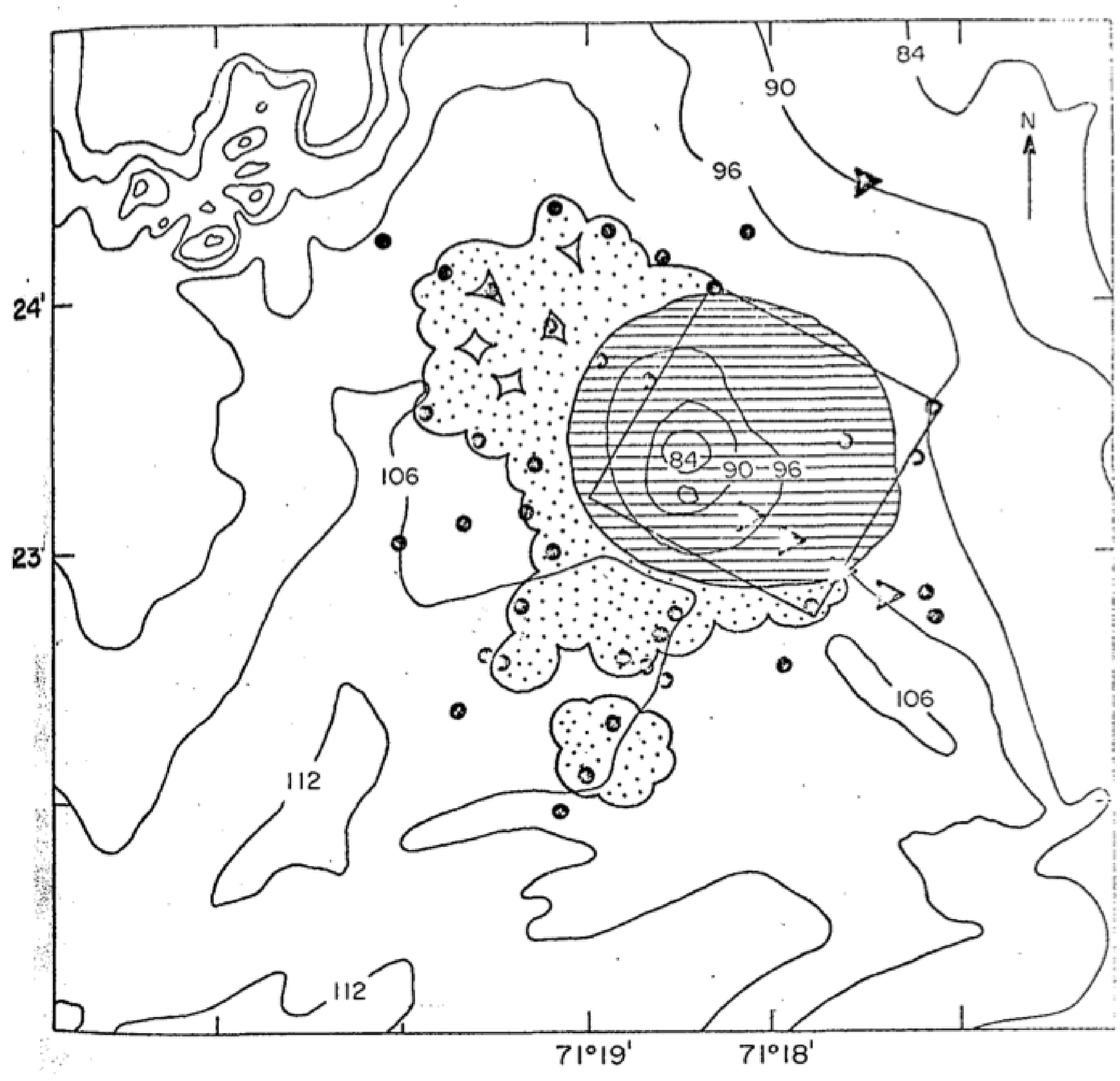

Figure A-5. Larger scale view bathymetric contour map. Data collected on September 25, 1970. Dredged material placed between October 22, 1969 and September 25, 1970: 2.1 million m³. Cumulative dredged material: 6.3 million m³. Hatched area shows dredged material thicker than 1 foot; dotted area had patches of dredged material (Pratt et al. 1973).

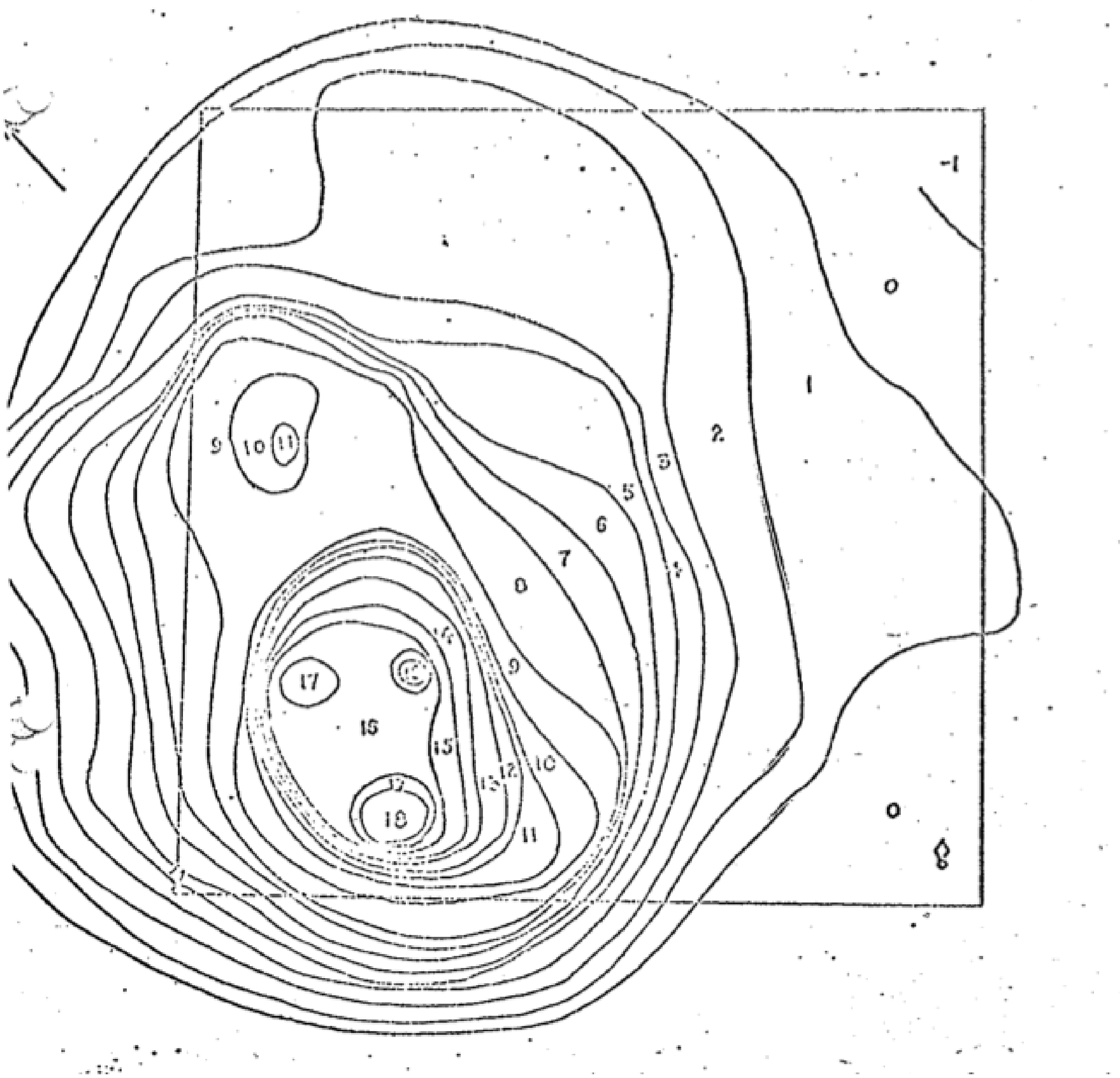

Figure A-6. Depth difference contour map. Isopachs compare December 15, 1967 data with September 25, 1970 data after 6.3 million m³ were placed (Saila et al. 1971).

Bathymetric Contour Maps of BRDS 1967 - 1987

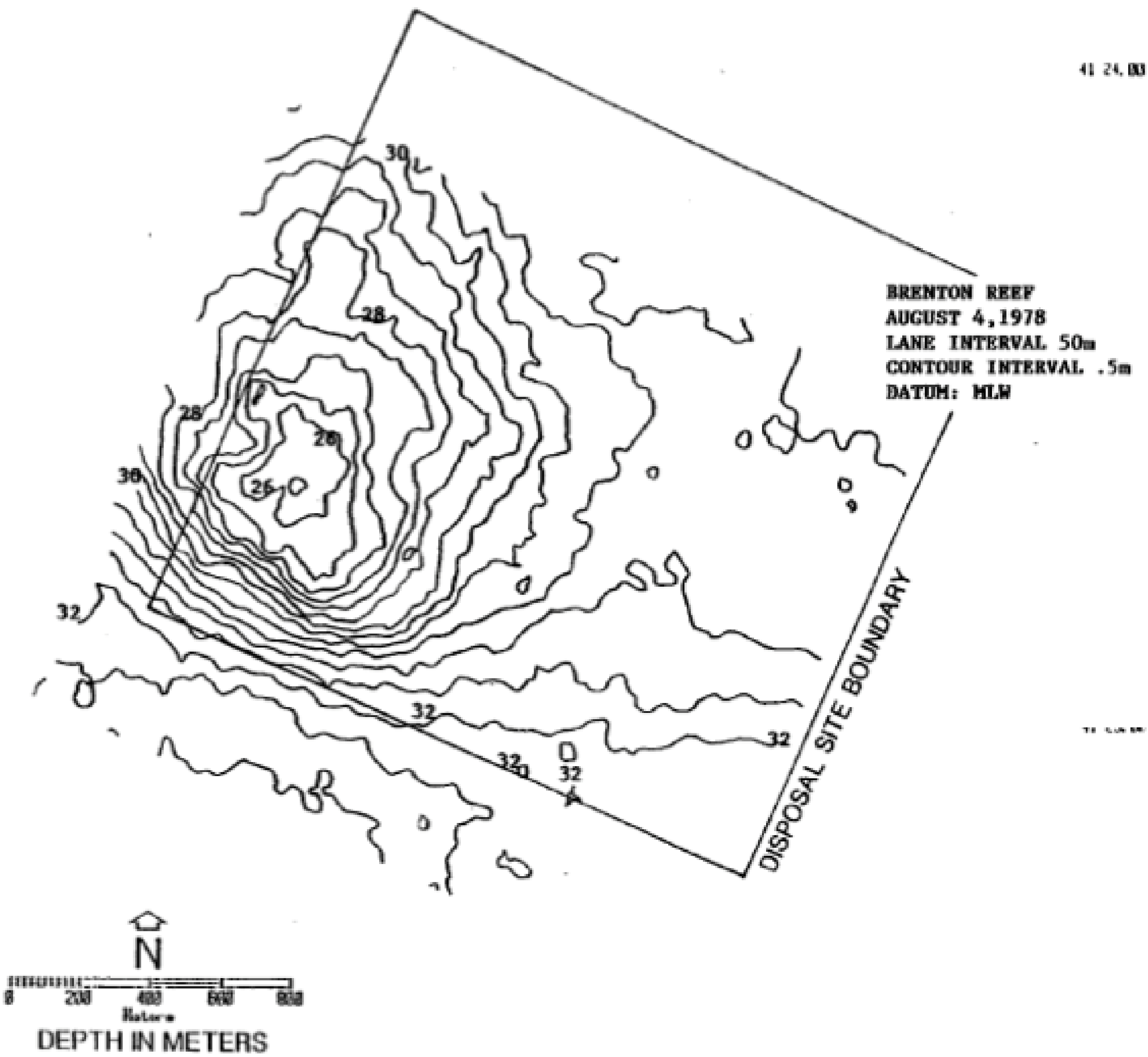

Figure A-7. Bathymetric survey data collected on August 4, 1978 (SAIC 1990)

Bathymetric Contour Maps of BRDS 1967 - 1987

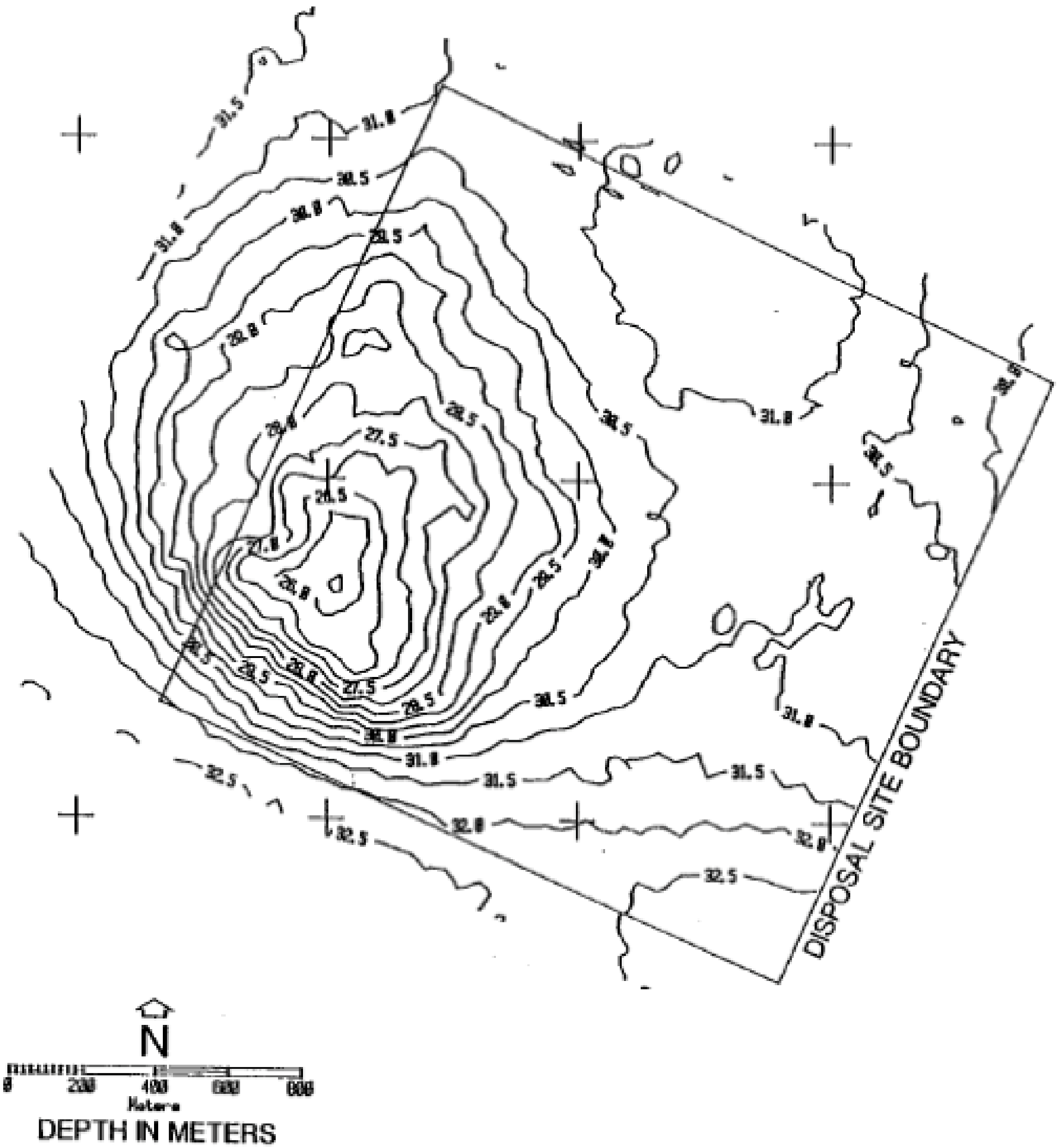

Figure A-8. Bathymetric survey data collected in October 1987 (SAIC 1990)

APPENDIX B

GRAIN SIZE SCALE FOR SEDIMENTS

APPENDIX B

Grain Size Scale for Sediments

Phi (Φ) size	Size range (mm)	Size class (Wentworth class)
< -1	> 2	Gravel
0 to -1	1 to 2	Very coarse sand
1 to 0	0.5 to 1	Coarse sand
2 to 1	0.25 to 0.5	Medium sand
3 to 2	0.125 to 0.25	Fine sand
4 to 3	0.0625 to 0.125	Very fine sand
> 4	< 0.0625	Silt/clay

APPENDIX C

SEDIMENT PROFILE AND PLAN-VIEW IMAGE RESULTS FOR BRDS

APPENDIX C

Sediment Profile and Plan-View Image Results for BRDS.

Reference stations 63–72, 94–97 are in bold text.

Station	Replicate	Date	Time	Calibration Constant	Penetration Area (sq.cm)	Penetration Mean (cm)	Penetration Minimum (cm)	Penetration Maximum (cm)	Boundary Roughness (cm)	Boundary Roughness Type	Grain Size Major Mode (phi)	Grain Size Maximum (phi)	Grain Size Minimum (phi)	Void #	Void Minimum Depth (cm)	Void Maximum Depth (cm)	Infaunal Succ. Stage
BR-01	A	7/25/2011	11:41	14.50	140.55	9.69	9.20	10.03	0.84	Physical	0 - -1	-4	>4	0	-	-	IND
BR-01	B	7/25/2011	11:42	14.50	103.31	7.12	5.27	8.32	3.05	Physical	0 - -1	-3	>4	0	-	-	IND
BR-01	C	7/25/2011	11:42	14.50	80.30	5.54	4.43	6.00	1.56	Physical	-1- -2	-4	>4	0	-	-	IND
BR-02	A	7/25/2011	11:17	14.50	174.51	12.04	11.45	12.50	1.05	Physical	2 - 1/>4	0	>4	0	-	-	3
BR-02	B	7/25/2011	11:18	14.50	175.45	12.10	11.71	12.32	0.62	Physical	1-0	-3	>4	0	-	-	IND
BR-02	C	7/25/2011	11:19	14.50	166.68	11.50	10.43	11.89	1.45	Physical	3-2/>4	0	>4	2	9.92	11.53	1 on 3
BR-03	A	7/25/2011	11:31	14.50	129.10	8.90	8.03	9.34	1.31	Physical	2 - 1/>4	0	>4	0	-	-	3
BR-03	B	7/25/2011	11:32	14.50	78.28	5.40	4.94	6.22	1.27	Physical	0 - -1	-3	>4	0	-	-	IND
BR-03	C	7/25/2011	11:33	14.50	98.23	6.77	6.33	7.74	1.42	Physical	2 - 1/>4	0	>4	0	-	-	1 on 3
BR-04	A	7/25/2011	11:10	14.50	142.58	9.83	9.34	10.21	0.87	Physical	2 - 1/>4	0	>4	1	4.94	7.53	1 on 3
BR-04	B	7/25/2011	11:11	14.50	122.60	8.46	7.05	10.25	3.20	Physical	0 - -1	-3	>4	0	-	-	1 on 3
BR-04	C	7/25/2011	11:12	14.50	146.22	10.08	10.03	10.21	0.18	Physical	2-1	0	>4	0	-	-	1
BR-05	A	7/25/2011	10:45	14.50	102.46	7.07	6.47	7.56	1.09	Physical	2-1	-3	>4	0	-	-	1
BR-05	B	7/25/2011	10:46	14.50	94.76	6.54	6.11	7.16	1.05	Physical	2-1	-3	>4	0	-	-	1
BR-05	C	7/25/2011	10:47	14.50	108.98	7.52	6.29	8.62	2.33	Physical	2-1	-1	>4	0	-	-	1
BR-06	B	7/25/2011	9:02	14.50	190.26	13.12	12.72	13.85	1.13	Physical	2 - 1/>4	0	>4	2	8.43	11.82	1 on 3
BR-06	C	7/25/2011	9:03	14.50	236.16	16.29	15.99	16.79	0.80	Physical	2 - 1/>4	0	>4	2	13.81	16.32	1 on 3
BR-06	F	7/25/2011	10:13	14.50	248.28	17.12	16.32	17.88	1.56	Physical	2 - 1/>4	0	>4	3	6.43	15.41	1 on 3
BR-07	A	7/25/2011	11:23	14.50	86.22	5.95	4.47	6.73	2.25	Physical	0 - -1	-2	>4	0	-	-	1
BR-07	B	7/25/2011	11:24	14.50	0.00	0.00	0.00	0.00	IND	IND	IND	IND	IND	IND	IND	IND	IND

Sediment Profile and Plan-View Image Results for BRDS.

Reference stations 63–72, 94–97 are in bold text.

Station	Replicate	Date	Time	Calibration Constant	Penetration Area (sq.cm)	Penetration Mean (cm)	Penetration Minimum (cm)	Penetration Maximum (cm)	Boundary Roughness (cm)	Boundary Roughness Type	Grain Size Major Mode (phi)	Grain Size Maximum (phi)	Grain Size Minimum (phi)	Void #	Void Minimum Depth (cm)	Void Maximum Depth (cm)	Infaunal Succ. Stage
BR-07	C	7/25/2011	11:25	14.50	126.01	8.69	8.14	9.27	1.13	Physical	1-0	-2	>4	0	-	-	1
BR-08	A	7/25/2011	10:36	14.50	240.33	16.57	16.25	17.05	0.80	Physical	2 - 1/>4	0	>4	2	8.43	15.16	1 on 3
BR-08	B	7/25/2011	10:37	14.50	181.86	12.54	11.12	13.45	2.33	Physical	3-2/>4	-5	>4	1	4.87	6.29	1 on 3
BR-08	C	7/25/2011	10:38	14.50	19.04	1.31	0.11	2.47	2.36	Physical	-4 - -5	-5	>4	0	-	-	IND
BR-09	A	7/25/2011	10:55	14.50	201.97	13.93	13.01	14.58	1.56	Physical	-2 - -3/>4	-4	>4	1	9.49	10.43	1 on 3
BR-09	B	7/25/2011	10:56	14.50	114.38	7.89	6.54	9.05	2.51	Physical	1 - -2	-3	>4	0	-	-	1
BR-09	C	7/25/2011	10:57	14.50	123.77	8.54	8.11	9.09	0.98	Physical	3-2/>4	-5	>4	2	3.42	8.29	1 on 3
BR-10	A	7/25/2011	11:03	14.50	197.84	13.64	12.65	14.00	1.34	Physical	2 - 1/>4	-2	>4	0	-	-	1 on 3
BR-10	B	7/25/2011	11:04	14.50	212.64	14.66	14.18	16.14	1.96	Physical	2 - 1/>4	-3	>4	0	-	-	1 on 3
BR-10	C	7/25/2011	11:05	14.50	48.40	3.34	2.87	4.29	1.42	Physical	1-0	-2	>4	0	-	-	IND
BR-19	A	7/27/2011	3:32	14.50	230.06	15.87	14.50	17.09	2.58	Biological	>4	2	>4	4	3.34	14.21	1 on 3
BR-19	B	7/27/2011	3:33	14.50	181.92	12.55	11.71	13.38	1.67	Biological	>4	2	>4	1	9.09	11.89	1 on 3
BR-19	C	7/27/2011	3:34	14.50	247.07	17.04	16.21	17.45	1.24	Biological	>4	2	>4	2	6.54	13.67	1 on 3
BR-21	A	7/27/2011	3:39	14.50	179.54	12.38	10.80	14.98	4.18	Physical	>4	2	>4	1	3.71	11.16	1 on 3
BR-21	B	7/27/2011	3:39	14.50	224.73	15.50	15.05	15.74	0.69	Biological	>4	2	>4	0	-	-	1 on 3
BR-21	C	7/27/2011	3:40	14.50	210.84	14.54	13.74	15.01	1.27	Biological	>4	2	>4	1	4.98	7.38	1 on 3
BR-24	A	7/27/2011	3:58	14.50	213.18	14.70	13.96	15.23	1.27	Biological	>4	2	>4	1	6.80	7.82	1 on 3
BR-24	B	7/27/2011	3:58	14.50	227.32	15.68	15.01	16.14	1.13	Biological	>4	2	>4	2	10.69	14.50	1 on 3
BR-24	C	7/27/2011	3:59	14.50	218.78	15.09	14.69	15.45	0.76	Biological	>4	2	>4	2	6.87	10.40	1 on 3
BR-25	A	7/27/2011	3:51	14.50	224.68	15.50	15.23	16.07	0.84	Biological	>4	2	>4	2	6.94	9.53	1 on 3

Sediment Profile and Plan-View Image Results for BRDS.

Reference stations 63–72, 94–97 are in bold text.

Station	Replicate	Date	Time	Calibration Constant	Penetration Area (sq.cm)	Penetration Mean (cm)	Penetration Minimum (cm)	Penetration Maximum (cm)	Boundary Roughness (cm)	Boundary Roughness Type	Grain Size Major Mode (phi)	Grain Size Maximum (phi)	Grain Size Minimum (phi)	Void #	Void Minimum Depth (cm)	Void Maximum Depth (cm)	Infaunal Succ. Stage
BR-25	B	7/27/2011	3:52	14.50	220.99	15.24	14.94	15.56	0.62	Biological	>4	1	>4	2	12.14	13.63	1 on 3
BR-25	C	7/27/2011	3:52	14.50	209.39	14.44	14.07	14.87	0.80	Biological	>4	1	>4	5	6.65	13.70	1 on 3
BR-26	A	7/27/2011	3:27	14.50	179.75	12.40	11.92	12.90	0.98	Biological	>4	2	>4	1	10.47	11.92	1 on 3
BR-26	B	7/27/2011	3:28	14.50	221.39	15.27	14.65	16.18	1.53	Biological	>4	1	>4	IND	-	-	1 on 3
BR-26	C	7/27/2011	3:29	14.50	227.26	15.67	15.27	16.58	1.31	Biological	>4	1	>4	3	5.78	11.38	1 on 3
BR-27	A	7/27/2011	3:15	14.50	185.15	12.77	11.63	13.49	1.85	Biological	4-3	1	>4	1	3.16	8.51	1 on 3
BR-27	B	7/27/2011	3:16	14.50	112.94	7.79	7.09	8.43	1.34	Physical	4-3	-5.00	>4	IND	-	-	IND
BR-27	C	7/27/2011	3:17	14.50	150.71	10.39	9.67	11.16	1.49	Physical	3-2/>4	-5.00	>4	1	8.36	9.71	1 on 3
BR-28	A	7/27/2011	3:21	14.50	208.04	14.35	14.10	15.30	1.20	Biological	>4	1	>4	1	5.27	8.65	1 on 3
BR-28	B	7/27/2011	3:22	14.50	231.73	15.98	15.27	17.16	1.89	Biological	>4	2	>4	4	8.73	15.49	1 on 3
BR-28	C	7/27/2011	3:23	14.50	219.48	15.14	14.36	15.52	1.16	Biological	>4	2	>4	3	9.67	12.80	1 on 3
BR-30	A	7/27/2011	3:09	14.50	159.85	11.02	8.72	12.03	3.31	Physical	>4	-4	>4	1	7.31	8.98	1 on 3
BR-30	B	7/27/2011	3:10	14.50	188.09	12.97	11.05	13.56	2.51	Biological	>4	2	>4	1	6.33	10.91	1 on 3
BR-30	C	7/27/2011	3:10	14.50	50.29	3.47	2.47	4.83	2.36	Physical	-2 - -3	-4	>4	IND	-	-	IND
BR-31	A	7/27/2011	2:13	14.50	34.07	2.35	1.24	3.93	2.69	Physical	IND	-4	>4	IND	-	-	IND
BR-31	B	7/27/2011	2:14	14.50	0.00	0.00	0.00	0.00	IND	Physical	-4 - -5	-5	>4	IND	-	-	IND
BR-31	C	7/27/2011	2:15	14.50	82.98	5.72	3.89	6.72	2.84	Physical	4-3	-2	>4	0	-	-	1->2
BR-32	A	7/27/2011	2:18	14.50	127.70	8.81	8.43	9.38	0.95	Physical	3-2/>4	-1	>4	2	6.29	8.43	1 on 3
BR-32	B	7/27/2011	2:19	14.50	202.68	13.98	12.61	14.98	2.36	Physical	3-2/>4	-1	>4	1	5.42	9.92	1 on 3
BR-32	C	7/27/2011	2:20	14.50	175.86	12.13	10.54	13.56	3.02	Physical	3-2/>4	-3	>4	1	4.65	5.56	1 on 3

Sediment Profile and Plan-View Image Results for BRDS.

Reference stations 63–72, 94–97 are in bold text.

Station	Replicate	Date	Time	Calibration Constant	Penetration Area (sq.cm)	Penetration Mean (cm)	Penetration Minimum (cm)	Penetration Maximum (cm)	Boundary Roughness (cm)	Boundary Roughness Type	Grain Size Major Mode (phi)	Grain Size Maximum (phi)	Grain Size Minimum (phi)	Void #	Void Minimum Depth (cm)	Void Maximum Depth (cm)	Infaunal Succ. Stage
BR-33	A	7/27/2011	2:07	14.50	208.95	14.41	14.54	14.87	0.33	Biological	>4	2	>4	1	12.21	13.30	1 on 3
BR-33	B	7/27/2011	2:08	14.50	211.01	14.55	13.60	15.41	1.82	Biological	>4	-3	>4	1	7.42	9.56	1 on 3
BR-33	C	7/27/2011	2:09	14.50	222.83	15.37	13.81	16.25	2.44	Biological	>4	2	>4	4	4.25	13.92	1 on 3
BR-34	A	7/27/2011	3:01	14.50	46.97	3.24	1.67	5.09	3.42	Physical	1-0	-4	>4	0	-	-	1
BR-34	B	7/27/2011	3:02	14.50	115.53	7.97	7.31	8.43	1.13	Physical	1-0	-3	>4	0	-	-	IND
BR-34	C	7/27/2011	3:03	14.50	95.80	6.61	5.63	7.92	2.29	Physical	-2 - -3	-3	>4	0	-	-	IND
BR-35	A	7/27/2011	1:37	14.50	265.39	18.30	17.41	19.23	1.82	Physical	2-1	0	>4	0	-	-	1
BR-35	B	7/27/2011	1:38	14.50	104.27	7.19	6.83	7.52	0.69	Physical	0 - -1	-3	>4	0	-	-	1
BR-35	C	7/27/2011	1:39	14.50	142.74	9.84	8.83	10.91	2.07	Physical	-3 - -4/2-1	-4	>4	0	-	-	1
BR-36	A	7/27/2011	1:53	14.50	136.85	9.44	8.36	11.27	2.91	Physical	>4	-4	>4	2	2.22	7.71	3
BR-36	B	7/27/2011	1:54	14.50	217.26	14.98	14.29	15.30	1.02	Physical	3-2/>4	-1	>4	1	13.60	15.12	1 on 3
BR-36	C	7/27/2011	1:56	14.50	187.06	12.90	12.03	13.67	1.64	Physical	3-2/>4	-1	>4	1	8.65	9.92	1 on 3
BR-37	A	7/27/2011	1:44	14.50	38.05	2.62	2.04	2.98	0.95	Physical	0 - -1	-8	>4	0	-	-	IND
BR-37	B	7/27/2011	1:45	14.50	71.33	4.92	4.51	5.27	0.76	Physical	3-2	0	>4	0	-	-	1
BR-37	C	7/27/2011	1:46	14.50	198.28	13.67	13.41	13.81	0.40	Physical	3-2/>4	-1	>4	1	11.74	12.54	1 on 3
BR-38	A	7/25/2011	2:28	14.50	127.53	8.80	7.85	9.12	1.27	Physical	3-2	0	>4	0	-	-	3
BR-38	B	7/25/2011	2:29	14.50	75.08	5.18	5.13	5.34	0.22	Physical	3-2	0	>4	0	-	-	1
BR-38	C	7/25/2011	2:30	14.50	60.54	4.18	4.00	4.54	0.55	Physical	3-2	0	>4	0	-	-	1
BR-39	A	7/25/2011	2:09	14.50	195.61	13.49	13.27	13.67	0.40	Biological	>4	1	>4	1	8.87	9.60	1 on 3
BR-39	B	7/25/2011	2:10	14.50	187.63	12.94	12.54	13.56	1.02	Biological	3-2/>4	1	>4	1	1.42	2.25	1 on 3

Sediment Profile and Plan-View Image Results for BRDS.
Reference stations 63–72, 94–97 are in bold text.

Station	Replicate	Date	Time	Calibration Constant	Penetration Area (sq.cm)	Penetration Mean (cm)	Penetration Minimum (cm)	Penetration Maximum (cm)	Boundary Roughness (cm)	Boundary Roughness Type	Grain Size Major Mode (phi)	Grain Size Maximum (phi)	Grain Size Minimum (phi)	Void #	Void Minimum Depth (cm)	Void Maximum Depth (cm)	Infaunal Succ. Stage
BR-39	C	7/25/2011	2:15	14.50	212.08	14.63	13.92	15.34	1.42	Biological	3-2/>4	1	>4	0	-	-	1 on 3
BR-40	A	7/25/2011	1:30	14.50	218.86	15.09	13.85	16.98	3.13	Biological	>4	1	>4	5	6.65	13.78	1 on 3
BR-40	B	7/25/2011	1:30	14.50	246.31	16.99	16.50	17.41	0.91	Biological	>4	1	>4	3	1.20	14.61	1 on 3
BR-40	C	7/25/2011	1:31	14.50	223.20	15.39	14.40	16.14	1.74	Biological	>4	1	>4	0	-	-	1 on 3
BR-41	A	7/25/2011	12:44	14.50	227.45	15.69	15.30	16.14	0.84	Biological	>4	1	>4	0	-	-	1 on 3
BR-41	B	7/25/2011	12:45	14.50	248.08	17.11	16.69	17.48	0.80	Biological	>4	1	>4	3	2.36	16.94	1 on 3
BR-41	C	7/25/2011	12:45	14.50	220.55	15.21	14.61	15.63	1.02	Biological	>4	1	>4	5	1.67	15.23	1 on 3
BR-42	A	7/25/2011	12:34	14.50	212.78	14.67	13.96	15.19	1.24	Biological	>4	1	>4	1	1.53	3.42	1 on 3
BR-42	B	7/25/2011	12:35	14.50	197.45	13.62	13.38	13.81	0.44	Biological	>4	1	>4	1	5.24	5.42	1 on 3
BR-42	C	7/25/2011	12:36	14.50	205.20	14.15	13.52	15.12	1.60	Biological	>4	1	>4	1	11.02	12.29	1 on 3
BR-43	A	7/25/2011	1:38	14.50	105.14	7.25	5.49	8.80	3.31	Physical	2-1	-3	>4	IND	-	-	IND
BR-43	B	7/25/2011	1:41	14.50	72.38	4.99	4.54	5.78	1.24	Physical	3-2	0	>4	0	-	-	1
BR-43	C	7/25/2011	1:42	14.50	148.82	10.26	8.32	11.16	2.84	IND	>4	0	>4	0	-	-	1 on 3
BR-44	A	7/25/2011	2:02	14.50	0.00	0.00	0.00	0.00	IND	IND	IND	IND	IND	IND	-	-	IND
BR-44	B	7/25/2011	2:03	14.50	125.67	8.67	7.92	8.94	1.02	Physical	3-2	1	>4	0	-	-	2
BR-44	C	7/25/2011	2:04	14.50	102.88	7.10	5.05	7.96	2.91	Physical	-1 - -2/>4	-4	>4	1	4.91	5.74	3
BR-45	A	7/25/2011	1:47	14.50	184.21	12.70	11.41	13.23	1.82	Physical	3-2/>4	1	>4	0	-	-	3
BR-45	B	7/25/2011	1:48	14.50	54.00	3.72	1.56	5.67	4.11	Physical	2 - -3	-4	>4	0	-	-	IND
BR-45	C	7/25/2011	1:49	14.50	163.04	11.24	9.23	12.58	3.34	Physical	3-2/>4	1	>4	1	3.09	5.13	1 on 3
BR-46	A	7/25/2011	1:55	14.50	54.14	3.73	2.80	4.40	1.60	Physical	1-0	-3	>4	0	-	-	IND

Sediment Profile and Plan-View Image Results for BRDS.
Reference stations 63–72, 94–97 are in bold text.

Station	Replicate	Date	Time	Calibration Constant	Penetration Area (sq.cm)	Penetration Mean (cm)	Penetration Minimum (cm)	Penetration Maximum (cm)	Boundary Roughness (cm)	Boundary Roughness Type	Grain Size Major Mode (phi)	Grain Size Maximum (phi)	Grain Size Minimum (phi)	Void #	Void Minimum Depth (cm)	Void Maximum Depth (cm)	Infaunal Succ. Stage
BR-46	B	7/25/2011	1:56	14.50	67.23	4.64	3.64	5.49	1.85	Physical	0 - -1	-2	>4	0	-	-	IND
BR-46	C	7/25/2011	1:57	14.50	72.46	5.00	3.60	6.29	2.69	Physical	>4	-3	>4	0	-	-	1.00
BR-47	A	7/27/2011	2:01	14.50	0.00	0.00	0.00	0.00	IND	IND	IND	IND	IND	IND	-	-	IND
BR-47	B	7/27/2011	2:02	14.50	210.73	14.53	14.14	14.76	0.62	Biological	3-2/>4	1	>4	5	2.87	14.40	1 on 3
BR-47	C	7/27/2011	2:03	14.50	196.92	13.58	12.76	14.14	1.38	Biological	3-2/>4	1	>4	1	12.69	13.34	1 on 3
BR-48	A	7/27/2011	10:25	14.50	182.67	12.60	12.10	12.90	0.80	Biological	>4	2	>4	3	2.36	9.02	1 on 3
BR-48	B	7/27/2011	10:26	14.50	217.89	15.03	14.65	15.41	0.76	Biological	>4	1	>4	4	4.80	13.60	1 on 3
BR-48	C	7/27/2011	10:27	14.50	193.76	13.36	12.69	13.96	1.27	Biological	>4	1	>4	1	10.98	11.89	1 on 3
BR-49	A	7/27/2011	10:18	14.50	21.52	1.48	0.84	2.40	1.56	Physical	4-3	0	>4	0	-	-	1.00
BR-49	B	7/27/2011	10:19	14.50	167.88	11.58	11.20	12.10	0.91	Physical	4-3	-2	>4	2	5.60	10.83	1 on 3
BR-49	C	7/27/2011	10:20	14.50	116.05	8.00	6.94	8.87	1.93	Physical	1-0	-2	>4	0	-	-	IND
BR-50	A	7/27/2011	10:13	14.50	180.08	12.42	11.81	13.12	1.31	Physical	2-1/>4	-2	>4	0	-	-	1.00
BR-50	B	7/27/2011	10:14	14.50	117.76	8.12	7.05	9.12	2.07	Physical	2-1	-2	>4	0	-	-	IND
BR-50	C	7/27/2011	10:15	14.50	184.63	12.73	11.81	14.14	2.33	Physical	2-1/>4	-1	>4	4	3.27	9.60	3.00
BR-51	A	7/27/2011	10:32	14.50	186.19	12.84	12.36	13.38	1.02	Physical	>4	2	>4	0	-	-	1 on 3
BR-51	B	7/27/2011	10:34	14.50	209.43	14.44	13.52	14.72	1.20	Physical	>4	2	>4	1	10.94	13.56	1 on 3
BR-51	C	7/27/2011	10:35	14.50	202.44	13.96	13.70	14.21	0.51	Biological	>4	2	>4	4	10.87	12.18	1 on 3
BR-52	A	7/27/2011	10:37	14.50	201.92	13.93	13.20	14.69	1.49	Biological	>4	0	>4	0	-	-	1 on 3
BR-52	B	7/27/2011	10:38	14.50	194.39	13.41	11.56	15.45	3.89	Physical	>4	0	>4	1	8.47	11.96	1 on 3
BR-52	C	7/27/2011	10:39	14.50	240.51	16.59	16.10	17.30	1.20	Biological	4-3/>4	1	>4	4	2.95	10.11	1 on 3

Sediment Profile and Plan-View Image Results for BRDS.

Reference stations 63–72, 94–97 are in bold text.

Station	Replicate	Date	Time	Calibration Constant	Penetration Area (sq.cm)	Penetration Mean (cm)	Penetration Minimum (cm)	Penetration Maximum (cm)	Boundary Roughness (cm)	Boundary Roughness Type	Grain Size Major Mode (phi)	Grain Size Maximum (phi)	Grain Size Minimum (phi)	Void #	Void Minimum Depth (cm)	Void Maximum Depth (cm)	Infaunal Succ. Stage
BR-53	A	7/27/2011	10:45	14.50	200.61	13.84	13.56	14.07	0.51	Physical	2-1/>4	-1	>4	2	5.31	13.86	1 on 3
BR-53	B	7/27/2011	10:46	14.50	183.55	12.66	11.05	13.52	2.47	Physical	3-2/>4	-1	>4	0	-	-	1 on 3
BR-53	C	7/27/2011	10:47	14.50	220.24	15.19	14.18	15.74	1.56	Physical	1-0/>4	-2	>4	1	4.73	7.20	1 on 3
BR-54	A	7/27/2011	10:58	14.50	217.35	14.99	14.25	15.63	1.38	Biological	>4	2	>4	2	7.20	12.29	1 on 3
BR-54	B	7/27/2011	11:00	14.50	217.60	15.01	14.32	15.49	1.16	Biological	>4	2	>4	3	8.98	14.62	1 on 3
BR-54	C	7/27/2011	11:01	14.50	205.80	14.19	13.52	15.27	1.74	Biological	>4	2	>4	2	7.45	12.21	1 on 3
BR-55	A	7/27/2011	11:05	14.50	221.35	15.27	14.40	15.99	1.60	Biological	>4	1	>4	5	2.18	13.67	1 on 3
BR-55	B	7/27/2011	11:06	14.50	194.46	13.41	12.90	14.18	1.27	Physical	>4	1	>4	2	2.80	11.24	1 on 3
BR-55	C	7/27/2011	11:07	14.50	230.16	15.87	15.49	16.14	0.65	Biological	>4	1	>4	3	8.87	13.34	1 on 3
BR-56	A	7/27/2011	11:10	14.50	131.80	9.09	8.07	10.47	2.40	Physical	>4	-2	>4	0	-	-	IND
BR-56	B	7/27/2011	11:11	14.50	138.63	9.56	8.00	10.69	2.69	Physical	>4	-4	>4	1	6.69	8.58	1 on 3
BR-56	C	7/27/2011	11:12	14.50	146.65	10.11	8.29	11.20	2.91	Physical	>4	-3	>4	1	3.71	7.24	1 on 3
BR-57	A	7/27/2011	10:51	14.50	161.26	11.12	10.73	11.96	1.23	Physical	3-2/>4	-1	>4	0	-	-	IND
BR-57	B	7/27/2011	10:51	14.50	151.52	10.45	9.67	10.73	1.06	Physical	1-0	-2	>4	0	-	-	1 on 3
BR-57	C	7/27/2011	10:52	14.50	160.57	11.07	9.31	12.69	3.38	Physical	1-0/>4	-2	>4	0	-	-	IND
BR-60	A	7/27/2011	11:16	14.50	49.91	3.44	2.04	5.05	3.02	Physical	2-1	-2	>4	0	-	-	IND
BR-60	B	7/27/2011	11:17	14.50	61.85	4.27	3.49	4.83	1.34	Physical	2-1	-4	>4	0	-	-	IND
BR-60	C	7/27/2011	11:18	14.50	159.29	10.99	10.40	11.38	0.98	Physical	1-0	-2	>4	0	-	-	IND
BR-61	A	7/27/2011	11:22	14.50	237.29	16.37	15.92	16.65	0.73	Biological	>4	-2	>4	3	2.51	9.53	1 on 3
BR-61	B	7/27/2011	11:23	14.50	190.07	13.11	12.25	13.89	1.64	Biological	3-2/>4	1	>4	0	-	-	1 on 3

Sediment Profile and Plan-View Image Results for BRDS.

Reference stations 63–72, 94–97 are in bold text.

Station	Replicate	Date	Time	Calibration Constant	Penetration Area (sq.cm)	Penetration Mean (cm)	Penetration Minimum (cm)	Penetration Maximum (cm)	Boundary Roughness (cm)	Boundary Roughness Type	Grain Size Major Mode (phi)	Grain Size Maximum (phi)	Grain Size Minimum (phi)	Void #	Void Minimum Depth (cm)	Void Maximum Depth (cm)	Infaunal Succ. Stage
BR-61	C	7/27/2011	11:24	14.50	225.85	15.58	15.12	16.43	1.31	Biological	>4	0	>4	4	5.89	15.23	1 on 3
BR-62	A	7/27/2011	2:54	14.50	121.33	8.37	7.52	9.52	2.00	Physical	2-1	-1	>4	0	-	-	1.00
BR-62	B	7/27/2011	2:54	14.50	36.36	2.51	0.73	3.38	2.65	Physical	-1 - -2	-3	>4	0	-	-	IND
BR-62	C	7/27/2011	2:55	14.50	115.34	7.95	6.87	9.63	2.76	Physical	-1 - -2	-3	>4	0	-	-	1.00
BR-63	A	7/27/2011	4:41	14.50	185.44	12.79	11.02	14.29	3.27	Biological	>4	2	>4	2	1.60	10.01	1 on 3
BR-63	B	7/27/2011	4:42	14.50	223.42	15.41	14.79	15.74	0.95	Biological	>4	2	>4	2	1.49	11.71	1 on 3
BR-63	C	7/27/2011	4:43	14.50	96.54	6.66	3.45	9.92	6.47	IND	>4	2	>4	1	4.58	6.11	1 on 3
BR-64	A	7/27/2011	4:35	14.50	215.02	14.83	14.65	15.16	0.51	Biological	>4	2	>4	4	3.02	14.94	1 on 3
BR-64	B	7/27/2011	4:36	14.50	211.29	14.57	14.00	15.05	1.05	Biological	>4	2	>4	3	1.16	12.72	1 on 3
BR-64	C	7/27/2011	4:37	14.50	189.20	13.05	12.00	14.29	2.29	Biological	>4	2	>4	0	-	-	1 on 3
BR-65	A	7/27/2011	4:31	14.50	215.62	14.87	14.21	15.30	1.09	Biological	>4	2	>4	0	-	-	1 on 3
BR-65	B	7/27/2011	4:32	14.50	243.47	16.79	16.43	16.87	0.44	Biological	>4	2	>4	4	9.60	16.36	1 on 3
BR-65	C	7/27/2011	4:33	14.50	208.78	14.40	13.56	14.87	1.31	Biological	>4	2	>4	0	-	-	1 on 3
BR-66	A	7/27/2011	4:47	14.50	205.08	14.14	13.49	15.05	1.56	Biological	>4	2	>4	2	2.51	10.55	1 on 3
BR-66	B	7/27/2011	4:48	14.50	213.69	14.74	13.78	14.98	1.20	Biological	>4	2	>4	0	-	-	1 on 3
BR-66	C	7/27/2011	4:49	14.50	200.42	13.82	13.23	14.14	0.91	Biological	>4	2	>4	2	9.74	12.36	1 on 3
BR-67	A	7/27/2011	4:53	14.50	161.85	11.16	8.62	13.85	5.23	Physical	>4	2	>4	0	-	-	1 on 3
BR-67	B	7/27/2011	4:54	14.50	218.43	15.06	14.69	15.38	0.69	Biological	>4	2	>4	3	8.58	14.07	1 on 3
BR-67	C	7/27/2011	4:55	14.50	243.81	16.81	15.56	17.63	2.07	Biological	>4	2	>4	3	1.56	2.94	1 on 3
BR-68	A	7/27/2011	5:13	14.50	149.34	10.30	9.89	10.87	0.98	IND	>4	2	>4	0	-	-	1 on 3

Sediment Profile and Plan-View Image Results for BRDS.

Reference stations 63–72, 94–97 are in bold text.

Station	Replicate	Date	Time	Calibration Constant	Penetration Area (sq.cm)	Penetration Mean (cm)	Penetration Minimum (cm)	Penetration Maximum (cm)	Boundary Roughness (cm)	Boundary Roughness Type	Grain Size Major Mode (phi)	Grain Size Maximum (phi)	Grain Size Minimum (phi)	Void #	Void Minimum Depth (cm)	Void Maximum Depth (cm)	Infaunal Succ. Stage
BR-68	B	7/27/2011	5:14	14.50	108.73	7.50	6.91	8.14	1.24	Physical	4-3	2	>4	0	-	-	1 on 3
BR-68	C	7/27/2011	5:15	14.50	181.86	12.54	12.29	12.76	0.47	Biological	>4	2	>4	1	2.33	2.62	1 on 3
BR-69	A	7/27/2011	5:18	14.50	223.57	15.42	15.01	15.81	0.80	Biological	>4	2	>4	2	4.22	11.05	1 on 3
BR-69	B	7/27/2011	5:19	14.50	196.86	13.58	13.34	13.89	0.55	Biological	>4	2	>4	2	4.11	9.56	1 on 3
BR-69	C	7/27/2011	5:20	14.50	154.07	10.63	10.25	11.49	1.24	Physical	>4	2	>4	2	2.73	9.78	1 on 3
BR-70	A	7/27/2011	5:24	14.50	170.35	11.75	11.38	12.32	0.95	Physical	>4	2	>4	0	-	-	1 on 3
BR-70	B	7/27/2011	5:25	14.50	193.76	13.36	12.47	13.78	1.31	Biological	>4	2	>4	1	5.78	6.65	1 on 3
BR-70	C	7/27/2011	5:25	14.50	188.53	13.00	11.74	14.00	2.25	Physical	>4	2	>4	0	-	-	1 on 3
BR-71	A	7/27/2011	5:04	14.50	147.21	10.15	9.96	10.65	0.69	Biological	>4	2	>4	0	-	-	1 on 3
BR-71	B	7/27/2011	5:05	14.50	170.85	11.78	10.18	13.20	3.02	Physical	>4	2	>4	1	1.75	2.29	1 on 3
BR-71	C	7/27/2011	5:06	14.50	152.43	10.51	10.43	10.69	0.26	Physical	>4	2	>4	0	-	-	1 on 3
BR-72	A	7/27/2011	5:08	14.50	124.45	8.58	8.29	8.76	0.47	Physical	4-3	2	>4	0	-	-	1 on 3
BR-72	B	7/27/2011	5:09	14.50	174.81	12.06	11.89	12.47	0.58	Biological	>4	2	>4	1	11.60	12.07	1 on 3
BR-72	C	7/27/2011	5:10	14.50	187.03	12.90	12.21	13.27	1.05	Biological	>4	2	>4	1	4.04	4.69	1 on 3
BR-73	A	7/27/2011	8:08	14.50	227.27	15.67	15.20	16.32	1.13	Biological	>4	2	>4	1	12.87	15.23	1 on 3
BR-73	B	7/27/2011	8:09	14.50	217.68	15.01	14.65	15.30	0.65	Biological	>4	2	>4	1	4.87	10.36	1 on 3
BR-73	C	7/27/2011	8:10	14.50	196.96	13.58	13.34	14.03	0.69	Biological	>4	2	>4	1	2.80	5.23	1 on 3
BR-74	A	7/27/2011	8:15	14.50	217.94	15.03	14.76	15.92	1.16	Biological	>4	2	>4	2	8.47	15.78	1 on 3
BR-74	B	7/27/2011	8:16	14.50	227.05	15.66	14.90	15.99	1.09	Biological	>4	2	>4	2	2.65	12.00	1 on 3
BR-74	C	7/27/2011	8:18	14.50	207.74	14.33	13.01	14.94	1.93	Biological	>4	2	>4	3	8.58	14.72	1 on 3

Sediment Profile and Plan-View Image Results for BRDS.

Reference stations 63–72, 94–97 are in bold text.

Station	Replicate	Date	Time	Calibration Constant	Penetration Area (sq.cm)	Penetration Mean (cm)	Penetration Minimum (cm)	Penetration Maximum (cm)	Boundary Roughness (cm)	Boundary Roughness Type	Grain Size Major Mode (phi)	Grain Size Maximum (phi)	Grain Size Minimum (phi)	Void #	Void Minimum Depth (cm)	Void Maximum Depth (cm)	Infaunal Succ. Stage
BR-75	A	7/27/2011	8:24	14.50	213.62	14.73	14.00	15.30	1.31	Biological	>4	1	>4	3	5.16	7.82	1 on 3
BR-75	B	7/27/2011	8:25	14.50	218.82	15.09	13.70	16.07	2.36	Biological	>4	2	>4	3	8.83	15.70	1 on 3
BR-75	C	7/27/2011	8:26	14.50	202.53	13.97	13.81	14.43	0.62	Biological	>4	2	>4	2	6.36	10.43	1 on 3
BR-76	A	7/27/2011	8:31	14.50	205.59	14.18	13.70	14.54	0.84	Physical	2-1/>4	0	>4	0	-	-	1.00
BR-76	B	7/27/2011	8:32	14.50	123.83	8.54	6.00	10.87	4.87	Physical	2-1/>4	0	>4	1	7.96	9.12	1 on 3
BR-76	C	7/27/2011	8:33	14.50	131.59	9.08	8.29	9.89	1.60	Physical	3-2/>4	-4	>4	0	-	-	1.00
BR-77	A	7/27/2011	8:41	14.50	62.98	4.34	2.44	5.31	2.87	Physical	3-2	0	>4	0	-	-	1.00
BR-77	B	7/27/2011	8:42	14.50	47.71	3.29	2.69	3.85	1.16	Physical	2-1	-1	>4	0	-	-	IND
BR-77	C	7/27/2011	8:43	14.50	65.21	4.50	3.42	5.96	2.54	Physical	2-1	-1	>4	0	-	-	1.00
BR-78	A	7/27/2011	8:48	14.50	69.05	4.76	4.36	5.09	0.73	Physical	1-0	-2	>4	0	-	-	IND
BR-78	B	7/27/2011	8:49	14.50	93.66	6.46	5.38	6.94	1.56	Physical	2-1	-4	>4	0	-	-	IND
BR-79	A	7/27/2011	8:55	14.50	212.38	14.65	12.61	15.78	3.16	Biological	>4	-3	>4	1	2.91	10.61	1 on 3
BR-79	B	7/27/2011	8:56	14.50	215.61	14.87	14.43	15.56	1.13	Biological	>4	1	>4	0	-	-	1 on 3
BR-79	C	7/27/2011	8:57	14.50	220.00	15.17	14.54	15.63	1.09	Biological	>4	1	>4	6	1.46	12.62	1 on 3
BR-80	A	7/27/2011	9:03	14.50	214.87	14.82	13.52	16.29	2.76	Biological	>4	1	>4	5	5.78	15.09	1 on 3
BR-80	B	7/27/2011	9:04	14.50	194.21	13.39	11.63	15.56	3.93	Biological	>4	1	>4	7	2.76	10.58	1 on 3
BR-80	C	7/27/2011	9:05	14.50	204.98	14.14	13.67	15.01	1.35	Biological	>4	1	>4	3	1.27	12.94	1 on 3
BR-81	A	7/27/2011	9:09	14.50	160.21	11.05	10.54	11.34	0.80	Physical	>4	-3	>4	1	7.05	10.52	1 on 3
BR-81	B	7/27/2011	9:10	14.50	163.03	11.24	10.29	12.65	2.36	Physical	3-2/>4	-6	>4	2	9.38	10.47	1 on 3
BR-81	C	7/27/2011	9:11	14.50	142.68	9.84	8.91	10.40	1.49	Physical	4-3	-4	>4	1	5.56	6.80	1 on 3

Sediment Profile and Plan-View Image Results for BRDS.

Reference stations 63–72, 94–97 are in bold text.

Station	Replicate	Date	Time	Calibration Constant	Penetration Area (sq.cm)	Penetration Mean (cm)	Penetration Minimum (cm)	Penetration Maximum (cm)	Boundary Roughness (cm)	Boundary Roughness Type	Grain Size Major Mode (phi)	Grain Size Maximum (phi)	Grain Size Minimum (phi)	Void #	Void Minimum Depth (cm)	Void Maximum Depth (cm)	Infaunal Succ. Stage
BR-82	A	7/27/2011	9:17	14.50	139.68	9.63	9.12	9.85	0.73	Physical	>4	1	>4	2	0.76	3.93	1 on 3
BR-82	B	7/27/2011	9:18	14.50	144.87	9.99	9.56	11.74	2.18	Physical	>4	1	>4	0	-	-	1 on 3
BR-82	C	7/27/2011	9:19	14.50	133.76	9.22	8.54	11.20	2.65	Physical	>4	1	>4	0	-	-	1 on 3
BR-83	A	7/27/2011	9:24	14.50	110.01	7.59	7.02	7.85	0.84	Physical	4-3	0	>4	0	-	-	1 on 3
BR-83	B	7/27/2011	9:25	14.50	56.85	3.92	3.56	4.14	0.58	Physical	4-3	0	>4	0	-	-	IND
BR-83	C	7/27/2011	9:26	14.50	95.66	6.60	6.22	7.16	0.95	Physical	4-3	0	>4	0	-	-	1 on 3
BR-91	A	7/27/2011	1:26	14.50	222.73	15.36	14.65	15.78	1.13	Biological	>4	2	>4	2	4.98	12.29	1 on 3
BR-91	B	7/27/2011	1:27	14.50	248.60	17.15	16.32	17.48	1.16	Biological	>4	2	>4	2	1.42	11.81	1 on 3
BR-91	C	7/27/2011	1:28	14.50	241.65	16.67	16.14	17.38	1.24	Biological	>4	2	>4	3	11.71	14.07	1 on 3
BR-92	A	7/27/2011	1:18	14.50	244.22	16.84	16.03	17.34	1.31	Biological	>4	2	>4	3	11.34	16.61	1 on 3
BR-92	B	7/27/2011	1:20	14.50	232.25	16.02	15.41	16.32	0.91	Biological	>4	2	>4	2	5.34	13.63	1 on 3
BR-92	C	7/27/2011	1:21	14.50	245.47	16.93	15.85	18.32	2.47	Biological	>4	2	>4	1	13.41	15.38	1 on 3
BR-93	A	7/27/2011	1:10	14.50	229.91	15.86	14.98	16.32	1.34	Biological	>4	2	>4	2	6.65	12.40	1 on 3
BR-93	B	7/27/2011	1:11	14.50	233.08	16.07	15.38	16.65	1.27	Biological	>4	2	>4	3	4.33	14.07	1 on 3
BR-93	C	7/27/2011	1:12	14.50	253.60	17.49	15.38	19.45	4.07	IND	>4	2	>4	4	2.98	16.18	1 on 3
BR-94	A	7/27/2011	5:37	14.50	178.33	12.30	10.69	14.00	3.31	IND	>4	2	>4	0	-	-	1 on 3
BR-94	B	7/27/2011	5:38	14.50	222.86	15.37	15.27	15.74	0.47	Biological	>4	2	>4	4	5.24	13.09	1 on 3
BR-94	C	7/27/2011	5:39	14.50	225.02	15.52	14.47	16.10	1.64	Biological	>4	2	>4	3	6.14	11.34	1 on 3
BR-95	A	7/27/2011	5:42	14.50	197.88	13.65	12.98	14.07	1.09	Physical	>4	2	>4	1	5.20	6.36	1 on 3
BR-95	B	7/27/2011	5:43	14.50	201.43	13.89	13.30	14.32	1.02	Biological	>4	2	>4	2	3.56	6.00	1 on 3

Sediment Profile and Plan-View Image Results for BRDS.

Reference stations 63–72, 94–97 are in bold text.

Station	Replicate	Date	Time	Calibration Constant	Penetration Area (sq.cm)	Penetration Mean (cm)	Penetration Minimum (cm)	Penetration Maximum (cm)	Boundary Roughness (cm)	Boundary Roughness Type	Grain Size Major Mode (phi)	Grain Size Maximum (phi)	Grain Size Minimum (phi)	Void #	Void Minimum Depth (cm)	Void Maximum Depth (cm)	Infaunal Succ. Stage
BR-95	C	7/27/2011	5:44	14.50	158.87	10.96	10.54	11.27	0.73	Physical	>4	2	>4	0	-	-	2.00
BR-96	A	7/27/2011	5:47	14.50	208.17	14.36	14.10	14.61	0.51	Biological	>4	2	>4	1	10.91	12.21	1 on 3
BR-96	B	7/27/2011	5:48	14.50	218.59	15.07	14.65	15.45	0.80	Biological	>4	2	>4	3	5.89	14.83	1 on 3
BR-96	C	7/27/2011	5:49	14.50	201.51	13.90	12.65	14.94	2.29	Biological	>4	2	>4	1	10.11	10.54	1 on 3
BR-97	A	7/27/2011	5:51	14.50	199.67	13.77	11.92	14.72	2.80	Biological	>4	2	>4	2	5.20	9.27	1 on 3
BR-97	B	7/27/2011	5:52	14.50	236.06	16.28	15.74	16.83	1.09	Biological	>4	2	>4	0	-	-	1 on 3
BR-97	C	7/27/2011	5:53	14.50	206.99	14.27	13.78	14.50	0.73	Biological	>4	2	>4	5	7.16	14.11	1 on 3
NE Ref 01	A			14.46	123.96	8.57	8.21	8.97	0.76	Physical	4-3	2	>4	1	6.71	7.02	1 on 3
NE Ref 01	B			14.46	132.67	9.18	8.74	9.76	1.02	Physical	4-3	2	>4	3	3.37	5.55	1 on 3
NE Ref 01	C			14.46	131.78	9.11	8.43	9.34	0.91	Physical	4-3	2	>4	3	3.37	8.89	1 on 3
NE Ref 02	A			14.46	66.98	4.63	4.41	4.98	0.57	Physical	3-2	1	>4	0	-	-	1->2

IND=Indeterminate

Sediment Profile and Plan-View Image Results for BRDS.

Reference stations 63–72, 94–97 are in bold text.

Station	REP	Total DM Area (Sq. cm.)	Total DM mean Thickness (cm)	DM Minimum Thickness (cm)	DM Maximum Thickness (cm)	Sorting	Debris	Plan-view	Facies	Comments
BR-01	A	140.55	9.69	9.20	10.03	Slightly Sorted	Gravel, shell		Reverse graded gravel	Tan, firm, slightly sorted gravelly very coarse sand. Very minor interstitial sands, appears to be lag deposit to depth.
BR-01	B	103.31	7.12	5.27	8.32	Slightly Sorted	Gravel, shell		Reverse graded gravel	Tan, firm, slightly sorted gravelly very coarse sand. Very minor interstitial sands, appears to be lag deposit to depth. DM > P.
BR-01	C	80.30	5.54	4.43	6.00	Sorted	Gravel, shell		Reverse graded gravel	Tan, hard very coarse sandy gravel with minor interstitial fines. Appears to be sorted lag deposit with slight armoring of gravel at SWI.
BR-02	A	174.51	12.04	11.45	12.50	Well Sorted	-		Transgressive sand	Tan, well sorted medium to coarse sand over gray silt/clay. Entire sediment column is dredged material with sorted lag at SWI that is 7.5 cm thick. Organism in old gray, fine DM 8.73 cm below SWI. Bedform.
BR-02	B	175.45	12.10	11.71	12.32	Sorted	Gravel, shell		Reverse graded gravel	Tan, sorted, coarse sand with minor gravel fragments at SWI. Very minor interstitial fines. Slightly armored. DM > P. Fines at bottom appear to be residual smear from previous rep. Sediment column appears to lag deposit.
BR-02	C	166.68	11.50	10.43	11.89	Well Sorted	Minor shell		Transgressive Sand	Tan, well sorted medium sand very gray silt/clay with voids. DM > P. 8.8 cm of well sorted lag over old gray silt DM with bioturbation/deposit feeding in old DM. Tubes at SWI.
BR-03	A	129.10	8.90	8.03	9.34	Well Sorted	Gravel, shell		Lag	Tan well sorted coarse sand with slight gravel armor at SWI over gray silt/clay. DM > P and upper 4.4 cm is well sorted and is likely long-term lag. Bioturbation into underlying older silt/clay. A few tubes and some biogenic aggregate at SWI.
BR-03	B	78.28	5.40	4.94	6.22	Poorly sorted	Gravel, shell		Lag	Tan poorly sorted very coarse sand with imbricated shell and gravel at SWI. Appears to be lag with some recent particulates.

Sediment Profile and Plan-View Image Results for BRDS.
Reference stations 63–72, 94–97 are in bold text.

Station	REP	Total DM Area (Sq. cm.)	Total DM mean Thickness (cm)	DM Minimum Thickness (cm)	DM Maximum Thickness (cm)	Sorting	Debris	Plan-view	Facies	Comments
BR-03	C	98.23	6.77	6.33	7.74	Well Sorted	Gravel, shell		Hard mixed sand/silt	Tan shelly well sorted medium to coarse sand over gray silt/clay with void at right. Tubes and biogenic aggregate at SWI. Bedform.
BR-04	A	142.58	9.83	9.34	10.21	Well Sorted	Gravel, shell		Transgressive Sand and gravel	Tan, well sorted medium to coarse sand over gray clay. Voids at left an Epizoans at left SWI. Top sand layer is 4.7 cm thick and has bedform and burrow. Appears to be sand lag over silt/clay.
BR-04	B	122.60	8.46	7.05	10.25	Sorted	Gravel, shell		Transgressive Sand and gravel	Tan, sorted coarse sand over light gray silt/clay. Minor gravels at SWI and minor fines in upper sand layer. Organism at bottom center and clay colored fecal pellets at left SWI indicating subsurface DM is being brought to SWI.
BR-04	C	146.22	10.08	10.03	10.21	Very well sorted	Shell		Transgressive Sand and gravel	Tan, exceptionally well sorted medium sand with interspersed shell fragments. Bedform in left SWI background. Appears to be sand lag or transgressive sand.
BR-05	A	102.46	7.07	6.47	7.56	Well Sorted	Shell		Transgressive Sand and gravel	Tan, well sorted medium sand with minor interstitial fines. Pebble at surface that is tablate. Either lag or transgressive sand.
BR-05	B	94.76	6.54	6.11	7.16	Slightly Sorted	Gravel, shell		Transgressive Sand and gravel	Tan gravelly sand with minor interstitial sand and no grading. Imbricated gravels at SWI and some tubes in background. Sand appears angular to subangular.
BR-05	C	108.98	7.52	6.29	8.62	Slightly Sorted	Gravel, shell		Transgressive Sand	Tan coarse sand with minor interstitial silt and no grading. Bedform slope.
BR-06	B	190.26	13.12	12.72	13.85	Well Sorted	-		Transgressive Sand and gravel	Tan, well sorted medium sand over gray DM with voids in DM and tubes at SWI.
BR-06	C	236.16	16.29	15.99	16.79	Well Sorted	-		Transgressive Sand	Tan, well sorted medium sand over gray DM with voids in DM at lower right. Sorted sand is 6.9 cm thick. Vector.

Sediment Profile and Plan-View Image Results for BRDS.

Reference stations 63–72, 94–97 are in bold text.

Station	REP	Total DM Area (Sq. cm.)	Total DM mean Thickness (cm)	DM Minimum Thickness (cm)	DM Maximum Thickness (cm)	Sorting	Debris	Plan-view	Facies	Comments
BR-06	F	248.28	17.12	16.32	17.88	Well Sorted	Shell		Transgressive Sand	Tan, well sorted medium sand with shell fragments over gray DM with voids in DM at lower right. Sorted sand is 4.2 cm thick. Biological Vector. Three reps are similar.
BR-07	A	86.22	5.95	4.47	6.73	Slightly Sorted	Shell		Transgressive Sand and gravel	Slightly sorted very coarse tan sand with bedform profile. Minor shell in sediment column. Minor detritus in sand.
BR-07	B	IND	IND	IND	IND	IND	IND		Transgressive Sand and gravel	Water shot
BR-07	C	126.01	8.69	8.14	9.27	Slightly Sorted	Shell		Transgressive Sand and gravel	Tan, firm, slightly sorted shelly coarse sand. Detritus trapped in sand interstices and shells at SWI. SWI appears washed free of fines.
BR-08	A	240.33	16.57	16.25	17.05	Well Sorted	-		Transgressive Sand	4 cm of tan well sorted medium sand over gray clay DM. Sand appears to transgressive or lad. Two large active voids and numerous small tubes at SWI that are likely scavenging the fines being brought up to the surface for the head down deposit feeders/burrowers. Active vector.
BR-08	B	181.86	12.54	11.12	13.45	Poorly sorted	Gravels		Transgressive Sand and gravel	Poorly sorted, gravelly fine to medium sand with high silt component over gray silt/clay DM. Void at right and patches of oxidized sediment at depth. Gravel at SWI that is presumably lag.
BR-08	C	19.04	1.31	0.11	2.47	Poorly sorted	Gravel, rock		Shell windrow and gravel	Hard, tan sandy grave/pebbles with little penetration. Appears to be a lag.
BR-09	A	201.97	13.93	13.01	14.58	Poorly sorted	Gravel, rock		Reverse graded gravel	Hard coarse sandy gravel over gray silt/clay DM that has void at left. Tubes at SWI. Reverse grading suggesting lag.
BR-09	B	114.38	7.89	6.54	9.05	Poorly sorted	Gravel		Reverse graded gravel	Coarse sand gravel with tubes at SWI. Mixed detritus in upper sediment column. Appears to be slightly reverse graded and a likely lag.

Sediment Profile and Plan-View Image Results for BRDS.

Reference stations 63–72, 94–97 are in bold text.

Station	REP	Total DM Area (Sq. cm.)	Total DM mean Thickness (cm)	DM Minimum Thickness (cm)	DM Maximum Thickness (cm)	Sorting	Debris	Plan-view	Facies	Comments
BR-09	C	123.77	8.54	8.11	9.09	Slightly sorted	Gravel, rock		Reverse graded gravel	Slightly sorted fine sand with coarse sand and gravels near SWI overlying gray silt/clay DM. Reverse grading, lag. Void/burrow gallery in with and several tubes at SWI. Distinct demarcation between sand/silt units. Active biological vector.
BR-10	A	197.84	13.64	12.65	14.00	Slightly sorted	fine gravel		Lag	3.9 cm thick layer of slightly sorted gravelly medium sand over mottled gray silt/clay DM. Organism in upper left and numerous epizoans at SWI along with some small tubes. Active biological vector.
BR-10	B	212.64	14.66	14.18	16.14	Slightly sorted	Gravel, shell		Lag	3.8 cm thick layer of medium sand with gravel over gray, mottled, silt/clay DM. Sand layer appears to be a lag based on embedded gravels. Tubes at SWI and patches of oxidized sediment at depth in undisturbed portion of the sediment column.
BR-10	C	48.40	3.34	2.87	4.29	Slightly sorted	Gravel		Lag	Hard, tan, gravelly coarse sand with scattered shell fragments. Based on comparison with previous reps, appears to be a coarser more impenetrable lag. DM.
BR-19	A	0.00	0.00	0.00	0.00	No sorting	-		Burrowed silt	Bioturbated, tan to gray very slightly fine sandy silt/clay. Voids and oxidized sediment throughout subsurface sediment and organism in mid-left. Tear scar in left-center.
BR-19	B	0.00	0.00	0.00	0.00	No sorting	-		Sandy silt	Tan to light gray, very fine sandy silt/clay that appears slightly depositional. Large void at lower right and sand appears to be concentrated in upper sediment column but not in a layer.
BR-19	C	0.00	0.00	0.00	0.00	No sorting	-		Sandy silt	Tan to medium gray slightly sandy silt/clay with sand more apparent in upper 3 cm od sediment column. Voids and organism. Reworked. Tubes at SWI.

APPENDIX C – (CONTINUED)

Sediment Profile and Plan-View Image Results for BRDS.

Reference stations 63–72, 94–97 are in bold text.

Station	REP	Total DM Area (Sq. cm.)	Total DM mean Thickness (cm)	DM Minimum Thickness (cm)	DM Maximum Thickness (cm)	Sorting	Debris	Plan-view	Facies	Comments
BR-21	A	0.00	0.00	0.00	0.00	No sorting	-		Sandy silt	Tan to light gray, slightly sandy silt/clay with dragdown and void in left. Appears to be depositional but there evidence of exposed tubes and washing at SWI. Minor shell.
BR-21	B	0.00	0.00	0.00	0.00	No sorting	-		Burrowed silt	Tan to light gray, bioturbated slightly fine sandy silt/clay with several patches of oxidized sediment at depth within the sediment column. Tubes at SWI.
BR-21	C	0.00	0.00	0.00	0.00	No sorting	-		Burrowed silt	Tan to light gray, bioturbated slightly fine sandy silt/clay. Appears slowly depositional with sand near the SWI but admixed.
BR-24	A	0.00	0.00	0.00	0.00	No sorting	-		Sandy silt	Bioturbated, tan to light gray slightly fine sandy silt/clay. Sand admixed near SWI. Sediment filled void in center.
BR-24	B	0.00	0.00	0.00	0.00	No sorting	-		Sandy silt	Bioturbated, tan to light gray slightly fine sandy silt/clay. Sand admixed near SWI Deep voids at left and several small tubes at SWI
BR-24	C	0.00	0.00	0.00	0.00	No sorting	-		Sandy silt	Bioturbated, tan to light gray slightly fine sandy silt/clay. Sand admixed near SWI. Voids at right.
BR-25	A	0.00	0.00	0.00	0.00	No sorting	-		Sandy silt	Tan to light gray fine sand silt/clay with large active voids and a few tubes at SWI. Increased sand at SWI.
BR-25	B	0.00	0.00	0.00	0.00	No sorting	-		Sandy silt	Tan to light gray fine sand silt/clay. Tube at SWI, shell dragdown at left and two well-formed active voids. Sand admixed at SWI.
BR-25	C	0.00	0.00	0.00	0.00	No sorting	-		Sandy silt	Tan to light gray, intensively bioturbated fine sandy silt/clay. A few small tubes at SWI and numerous active voids in sediment column. Covered sediment at right.

Sediment Profile and Plan-View Image Results for BRDS.

Reference stations 63–72, 94–97 are in bold text.

Station	REP	Total DM Area (Sq. cm.)	Total DM mean Thickness (cm)	DM Minimum Thickness (cm)	DM Maximum Thickness (cm)	Sorting	Debris	Plan-view	Facies	Comments
BR-26	A	0.00	0.00	0.00	0.00	No sorting	Shell		IND	Tan to very light gray, very sandy silt/clay with void in lower right. Small shell frags at SWI and SWI appears slightly washed.
BR-26	B	0.00	0.00	0.00	0.00	No sorting	-		Sandy silt	Tan to very light gray, fine sandy silt/clay. Dragdown scars in sediment column preclude void ID but large biogenic mound at SWI. Sand at SWI and is admixed.
BR-26	C	0.00	0.00	0.00	0.00	No sorting	-		Sandy silt	Tan to light gray, slightly fine sandy silt/clay. Bioturbated with voids at center and left. Tubes at SWI, biogenic mound at right.
BR-27	A	0.00	0.00	0.00	0.00	No sorting	-		Sandy silt	Tan to light gray very silty very fine sand. Large void in center and abundant tubes at SWI that appear related to burrow exhaust, biogenic depression in center SWI.
BR-27	B	0.00	0.00	0.00	0.00	No sorting	Gravel, shell		Lag on silt	Tan to very light gray, gravely, very silty fine and. Gravels and shell at SWI that are mostly free of detritus suggest erosion or no/little sediment input. Shell and gravels appear as a lag.
BR-27	C	0.00	0.00	0.00	0.00	No sorting	Gravel, shell		Lag on silt	Tan to gray gravelly sand over very sandy silt/clay without a distinct contact. Appears to have lag deposit at SWI. Void/patch of oxidized sediment at depth at left.
BR-28	A	0.00	0.00	0.00	0.00	No sorting	Shell		Sandy silt	Tan to medium gray, slightly fine sandy silt. Biogenic mound at left and burrow/void underneath. Appears sandier at SWI with sand admixed, but may be an artifact.
BR-28	B	0.00	0.00	0.00	0.00	No sorting	-		Sandy silt	Tan to light gray slightly fine sandy silt/clay with increased proportion of sand at the SWI. Voids at depth and several burrows. A few tubes at SWI and appears depositional.

Sediment Profile and Plan-View Image Results for BRDS.

Reference stations 63–72, 94–97 are in bold text.

Station	REP	Total DM Area (Sq. cm.)	Total DM mean Thickness (cm)	DM Minimum Thickness (cm)	DM Maximum Thickness (cm)	Sorting	Debris	Plan-view	Facies	Comments
BR-28	C	0.00	0.00	0.00	0.00	No sorting	-		Sandy silt	Tan to light gray slightly fine sandy silt/clay with increased proportion of sand at the SWI. Voids at lower left and several tubes at right SWI.
BR-30	A	0.00	0.00	0.00	0.00	No sorting	Gravel, shell		Lag on silt	Tan to light gray slightly gravelly and slightly sandy silt/clay with graves and sand at SWI. Void and organism at lower left.
BR-30	B	0.00	0.00	0.00	0.00	No sorting	-		Lag on silt	Tan to very light gray, slightly sandy silt/clay with large prominent void at SWI. Shrimp at SWI. Sand fraction appears increased at SWI but is not present as a discrete layer.
BR-30	C	0.00	0.00	0.00	0.00	No sorting	-		Lag on silt	Gravel with silts, little penetration. Possible lag. Origin of coarse fraction unclear.
BR-31	A	0.00	0.00	0.00	0.00	No sorting	-		Lag on silt	Gravels at SWI with silty fine sand below. Major mode is indeterminate due to dragdown and disruption of sediment column. Epizoans in background. Possible lag and origin of coarse fraction unclear.
BR-31	B	0.00	0.00	0.00	0.00	No sorting	-		Lag on silt	No penetration, angular cobbles in background and minor shell fragments. Unclear as to origin. Lack of mantling suggests dynamic.
BR-31	C	0.00	0.00	0.00	0.00	No sorting	-		Lag on silt	Hard, tan to light gray very silty very fine sand with gravel/shell at SWI. Shallow oxidized burrows at left. Possible bedform. Three reps show different features but all have coarse component at SWI.
BR-32	A	127.70	8.81	8.43	9.38	Layered	Shell		Shell windrow	Poorly sorted medium sand over gray silt/clay with active voids at depth. Sand is present as a discrete layer at SWI and is 3.5 cm thick. Appears transgressive rather than lag.

Sediment Profile and Plan-View Image Results for BRDS.

Reference stations 63–72, 94–97 are in bold text.

Station	REP	Total DM Area (Sq. cm.)	Total DM mean Thickness (cm)	DM Minimum Thickness (cm)	DM Maximum Thickness (cm)	Sorting	Debris	Plan-view	Facies	Comments
BR-32	B	202.68	13.98	12.61	14.98	Layered, well sorted	-		Transgressive Sand	
BR-32	C	175.86	12.13	10.54	13.56	Slightly sorted	Gravel, shell		Transgressive Sand and gravel	2.7 cm layer of poorly sorted fine to medium sand over gray silt/clay that has void in upper right. Gravel at SWI without detrital mantling. Appears to be old DM at depth.
BR-33	A	208.95	14.41	14.54	14.87	No sorting	-		Lag on silt	Tan very fine sand silt over mottle silty clay that appears to be DM based on fabric and clay clots. Void lower left. And tubes at SWI. Appears to be mixed sediment over old DM.
BR-33	B	211.01	14.55	13.60	15.41	No sorting	Gravel		Lag on silt	Very fine sandy silt over gray chaotic silt/clay with dragdown and void in center. 9 cm of mixed sediment, sand over old DM in various states of biogenic reworking.
BR-33	C	0.00	0.00	0.00	0.00	No sorting	-		Sandy silt	Fine sandy silt clay with increased proportion of sand in upper sediment column. Voids at left and mid-right. Biogenic depression. Appears to be native. Sand at SWI is admixed.
BR-34	A	46.97	3.24	1.67	5.09	Poorly sorted	Gravel		Lag	Poorly sorted coarse sand with admixed detritus. Gravels at SWI. Appears to be lag at that is temporarily depositional.
BR-34	B	115.53	7.97	7.31	8.43	Slightly sorted	Gravel, shell		Reverse graded gravel	Reversely graded slightly sorted gravelly coarse sand with interstitial detritus. Oyster shell at SWI and gravels at SWI. Appears to be lag deposit that is presently accumulating detritus. Similar to A.
BR-34	C	95.80	6.61	5.63	7.92	Slightly sorted	Gravel, shell		Lag	Ungraded coarse sandy gravel with old shell at SWI. Surficial gravels appear imbricated. Lag. Likely old DM residue.

Sediment Profile and Plan-View Image Results for BRDS.

Reference stations 63–72, 94–97 are in bold text.

Station	REP	Total DM Area (Sq. cm.)	Total DM mean Thickness (cm)	DM Minimum Thickness (cm)	DM Maximum Thickness (cm)	Sorting	Debris	Plan-view	Facies	Comments
BR-35	A	265.39	18.30	17.41	19.23	Well sorted	-	sand, tracks, mud interfingered	Transgressive Sand	Thick accumulation of tan well sored medium to coarse sand with tubes at SWI. Sands are loose grain-to grain contact based on deep penetration and are either transgressive or transgressive lag. Appears DM related but physically reworked.
BR-35	B	IND	IND	IND	IND	Slightly sorted	Gravel	sand, tracks, mud interfingered	Reverse graded gravel	Reversely graded, coarse sandy fine gravel with thin incipient flaser of silt at SWI with fine tubes at surficial silt lens. Gravel without detritus mantling in background. A lag deposit that is temporarily depositional. Possibly DM but unclear.
BR-35	C	IND	IND	IND	IND	Slightly sorted	Gravel, shell	poor visibility sand/mud interfingered	Reverse graded gravel	Reversely graded gravel over coarse sand with interstitial fines in sand. Old shell at SWI that appears to scallop and oyster. Likely old DM but cannot be sure. Tubes in background. Lag.
BR-36	A	136.85	9.44	8.36	11.27	No sorting	Gravel, shell		Shell windrow and gravel	Gravelly sand over gray silt clay that is in the process of being reworked. Shells and gravel SWI suggest that this is lag.
BR-36	B	217.26	14.98	14.29	15.30	Sorted	-		Hard mixed sand/silt	6.4 cm layer of sorted medium sand over gray silt/clay. Void in lower center. Appears to be dynamic with transgressive sand or transgressive lag at SWI. Fines at depth are reworked but pale clays apparent. Small tubes at SWI.
BR-36	C	IND	IND	IND	IND	Poorly sorted	-		Transgressive Sand	7.3 cm layer of poorly sorted normally graded fine to medium sand over sand silt/clay that appears partially reworked and not distinct enough to say its DM. Sediment filled void at left and a few small tubes at SWI. Transgressive or transgressive lag.
BR-37	A	IND	IND	IND	IND	Poorly sorted	Cobble		Lag	Hard coarse sandy gravel with large rock that exceed 14.5 cm window width at SWI background. Epizoans. Origin unclear.

Sediment Profile and Plan-View Image Results for BRDS.
Reference stations 63–72, 94–97 are in bold text.

Station	REP	Total DM Area (Sq. cm.)	Total DM mean Thickness (cm)	DM Minimum Thickness (cm)	DM Maximum Thickness (cm)	Sorting	Debris	Plan-view	Facies	Comments
BR-37	B	IND	IND	IND	IND	Poorly sorted	-		Hard mixed sand/silt	Hard medium sand with abundant admixed fines/detritus. Several small tubes at SWI. Entire sediment column oxidized and origin of sands unclear.
BR-37	C	198.28	13.67	13.41	13.81	Slightly sorted	-		Transgressive Sand and gravel	8.9 cm layer of slightly sorted, normally graded medium sand over gray silt/clay that appears to be DM. Void at left and tubes at SWI. Sand appears to be thick transgressive layer.
BR-38	A	0.00	0.00	0.00	0.00	Poorly sorted	Shell	burrows, shell frags	Hard mixed sand/silt	Poorly sorted, normally graded tan medium sand with deep oxidized burrows, surficial detritus and admixed detritus. Minor shell fragments at SWI. Signature of sand different and appears native.
BR-38	B	0.00	0.00	0.00	0.00	Poorly sorted	Shell		Hard mixed sand/silt	Poorly sorted, very silty, hard, medium sand. Entire sediment column oxidized. A few small tubes at SWI. Sand appears native.
BR-38	C	0.00	0.00	0.00	0.00	Poorly sorted	Shell		Hard mixed sand/silt	Poorly sorted, very silty, hard, medium sand. Entire sediment column oxidized. A few small tubes at SWI. Sand appears native. Three reps are generally similar and have distinct differences with other sands.
BR-39	A	0.00	0.00	0.00	0.00	No sorting	-		Transgressive Sand	Slightly sandy silt/clay with shell at depth and numerous very deep oxidized burrow traces. Void at left and organism at right. Tubes at SWI. Thin 0.7 cm band of recently deposited fines at SWI that may be due to upward biogenic conveying. Sediment column well-processed.

APPENDIX C – (CONTINUED)

Sediment Profile and Plan-View Image Results for BRDS.
Reference stations 63–72, 94–97 are in bold text.

Station	REP	Total DM Area (Sq. cm.)	Total DM mean Thickness (cm)	DM Minimum Thickness (cm)	DM Maximum Thickness (cm)	Sorting	Debris	Plan-view	Facies	Comments
BR-39	B	0.00	0.00	0.00	0.00	Layered	-		Transgressive Sand	Poorly sorted fine to medium sand over olive to light gray silt/clay. Void upper left and abundant tubes at SWI. Sand appears transgressive and normally graded. Subsurface sediment appears processed. Contact between sand and lower silts is becoming obscured.
BR-39	C	0.00	0.00	0.00	0.00	Layered	-		Transgressive Sand	Poorly sorted fine to medium sand over olive to light gray silt/clay. Sand is 6 cm thick. Mixed shell fragments at bottom of frame and numerous deep oxidized burrow traces. Several tubes at SWI. Event that produced sand layer appears to have been older and sand layer signature is becoming obscured.
BR-40	A	0.00	0.00	0.00	0.00	No sorting	-		Sandy silt	Intensely bioturbated, very slightly sandy silt/clay that appears to be native. Higher proportion of sand at SWI. Voids throughout and biogenic surface. Tube at right.
BR-40	B	0.00	0.00	0.00	0.00	No sorting	-		Sandy silt	Intensely bioturbated, very slightly sandy silt/clay that appears to be native. Enormous voids/burrows in sediment column, biogenic mound at SWI and numerous large tubes. Sand percentage higher at SWI.
BR-40	C	0.00	0.00	0.00	0.00	No sorting	-		Sandy silt	Tan to medium gray slightly fine sandy silt/clay with several deep burrow and patches of oxidized sediment at depth. Dense tubes at SWI. Native. Three reps are similar.
BR-41	A	0.00	0.00	0.00	0.00	No sorting	-		Sandy silt	Tan to olive gray slightly fine sandy silt/clay with shell dispersed throughout entire sediment column. Deep oxidized burrow traces. Native.
BR-41	B	0.00	0.00	0.00	0.00	No sorting	-		Sandy silt	Tan to olive gray slightly fine sandy silt/clay with shell dispersed throughout entire sediment column. Voids upper right and bottom. Organism at left and tubes at SWI. Native.

Sediment Profile and Plan-View Image Results for BRDS.

Reference stations 63–72, 94–97 are in bold text.

Station	REP	Total DM Area (Sq. cm.)	Total DM mean Thickness (cm)	DM Minimum Thickness (cm)	DM Maximum Thickness (cm)	Sorting	Debris	Plan-view	Facies	Comments
BR-41	C	0.00	0.00	0.00	0.00	No sorting	-		Sandy silt	Tan to olive gray slightly fine sandy silt/clay with shell dispersed throughout entire sediment column. Voids throughout sediment column and tubes at SWI. Three reps are similar. Native.
BR-42	A	0.00	0.00	0.00	0.00	No sorting	-		Sandy silt	Tan to olive gray slightly fine sandy silt/clay. Oxidized burrow trace deep into sediment column and small void/burrow upper right. Dragdown at left. Tubes at SWI.
BR-42	B	0.00	0.00	0.00	0.00	No sorting	-		Sandy silt	Tan to olive gray fine sandy silt/clay. Scattered tubes and small void/burrow at left. Appears faintly depositional. Organism lower right.
BR-42	C	0.00	0.00	0.00	0.00	No sorting	-		Sandy silt	Tan to olive fine sandy silt/clay with thin band of gray sand at right SWI that appears localized. Large void lower left. Small tube at right.
BR-43	A	IND	IND	IND	8.80	Poorly sorted	Gravel, shell		Shell windrow	Dense shell hash over poorly sorted medium to coarse sand. Material is physically reworked with shell surficial lag. Presumably DM. Starfish.
BR-43	B	0.00	0.00	0.00	0.00	Slightly sorted	Minor shell		Hard mixed sand/silt	Hard, tan slightly silt fine to medium sand. Bedform. Tubes at SWI oxidized to depth. Appears native in contrast to previous rep.
BR-43	C	0.00	0.00	0.00	0.00	No sorting	-		Sandy silt	High relief, tan to light gray shelly very fine sandy silt/clay that has shell fragments distributed throughout sediment column. Three reps from this station are very different.
BR-44	A	IND	IND	IND	IND	IND	IND	muddy sand wave and shell and gravel, burrows	Shell windrow and gravel	No penetration water shot.

Sediment Profile and Plan-View Image Results for BRDS.

Reference stations 63–72, 94–97 are in bold text.

Station	REP	Total DM Area (Sq. cm.)	Total DM mean Thickness (cm)	DM Minimum Thickness (cm)	DM Maximum Thickness (cm)	Sorting	Debris	Plan-view	Facies	Comments
BR-44	B	0.00	0.00	0.00	0.00	Poorly sorted	-	burrows, small shells and frags	Hard mixed sand/silt	Firm tan to light gray very silty very fine to fine sand. Low relief bedform surface. Crab. Shell fragments throughout sediment column. Several shallow oxidized burrows.
BR-44	C	102.88	7.10	5.05	7.96	No sorting	Gravel, shell	plaice, cobble, shell frags, burrows, large cobble	Lag	Firm, coarse sandy graver over gray silt/clay. Appears to lag over old DM. Very different from previous rep and likely true spatial heterogeneity based on mobile (periodically) sands. Small void in lower right and organism at left. Unusual.
BR-45	A	184.21	12.70	11.41	13.23	Poorly sorted	Gravel, shell		Lag	3.5 cm layer of poorly sorted fine to medium sand over gray silt/clay that has characteristics of old d m. Patch of oxidized sediment at depth at right. Shell fragments at SWI and appears to be periodically dynamic/transgressive.
BR-45	B	IND	IND	IND	8.80	Poorly sorted	Gravel, shell		Lag	Gravel lag with interstitial san and shell fragments. Possible DM residue.
BR-45	C	163.04	11.24	9.23	12.58	Sorted	Shell		Transgressive Sand and gravel	6.8 cm layer of sorted sand with minor interstitial detritus over gray silt/clay that looks like old DM based on clays. Tubes at SWI and void at left. Sand appears as a transgressive lag. High variability at station.
BR-46	A	54.14	3.73	2.80	4.40	Poorly sorted	Gravel, shell		Lag	DM lag residue. Old shell at SWI and bedform profile. Interstitial detritus.
BR-46	B	67.23	4.64	3.64	5.49	Poorly sorted	Gravel, shell		Lag	Gravelly very coarse san with interstitial detritus. Old shell at SWI. Hard. Old DM lag.
BR-46	C	67.23	4.64	3.64	5.49	No sorting	Gravel, shell		Lag	Gray silt clay with scattered gravel and shell fragments at SWI. Appears to be old DM. Lag or erratics at SWI.
BR-47	A	IND	IND	IND	IND	IND	IND		Lag	No penetration water shot.

Sediment Profile and Plan-View Image Results for BRDS.

Reference stations 63–72, 94–97 are in bold text.

Station	REP	Total DM Area (Sq. cm.)	Total DM mean Thickness (cm)	DM Minimum Thickness (cm)	DM Maximum Thickness (cm)	Sorting	Debris	Plan-view	Facies	Comments
BR-47	B	210.73	14.53	14.14	14.76	Layered, sorted	-		Transgressive Sand	3.7 cm layer of well sorted transgressive medium sand over mottled/chaotic silt clay that has glacial/DM characteristics. Sediment column riddled with voids. Tubes at SWI. Interesting pic. Possible vector.
BR-47	C	196.92	13.58	12.76	14.14	Layered, sorted	-		Transgressive Sand	5.6 cm layer of sorted fine sand over light bluish gray silt/clay with sediment filled void in lower right center. Tubes at SWI. Transgressive sand over old DM.
BR-48	A	IND	IND	IND	IND	No sorting	Shell		Sandy silt	Tan to light gray, slightly sandy, silt/clay with Voids and organism in center. A few tubes at SWI. Small shell fragments to depth. Has characteristics of native or reworked sediment.
BR-48	B	Present	IND	IND	IND	No sorting	-		Sandy silt	Tan to mottled gray slightly sandy silt clay that appears to have older DM at depth that has been reworked and cannot be quantified. Upper sediment column highly bioturbated. Organism at center. Upper sediment column appears sandier.
BR-48	C	0.00	0.00	0.00	0.00	No sorting	Shell		Sandy silt	Tan to gray fine sandy silt/clay. If DM present it has been reworked beyond recognition. Shell fragments throughout sediment column and tubes at SWI.
BR-49	A	IND	IND	IND	IND	Well sorted	Gravel, shell		Transgressive Sand	Hard tan very fine sand with gravel, shell and sand dollar at SWI. Bedform. Unclear on origin of sand.
BR-49	B	0.00	0.00	0.00	0.00	Slightly sorted	Gravel, shell		Transgressive Sand	Tan to gray silty fine sand with patch of trapped organics at left. Appears transgressive and minor fine gravel at SWI. Organism/burrow at right. Unusual.
BR-49	C	IND	IND	IND	IND	Slightly sorted	Gravel, shell		Shell windrow and gravel	Tan to very light gray slightly sorted very coarse sand with interstitial fines. Gravel and shell at SWI along with epizoans. Lag, possibly DM but insufficient diagnostic evidence.

Sediment Profile and Plan-View Image Results for BRDS.

Reference stations 63–72, 94–97 are in bold text.

Station	REP	Total DM Area (Sq. cm.)	Total DM mean Thickness (cm)	DM Minimum Thickness (cm)	DM Maximum Thickness (cm)	Sorting	Debris	Plan-view	Facies	Comments
BR-50	A	180.08	12.42	11.81	13.12	Sorted	Dense shell		Shell windrow	Sorted coarse sand and shell hash over dark gray silt/clay. Lag/transgressive sand over DM. Old limpets shells.
BR-50	B	117.76	8.12	7.05	9.12	Poorly sorted	Dense shell		Shell windrow	Imbricated shell lag over poorly sorted coarse sand. Shell appears old and to be *Mya*. DM lag/transgressive deposit.
BR-50	C	184.63	12.73	11.81	14.14	Sorted	-		Shell windrow	Reversely graded coarse and medium sand over gray to olive silt/clay. Subsurface sediment like a mix of DM or reworked DM, clay clot at left. Voids in sediment column. Sand present in a 4-8 cm thick distinct layer. Transgressive or lag.
BR-51	A	0.00	0.00	0.00	0.00	No sorting	-		Sandy silt	Tan to light gray silt/clay with dragdown scar at right and deep oxidized burrows. Several small tubes at SWI. Native.
BR-51	B	0.00	0.00	0.00	0.00	No sorting	-		Sandy silt	Tan to light olive-gray silt/clay. Well processed, dragdown at left and oxidized void/burrow in bottom center. Native.
BR-51	C	0.00	0.00	0.00	0.00	No sorting	-		Sandy silt	Tan to light olive-gray slightly fine sandy silt/clay. Well processed. Voids at a distinct horizon at bottom of sediment column and several tubes at SWI. Native.
BR-52	A	0.00	0.00	0.00	0.00	No sorting	Shell		Sandy silt	Tan to gray fine sandy silt/clay with increased proportion of sands in upper sediment column. Patches of oxidized sediment at depth and deep burrow traces. Numerous small tubes at SWI. Possible DM but well mixed so that it, if present, it is indistinguishable from native.
BR-52	B	IND	IND	IND	IND	IND	Shell		Sandy silt	Disturbed from sampling. Highly unusual.

APPENDIX C – (CONTINUED)

Sediment Profile and Plan-View Image Results for BRDS.
Reference stations 63–72, 94–97 are in bold text.

Station	REP	Total DM Area (Sq. cm.)	Total DM mean Thickness (cm)	DM Minimum Thickness (cm)	DM Maximum Thickness (cm)	Sorting	Debris	Plan-view	Facies	Comments
BR-52	C	Present	IND	IND	IND	Slightly sorted	-		Sandy silt	Thin band (1-1.5 cm) of very fine sand over gray to olive silt/clay with upper portion of sediment column showing the gray and blue gray clays characteristic of site DM. Tubes at SWI. Possible minor transgressive sequence over native, but true amount of DM present is not measurable due to physical and biological mixing. Best guess is that DM is 11 cm from SWI down.
BR-53	A	200.61	13.84	13.56	14.07	Layered, well sorted	Gravel, shell		Shell windrow and gravel	2.6 cm layer of well sored medium to coarse sand with scattered gravel and shell at SWI. Subsurface sediment is old DM with clay clots and some chaotic fabric. Voids in center and active biological vector.
BR-53	B	183.55	12.66	11.05	13.52	Slight sorted.	Shell		Shell windrow and gravel	Thin 0.5 -1 cm band of slightly sorted fine to medium sand over gray silt/clay that is old DM that retains clay clots and chaotic fabric. Shell lag at SWI. Dynamic. Oxidized sediment at depth indicates biogenic reworking and vector.
BR-53	C	220.24	15.19	14.18	15.74	Slightly sorted	Gravel		Shell windrow and gravel	2.5 cm band of slightly sorted coarse sand with minor gravel at SWI that overlies dark and light gray chaotic old DM that had distinct light and blue=gray clay clasts. Void in upper right. Transport/transgressive sand/lag. Active vector.
BR-54	A	Present	Present	IND	IND	No sorting	-		Sandy silt	Tan to medium gray, slightly sandy silt/clay with active voids in center of frame. Appears to be some old mixed DM at lower left but DM not present as discrete layer and is buried. Sand fraction greater at SWI.
BR-54	B	0.00	0.00	0.00	0.00	No sorting	-		Sandy silt	Tan to light gray, intensively bioturbated, slightly fine sandy silt/clay. Native. Prominent voids in lower sediment column, biogenic mound and organism at left.

Sediment Profile and Plan-View Image Results for BRDS.

Reference stations 63–72, 94–97 are in bold text.

Station	REP	Total DM Area (Sq. cm.)	Total DM mean Thickness (cm)	DM Minimum Thickness (cm)	DM Maximum Thickness (cm)	Sorting	Debris	Plan-view	Facies	Comments
BR-54	C	0.00	0.00	0.00	0.00	No sorting	-		Sandy silt	Tan to light gray, intensively bioturbated, slightly fine sandy silt/clay. Native. Voids at left and center with large organism in one void, another organism far right. Light smears at left appear to be shell dissolution tracks rather than clay clots. Tubes at SWI.
BR-55	A	0.00	0.00	0.00	0.00	No sorting	-		Sandy silt	Tan to gray well bioturbated, slightly sandy silt/clay that appears native and depositional. Shell at SWI. Numerous voids throughout the sediment column.
BR-55	B	Present	Present	IND	IND	No sorting	-		Sandy silt	Tan to gray very slightly fine sandy silt clay. Possible old DM at bottom of frame based on clay smear and reflectivity. Dense tubes at SWI and large void accentuated by a tear in center of frame. DM is unmeasurable as a distinct stratum.
BR-55	C	0.00	0.00	0.00	0.00	No sorting	-		Sandy silt	Tan to gray well bioturbated, slightly sandy silt/clay that appears native and depositional. Large and two small voids in center of frame. Tubes at SI. If DM present it has been reworked beyond recognition.
BR-56	A	Present	Present	IND	IND	No sorting	Gravel, shell		Lag	Tan to gray slightly sorted fine sand with gravel and shell lag at SWI that overlies gray silt/clay. DM presumably present at part of surficial lag but sediment column disturbed from dragdown.
BR-56	B	0.00	0.00	0.00	0.00	No sorting	Gravel, shell		Lag	Tan to light gray very fine sandy, shelly, silt/clay with shell and gravel at SWI. Id DM is present it has been reworked to the point where it converges with native sediment in optical properties. Shell Gravel appears to be lag.

Sediment Profile and Plan-View Image Results for BRDS.

Reference stations 63–72, 94–97 are in bold text.

Station	REP	Total DM Area (Sq. cm.)	Total DM mean Thickness (cm)	DM Minimum Thickness (cm)	DM Maximum Thickness (cm)	Sorting	Debris	Plan-view	Facies	Comments
BR-56	C	0.00	0.00	0.00	0.00	No sorting	Gravel, shell		Lag	Tan to light gray very fine sandy, shelly, silt/clay with shell at SWI. Shell appears to older scallop and clam shells and is possible related to old DM. Subsurface sediment does not have characteristics of DM. Small void in center.
BR-57	A	161.26	11.12	10.73	11.96	Layered	Gravel, shell		Shell windrow and gravel	Tan to light gray, faintly layered medium shelly sand over silt/clay. Appears to be old DM with surficial shell lag,
BR-57	B	151.52	10.45	9.67	10.73	Sorted	Gravel		Shell windrow and gravel	Tan to light gray sorted coarsen sand that has minor interstitial fines. Old DM silt/clay at bottom of frame. Tubes at SWI and organism lower right. Fine dusting of detritus at SWI.
BR-57	C	160.57	11.07	9.31	12.69	Layered, slightly sorted	Gravel, shell		Shell windrow and gravel	Reversely graded gravelly coarse sand over gray old DM silt/clay. Shell fragments at SWI. Deposit appears to be a lag and three reps show similarities.
BR-60	A	49.91	3.44	2.04	5.05	Poorly sorted	Gravel, shell		Shell windrow and gravel	Hard poorly sorted coarse sand with scattered surficial gravels and shell. Appears to be a lag deposit or a lagged transgressive deposit.
BR-60	B	61.85	4.27	3.49	4.83	Poorly sorted	Gravel, shell		Shell windrow and gravel	Hard poorly sorted coarse sand with scattered surficial gravels and shell. Appears to be a lag deposit or a lagged transgressive deposit.
BR-60	C	159.29	10.99	10.40	11.38	Well sorted	Gravel, shell		Reverse graded gravel	Beautifully reverse graded well sorted coarse sand. Dynamic. Great pic. Shrimp in background.
BR-61	A	0.00	0.00	0.00	0.00	No sorting	Gravel		Burrowed silt	Tan, fine sandy silt/clay that is biogenically reworked. Possible old DM is present but if so it has been reworked to the point where it no longer distinguishable. Shell at depth.

Sediment Profile and Plan-View Image Results for BRDS.

Reference stations 63–72, 94–97 are in bold text.

Station	REP	Total DM Area (Sq. cm.)	Total DM mean Thickness (cm)	DM Minimum Thickness (cm)	DM Maximum Thickness (cm)	Sorting	Debris	Plan-view	Facies	Comments
BR-61	B	0.00	0.00	0.00	0.00	Poorly sorted	-		Transgressive Sand	Tan normally graded fine sand over gray silt clay in a depositional sequence. Possible physically reworked DM in upper layer but it is not optically distinguishable. Interesting pic. Oxidized sediment at depth and dense tubes at SWI.
BR-61	C	0.00	0.00	0.00	0.00	No sorting	-		Transgressive Sand	Tan very fine sandy silt/clay with dense tubes at SWI and shell fragments distributed throughout sediment column. If DM present it cannot be distinguished. Upper sediment column is enriched in sand relative to lower sediment column.
BR-62	A	121.33	8.37	7.52	9.52	Slightly sorted	Gravel, shell	Large oyster shells, brick	Shell windrow and gravel	Tan, slightly sorted coarse sand with interstitial fines. Physically reworked and is either transgressive or a lag. DM that has been physically reworked.
BR-62	B	36.36	2.51	0.73	3.38	Slightly sorted	Gravel, shell	Large oyster shells	Shell windrow and gravel	Imbricated fine gravel with minor coarse sand and fines. Hard, washed lag that is presumably DM residue or transgressive residue.
BR-62	C	115.34	7.95	6.87	9.63	Slightly sorted	Gravel, shell	Large oyster shells	Shell windrow and gravel	Coarse sandy fine gravel that has interstitial fines. Epizoan in background. Physically reworked. Appears to be lag or mobile coarse deposit.
BR-63	A	0.00	0.00	0.00	0.00	No sorting	Shell		Burrowed silt	Tan to gray silt/clay. Native. Burrow void upper right, void and dragdown at left and a few small tubes at SWI.
BR-63	B	0.00	0.00	0.00	0.00	No sorting	-		Burrowed silt	Tan to gray silt/clay. Native. Burrow void upper right, void at left, worm in center-right and a numerous tubes at SWI.
BR-63	C	0.00	0.00	0.00	0.00	No sorting	-		Burrowed silt	Limited penetration, tan to light gray silt/clay. Clam at SWI and organism lower left.
BR-64	A	0.00	0.00	0.00	0.00	No sorting	-		Burrowed silt	Tan to light gray fine sandy silt/clay that is extensively biogenically reworked. Native voids in sediment column and dense tubes at SWI.

Sediment Profile and Plan-View Image Results for BRDS.

Reference stations 63–72, 94–97 are in bold text.

Station	REP	Total DM Area (Sq. cm.)	Total DM mean Thickness (cm)	DM Minimum Thickness (cm)	DM Maximum Thickness (cm)	Sorting	Debris	Plan-view	Facies	Comments
BR-64	B	0.00	0.00	0.00	0.00	No sorting	-		Burrowed silt	Tan to light gray fine sandy silt/clay that is extensively biogenically reworked. Numerous worms in sediment column. Native Similar to A.
BR-64	C	0.00	0.00	0.00	0.00	No sorting	-		Burrowed silt	Tan to light gray fine sandy silt/clay. Organism at right and tubes at SWI. Native.
BR-65	A	0.00	0.00	0.00	0.00	No sorting	-		Burrowed silt	Tan to light gray fine sandy silt/clay. Oxidized sediment at depth within the sediment column. Abundant tubes of multiple types at SWI. Upper sediment column does appear sandier.
BR-65	B	0.00	0.00	0.00	0.00	No sorting	-		Burrowed silt	Tan to light gray fine sandy silt/clay that is well-processed. Numerous voids in sediment column and tubes at SWI. Nice pic. Native.
BR-65	C	0.00	0.00	0.00	0.00	No sorting	-		Burrowed silt	Tan to light gray fine sandy silt/clay that is well-processed. No voids but oxidized sediment and burrow traces at depth, tubes at SWI Native. Three reps similar.
BR-66	A	0.00	0.00	0.00	0.00	No sorting	-		Burrowed silt	Tan to light gray silt/clay that is well-processed. Void upper right and organism and void lower left. Very slight fine sand at SWI. Native.
BR-66	B	0.00	0.00	0.00	0.00	No sorting	-		Burrowed silt	Tan to light gray silt/clay. No voids but oxidized sediment and burrow traces at depth, tubes at SWI Native. Organism at right.
BR-66	C	0.00	0.00	0.00	0.00	No sorting	-		Burrowed silt	Tan to light gray silt/clay that is well-processed. Voids in lower center and left with organism at right. Numerous tubes at SWI. Three reps very similar.
BR-67	A	0.00	0.00	0.00	0.00	No sorting	-		Burrowed silt	Tan to light gray very fine sandy silt/clay with bedform at right. Clumped biogenic aggregated sediment in trough. Oxidized burrow and organism at right. Native.

Sediment Profile and Plan-View Image Results for BRDS.

Reference stations 63–72, 94–97 are in bold text.

Station	REP	Total DM Area (Sq. cm.)	Total DM mean Thickness (cm)	DM Minimum Thickness (cm)	DM Maximum Thickness (cm)	Sorting	Debris	Plan-view	Facies	Comments
BR-67	B	0.00	0.00	0.00	0.00	No sorting	-		Burrowed silt	Tan to light gray very fine sandy silt/clay. Voids at left. Appears to have faint layering of pulsed deposition. Abundant tubes at SWI.
BR-67	C	0.00	0.00	0.00	0.00	No sorting	-		Burrowed silt	Tan to light gray very fine sandy silt/clay. Small voids in upper sediment column and deep oxidized burrows. Tubes at SWI native.
BR-68	A	0.00	0.00	0.00	0.00	No sorting	-		Burrowed silt	Tan to minor light gray very fine sandy silt/clay. Organisms lower left and mid-right as well as tubes at SWI.
BR-68	B	0.00	0.00	0.00	0.00	No sorting	-		Burrowed silt	Tan, very silty very fine sand with bedform profile. Abundant tubes at SWI. Oxidized to depth.
BR-68	C	0.00	0.00	0.00	0.00	No sorting	-		Burrowed silt	Tan, very fine sandy silt/clay with small void in upper right and numerous tubes at SWI. Organism at depth and buried shell fragments.
BR-69	A	0.00	0.00	0.00	0.00	No sorting	-		Burrowed silt	Tan to gray, slightly fine sandy silt/clay that is well bioturbated. Voids at far left and far right. Numerous tubes at SWI and pellets. Oxidized burrow traces.
BR-69	B	0.00	0.00	0.00	0.00	No sorting	-		Burrowed silt	Tan to gray, slightly fine sandy silt/clay that is well bioturbated. Voids at right and tubes at SWI. Unusual organism cluster at far left SWI. Shell fragments at right. Tubes in right background have characteristics of amphipod tubes. Native.
BR-69	C	0.00	0.00	0.00	0.00	No sorting	-		Burrowed silt	Tan to gray, slightly fine sandy silt/clay. Abundant broken tubes and a few intact at SWI/ Bedform profile in background
BR-70	A	0.00	0.00	0.00	0.00	No sorting	-		Burrowed silt	Tan to gray, slightly fine sandy silt/clay. Tears at depth and organism lower right. Deep oxidized burrows. Abundant tubes at SWI.

Sediment Profile and Plan-View Image Results for BRDS.

Reference stations 63–72, 94–97 are in bold text.

Station	REP	Total DM Area (Sq. cm.)	Total DM mean Thickness (cm)	DM Minimum Thickness (cm)	DM Maximum Thickness (cm)	Sorting	Debris	Plan-view	Facies	Comments
BR-70	B	0.00	0.00	0.00	0.00	No sorting	-		Burrowed silt	Tan to gray, fine sandy silt/clay. Biogenic mound at left and sediment filled void at right. Tubes and abundant broken tubes at SWI.
BR-70	C	0.00	0.00	0.00	0.00	No sorting	-		Burrowed silt	Tan to gray, fine sandy silt/clay. Abundant tubes at SWI and unclear whether mound or ripple but has ripple profile. Deep, oxidized burrow traces.
BR-71	A	0.00	0.00	0.00	0.00	No sorting	-		Burrowed silt	Tan to gray, very fine sandy silt/clay. Dense tubes at SWI. Organism in center. Appears static in deposition.
BR-71	B	0.00	0.00	0.00	0.00	No sorting	-		Burrowed silt	Tan to gray, very fine sandy silt/clay. Numerous oxidized burrow trace and several tubes at SWI.
BR-71	C	0.00	0.00	0.00	0.00	No sorting	Shell		Burrowed silt	Tan to gray, very fine sandy silt/clay. Shell at SWI and SWI appears washed. Broken tubes.
BR-72	A	0.00	0.00	0.00	0.00	No sorting	-		Burrowed silt	Tan very silty very fine sand with bedform/washed profile. Oxidized to depth and numerous tubes at SWI.
BR-72	B	0.00	0.00	0.00	0.00	No sorting	-		Burrowed silt	Tan to very light olive gray very fine sandy silt/clay with void at bottom center. Dense tubes at SWI.
BR-72	C	0.00	0.00	0.00	0.00	No sorting	-		Burrowed silt	Tan to very light olive gray very fine sandy silt/clay, void at right and dense tubes at SWI. Nice layer of detritus at SWI. Well processed.
BR-73	A	0.00	0.00	0.00	0.00	No sorting	-		Burrowed silt	Tan to olive gray, well processed silt clay with prominent void and anemone tentacular crown at SWI. Native.
BR-73	B	0.00	0.00	0.00	0.00	No sorting	-		Burrowed silt	Tan to olive gray, well processed silt clay. Patch of organics lower left and smeared organism and void complex at left. Tubes at SWI. Native.

Sediment Profile and Plan-View Image Results for BRDS.
Reference stations 63–72, 94–97 are in bold text.

Station	REP	Total DM Area (Sq. cm.)	Total DM mean Thickness (cm)	DM Minimum Thickness (cm)	DM Maximum Thickness (cm)	Sorting	Debris	Plan-view	Facies	Comments
BR-73	C	0.00	0.00	0.00	0.00	No sorting	-		Burrowed silt	Tan to gray very slightly fine sandy silt/clay. Void/burrow in center and small biogenic mound at left SWI. A few small tubes at SWI. Native.
BR-74	A	0.00	0.00	0.00	0.00	No sorting	-		Burrowed silt	Tan to gray very slightly fine sandy silt/clay that is well-processed and bioturbated. Numerous tubes at SWI. Native.
BR-74	B	0.00	0.00	0.00	0.00	No sorting	-		Burrowed silt	Tan to gray very slightly fine sandy silt/clay that is well-processed and bioturbated. Void at left and center. Native.
BR-74	C	0.00	0.00	0.00	0.00	No sorting	-		Burrowed silt	Tan to gray very slightly fine sandy silt/clay that is well-processed and bioturbated. Void complex in lower right and tubes at SWI. Native. Three reps are similar.
BR-75	A	0.00	0.00	0.00	0.00	No sorting	-		Burrowed silt	Tan to gray slightly fine sandy silt with voids at center and right. Several small tubes at SWI. Organism at lower right. Native.
BR-75	B	0.00	0.00	0.00	0.00	No sorting	-		Burrowed silt	Tan to gray slightly fine sandy silt. Voids at bottom of frame. Biogenic mound and tubes at SWI. Well bioturbated.
BR-75	C	0.00	0.00	0.00	0.00	No sorting	-		Burrowed silt	Tan to gray slightly fine sandy silt. Void complex at far left. A few small tubes at SWI. Native. Three reps are similar.
BR-76	A	205.59	14.18	13.70	14.54	Well sorted	Shell		Lag	Well sorted coarse sand over gray uniform silt/clay. Dynamic and transgressive/lag. Several small tubes at SWI.
BR-76	B	123.83	8.54	6.00	10.87	Sorted	Shell		Transgressive Sand	Sorted coarse sand over gray/blue silt/clay. Void in lower center and several tubes at SWI. Sand has shell evenly reworked throughout. Possible bedform flank.
BR-76	C	131.59	9.08	8.29	9.89	Well sorted	Gravel, shell		Transgressive Sand and gravel	Tan, well sorted medium sand with gravel at SWI that overlies blue/gray silt/clay. Gravels in background.

Sediment Profile and Plan-View Image Results for BRDS.

Reference stations 63–72, 94–97 are in bold text.

Station	REP	Total DM Area (Sq. cm.)	Total DM mean Thickness (cm)	DM Minimum Thickness (cm)	DM Maximum Thickness (cm)	Sorting	Debris	Plan-view	Facies	Comments
BR-77	A	IND	IND	IND	IND	Well sorted	-		Transgressive Sand and gravel	Hard well sorted tan medium sand with broken reworked shell fragments throughout. Bedform flank. Broken tube accumulation at right SWI. Possible lag, unclear without additional evidence.
BR-77	B	47.71	3.29	2.69	3.85	Sorted	Shell		Transgressive Sand and gravel	Hard, sorted medium to coarse sand with shell fragments at SWI. Shell appears old and stained. Bedforms in background. Appears to be transgressive/lag.
BR-77	C	IND	IND	IND	IND	Sorted	Shell		Transgressive Sand and gravel	Hard tan medium sand with scattered shell. Thin veneer of fines at SWI that appears transient. Three reps show many similar physical features.
BR-78	A	69.05	4.76	4.36	5.09	Slightly sorted	Gravel, Shell		Reverse graded gravel	Coarse lag with old shells at SWI.
BR-78	B	93.66	6.46	5.38	6.94	Poorly sorted	Gravel, Shell		Reverse graded gravel	Coarse lag with old shells at SWI. Rectangular object in background. Appears to be DM lag.
BR-79	A	0.00	0.00	0.00	0.00	No sorting	Gravel		Burrowed silt	Tan to gray slightly fine sandy silt. Void and dragdown scar at left. Gravel in SWI background and organism at right. Bioturbated. A few tubes at SWI. If DM present it has been reworked to point where it cannot be discerned.
BR-79	B	0.00	0.00	0.00	0.00	No sorting	-		Burrowed silt	Tan to gray slightly fine sandy silt. Bioturbated. Numerous tubes at SWI, oxidized sediment at depth and organism at left. If DM present it has been reworked to the point where it cannot be discerned.
BR-79	C	0.00	0.00	0.00	0.00	No sorting	-		Burrowed silt	Tan to gray slightly fine sandy silt. Highly bioturbated. Voids throughout sediment column and numerous tubes at SWI. If DM present it has been reworked to the point where it cannot be discerned. Three reps are similar.

Sediment Profile and Plan-View Image Results for BRDS.

Reference stations 63–72, 94–97 are in bold text.

Station	REP	Total DM Area (Sq. cm.)	Total DM mean Thickness (cm)	DM Minimum Thickness (cm)	DM Maximum Thickness (cm)	Sorting	Debris	Plan-view	Facies	Comments
BR-80	A	0.00	0.00	0.00	0.00	No sorting	-		Burrowed silt	Tan to gray slightly fine sandy silt. Highly bioturbated. Voids throughout sediment column and dense tubes at SWI. Appears native.
BR-80	B	0.00	0.00	0.00	0.00	No sorting	-		Burrowed silt	Tan to gray slightly fine sandy silt. Highly bioturbated. Cluster of voids in center of sediment column. Several tubes at SWI. Appears native.
BR-80	C	0.00	0.00	0.00	0.00	No sorting	-		Burrowed silt	Tan to gray slightly fine sandy silt. Bioturbated. Small void in upper right and void+dragdown in bottom center. Has characteristics of native, if DM present it is so reworked as to be indistinguishable from native.
BR-81	A	0.00	0.00	0.00	0.00	No sorting	-		Lag on silt	Tan to olive gray very sandy silt with scattered rounded gravels at SWI. Void and dragdown in center. Gravels appear dissociated from underlying material. Subsurface sediment appears processed. No distinct layering of coarser sediment at top but is gradational. Does not share that characteristic with the DM deposit.
BR-81	B	0.00	0.00	0.00	0.00	No sorting	-		Lag on silt	Tan to olive sand over silt/clay. Rounded gravels at SWI and colonization of gravels by epizoans. Optical signature of subsurface sediment is different than DM. Small voids in lower left. Unusual.
BR-81	C	0.00	0.00	0.00	0.00	No sorting	-		Lag on silt	Tan to light gray very silty, gravelly fine sand. Surface is armored with rounded gravel. Void at left and numerous dragdown/tearing scars. Highly unusual but portions of subsurface sediment appear to older and reworked rather than exposed DM.

Sediment Profile and Plan-View Image Results for BRDS.

Reference stations 63–72, 94–97 are in bold text.

Station	REP	Total DM Area (Sq. cm.)	Total DM mean Thickness (cm)	DM Minimum Thickness (cm)	DM Maximum Thickness (cm)	Sorting	Debris	Plan-view	Facies	Comments
BR-82	A	0.00	0.00	0.00	0.00	No sorting	-		Burrowed silt	Tan to light olive gray very fine sandy firm silt/clay. Shallow burrow and void in upper center. Sediment column appears processed. Numerous tubes at SWI.
BR-82	B	0.00	0.00	0.00	0.00	No sorting	-		Burrowed silt	Tan to light olive gray very fine sandy firm silt/clay. Very dense tubes at SWI. Some appear to be amphipod tubes.
BR-82	C	0.00	0.00	0.00	0.00	No sorting	-		Burrowed silt	Tan to light olive gray very fine sandy firm silt/clay. Very dense tubes at SWI. Organism at right and broken tubes at SWI also. Bedform. Three reps are similar.
BR-83	A	0.00	0.00	0.00	0.00	No sorting	-		Hard mixed sand/silt	Tan to very light gray very silty very fine sand. Bedform profile tubes at SWI and several deep oxidized burrows. Burrow/organism at bottom right. Slightly sandier than 82.
BR-83	B	0.00	0.00	0.00	0.00	No sorting	-		Hard mixed sand/silt	Tan very silty very fine sand. Bedform profile. Hard, oxidized to depth.
BR-83	C	0.00	0.00	0.00	0.00	No sorting	-		Hard mixed sand/silt	Tan to very light gray very silty very fine sand. Tubes at SWI and several deep oxidized burrows. Burrow/organism at bottom right. Possible biogenic depression in background. Nearly oxidized to depth.
BR-91	A	0.00	0.00	0.00	0.00	No sorting	-		Sandy silt	Tan to gray silt/clay with voids at left. Upper portion sediment column biogenically reworked. Tubes at SWI. Native.
BR-91	B	0.00	0.00	0.00	0.00	No sorting	-		Sandy silt	Tan to light olive gray silt/clay. Upper portion sediment column biogenically reworked. Tubes at SWI. Burrow void and dragdown at upper right and sediment filled void in left center. Appears to 1.5 cm of RDS at SWI. Native.
BR-91	C	0.00	0.00	0.00	0.00	No sorting	-		Sandy silt	Tan to olive to gray silt/clay. Upper portion sediment column biogenically reworked. Tubes at SWI. Native.

Sediment Profile and Plan-View Image Results for BRDS.

Reference stations 63–72, 94–97 are in bold text.

Station	REP	Total DM Area (Sq. cm.)	Total DM mean Thickness (cm)	DM Minimum Thickness (cm)	DM Maximum Thickness (cm)	Sorting	Debris	Plan-view	Facies	Comments
BR-92	A	0.00	0.00	0.00	0.00	No sorting	-		Sandy silt	Tan to gray, slightly fine sandy silt/clay with large, deep voids. Minor shell fragments at SWI. Reworked and appears native. SWI slightly sandier but sand is not in distinct layer.
BR-92	B	0.00	0.00	0.00	0.00	No sorting	-		Sandy silt	Tan to gray, slightly fine sandy silt/clay. Tubes at SWI. Reworked and appears native though there are some olive-gray organics at depth. SWI slightly sandier but sand is not in distinct layer.
BR-92	C	0.00	0.00	0.00	0.00	No sorting	-		Sandy silt	Tan to gray, slightly fine sandy silt/clay. Tubes at SWI. Void at lower left. Unusual mottling of subsurface sediment that almost suggest fain layering. SWI slightly sandier but sand is not in distinct layer.
BR-93	A	0.00	0.00	0.00	0.00	No sorting	-		Sandy silt	Tan to light gray, mottled, slightly sandy silt clay. Appears native. Dense tubes at SWI and voids at far right and mid left. Biogenic depression/burrow opening at right SWI.
BR-93	B	0.00	0.00	0.00	0.00	No sorting	-		Sandy silt	Tan to light gray, slightly sandy silt clay. Large active voids and numerous tubes at SWI. Well-bioturbated. Native.
BR-93	C	0.00	0.00	0.00	0.00	No sorting	-		Sandy silt	Bioturbated, native, slightly fine sandy silt/clay with voids throughout sediment column. Small tubes at SWI and oxidized burrows at far left.
BR-94	A	0.00	0.00	0.00	0.00	No sorting	-		Burrowed silt	Olive silt/clay with RDSI that ranges from 3 to 5 cm thick. High light clay proportion RDSI. Very unusual. Large organism in center and several tubes at SWI. Origin of RDSI is unclear.

Sediment Profile and Plan-View Image Results for BRDS.

Reference stations 63–72, 94–97 are in bold text.

Station	REP	Total DM Area (Sq. cm.)	Total DM mean Thickness (cm)	DM Minimum Thickness (cm)	DM Maximum Thickness (cm)	Sorting	Debris	Plan-view	Facies	Comments
BR-94	B	IND	IND	IND	IND	Layered silt	-		Burrowed silt	Layered tan to gray to olive silt. Appear to be episodic deposition with layering on the 3-5 cm scale. Bioturbation does not obscure layering. Origin of layering unclear. Dense tubes at SWI.
BR-94	C	IND	IND	IND	IND	No sorting	-		Burrowed silt	Tan to olive, bioturbated slightly sandy silt/clay with voids, organism and abundant tubes at the SWI.
BR-95	A	IND	IND	IND	IND	Layered silt	-		Burrowed silt	Tan to gray to olive layered silt. Layering is on 3-4 cm intervals and relict RPD discernible. There does not appear to be a compositional shift. SWI has been recently disturbed and top down incipient RPD. Abundant tubes at SWI and void in center. Several couplets observable. Origin of material is not apparent.
BR-95	B	IND	IND	IND	IND	Layered silt	-		Burrowed silt	Tan to gray to olive layered silt. Layering is on 3-4 cm intervals and relict RPD discernible. Compositionally material similar throughout sediment column. Voids in upper sediment column and smeared organism in center. Layering is on 5-7 cm scale. Tubes at SWI
BR-95	C	IND	IND	IND	IND	Layered silt	-		Burrowed silt	Tan to gray fine sandy silt with very faint banding. On the 3-4 cm scale. Shallow oxidized burrows and a few tubes at SWI. Three reps show some similar features and origin of layering is unclear.
BR-96	A	IND	IND	IND	IND	Layered silt	-		Burrowed silt	Tan to gray slightly fine sandy silt that is layered in a 7-8 cm scale. Relict RPD visible. There does not appear to be a large compositional shift between layers. Void in lower left and organism in lower right. Several tubes at SWI.

Sediment Profile and Plan-View Image Results for BRDS.

Reference stations 63–72, 94–97 are in bold text.

Station	REP	Total DM Area (Sq. cm.)	Total DM mean Thickness (cm)	DM Minimum Thickness (cm)	DM Maximum Thickness (cm)	Sorting	Debris	Plan-view	Facies	Comments
BR-96	B	IND	IND	IND	IND	No sorting	-		Burrowed silt	Tan to light gray silt/clay. Possible banding but is very faint. Voids at left and center as well as several tubes at SWI.
BR-96	C	IND	IND	IND	IND	No sorting	-		Burrowed silt	Tan to light gray biogenically mixed silt/clay. Patches of organics at left. Oxidized sediment at bottom frame from infaunal activity. Numerous tubes at SWI.
BR-97	A	0.00	0.00	0.00	0.00	No sorting	-		Burrowed silt	Tan to olive gray silt/clay with voids in center and abundant tubes at SWI. Tinge of blue clay at lower left but if DM present it has been reworked beyond recognition.
BR-97	B	0.00	0.00	0.00	0.00	No sorting	-		Burrowed silt	Tan to olive gray silt/clay that appear to be native in optical signature.
BR-97	C	0.00	0.00	0.00	0.00	No sorting	-		Burrowed silt	Tan to olive gray silt/clay that appear to be native in optical signature. Large voids and organism at left. Several small tubes at SWI/
NE Ref 01	A									Tan to light gray silty very fine sand. Void in lower center. Burrow and mound at upper left. Polychaete above void. RPD physically influenced. Appears siltier at depth. SWI washed. A few sand tubes at SWI.
NE Ref 01	B									Tan to light gray silty very fine sand. RPD physically influenced. Appears siltier at depth. SWI washed. A few sand tubes at SWI. Void at far left and two voids at far right, one lined to SWI with a burrow. Algae in background. Sorting greater in upper 2-3 cm of sediment column corresponding to RPD. Patches of oxidized sediment at depth.

Sediment Profile and Plan-View Image Results for BRDS.

Reference stations 63–72, 94–97 are in bold text.

Station	REP	Total DM Area (Sq. cm.)	Total DM mean Thickness (cm)	DM Minimum Thickness (cm)	DM Maximum Thickness (cm)	Sorting	Debris	Plan-view	Facies	Comments
NE Ref 01	C									Tan to light gray silty very fine sand. RPD physically influenced. Appears siltier at depth. SWI washed. A few sand tubes at SWI. Bedforms. Voids in upper center, lower center and lower left. Polychaete in left void. Algae in background. Sorting greater in upper 2-3 cm of sediment column corresponding to RPD. Patches of oxidized sediment at depth. Three reps very similar.
NE Ref 02	A									Tan to medium gray, firm, slightly silty fine sand. SWI washed. Upper 2-3 cm well-sorted. Several shallow, oxidized burrows and a few tubes at SWI. RPD dominantly physical in nature. Minor shell fragments at SWI.

IND=Indeterminate

APPENDIX D

FULL LENGTH SEDIMENT CORE PHOTOGRAPHS
WITH CHARACTERISTICS AND DESCRIPTIONS

APPENDIX D
FULL LENGTH SEDIMENT CORE PHOTOGRAPHS WITH CHARACTERISTICS AND DESCRIPTIONS

LIST OF FIGURES

Page

Full Length Sediment Core Photographs with Characteristics and Descriptions

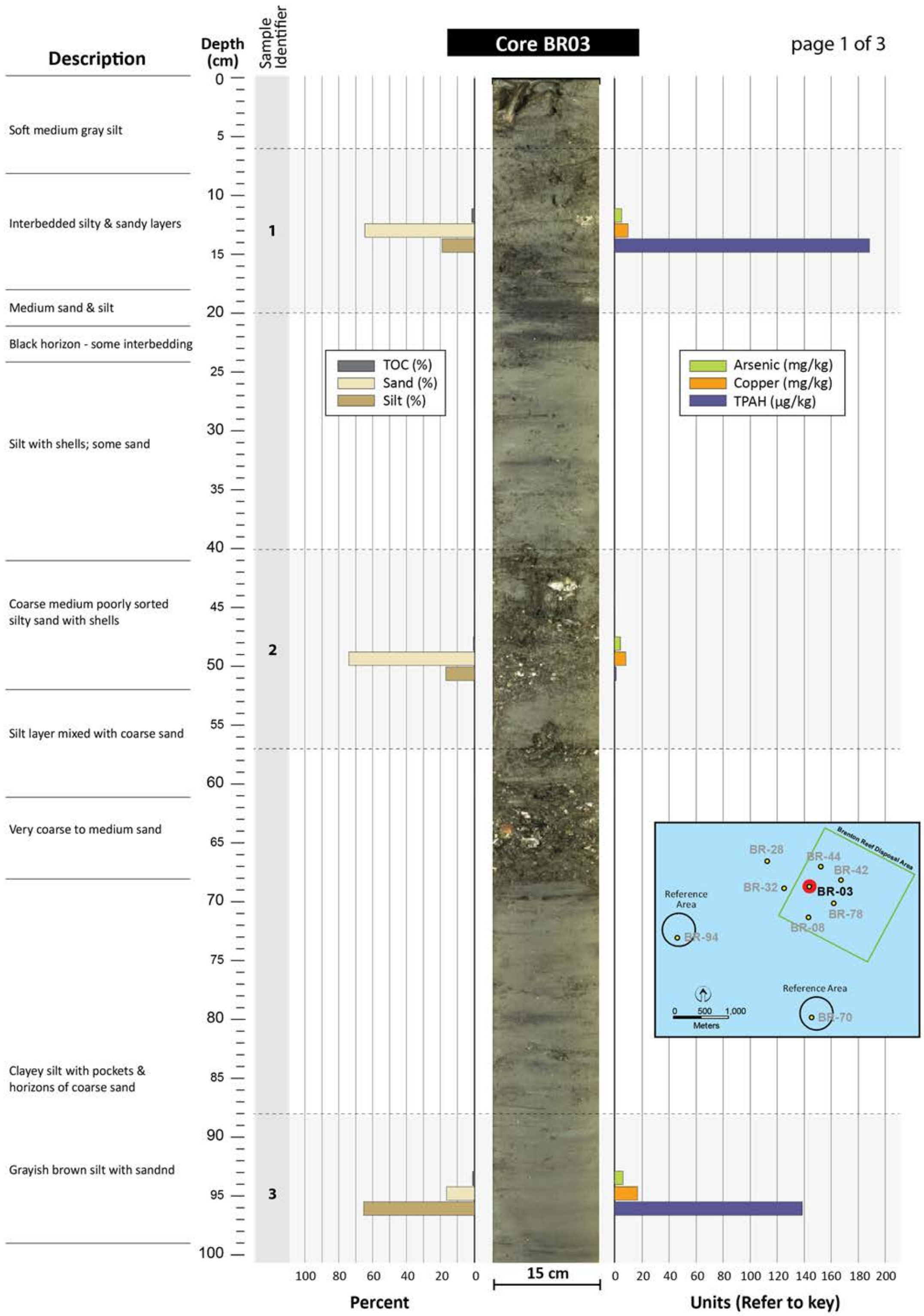

Figure D-1a. Full core BR03 characteristics, horizon descriptions and selected analyte values.

Full Length Sediment Core Photographs with Characteristics and Descriptions

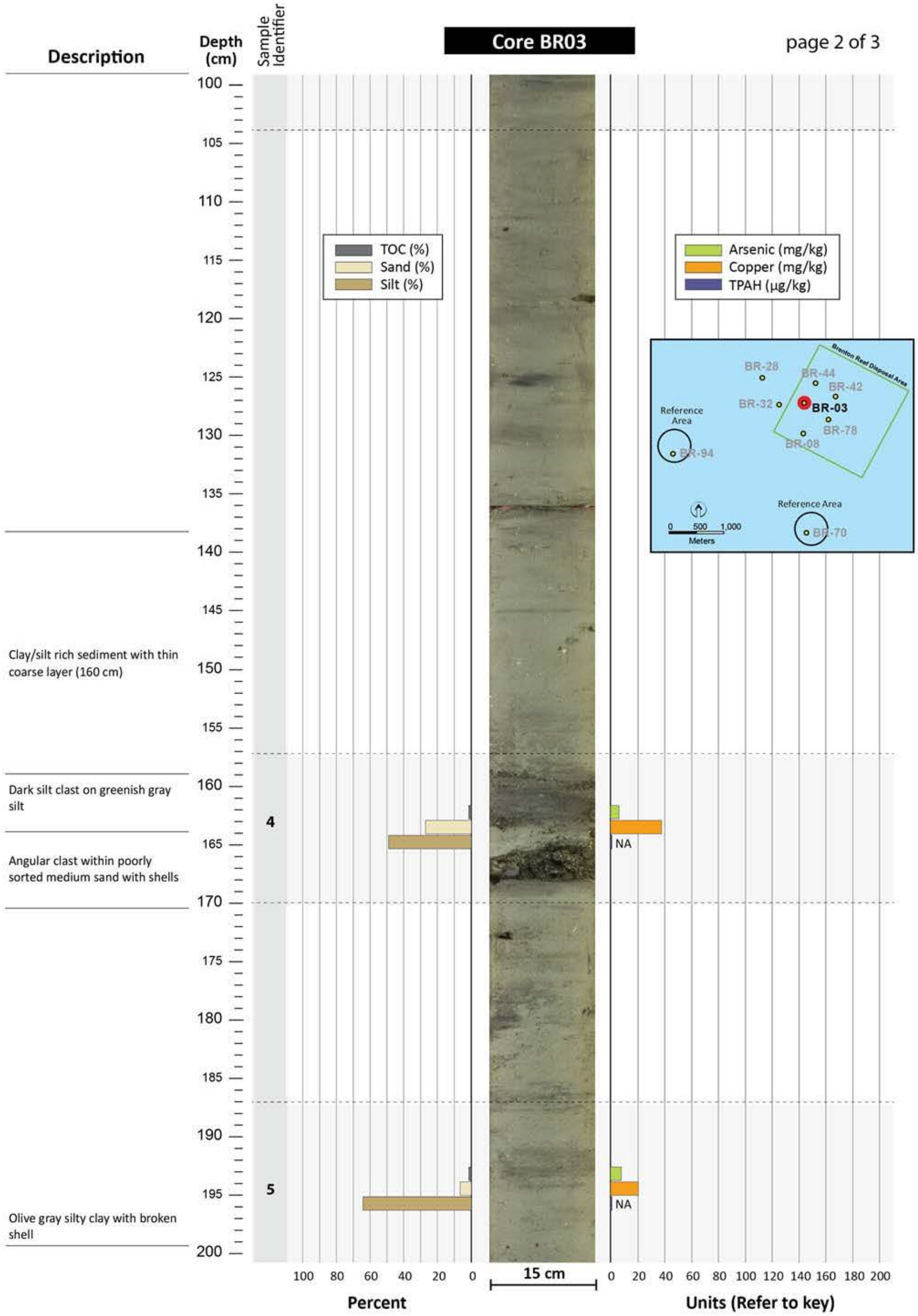

Figure D-1b. Full core BR03 characteristics, horizon descriptions and selected analyte values (continued).

Full Length Sediment Core Photographs with Characteristics and Descriptions

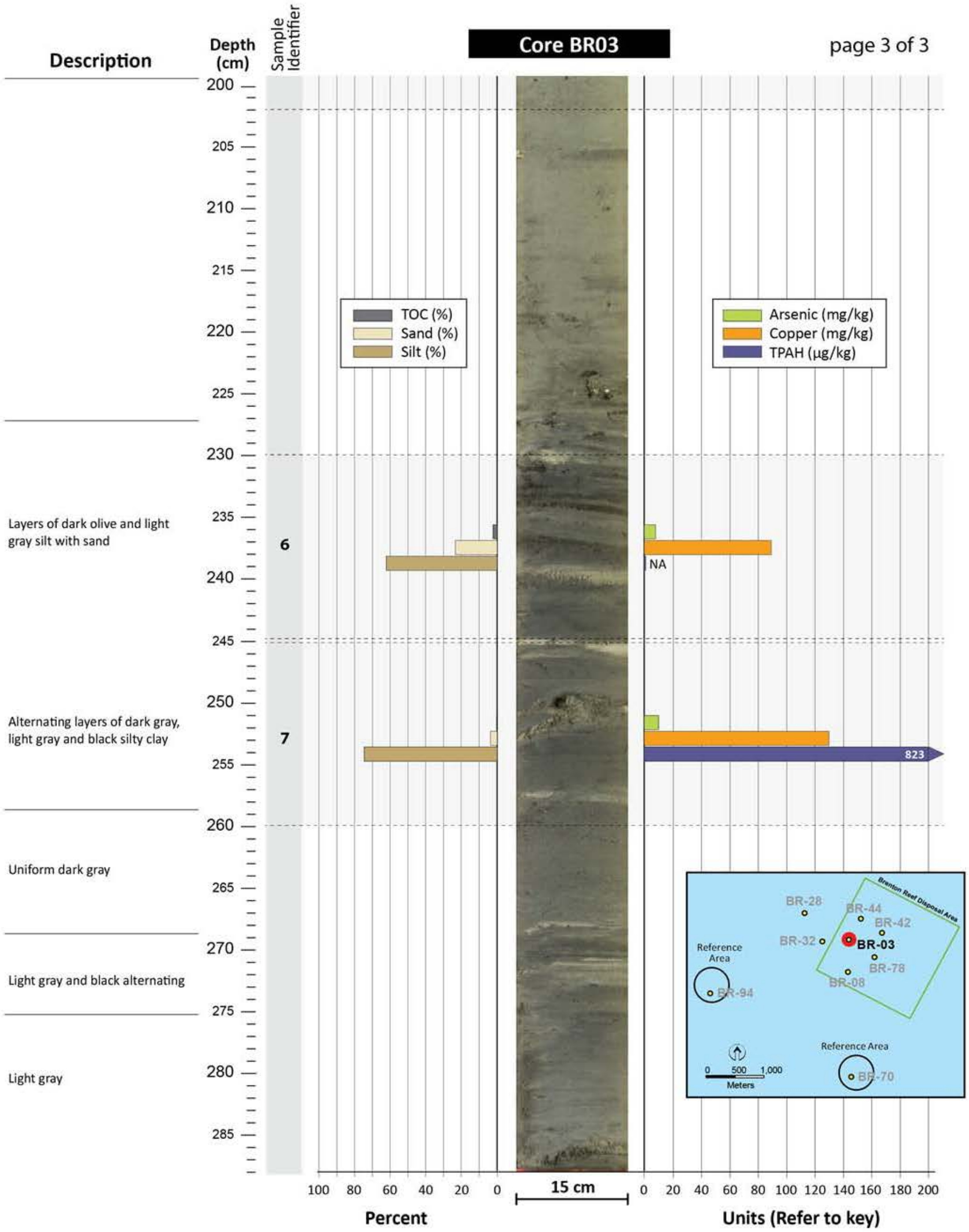

Figure D-1c. Full core BR03 characteristics, horizon descriptions and selected analyte values (continued).

Full Length Sediment Core Photographs with Characteristics and Descriptions

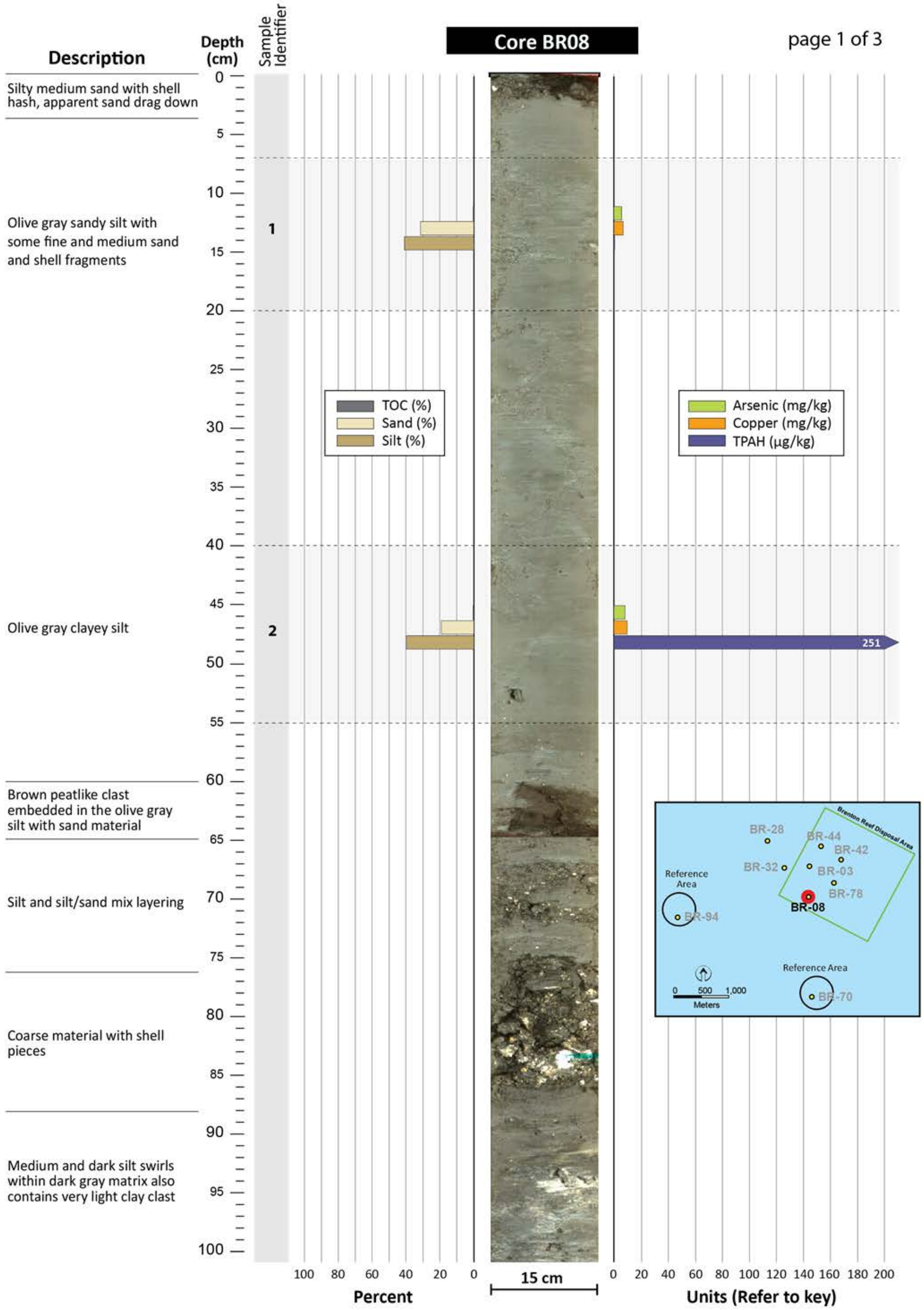

Figure D-2a. Full core BR08 characteristics, horizon descriptions and selected analyte values.

Full Length Sediment Core Photographs with Characteristics and Descriptions

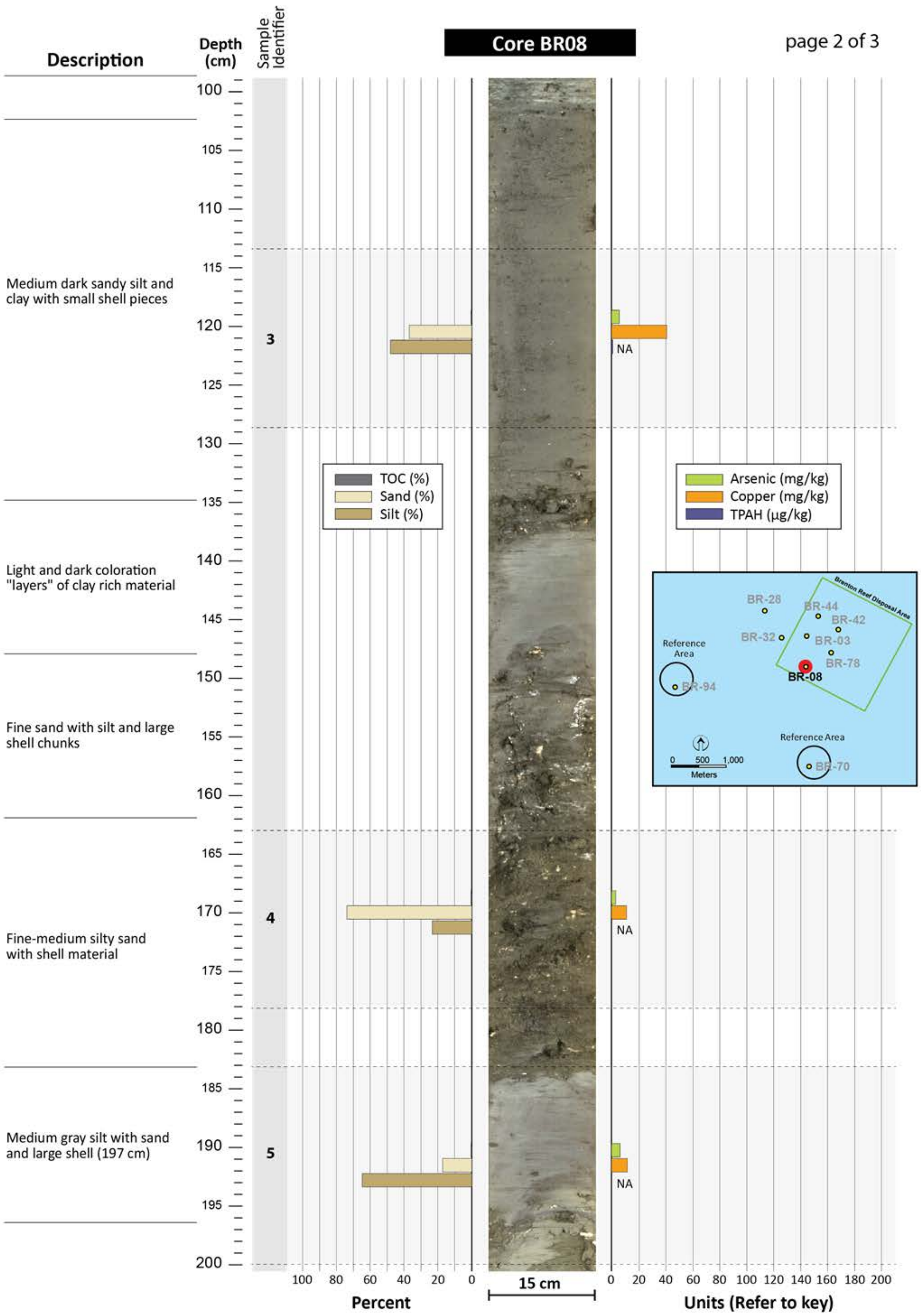

Figure D-2b. Full core BR08 characteristics, horizon descriptions and selected analyte values (continued).

Full Length Sediment Core Photographs with Characteristics and Descriptions

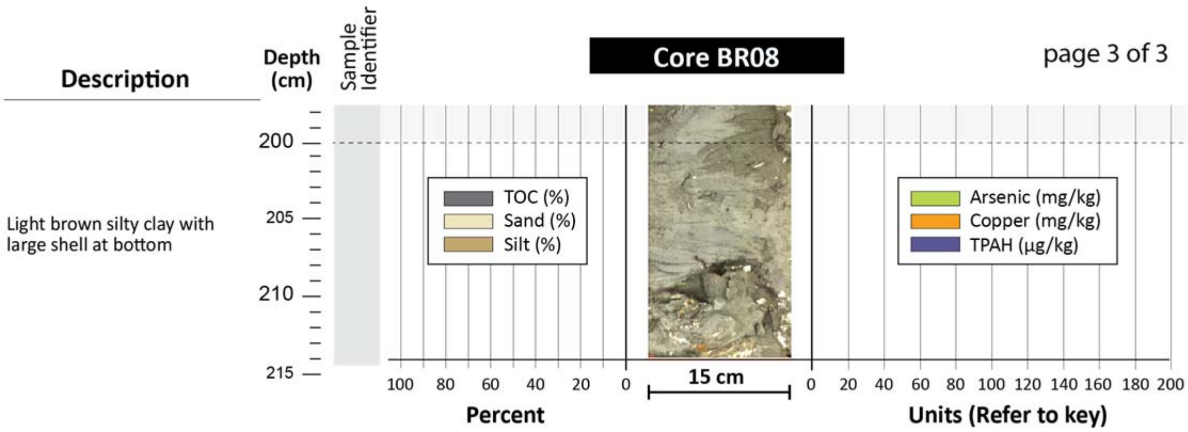

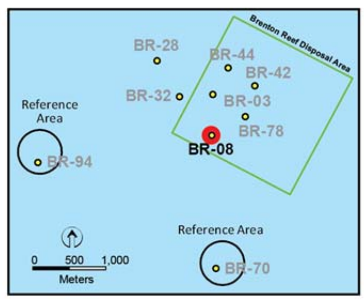

Figure D-2c. Full core BR08 characteristics, horizon descriptions and selected analyte values (continued).

Full Length Sediment Core Photographs with Characteristics and Descriptions

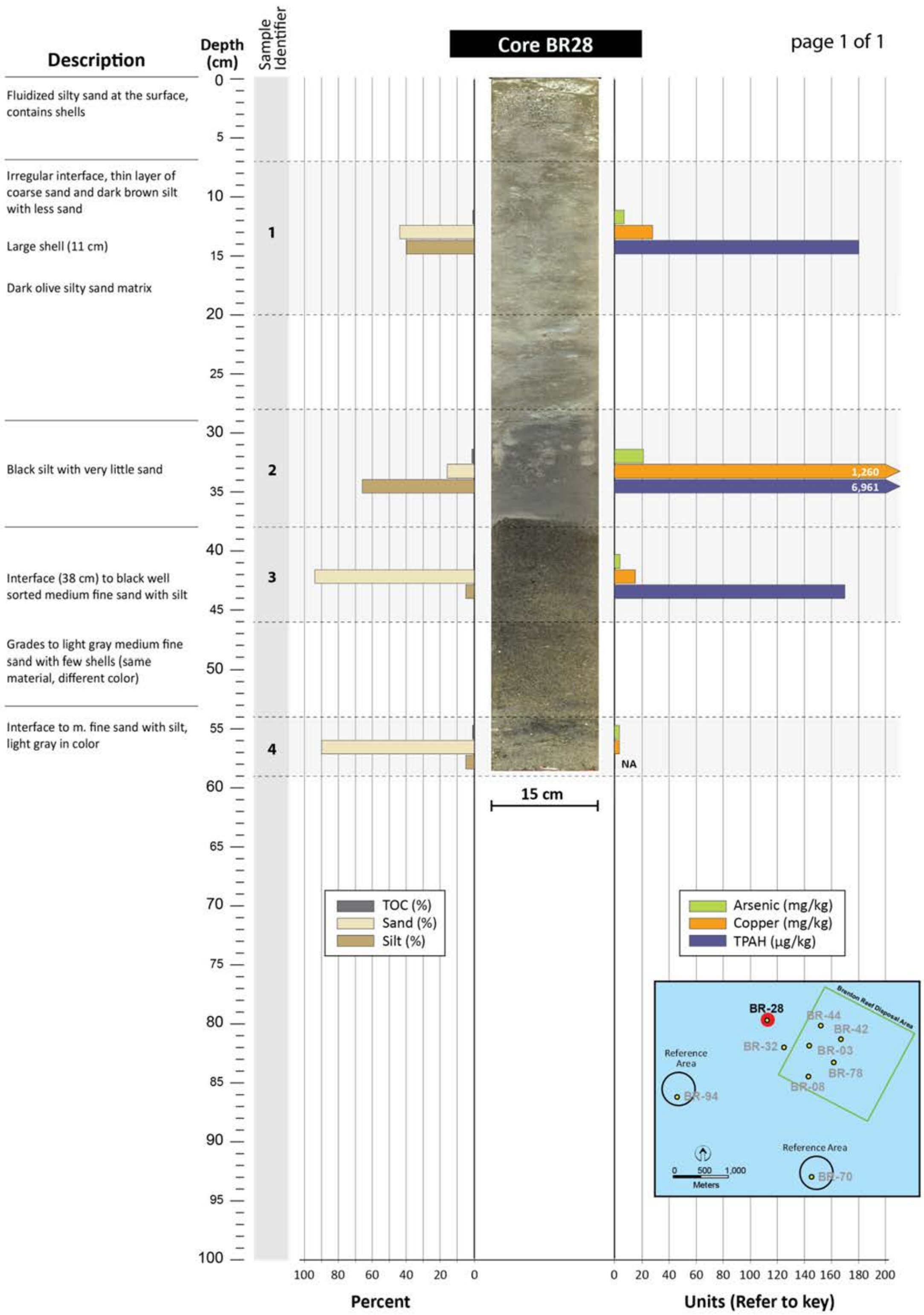

Figure D-3. Full core BR28 characteristics, horizon descriptions and selected analyte values.

Full Length Sediment Core Photographs with Characteristics and Descriptions

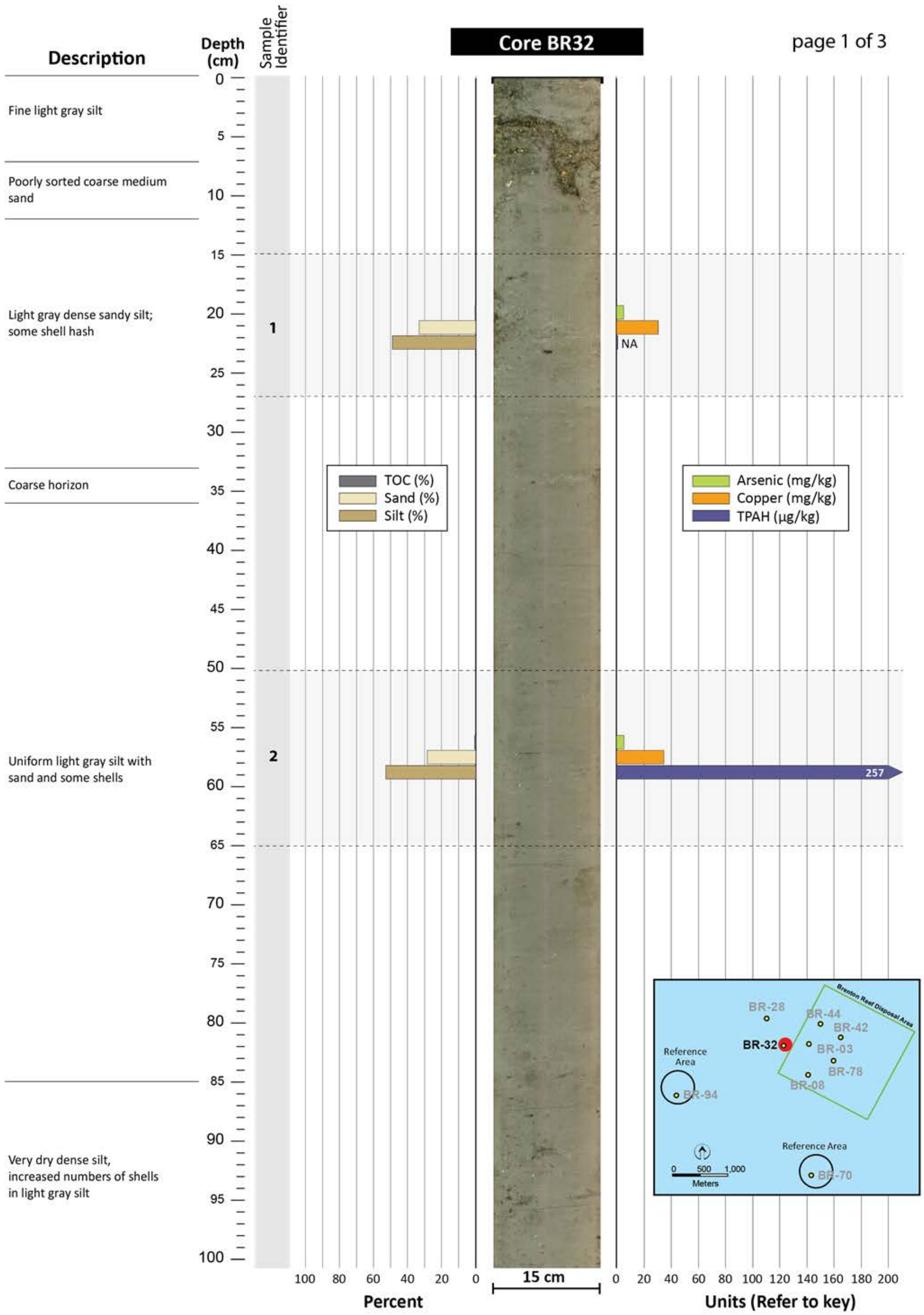

Figure D-4a. Full core BR32 characteristics, horizon descriptions and selected analyte values.

Full Length Sediment Core Photographs with Characteristics and Descriptions

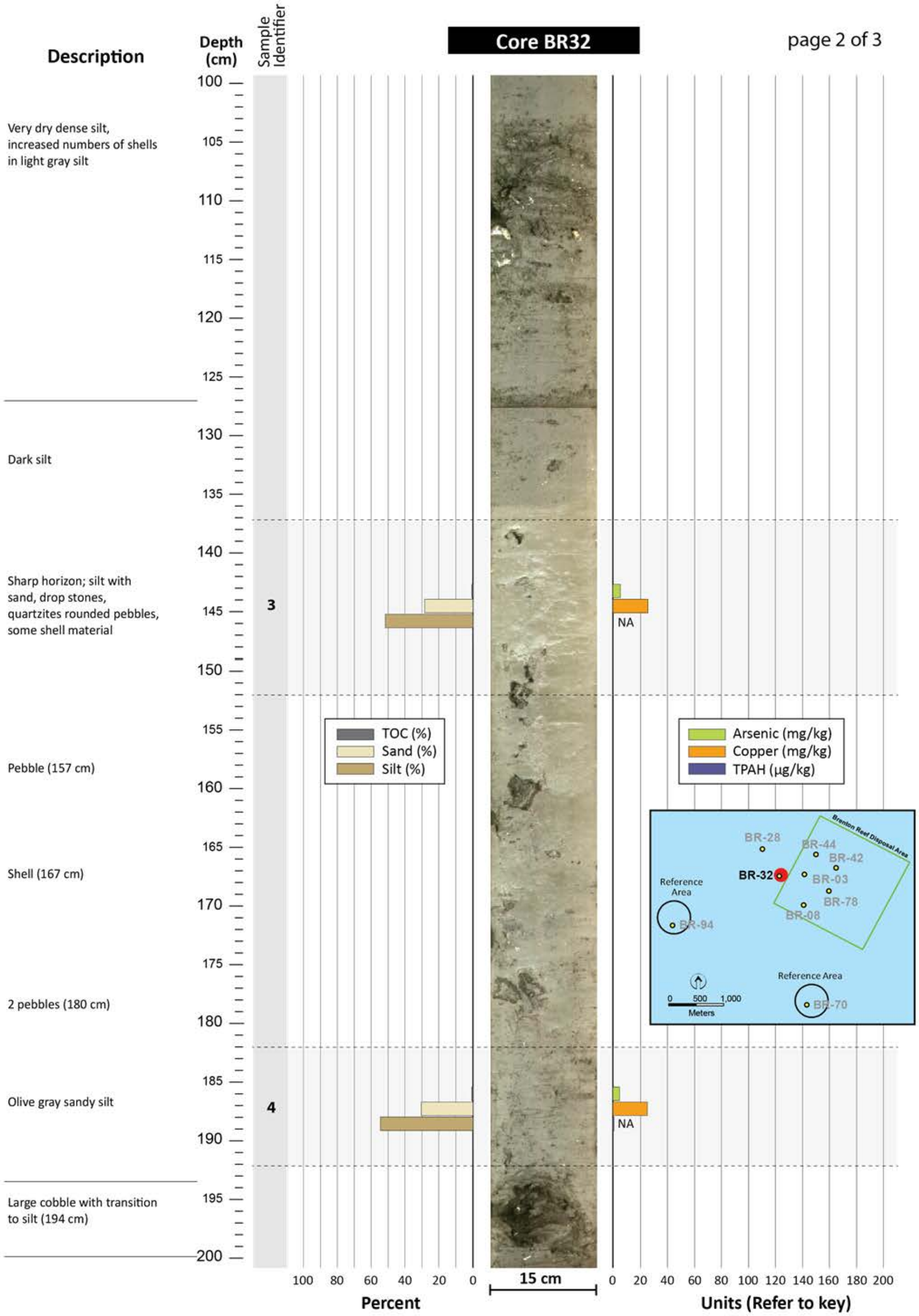

Figure D-4b. Full core BR32 characteristics, horizon descriptions and selected analyte values (continued).

Full Length Sediment Core Photographs with Characteristics and Descriptions

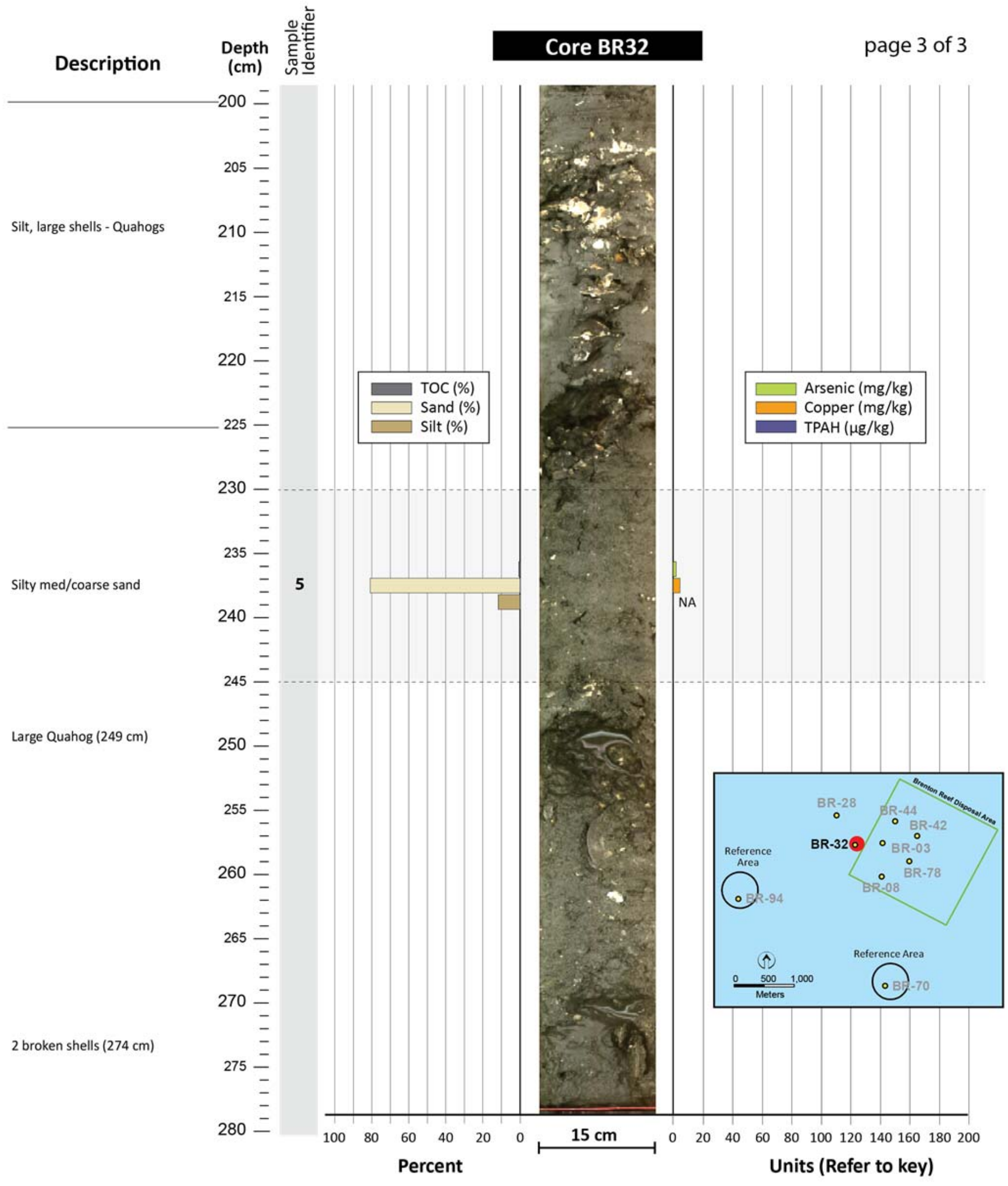

Figure D-4c. Full core BR32 characteristics, horizon descriptions and selected analyte values (continued).

Full Length Sediment Core Photographs with Characteristics and Descriptions

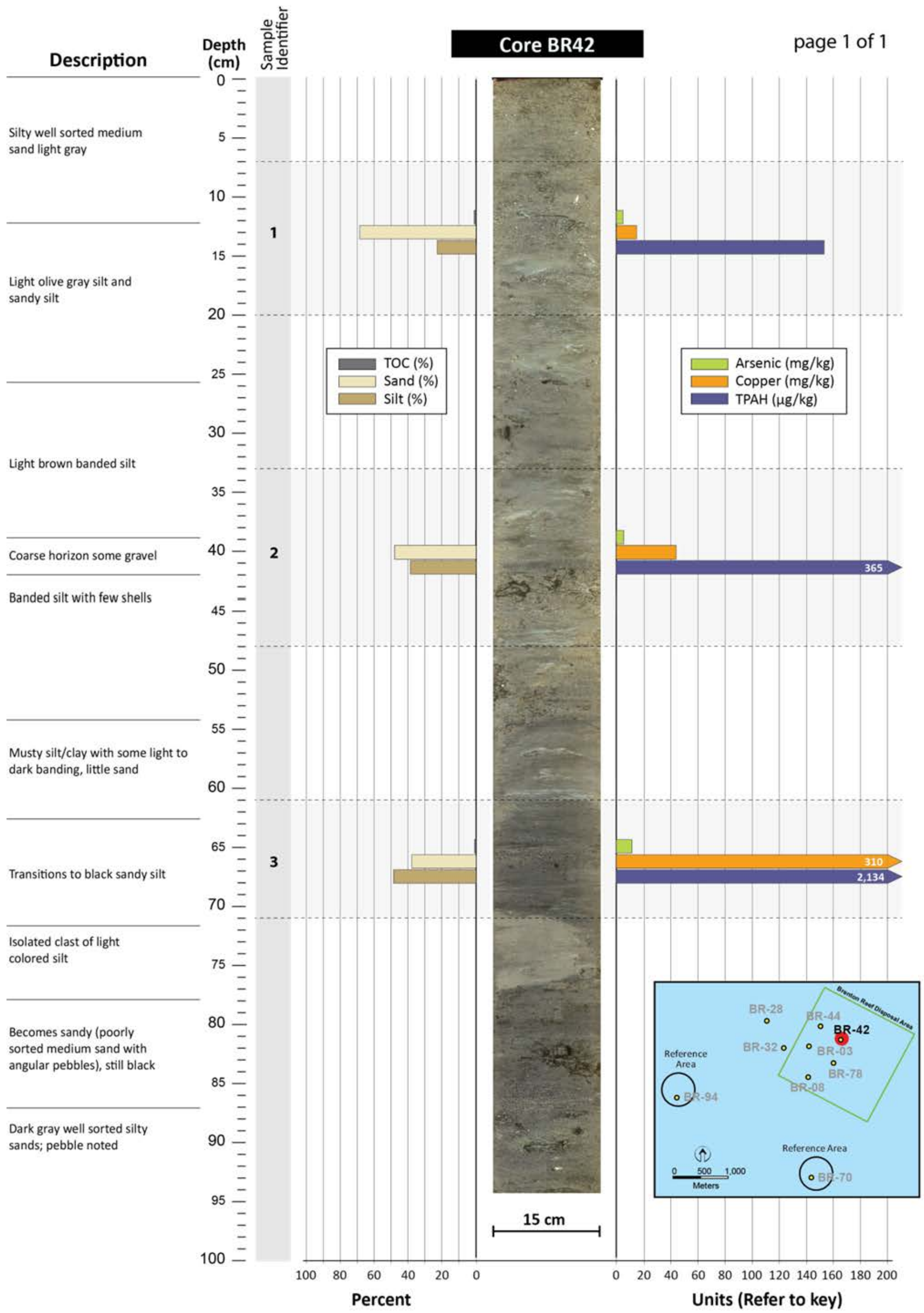

Figure D-5. Full core BR42 characteristics, horizon descriptions and selected analyte values.

Full Length Sediment Core Photographs with Characteristics and Descriptions

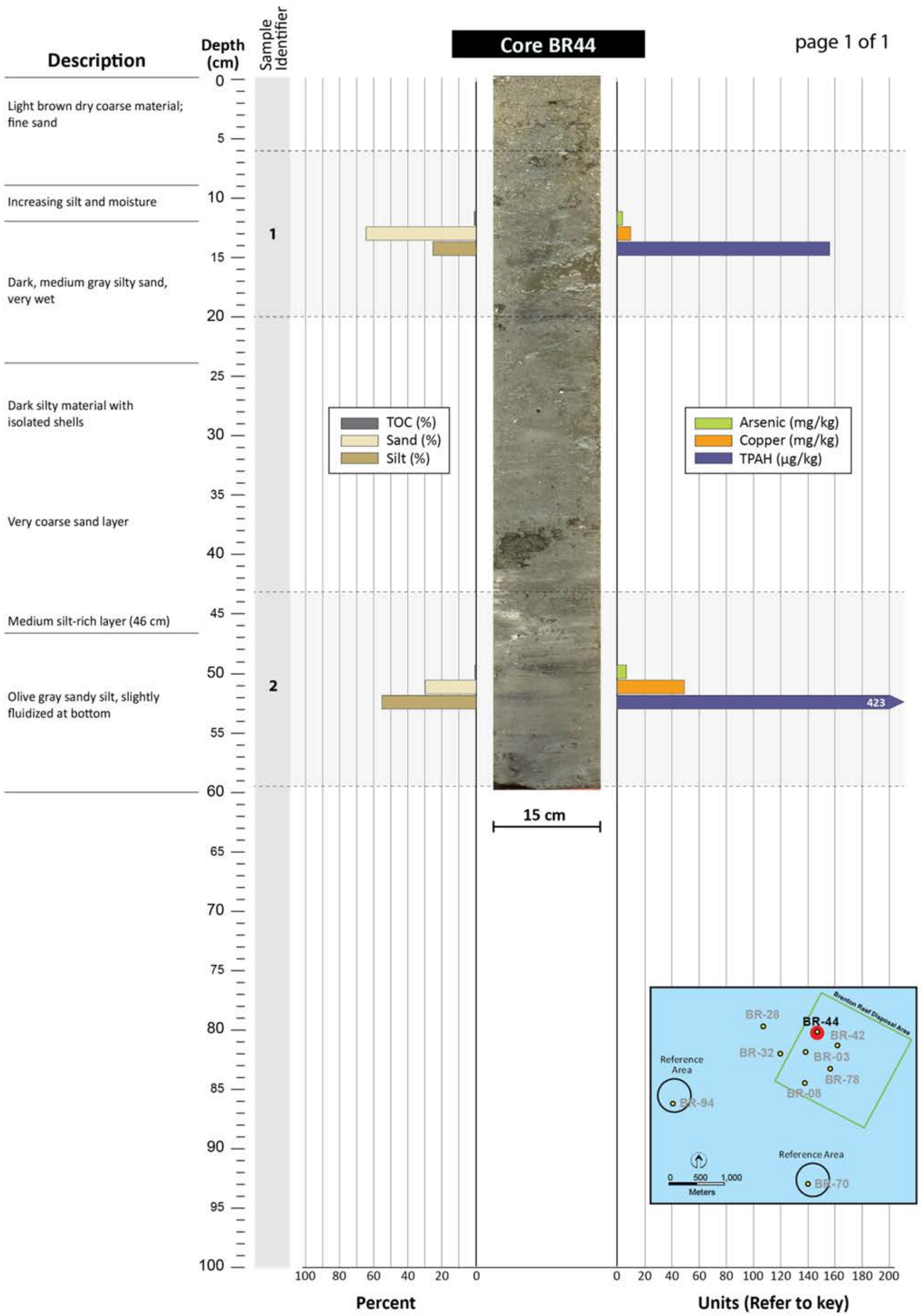

Figure D-6. Full core BR44 characteristics, horizon descriptions and selected analyte values.

Full Length Sediment Core Photographs with Characteristics and Descriptions

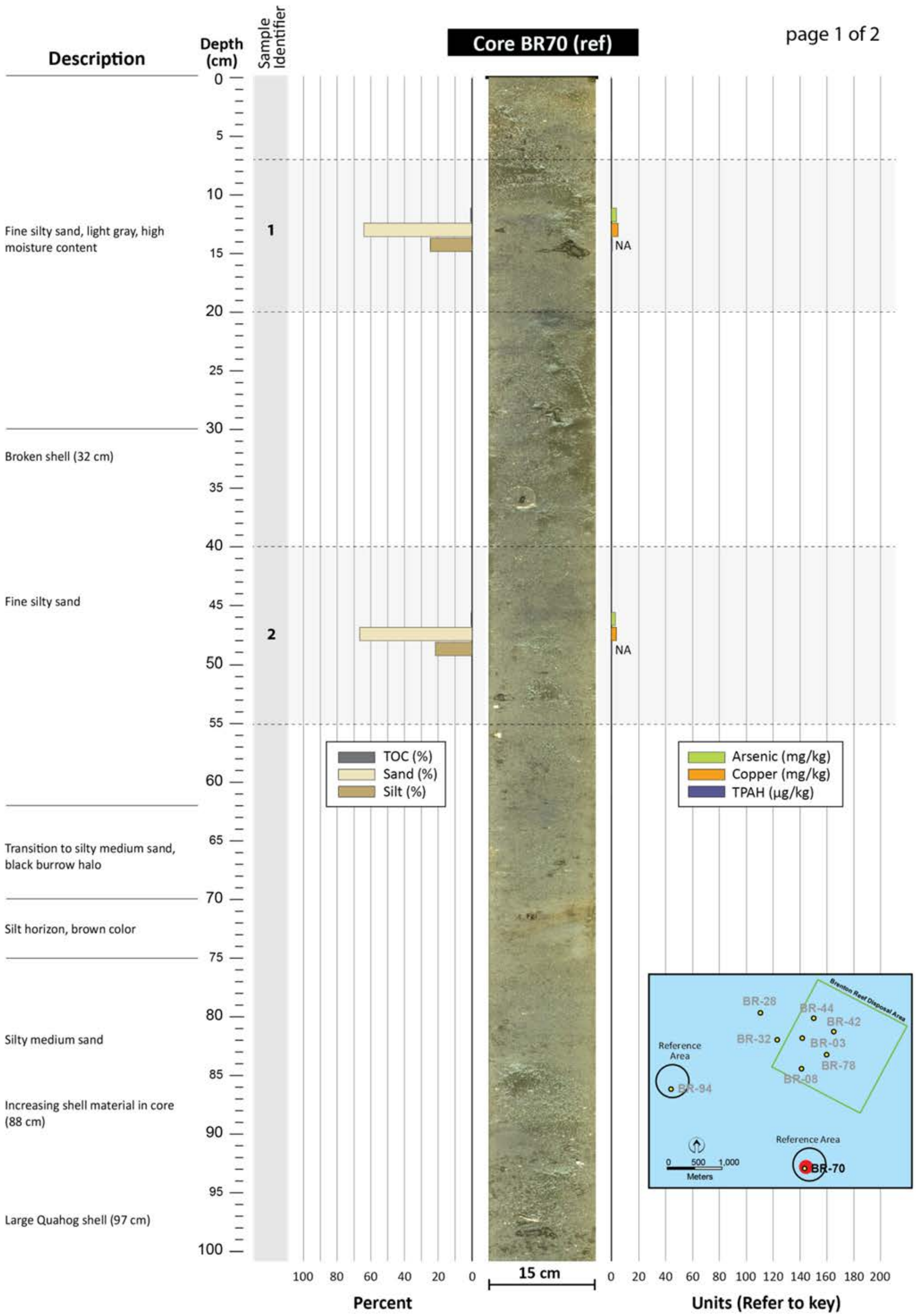

Figure D-7a. Full core BR70 characteristics, horizon descriptions and selected analyte values.

Full Length Sediment Core Photographs with Characteristics and Descriptions

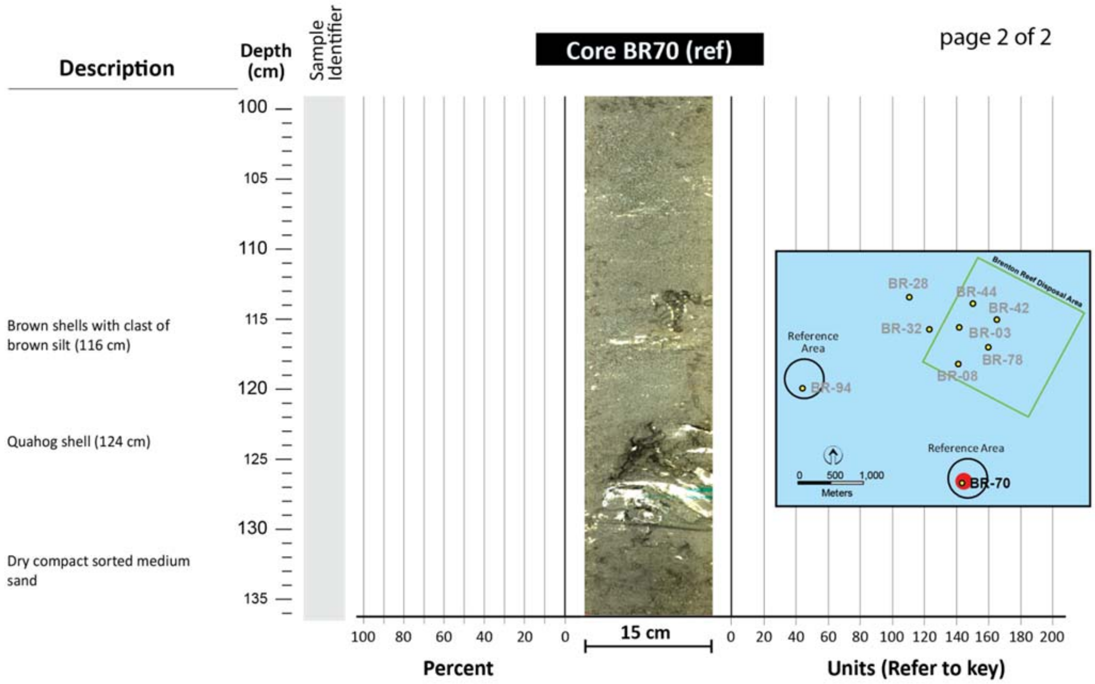

Figure D-7b. Full core BR70 characteristics, horizon descriptions and selected analyte values (continued).

Full Length Sediment Core Photographs with Characteristics and Descriptions

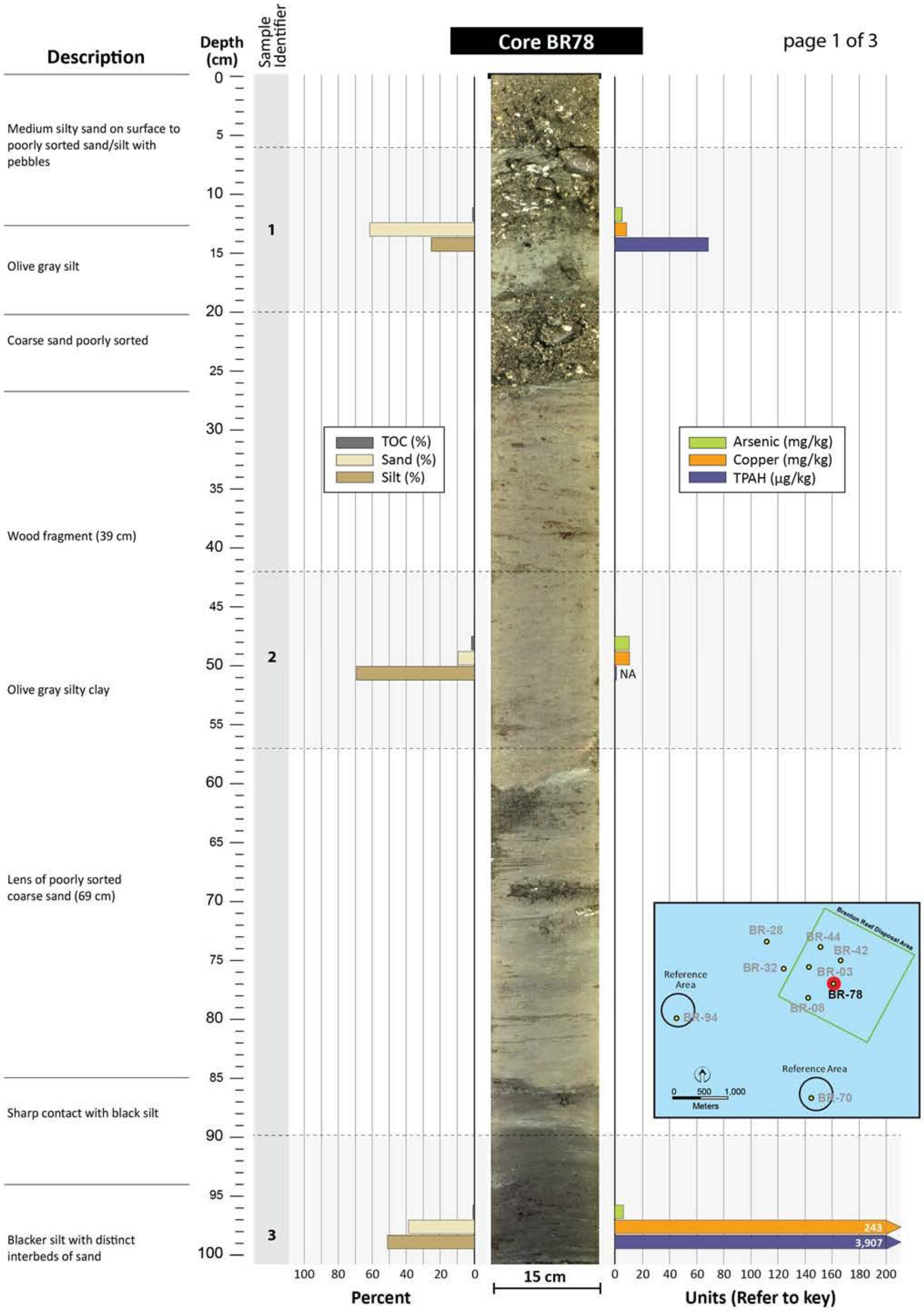

Figure D-8a. Full core BR78 characteristics, horizon descriptions and selected analyte values.

Full Length Sediment Core Photographs with Characteristics and Descriptions

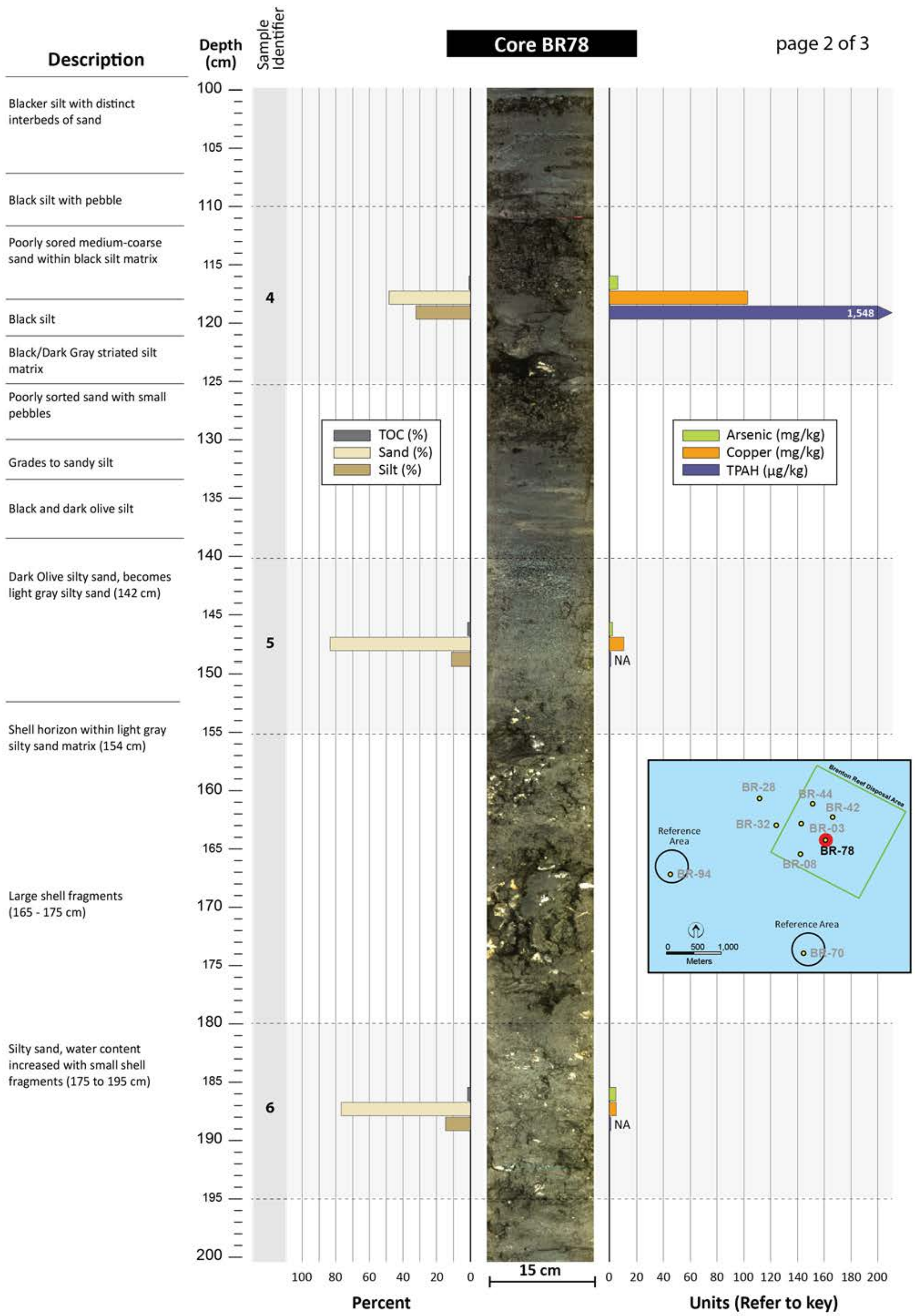

Figure D-8b. Full core BR78 characteristics, horizon descriptions and selected analyte values (continued).

Full Length Sediment Core Photographs with Characteristics and Descriptions

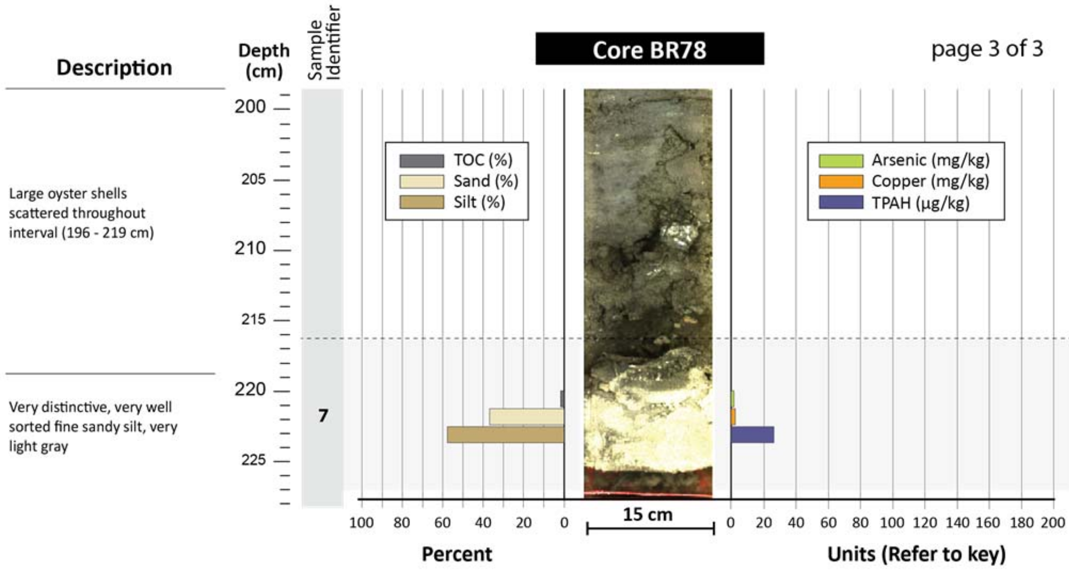

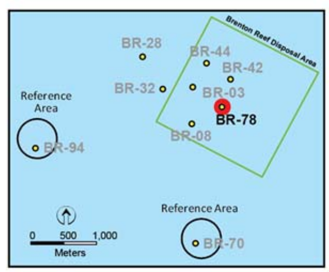

Figure D-8c. Full core BR78 characteristics, horizon descriptions and selected analyte values (continued).

Full Length Sediment Core Photographs with Characteristics and Descriptions

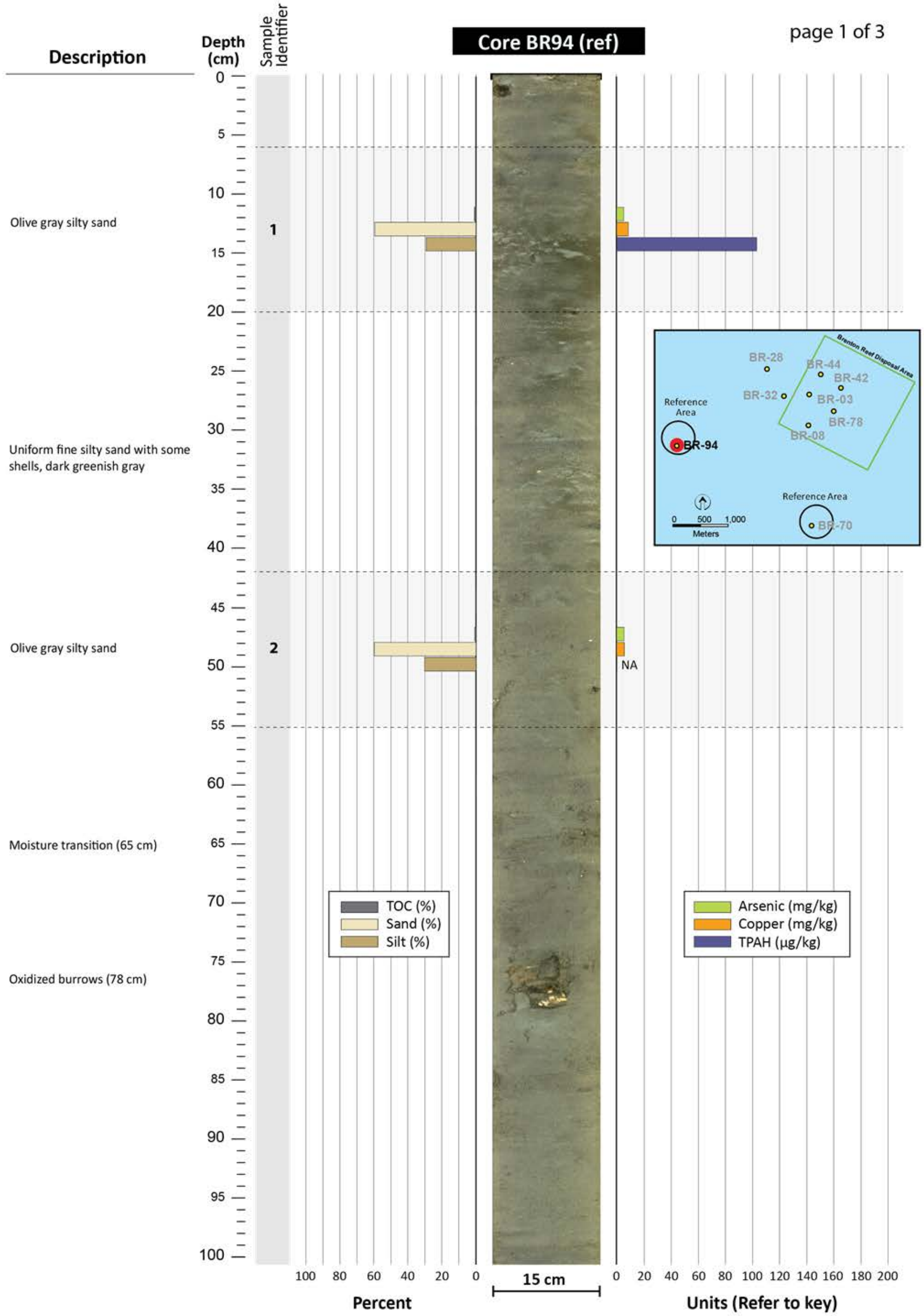

Figure D-9a. Full core BR94 characteristics, horizon descriptions and selected analyte values.

Full Length Sediment Core Photographs with Characteristics and Descriptions

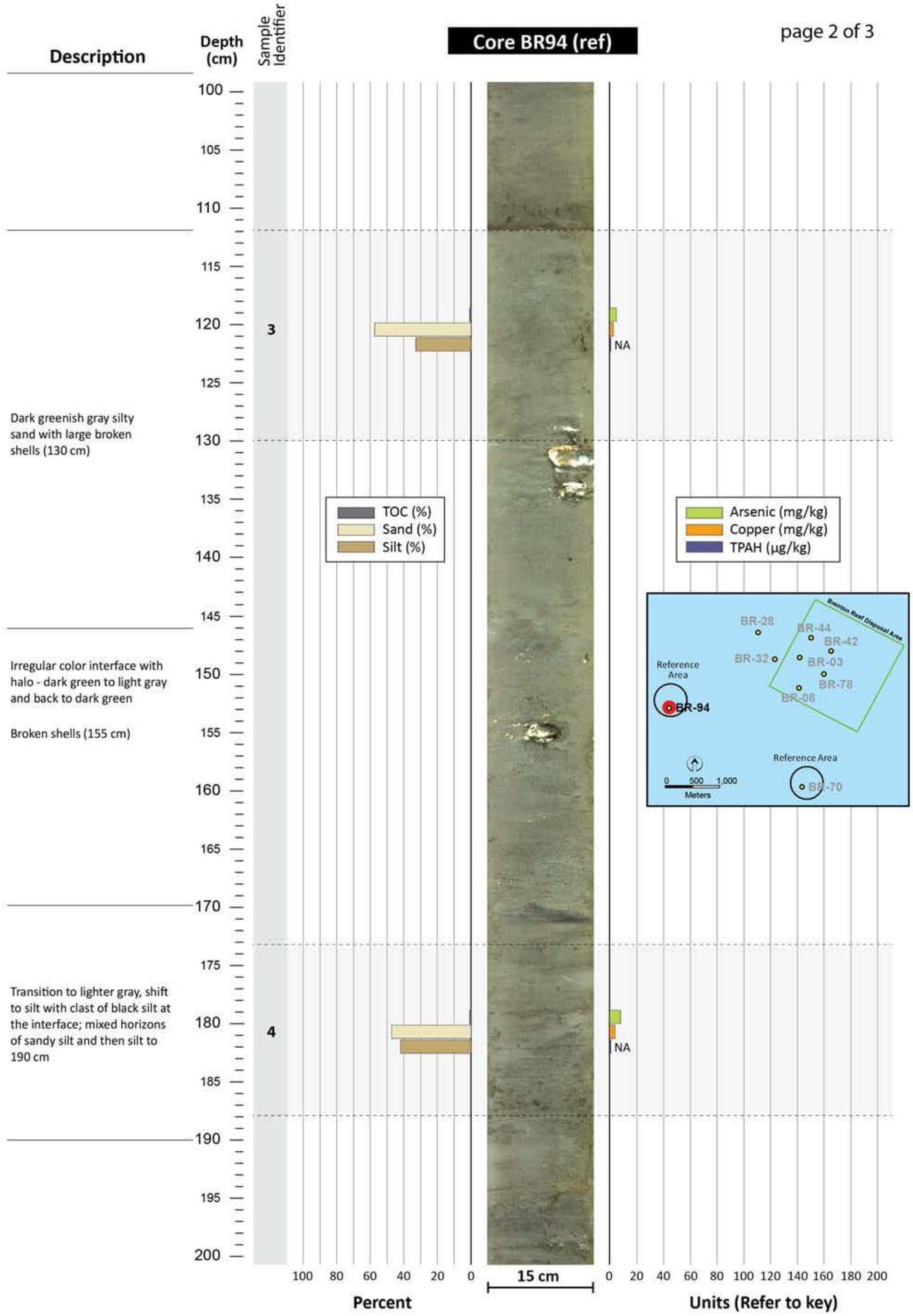

Figure D-9b. Full core BR94 characteristics, horizon descriptions and selected analyte values (continued).

Full Length Sediment Core Photographs with Characteristics and Descriptions

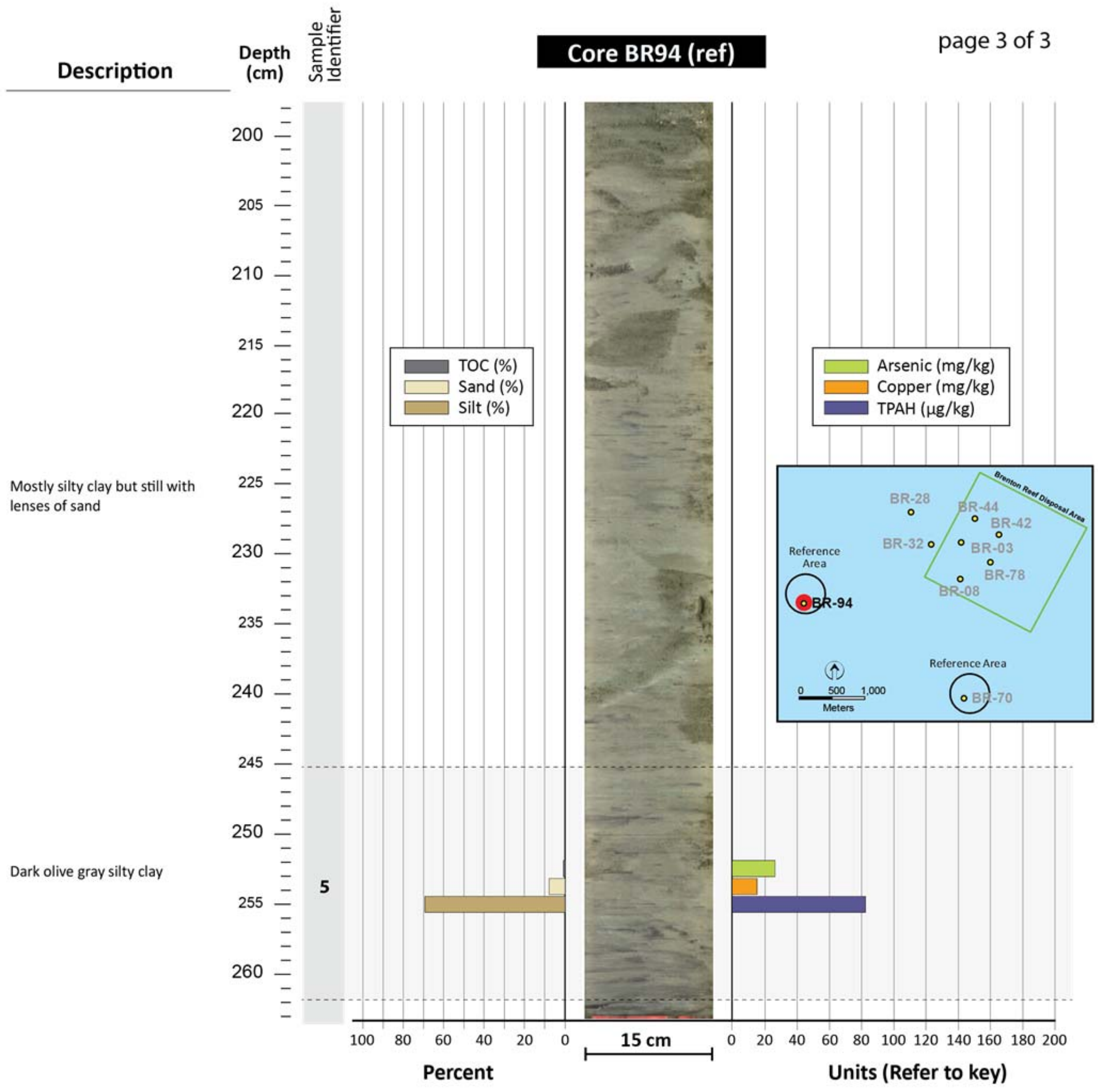

Figure D-9c. Full core BR94 characteristics, horizon descriptions and selected analyte values (continued).

APPENDIX E

PRINCIPAL COMPONENTS ANALYSIS OF SEDIMENT CORE DATA

APPENDIX E
PRINCIPAL COMPONENTS ANALYSIS OF SEDIMENT CORE DATA

LIST OF FIGURES

Page

E1 Data Analysis and Statistical Methods

Principal components analysis is an exploratory data analysis tool that can be used to investigate relationships between samples, and also for data reduction of a multivariate dataset. Sample relationships are illustrated using graphical representations of the data in terms of a small number of principal components (PCs) which are linear combinations of the original variables. Correlations between the principal components and the original variables allow us to interpret which variables drive the primary differences among samples. Principal components analysis (PCA) was applied using the statistical software S-Plus (MathSoft 1999).

Prior to conducting the PCA, metals and PAH data were normalized. Normalizing metals concentrations is useful to diminish the concentration fluctuations that may be due to the innate character of the sediment, rather than anthropogenic input. Metals data were normalized to the fine-grained fraction (silt+clay) of the sediment, since metals in surface water readily sorb to fine particles. Consequently, unusually high concentrations of fines-normalized metals data would indicate excessive metals contributions from an anthropogenic source. The organic constituents (PAHs) were evaluated both as bulk (dry weight) concentrations, and normalized to total organic carbon (TOC), because non-polar organic contaminants tend to be correlated with the organic matter in sediments. Gradients of chemical concentration associated with a source may be more easily observed when the data are OC-normalized than when they are presented as bulk concentrations.

Normalized concentrations were calculated as described in the following formulas. PAHs were normalized to organic carbon as:

$$\frac{\mu g\ chemical}{kg\ DW\ sed} \times \frac{kg\ DW\ sed}{mg\ OC} \times \frac{10^6\ mg}{kg} = \frac{\mu g\ chemical}{kg\ OC}$$

Similarly, metals were normalized to fines as:

$$\frac{mg\ metal}{kg\ DW\ sed} \times \frac{100}{\%\ fines} = \frac{mg\ metal}{kg\ \ fines}$$

(where DW sed is the dry weight of the sediment sample).

PCA is a statistical method that summarizes the covariance or correlation structure of the original data set using a set of principal components that are constructed as linear combinations of the original variables. Each principal component (PC) is constrained by the method to be uncorrelated with the other principal components. The first PC summarizes as much of the variability in the data as possible, and variables that load highly on this first PC will be correlated with one another. The second PC summarizes as much of the remaining variability as possible, and so on. The second PC will identify the variables that are either not well correlated over-all with the set of variables that contributed to the first PC, or for which some samples show a different pattern.

A PCA plot illustrates the relationships summarized by the principal components: correlations common among all samples will be indicated by a string of samples along the axis of one of the PCs (e.g., COMP1 in Figure E-1); correlation patterns driven by one or two extreme samples will be indicated by outliers on the PCA plot (e.g., sample BR28-2 in Figure E-1). When a set of principal components cumulatively summarizes most (e.g., 80%–90%) of the total sample variance, then these principal components can replace the original variables without much loss of information. When a set of principal components summarizes only a moderate proportion of the total sample variance (e.g., 50%–70%), then these results should be used primarily for interpretation of how the original variables contribute to the sample variance-covariance structure.

PCAs were conducted on the 20 samples with reported PAHs (both dry weight- and TOC-normalized), using all compounds with at least 50% detection frequency. Three PAH compounds were excluded due to low detection frequency: 2-methylnaphthalene (35% detected), acenaphthene (40% detected), and naphthalene (35% detected). The remaining PAH compounds had detection frequencies ranging from 55% to 90% detected. The sample BR03-7 was excluded from the TOC-normalized analysis due to extremely low TOC (0.006%).

PCAs also were conducted on all 40 samples with metals reported at 50% detection frequency (both as dry weight and as metals normalized to percent fines). Selenium (48% detected) and silver (38% detected) were excluded due to low detection frequency. The remaining metals had detection frequencies ranging from 88% to 100%.

E2 PCA Results for Metals

A PCA was conducted among all samples with reported metals in order to evaluate the relationship among the samples, and to note how the metals covaried (Figure E-1). Two metals were excluded from the analysis due to low detection frequency (selenium and silver). The first principal component (Comp. 1) was an overall average of the individual metals, accounting for 68% of the total variation. Higher values of Comp. 1 represent higher metals concentrations. The second principal component (Comp. 2, accounting for an additional 25% of the total variation), represented changes in the relative contribution of individual metals. The sample BR28-2 (28–38 cm) stands out near the top of the plot due to its disproportionately higher concentrations of cadmium, copper, chromium, lead, and zinc. The string of samples that stretch out in the negative direction of Comp. 2 have increasing concentrations of aluminum, beryllium, vanadium, and iron. Because all four of these metals have strong associations with natural metals content in aluminosilicate minerals, and less of an association with contaminant input in Narragansett Bay, the PCA analysis was rerun with metals normalized to grain size.

Similar patterns were seen in the PCA on metals normalized to percent fines (Figure E-2), although many samples clustered closely together. An inference can be made that those samples (including reference samples) are more representative of expected metals concentrations in outer Narragansett Bay, while the outliers are most likely influenced by the levels of metals concentrations associated with material dredged from areas closer to inner Providence Harbor. The distinctly different samples included three samples from the station BR28, starting from the second sample or 28–38 cm; four samples from mound station BR78 starting at the third sample or from 90–110 cm; and one sample from station BR42 (61–71 cm). In summary, many of the metals were found to covary within the metals group and also with grain size.

E3 PCA Results for Polycyclic Aromatic Hydrocarbons

All of the polycyclic aromatic hydrocarbon (PAH) results discussed below are reported in dry weight. A PCA was conducted among all samples with reported individual PAHs in order to evaluate the relationship among samples, and to note how the PAHs covaried (Figure E-3). Three PAH compounds with detection frequencies below 50% were excluded from this analysis (2-methylnaphthalene, acenaphthene, and naphthalene). The individual PAHs were all highly correlated (Appendix D) and the first principal component (Comp. 1, accounted for 99.6% of the total variance) was an average of all individual compounds. The samples with increasing values along the first principal component axis represent a gradient of increasing PAH concentration. Sample BR28-2 (28–38cm) had the highest concentration of every individual PAH. This station stands out on the second principal component (Comp.2) due to disproportionately higher concentrations of fluorene, benzo[k]fluoranthene, anthracene, benzo[a]anthracene, and acenaphthylene.

A second PCA was conducted on the PAHs normalized to total organic carbon, again excluding three compounds with low detection frequency (Figures E-4 and E-5). Sample BR03-7 (246–261 cm) was excluded from this PCA because it had no detectable TOC. Patterns among samples were very similar to those from the nonnormalized analysis. The correlation among the individual normalized PAHs was still high, so that the first principal component (Comp.1, accounted for 97% of the total variance) was again an average of all individual compounds. The majority of samples fell within a small area of the plot, and had normalized PAHs with similar patterns and magnitudes. The outlying samples formed a group similar to that for the metals outliers: BR42 (BR42-2 at 33–48 cm, BR42-3 at 61–71 cm); BR78 (BR78-4 at 110–125 cm, BR78-7 at 218–224 cm); and BR28 (BR28-2 at 28–38 cm, BR28-3 at 38–46 cm).

E4 Summary

A PCA was applied to illustrate relationships among individual samples (all groups, all depths) on patterns of contamination. It provided useful insights by summarizing the multivariate data sets. The PCA on PAHs found that the total PAH covaried very closely with individual PAHs. Based on the PCA findings for the individual PAHs, we may accurately represent PAH results in a summary format, such as total PAH, low PAH and high PAH.

In the metals PCA, the first principal component (Comp. 1) represents an average of all the individual metals, and explains 68% of the total variation. This kind of "average" and moderate variance PC indicates that the original data set is fairly strongly correlated, but that some samples have a different metals contamination pattern. This could be indicative of different source materials. Some samples appear to have metals concentrations that are more like “native” sediment (i.e., dominated by aluminum, beryllium, vanadium, and iron), while other samples have contaminant patterns more similar to Narragansett Bay sediments (i.e., dominated by cadmium, chromium, copper, lead, and zinc) even if their concentrations are low.

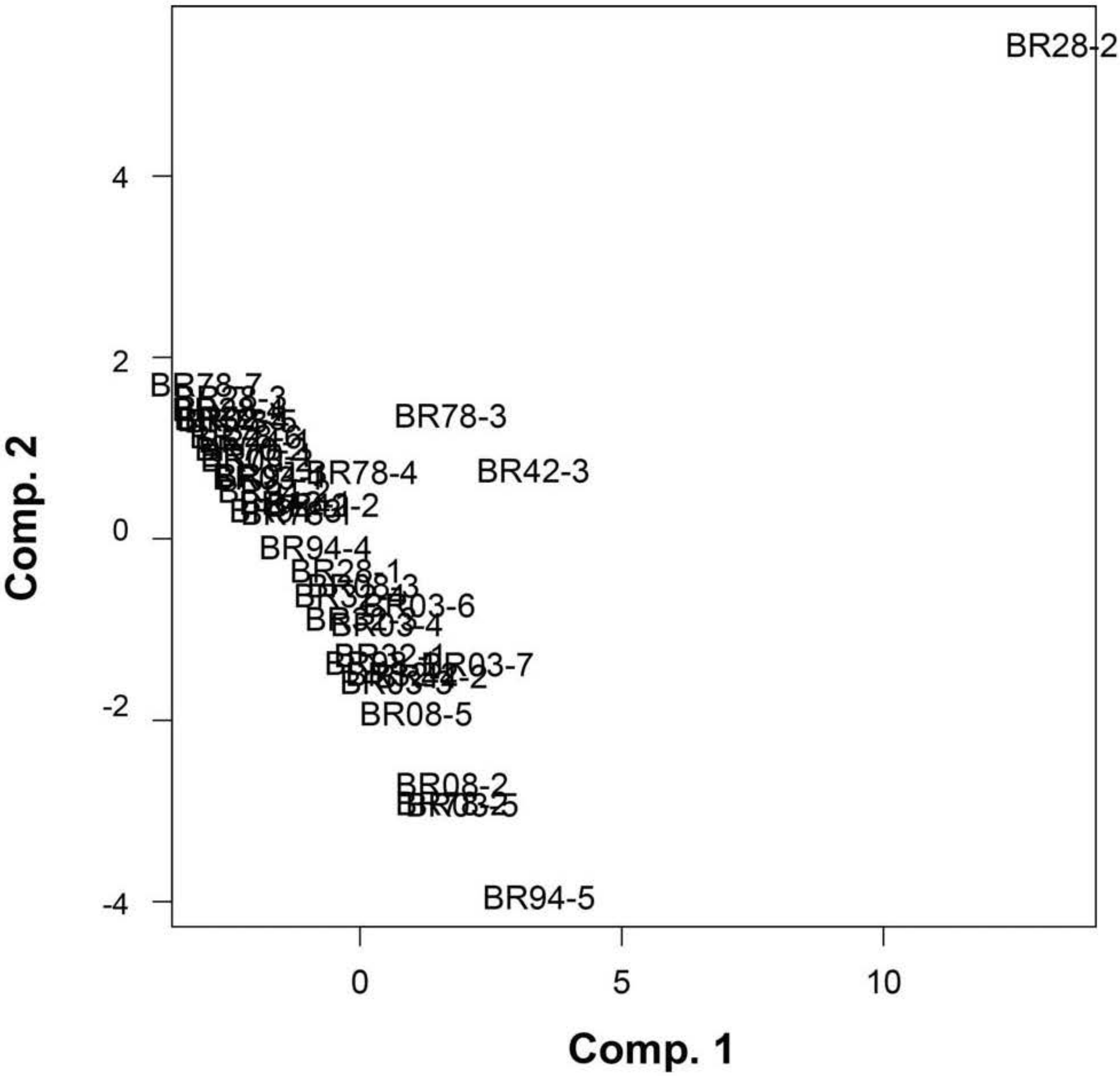

Figure E-1. Plot of the first two principal components for the PCA on metals (n=40), excluding Se and Ag. The first two principal components account for 68% and 25%, respectively, of the total variation.

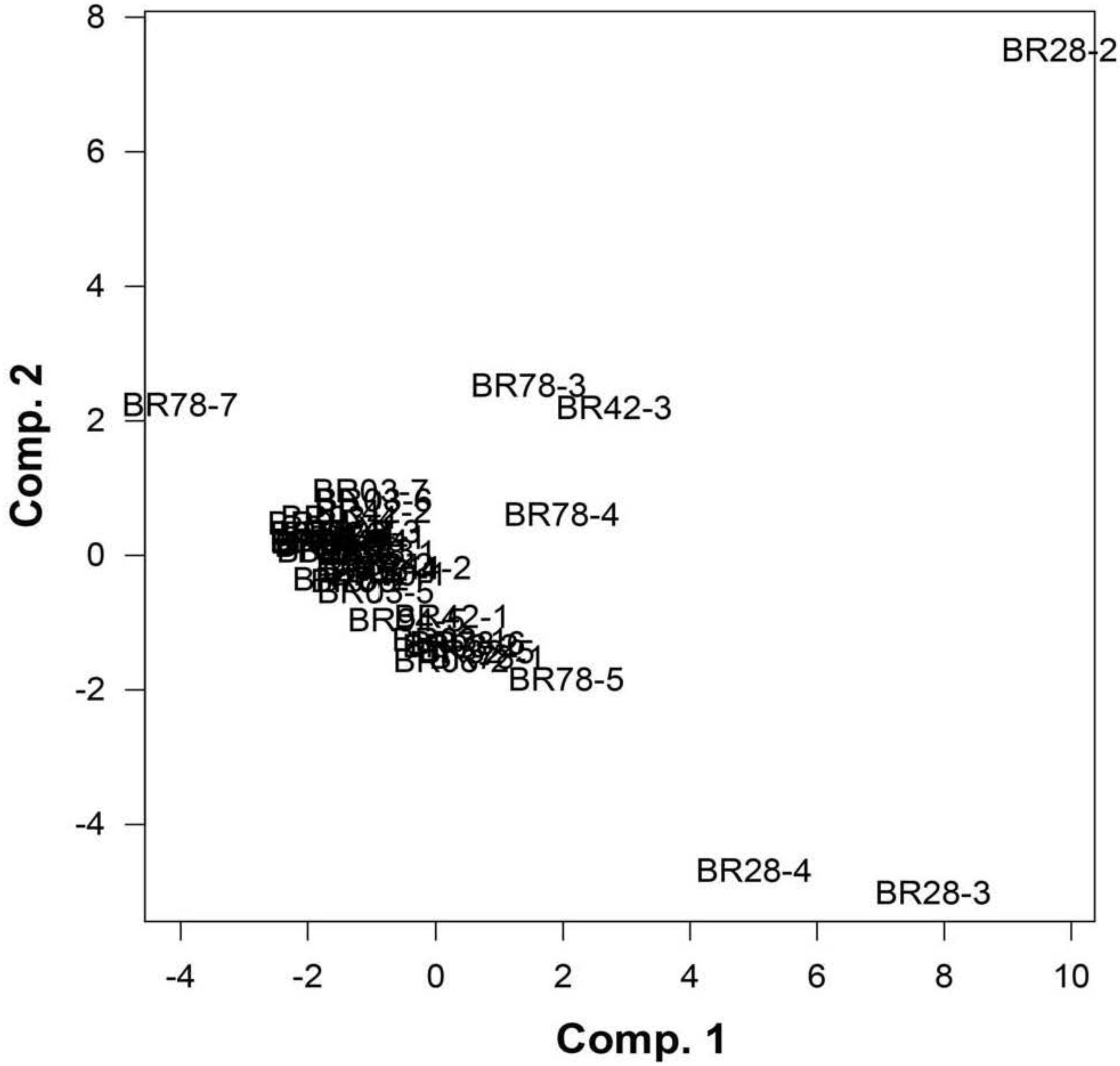

Figure E-2. Plot of the first two principal components for the PCA on metals normalized to fines (n=40), excluding Se and Ag. The first two principal components account for 59% and 32%, respectively, of the total variation.

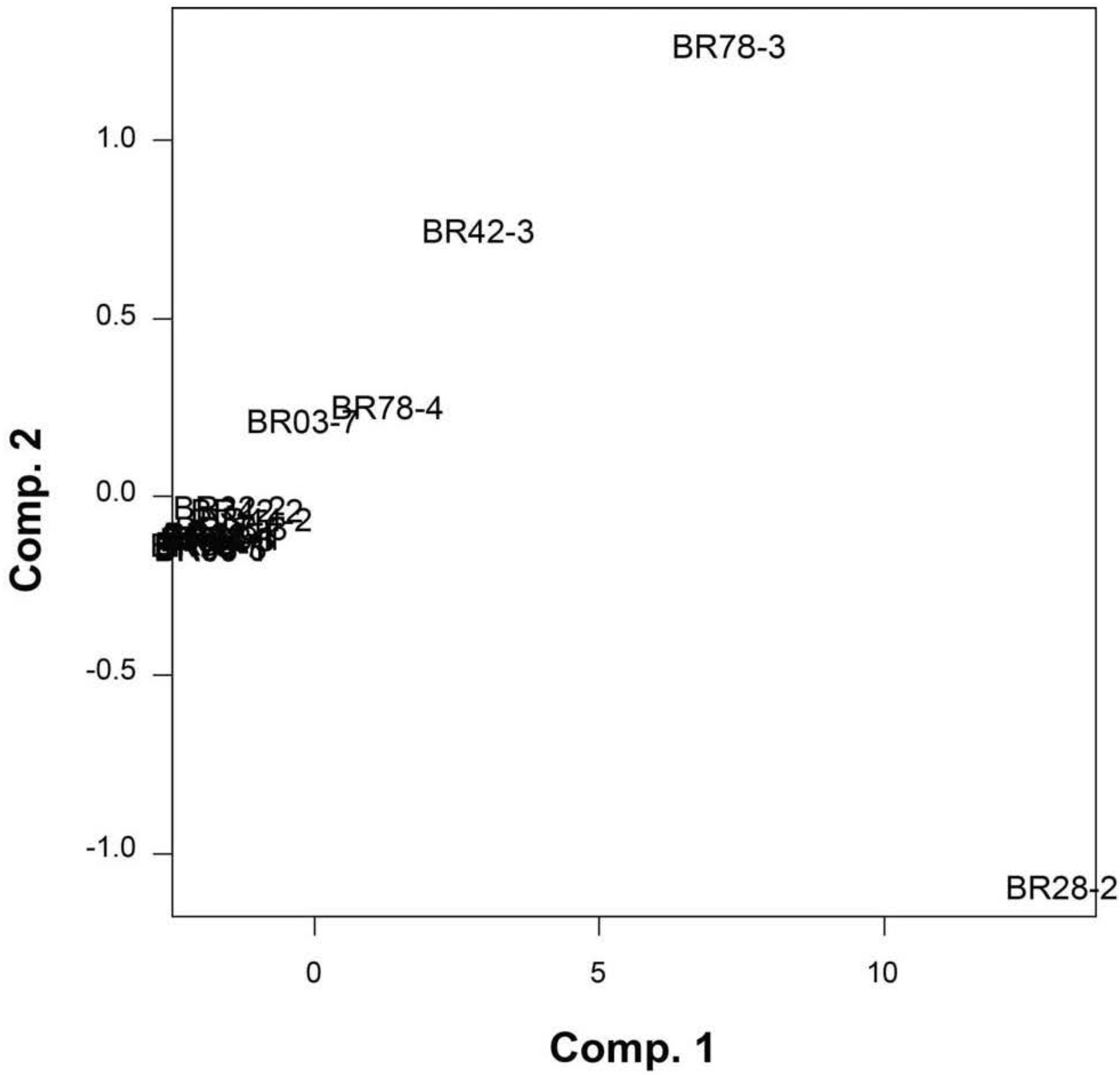

Figure E-3. Plot of the first two principal components for the PCA on PAHs (n=20), excluding three compounds with low detection frequency. The first two principal components account for 98.3% and 1.3%, respectively, of the total variation.

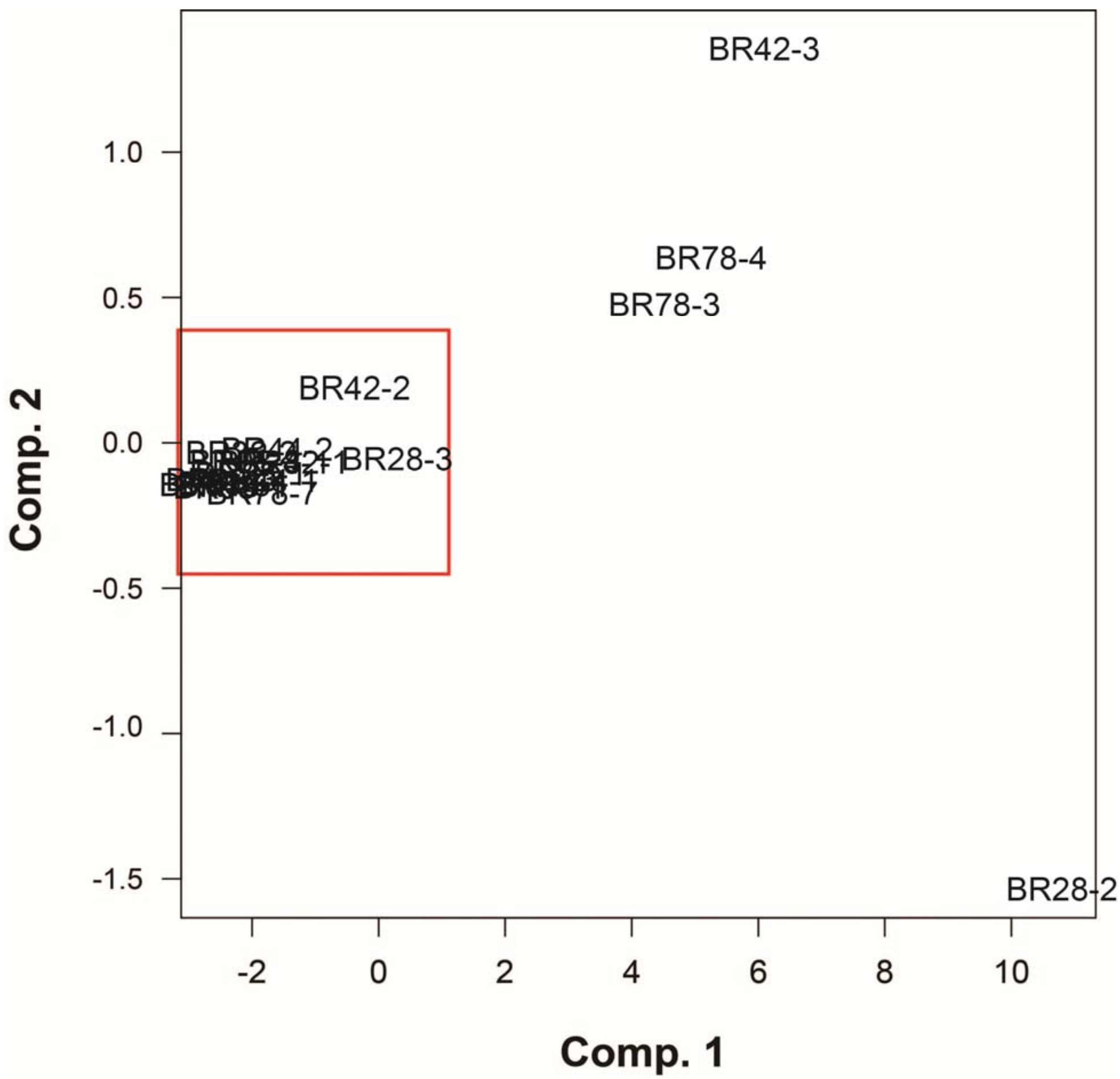

Figure E-4. Plot of the first two principal components for the PCA on OC-normalized PAHs (n=19), excluding three compounds with low detection frequency and sample BR03-7. The first principal component accounts for 97% of the total variation. The samples within the red box are shown on an expanded scale in Figure E-5.

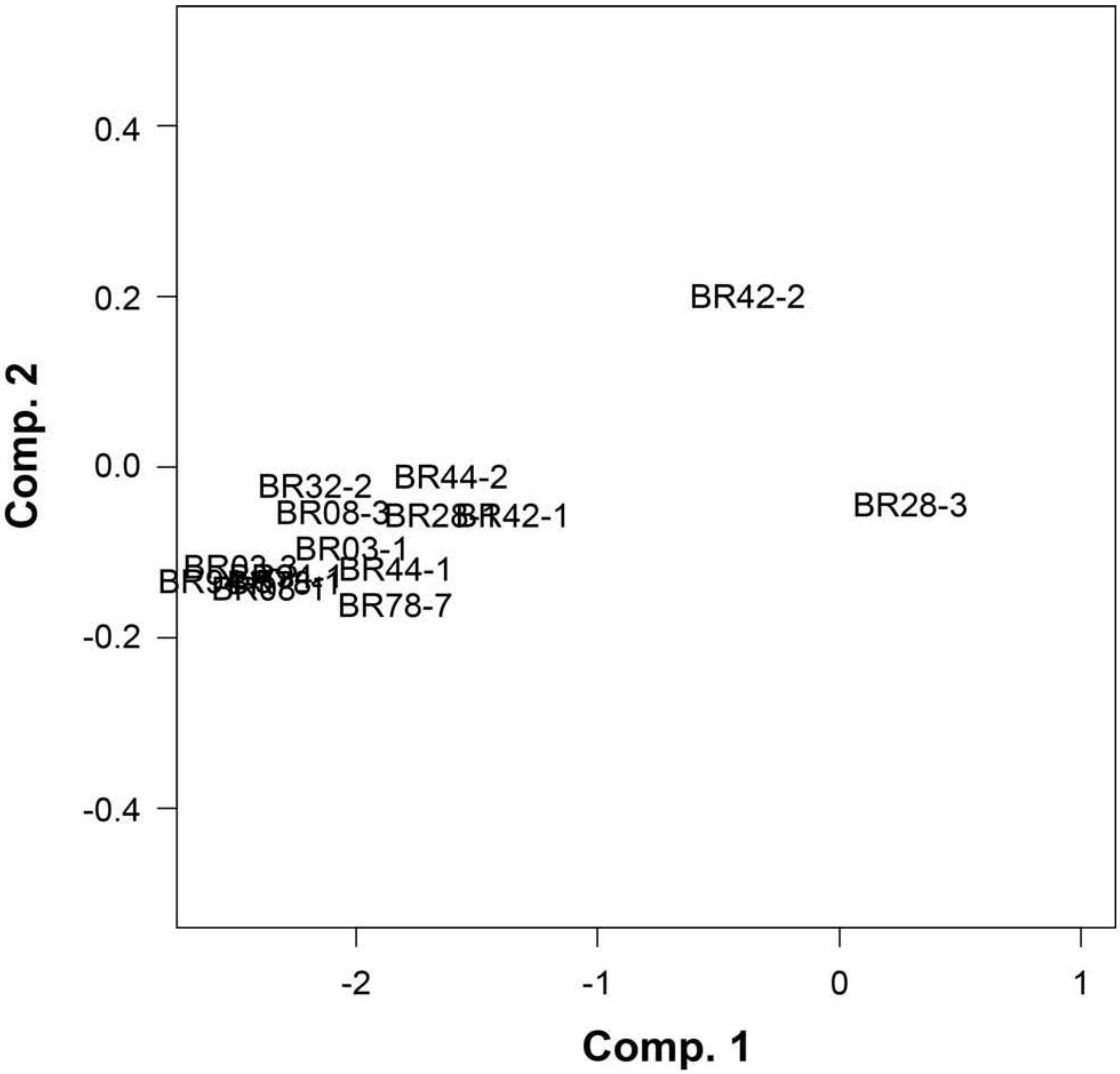

Figure E-5. Plot of the first two principal components for the PCA on OC-normalized PAHs (n=19), excluding three compounds with low detection frequency and sample BR03-7. This plot includes only the area within the red square shown in Figure E-4.

APPENDIX F

CORE LOGGING RESULTS AND ANALYSIS

APPENDIX F
CORE LOGGING RESULTS AND ANALYSIS

LIST OF TABLES AND FIGURES

Page

Core Logging Results

Core logging provided continuous photographs and measurements of gamma density, P-wave velocity, magnetic susceptibility, and electrical resistivity (Figure F-1). Evidence from the visual descriptions, core logging and the chemistry results provided a record of sedimentary processes at the site including predisposal, disposal, and postdisposal history. This vertical record was used to identify where and when dredged material disposal had occurred. Continuous core logging results are particularly useful in detecting interbedded silts and sands (e.g., Figures F-1a and d) and correlating horizons in widespread sedimentary sequences. We did not expect to see distinct sedimentary horizons that could be correlated across cores, even in the ambient sediments. We investigated the possibility of using this evidence to interpolate metals concentrations between horizons that were sampled for chemical analysis. Gamma density is a remote measure of bulk density of the sediments reflecting sediment grain density and porosity; it can be a reliable measure of porosity in saturated sediments but may also be affected by large shells or gravel. P-wave velocity is particularly useful for evaluating grain size variation with acoustic properties. Acoustic impedance is calculated by the product of bulk density and p-wave velocity and has been used as a grain-size estimator in carbonate-free sediments (Weber et al. 1997). Magnetic susceptibility relates to sediment composition. Magnetic susceptibility in marine sediments is generally correlated with deposition of detrital magnetic minerals (i.e., iron-bearing minerals such as magnetite, pyrrhotite, hematite, olivine, biotite, pyrite, and iron-oxide), often as a result of transport of fragments of glacially scoured bedrock or ice-rafting (Currie and Bornhold 1983, Andrews and Stravers 1995). Electrical resistivity is another technique for estimating porosity or grain size variation.

The reference cores in particular provided insight into pre- and postdisposal history of sediment processes. The presence of sand layers, intact shells, oxidized burrows, and deep compacted silt layers (BR94; Appendix D) indicated that this site had experienced episodic changes in sediment transport conditions. The sand layers and shell horizons represent periods with increased wave energy, and the burrows and silt horizons periods with much lower wave energy.

The core logging results can be compared to bulk sediment sample results to determine if the higher frequency core logging data can be used to infer lithology or perhaps even provenance of sediment layers. Core log data was averaged for each bulk sediment sample interval, and gamma ray density and p-wave velocity were converted to acoustic impedance for comparison with percent fines (silt+clay) and iron (Fe) concentration (Table F-1). Electrical resistivity and acoustic impedance are frequently correlated with grain-size or porosity, but exhibited a poor relationship with percent fines in these cores (Figure F-2a). There may have been confounding factors such as variable water content, presence of carbonate shells or blurring of results through averaging. Fe concentration is often strongly influenced by percent fines and in these results showed a relatively close correlation with grain size (Figure F-2b).

Magnetic susceptibility is also strongly influenced by percent fines as much of the natural signal comes from detrital minerals transported long distances in suspended load. In these results it was generally correlated with grain size, but there were notable deviations (Figure F-3a). Some samples were above average in magnetic strength compared to the fines content (BR28-4, BR32-3, BR32-4, BR44-1, BR78-3, BR78-4, BR78-5, BR94-5). There may be several factors that influence this result: silty sands with enriched metal content in the silt fraction (BR28-4 was a distinct well-sorted sand with silt and clay, BR44-1 was a wet silty sand, BR78-5 was a silty sand); clayey silts strongly enriched in metals (BR32-3, BR32-4, BR94-5); or interbedded sands and silts that contained highly enriched fractions (BR78-3, BR78-4). Some samples were strongly below average in magnetic strength compared to the fines content (BR3-3, BR3-4, BR3-5, BR8-1, BR8-2, BR28-2, BR32-1, BR32-2, BR44-2, BR78-2, BR78-7). These samples included a number of distinctive lithologies but also some surprisingly high metal contents (Table 3-2). The logical comparison is between magnetic susceptibility and Fe content, normalized to fines (Figure F-2b). Remarkably, there appears to be no clear correlation between magnetic susceptibility and Fe content; the magnetic susceptibility variation is flattened by normalization but some outliers still persist that are not reflected in Fe variation (Figure F-2b). The Fe variation is flattened by use of a logarithmic scale but there are still deviations from average values that are distinct between the two datasets.

A comparison of the Principal Components Analysis (PCA) results for metals and the magnetic susceptibility results provides some further insight into potential sources of metal concentrations in some of the sediment layers (Appendix E and Table F-1). Not surprisingly, the PCA results indicated that many of the sediment layers discussed above (BR28-3,4; BR78-3, BR78-4, BR78-5, BR78-7, and BR42-3) all had outlier results for metals normalized to fines (Figure E-2). These mixed sediments and strong variations in metal content are diagnostic of dredged material (Fredette et al. 1992, Myre and Germano 2007) and are not typical of sediments deposited under equilibrium conditions in the open ocean. However, there is one sample that is the exception to this conclusion.

At the base of BR94, a sample (247–262 cm) with unusually high silt content (92%) had enriched metal content and a very high value of magnetic susceptibility in the core logs (Table F-1). It had the maximum measured value of all samples for As and Fe, and near the maximum values for Al, Ni, and Se (Table 3-2). When metal concentrations were normalized to fine-grained sediment percentage, only As and Fe were above average relative to other samples. The anomalous results at the bottom of this >2.5 m core are likely the result of reworking and transport of fine-grained heavy minerals or clays and deposition in an estuarine basin during the most recent marine transgression, rather than deposition of dredged material. There was no evidence of a 2.5-m deposit of dredged material at the location of the core and the core was located above a buried postglacial fluvial channel (Needell et al. 1983). The fluvial channels in Rhode Island Sound were buried by Holocene estuarine deposits of silt during postglacial sea level rise (O'Hara and Oldale 1980, Needell et al. 1983).

The other reference core (BR70) was only 1.3 m long and did not appear to sample this metal-enriched horizon. There was a small magnetic spike at 25 cm below the surface, but this level was not analyzed for metals. In other respects the core was quite similar to BR94, reflecting the same changing sediment transport conditions.

It is tempting to use magnetic susceptibility profiles to extrapolate anthropogenic metal concentrations within the cores from Brenton Reef (see Reynolds et al. 2010, Corbin 1989). There are clearly confounding factors, however, as Fe does not always serve as a proxy for all other metals and may be enriched or depleted in harbor sediments or background materials. In particular, the highly heterogeneous nature of dredged material deposits precludes generalization about trends: chaotic fabrics, chaotic lithologies, and chaotic chemistry are the norm.

Table F-1.

Magnetic Susceptibility, Acoustic Impedance and Electrical Resistivity Compared to Grain Size and Fe Concentration in Cores

Core Interval	Location	Percent Fines	Interval (cm)	Magnetic (SI)	Acoustic Impedance (Z)	Elec. Res (Ohm-m)	Fe (mg/kg)
BR03-1	Mound	26.3	6 –19	26.2	2588	1.2	11,000E
BR03-2	Mound	23.4	41–56	12.3	2530	1.0	9,880E
BR03-3	Mound	83.4	88–103	11.8	1245	0.7	21,900E
BR03-4	Mound	64.4	159–170	27.5	959	0.9	20,200E
BR03-5	Mound	93.0	187–202	7.1	808	0.7	33,900E
BR03-6	Mound	77.6	231–246	63.3	786	1.1	20,600E
BR03-7	Mound	95.9	246– 261	64.2	699	1.0	29,200E
BR08-1	Mound	65.6	7–20	7.7	2612	0.7	20,100
BR08-2	Mound	64.7	40–55	8.0	2569	0.6	30,200
BR08-3	Mound	63.1	114–129	40.7	3125	1.0	17,500E
BR08-4	Mound	26.6	165–180	24.7	962	1.9	7,720
BR08-5	Mound	82.5	185–200	68.8	2719	1.7	23,900E
BR28-1	Mound	54.1	7–20	25.4	2825	0.8	15,900E
BR28-2	Mound	84.1	28–38	12.1	2040	0.5	28,500E
BR28-3	Mound	6.4	38–46	9.4	2024	1.0	7,060E
BR28-4	Mound	7.8	54–59	18.5	1008	4.2	7,190E
BR32-1	Mound	66.4	15–28	22.2	3022	0.9	24,900
BR32-2	Mound	71.4	50–65	29.4	3013	0.7	26,300
BR32-3	Mound	65.0	139–154	130.0	3256	1.0	23,200E
BR32-4	Mound	67.2	181–192	92.3	2026	1.0	18,100E
BR32-5	Mound	16.6	231–246	16.9	909	1.3	7,680E
BR42-1	Mound	31.3	7–20	41.1	3300	1.0	12,200E
BR42-2	Mound	50.1	33–48	42.3	2630	0.7	13,600E
BR42-3	Mound	61.8	61–71	50.1	2628	0.6	19,400
BR44-1	Mound	31.2	7–20	64.8	3263	1.1	9,210E
BR44-2	Mound	69.9	44–59	23.8	2647	0.6	22,900
BR70-1	Reference	28.9	7–20	26.3	3549	1.3	10,100E
BR70-2	Reference	33.6	40–55	14.3	2843	1.0	8,660E

E = Estimated value

Table F-1., continued.

Magnetic Susceptibility, Acoustic Impedance and Electrical Resistivity Compared to Grain Size and Fe Concentration in Cores

Core	Location	Percent Fines	Interval (cm)	Magnetic (SI)	Acoustic Impedance (Z)	Elec. Res (Ohm-m)	Fe (mg/kg)
BR78-1	Mound	29.0	6–20	22.2	1049	1.5	12,800E
BR78-2	Mound	90.5	42–57	5.4	2440	0.6	34,900E
BR78-3	Mound	60.2	90–110	91.2	2050	1.0	15,100E
BR78-4	Mound	37.7	110–125	123.0	1965	1.7	14,679E
BR78-5	Mound	15.1	140–155	34.6	3250	1.0	8,200E
BR78-6	Mound	19.6	180–195	12.8	2385	1.3	8,610E
BR78-7	Mound	61.8	218–224	14.2	729	8.2	4,950
BR94-1	Reference	41.2	7–20	35.3	3149	0.8	10,700E
BR94-2	Reference	40.2	40–55	29.0	3286	0.8	11,600E
BR94-3	Reference	43.0	114–129	19.7	3016	1.8	13,000E
BR94-4	Reference	53.0	174–189	41.9	3329	1.0	14,500E
BR94-5	Reference	91.5	247–262	164.4	1901	1.3	47,900E

E = Estimated value

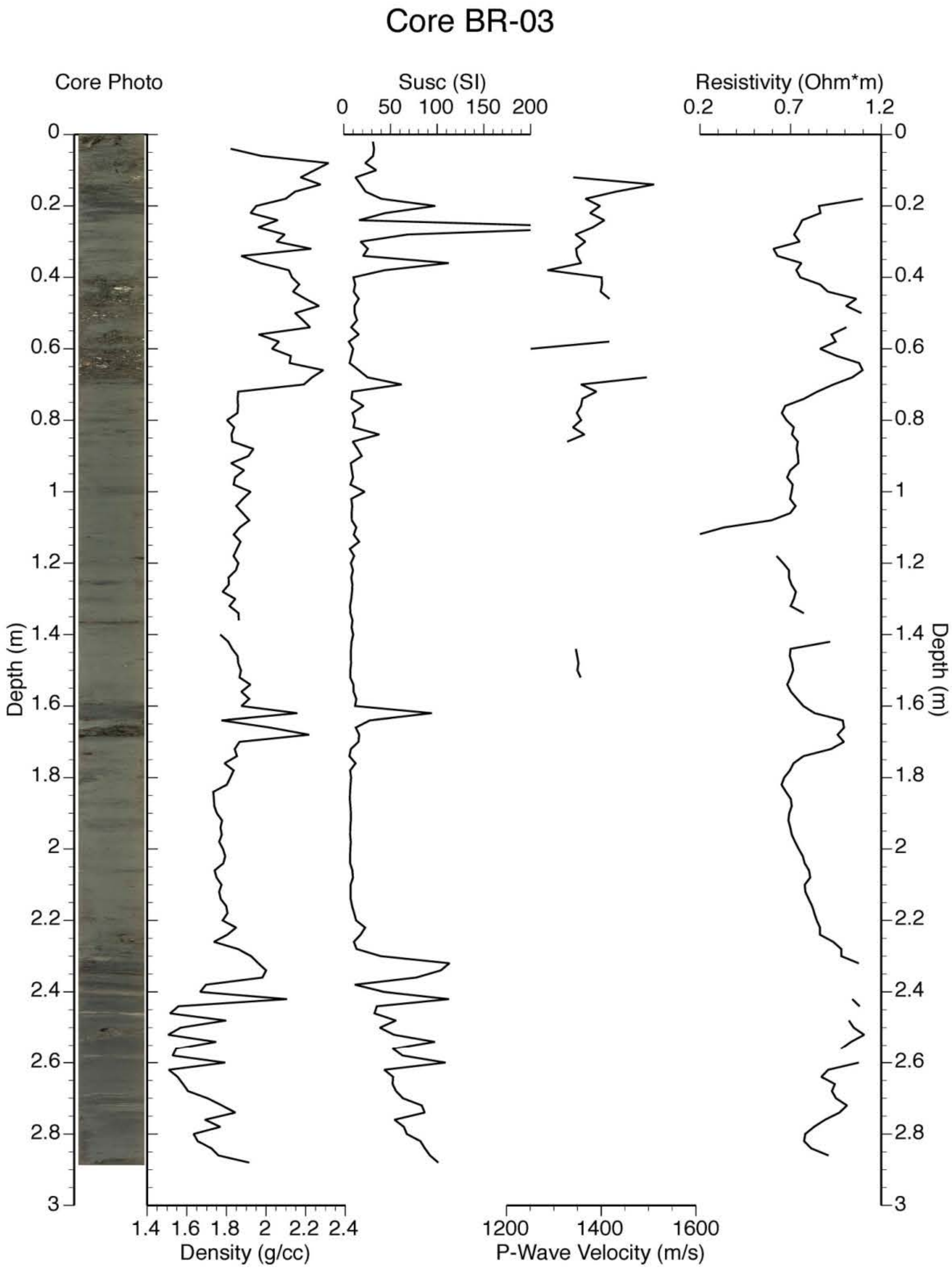

Figure F-1 a. Core logging results from core BR-03.

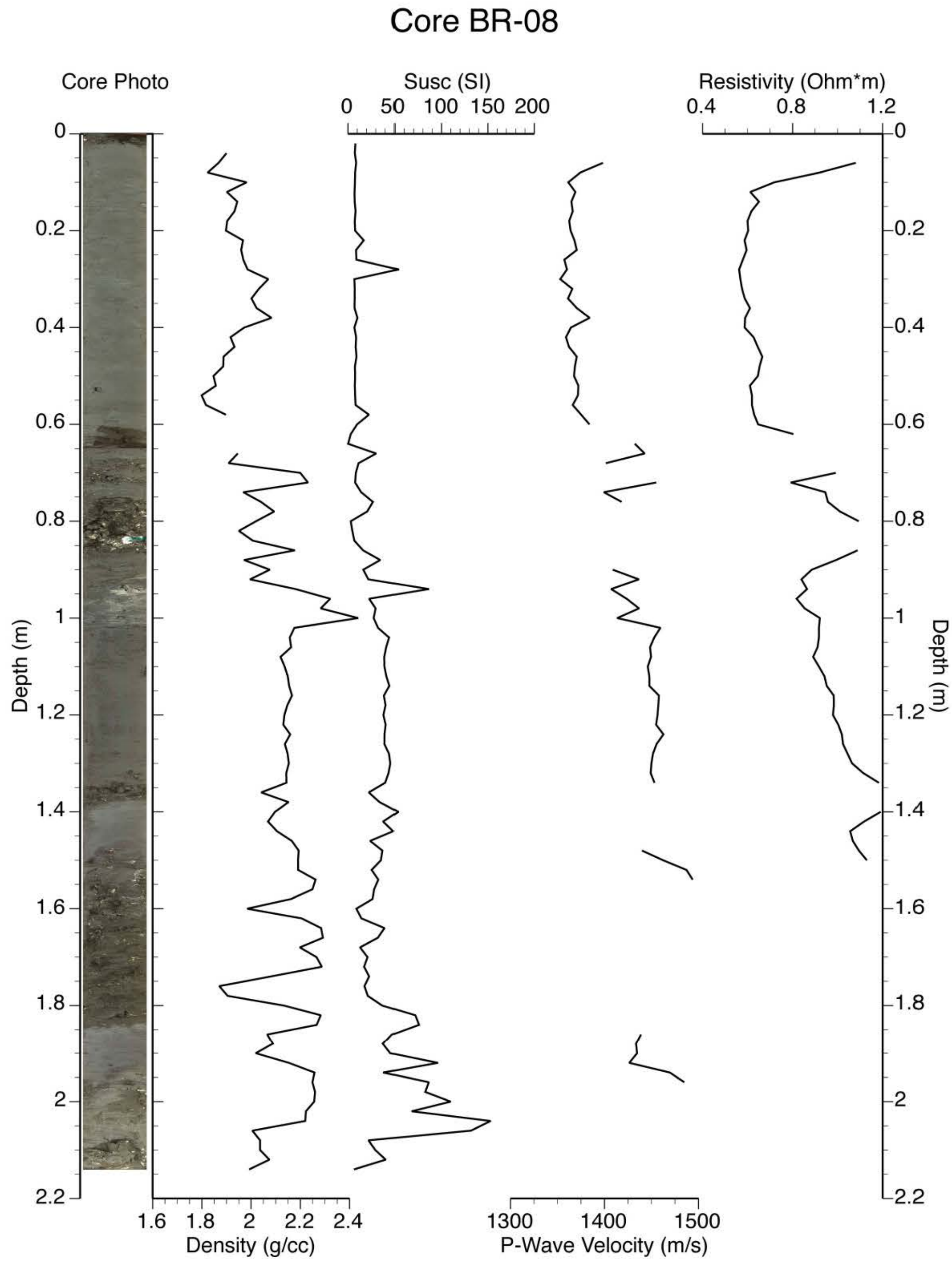

Figure F-1 b. Core logging results from core BR-08.

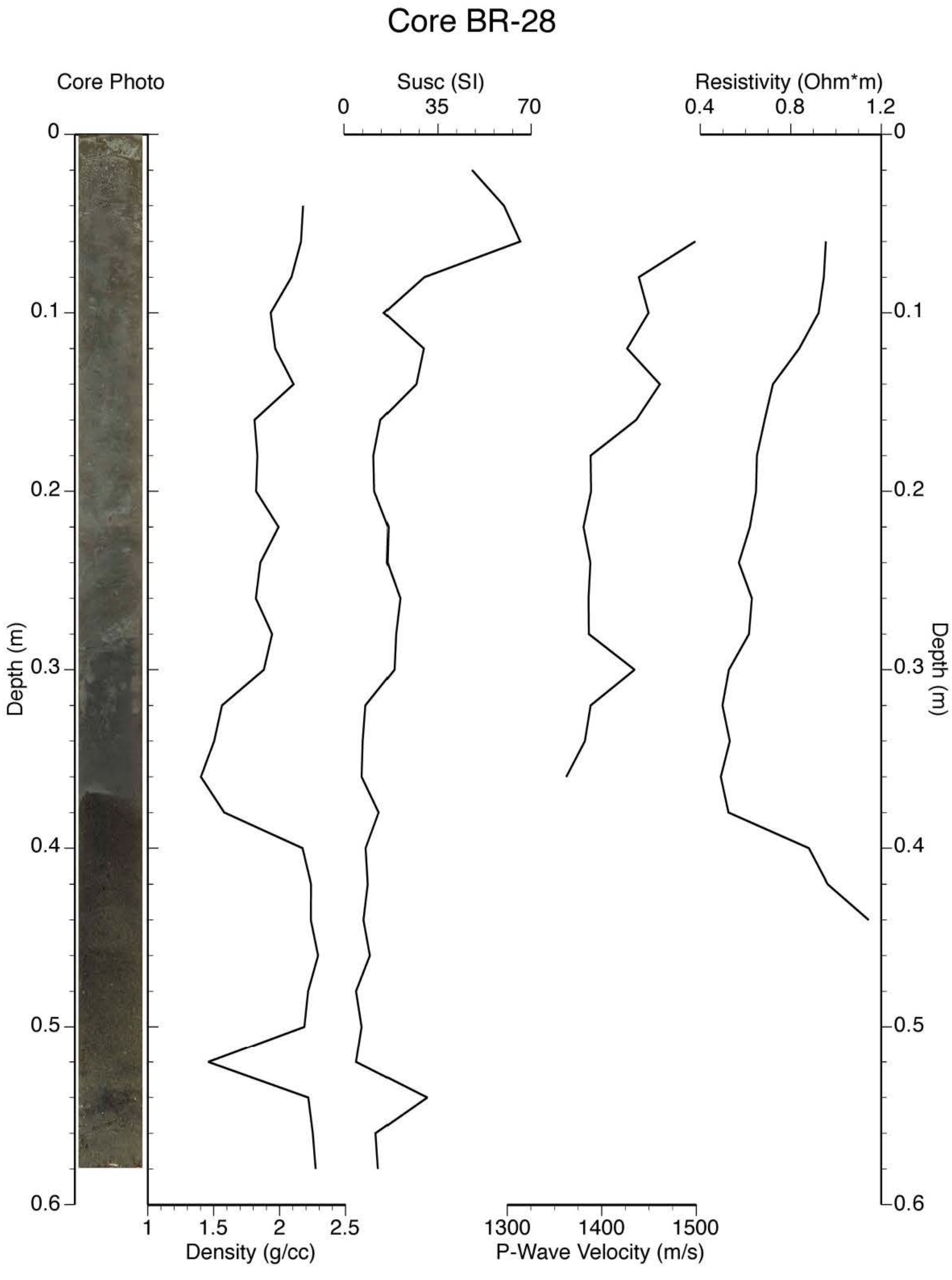

Figure F-1 c. Core logging results from core BR-28.

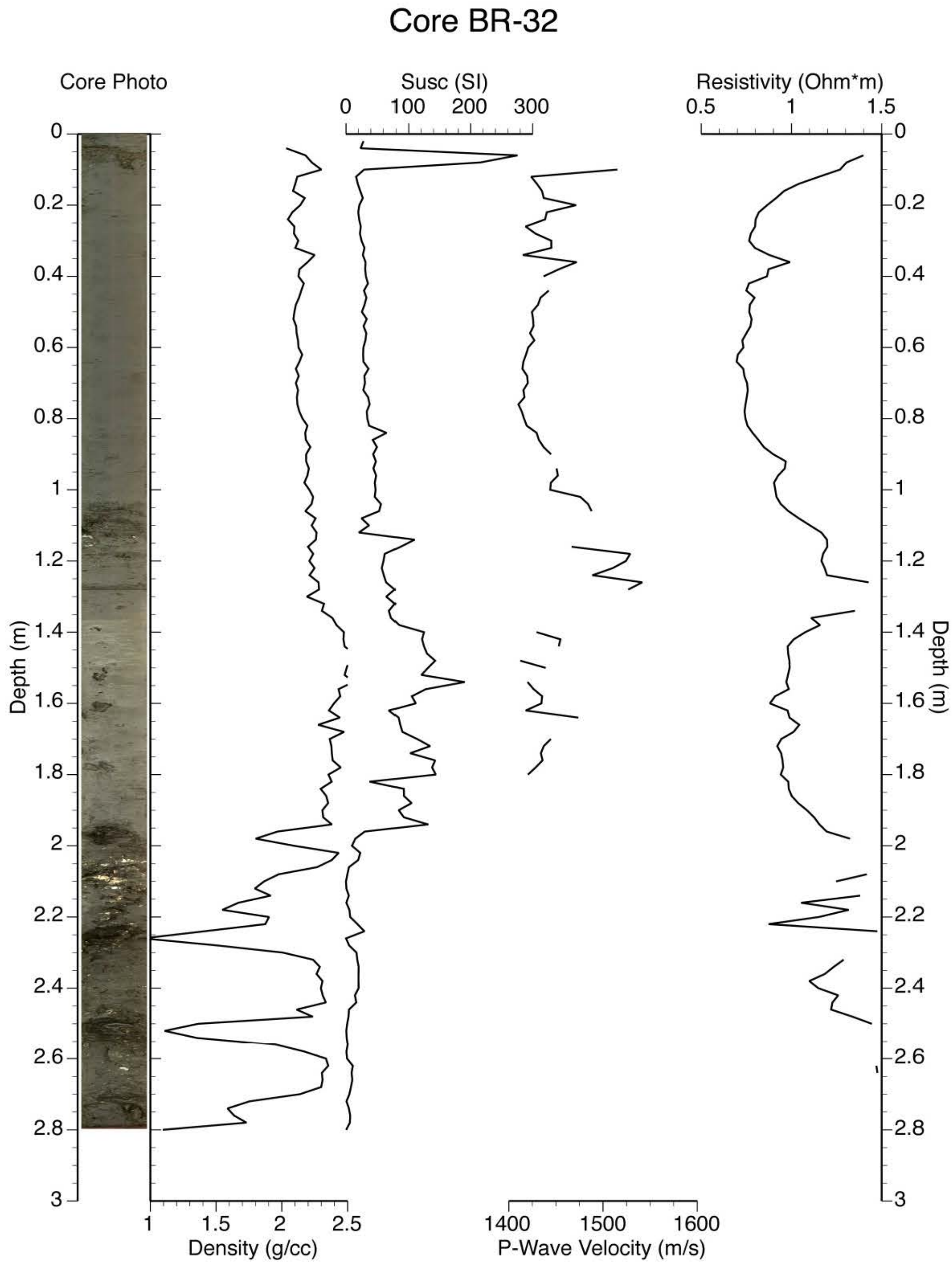

Figure F-1 d. Core logging results from core BR-32.

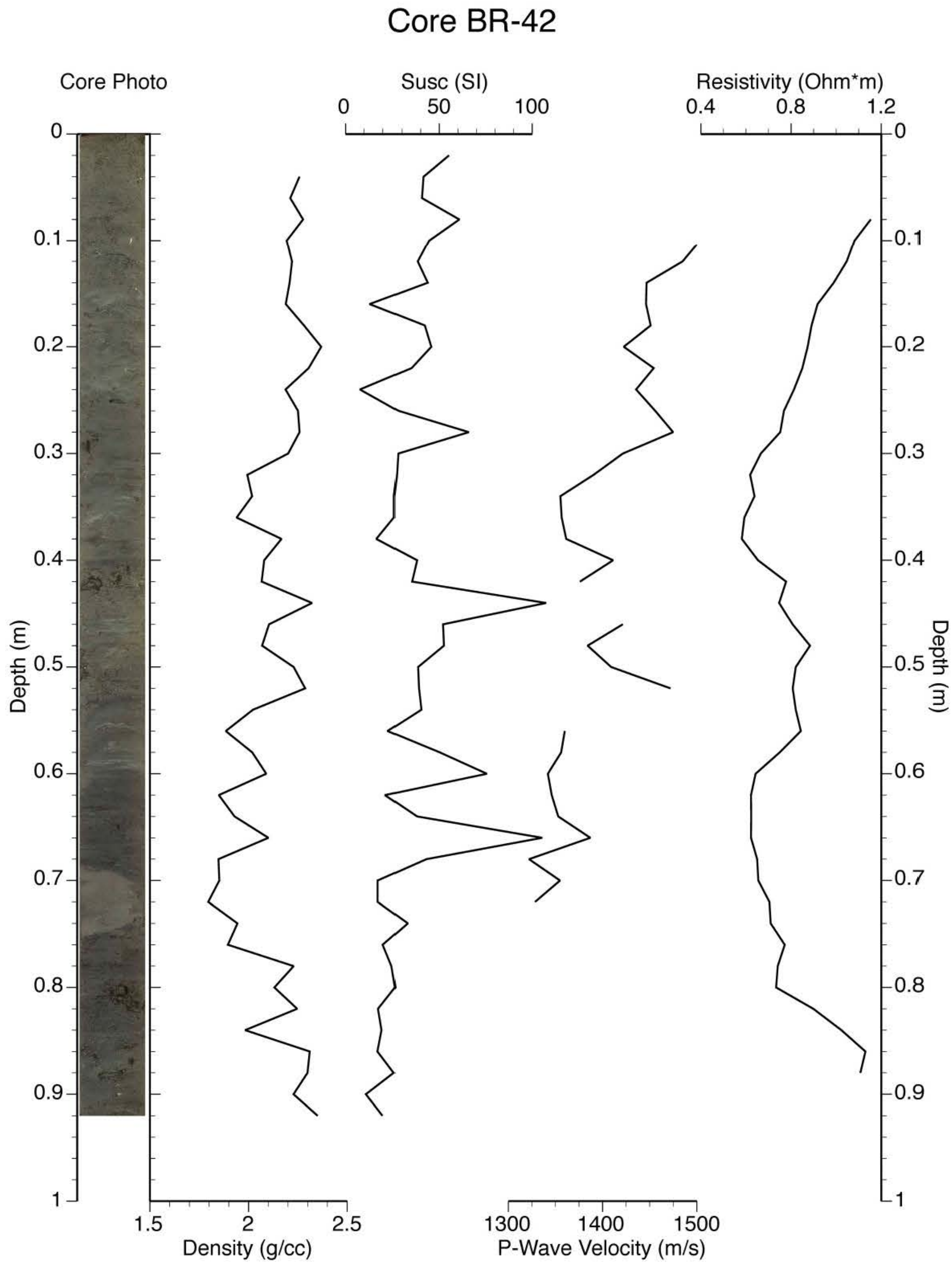

Figure F-1 e. Core logging results from core BR-42.

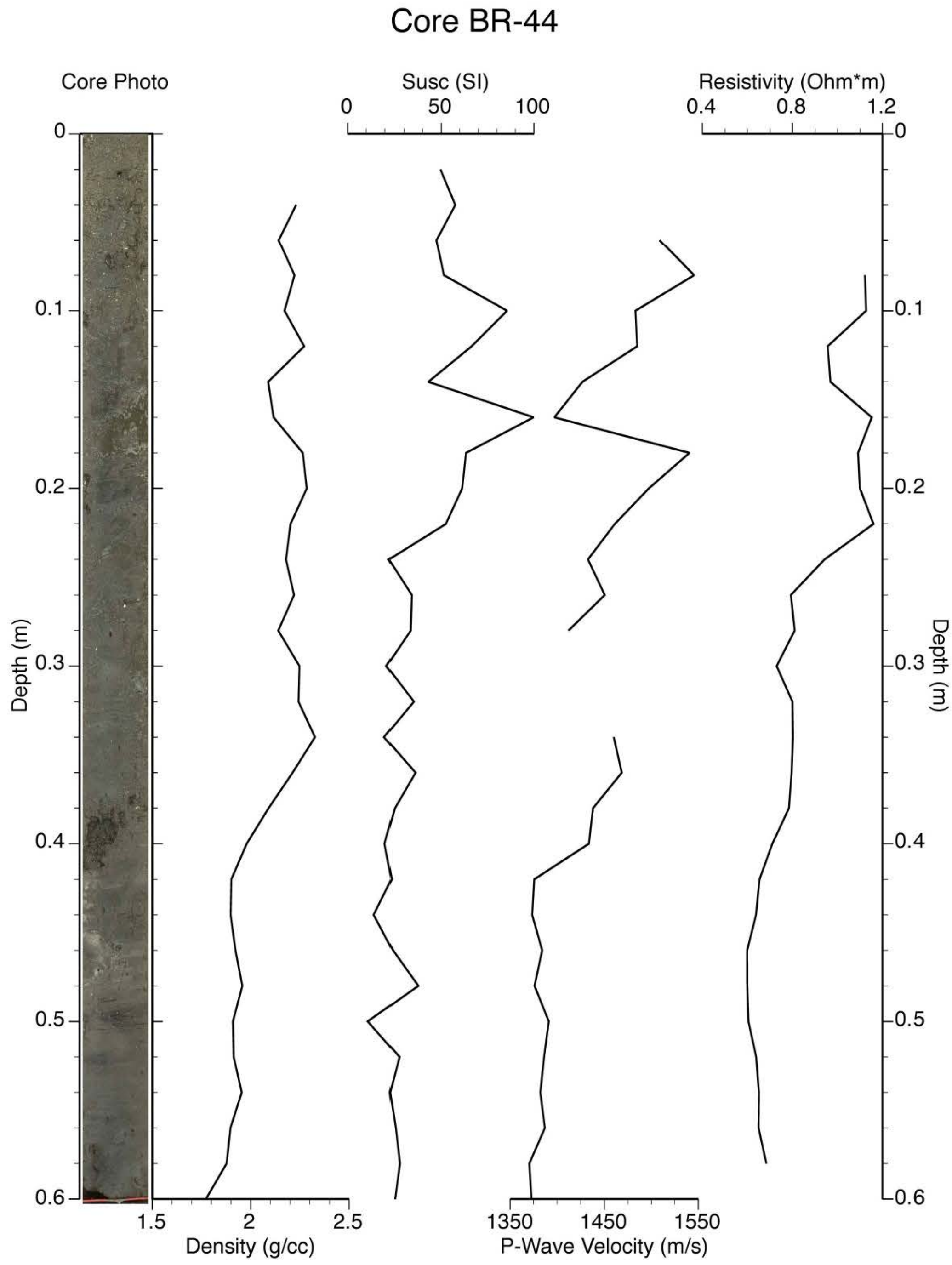

Figure F-1 f. Core logging results from core BR-44.

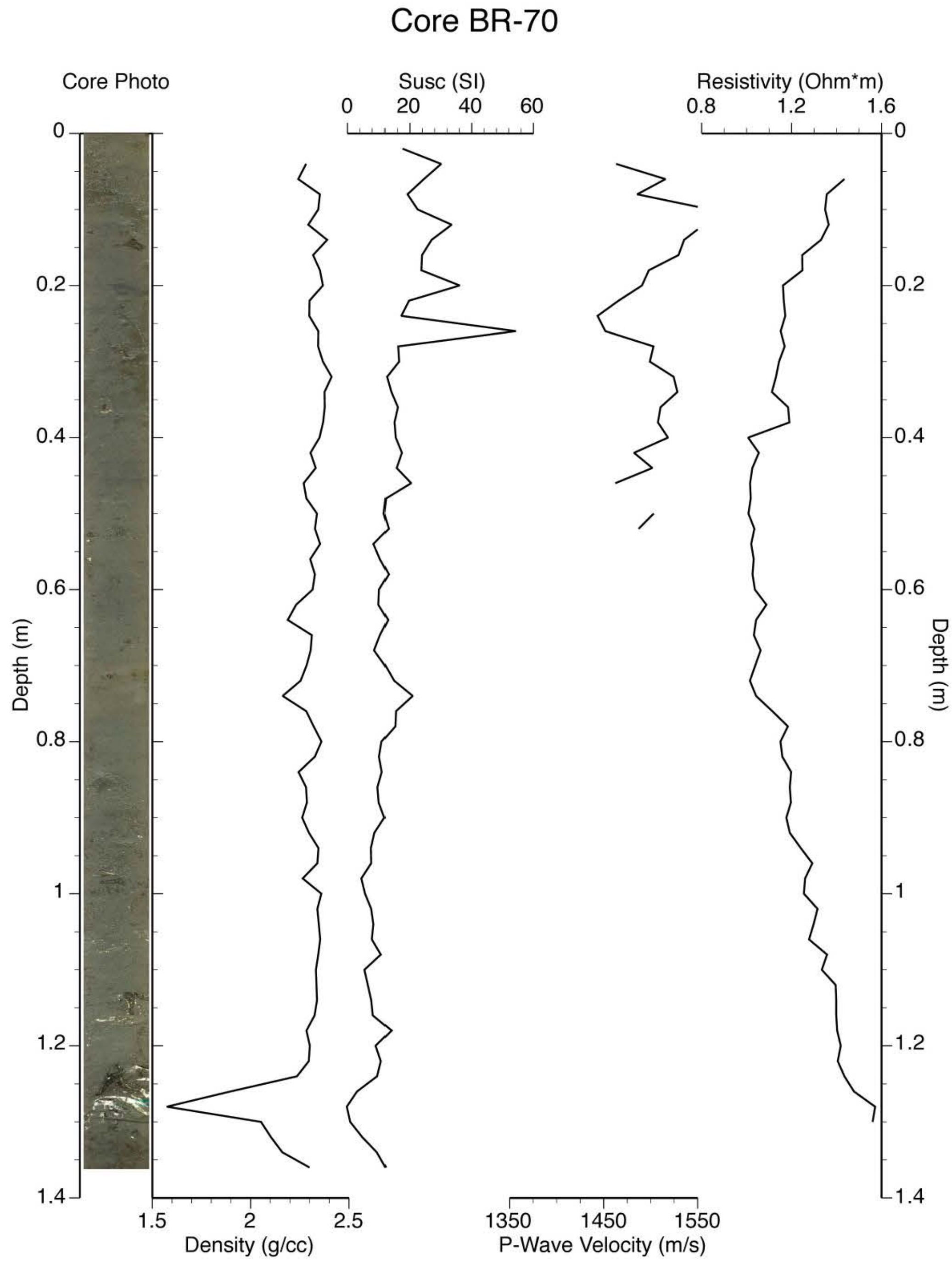

Figure F-1 g. Core logging results from core BR-70.

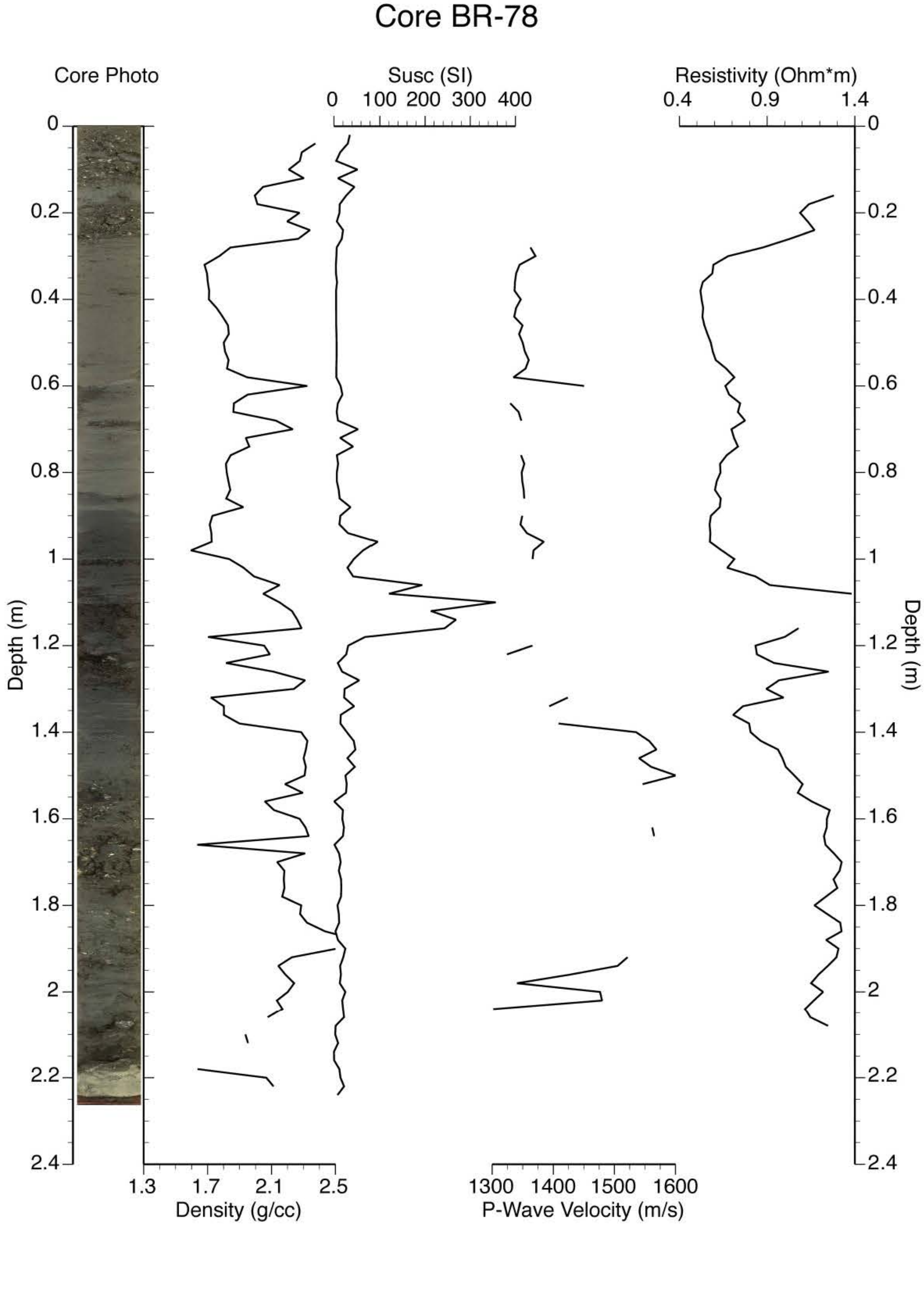

Figure F-1 h. Core logging results from core BR-78.

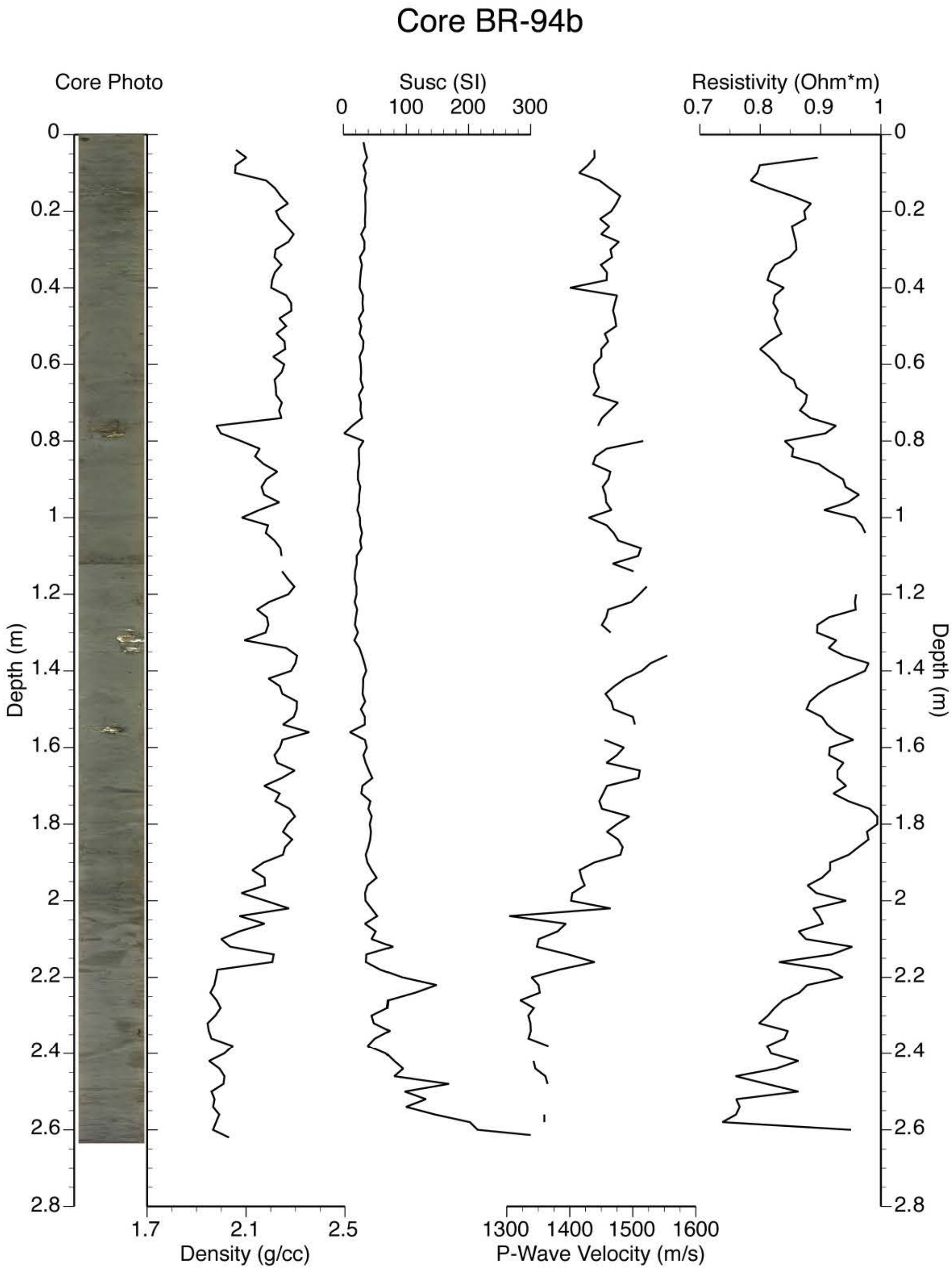

Figure F-1 i. Core logging results from core BR-94b.

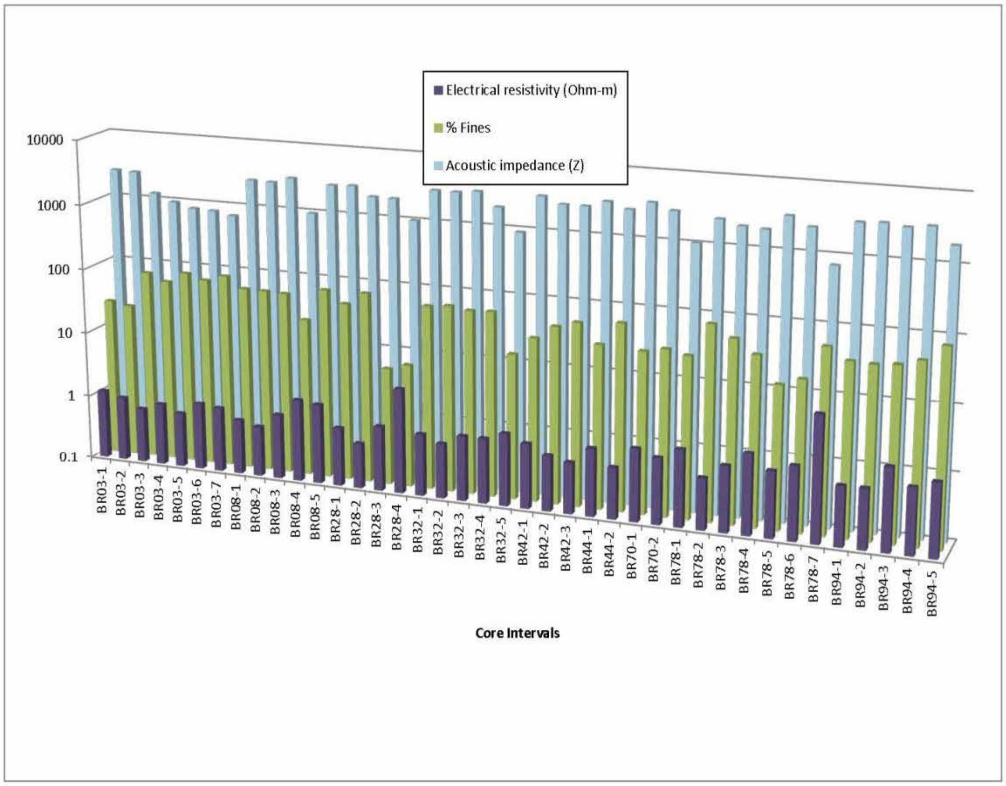

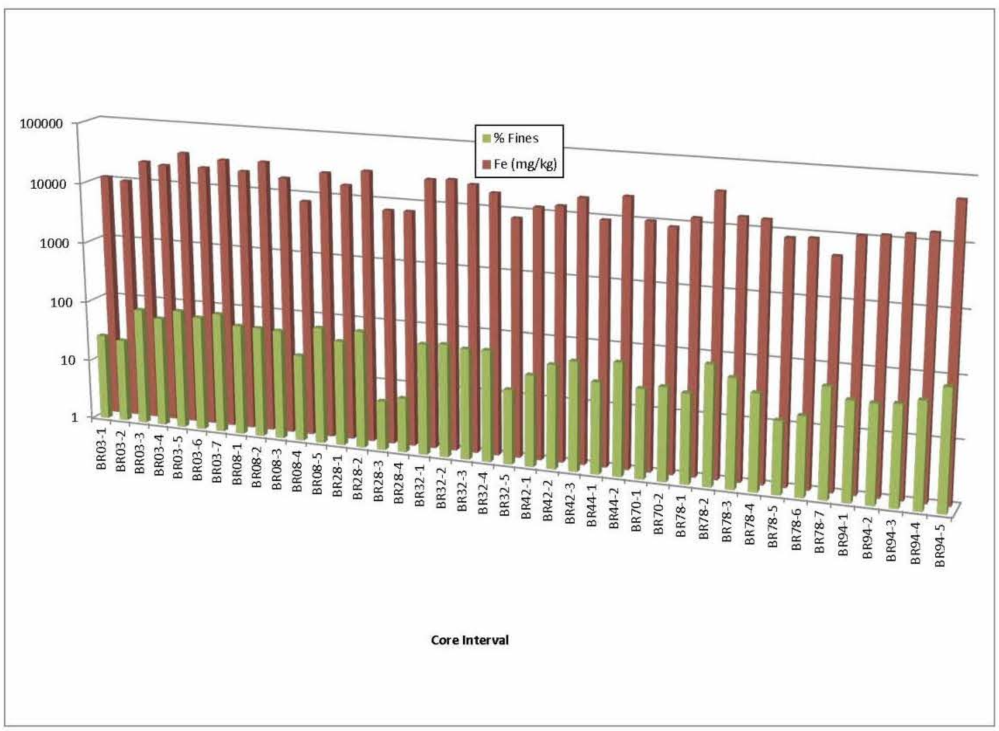

Figure F-2. a.Core logging results averaged by sediment sampling interval compared to percent fines from sample analysis. b. Percent fines compared to total iron (Fe) concentration from sample analysis.

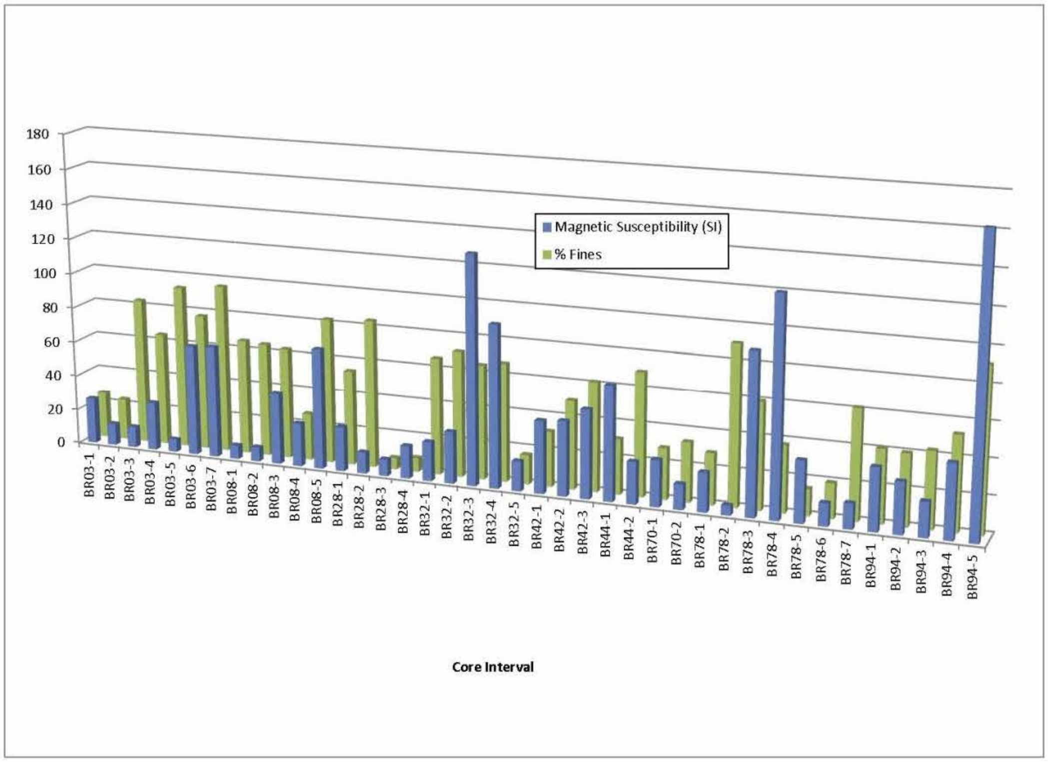

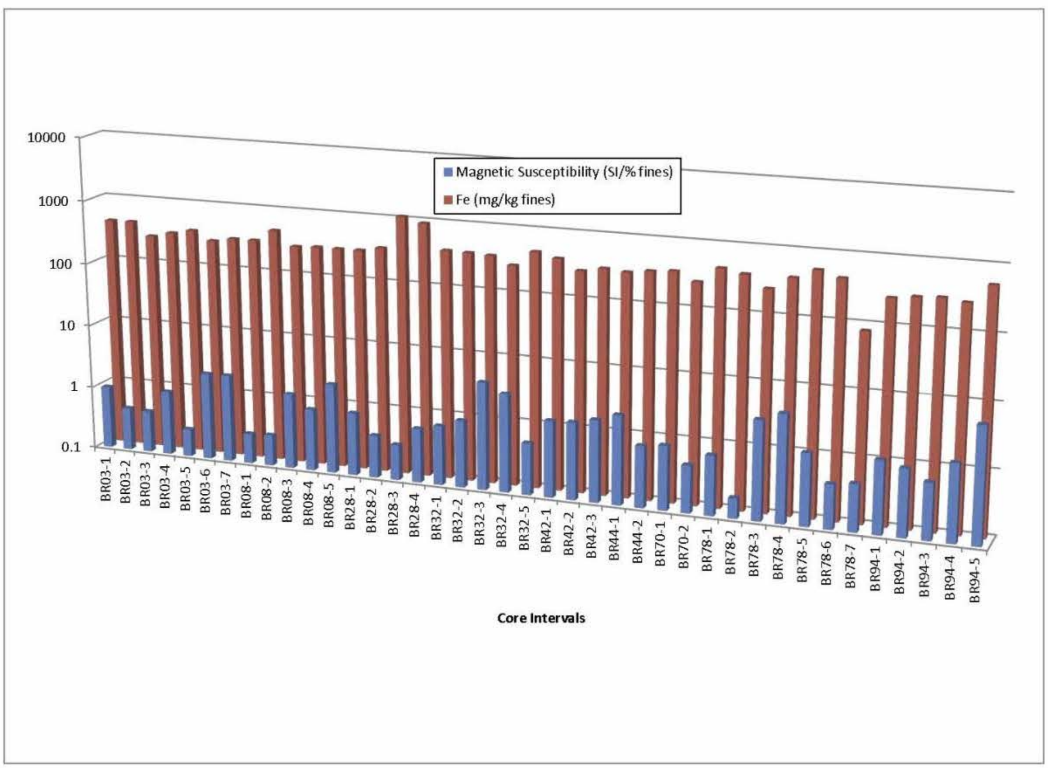

Figure F-3. a. Magnetic susceptibility results from core logging averaged by sample interval compared to percent fines. b. Magnetic susceptibility normalized to percent fines compared to iron (Fe) concentration normalized to fines.

APPENDIX G

SURFICIAL SEDIMENT ANALYSIS AND ACOUSTIC DATA PROCESSING

APPENDIX G
SURFICIAL SEDIMENT ANALYSIS AND ACOUSTIC DATA PROCESSING

LIST OF FIGURES

Facies Model Development

In order to resolve some of the complexity and provide a descriptive framework, nine facies were defined (Table 4-1) based on analysis of PUC and SPI images. The PUC images were typically 43 cm wide, whereas the SPI images provided a 15-cm wide sample of the PUC field of view. These imaging scales provided detail of the surface sediment type, degree of sorting, small bedforms, sediment layers, graded bedding and the presence or absence of larger shells or sediment particles on the surface (lag deposits). The variation between replicates may represent sampling across distinct sediment features (Figure G-1), but the features themselves were highly complex in three dimensions. Many coarse sediment layers were thin and patchy and underlain by burrowed silt; the presence of the silt might result in a lower backscatter response. At the sampling density and scale of the images it was not possible to accurately map the distribution of these facies, but the point distribution of facies could be compared with the patterns of backscatter derived from data processing.

Across the surface of the mound, there were small rises of various sizes and shapes. Many of these are characterized by moderate backscatter returns. Lower backscatter returns indicate some features of the surface are absorbing sound waves, and the returning signal to the transducer has less resulting energy. This is often the case with soft sediments such as silt or mud, but lower backscatter may also result from higher water content or relatively smooth surface features (low boundary roughness). One of the small rises on the mound, characterized by low backscatter, was sampled by SPI and plan-view (Station 45; Figure G-2). The surface sediments consisted of uneven, poorly sorted medium sand overlying burrowed silt. In contrast, a slight depression close to Station 45, also sampled by SPI and PUC, was characterized by relatively high backscatter (Station 62; Figure G-3). The surface sediments in the depression were a rough surface of large oyster shells and imbricated gravel and sand. If the simple relationship shown in these examples could be applied to backscatter distribution generally (coarse material = high backscatter; fine material = low backscatter), the patterns of the backscatter would be readily interpretable (Figure G-4). However, the complexity of these relationships required more extensive analysis.

Acoustic Backscatter Data Processing and Analysis Methods

As part of the effort to support evaluation of surficial sediment characteristics at the BRDS mound additional acoustic backscatter data processing and analysis were performed beyond that described in Section 2.3.3.

After side-scan data were processed into a mosaic with GeoCoder, QTC Sideview software was used to analyze the mosaicked backscatter data. QTC Sideview is an image-based backscatter analysis program which attempts to identify and map acoustically similar classes of seafloor. Digital sonar data were first converted to images which were rectified for beam spreading and signal attenuation. The contrast (gray-scale shading) variations in side-scan images are presumed by Sideview to be due to variations in backscatter and seafloor composition. Sideview divided the sonar image for each transect into a grid of rectangular small patches, approximately 12 m across-track and 8.5 m along-track (65 samples × 17 pings), then conducted statistical evaluation of the data within each patch to reduce data to acoustic "features". Calculated statistics/metrics included gray-level co-occurrence matrices; basic descriptive statistics (mean, maximum, standard deviation, etc.); quantile and histogram; Fast Fourier Transforms (FFTs); ratios based on power spectra (Pace and Gao 1988); and fractal dimension. These features were next evaluated using multivariate statistical processing, and the three dominant components were selected by Sideview. These components (termed Q1, Q2, and Q3) were plotted in three-dimensional "Q-Space" with one axis for each of the three components. Seabed types with similar acoustic properties will occupy a similar Q-space due to similar Q-values. Bayesian statistics (iterative numerical hypothesis testing) were used to isolate clusters of similar signals. Clusters were assigned to "classes" which possessed similar acoustic characteristics. Points nearest each cluster were attributed with the class value of the cluster, as well as with a statistical description of each point's separation from the center of its cluster. Because all of the points used in the analysis were associated with positioning information from the survey vessel's DGPS, the classified points could be assigned real-world coordinates, allowing geographic analysis of the distribution of acoustically similar regions of the seabed.

The database of classified points was used to create a map of seabed classes using QTC CLAMS interpolation software. This software uses the frequency distribution of classes surrounding a grid node when assigning each node to a class. Gridded data were exported from CLAMS in a format suitable for import and manipulation using Golden Software's Surfer® software. Surfer® was used to assign colors to classes and to merge QTC data with other layers of interest (e.g., bathymetry, backscatter). Maps were then exported as georeferenced TIFs and polyline DXF files for scaling and analysis using ESRI ArcGIS software.

Backscatter data from the MBES was further evaluated using IDRISI processing software in order to identify gray-scale patterns which might not be easily distinguished by visual inspection. Because pixel values exported from GeoCoder are representations of seafloor backscatter (and presumably composition), multivariate clustering of pixel values should generate a map which identifies similar seabed textures based on backscatter similarity and distribution. A K-means clustering algorithm was selected due to high processing efficiency of large images relative to other methods. The K-means process randomly ""seeds" " the image with a number of cluster centroids which is assigned based on existing knowledge of the data. Pixels are then assigned to the nearest randomly ""seeded" " cluster centroid, the position of which is iteratively re-calculated based on the added data points.

The mosaic created using GeoCoder was first passed through a low-pass Gaussian filter to minimize fine-scale acoustic artifacts unrelated to seabed composition. The filtered mosaic was then evaluated using a histogram analysis algorithm to estimate the maximum number of distinct gray-scale clusters which might be reasonably be present. IDRISI's K-means clustering routine was applied to the mosaic specifying: a maximum of 16 clusters; 50 iterations; termination when the percentage of migrating pixels was less than or equal to 1- percent; and fusion of clusters with proportions less than or equal to 2-percent.

Results of Acoustic Backscatter Data Processing and Analysis

The backscatter was processed in a variety of ways to reduce its complexity and provide a means to compare it with the visual information. The results of classification routines (QTC, dB binning, K-means) were compared to facies distribution and individual SPI physical parameters (Figures F-1, F-2, F-3). The QTC approach placed ranges of backscatter distributions into a small number of classes and was more successful in delineating broad distributions of sediments than other classifying routines (Figure G-5). The patterns do not match the medium-scale sediment transport patterns (20-100 m) but they do identify the top of the mound and alternating areas of high and low backscatter without a "noisy" distribution. Grouping the backscatter into simple dB ranges produced an image with many of the medium-scale features delineated but does have a lot of small scale noise (Figure G-6).

The K-means grouping of backscatter intensity had no intrinsic meaning but seemed to bridge the scales of QTC and simple binning (Figure G-7).

The distribution of the facies, which is simply a descriptive classification of imaging results into process classes, demonstrated that the sediment transport activities were most pronounced over the south slope and top of the mound (Figure G-8). Lag deposits, shell windrows, and gravel dominated the southern edge of the mound while transgressive sands and gravels were clustered on the top of the mound and between shell windrows and reverse- graded gravels along the northern margin of the mound. Burrowed silts surrounded the mound and mound margins and were intermixed with thin lag deposits on silt and thin sand layers.

When these facies classes are compared to the K-means classes, the relationships are difficult to discern (Figure G-9). Because the variation in sediment characteristics occurs on such small scales, even the finely textured K-means grouping of backscatter displays very small patches of hard and soft returns within a larger pattern. The facies are based on 15-cm wide slices of the seafloor which are much smaller than the patches of processed backscatter data. In addition the exact location of the SPI and PUC images may vary by as much as 10-15 m (location based on vessel position not camera) making integration of small units very difficult. Looking in detail at the grain size distribution to K-means classes (Figure G-10) suggests that the harder backscatter returns could be associated with the coarse sediments and the softer backscatter returns associated with the finer sediments.

The facies classes were clustered with QTC CLAMS interpolation software. The CLAMS routine used the frequency distribution of each classified replicate to create a grid of classes. The facies classes were reduced to eight groups and exported to Surfer for generation of a map that could be projected onto the bathymetry and backscatter images (Figure G-11). The clustering of similar facies classes helps to visualize the medium-scale sediment transport patterns. The depositional silt horizons surround the mound. Patches of lag alternate with shell windrow and reverse-graded gravel surrounding the transgressive sand and sand/gravel on the highest part of the mound. Two patches of transgressive sand lie shoreward of a patch of lag. Lag overlying silt clusters at the shoreward side of the mound. These clustered results are highly dependent on the spacing of the SPI stations but they provide some indication of the variation in energy and sediment types across the mound. These results are comparable in scale but not the same as the QTC backscatter classification (Figure G-12).

Table G-1.

Summary Sediment Data Based on Analysis of Sediment Profile (SPI) and Plan-view Underwater Camera (PUC) Images

Sedimentary Environment	Facies	Surface Sediment	Bedforms	Sediment texture	Camera penetration	Example station	Frequency
Depositional	Burrowed silt	Very pale brown to gray fine sandy silt to Very pale brown to olive gray silt/clay	Burrows, mounds, tubes	Highly bioturbated, some fine sand mixed in surface layer	Good penetration by SPI camera	97-B	65
Reworking	Sandy silt	Fine sandy silt, with slight concentration of fine sand at SWI	Burrows, mounds, tubes, ripples, protruding tubes	Increased proportion of sand in upper sediment column, not sorted or layered	Good penetration by SPI camera	33-C	50
Reworking	Hard mixed sand/silt	Very pale brown to light gray silty sand, shell fragments	Burrows, mounds, tubes, ripples, no gravel visible	Bioturbated silty sand overlying silt, no defined layer	Poor penetration by SPI camera	44-B	8
Reworking or bedload transport	Transgressive sand	Very pale brown, well-sorted, medium to coarse sand	Sand ripples, burrows, tracks	Well -defined layer of well-sorted sand over silt	Poor to moderate penetration by SPI camera	02-A	17
Reworking or bedload transport	Transgressive sand and gravel	Very pale brown, well-sorted, medium to coarse sand with gravel and shells	Sand ripples, burrows, tracks, gravel ribbons	Well-defined layer of gravel and sorted sand over silt	Poor penetration by SPI camera	04-B	16
Erosion or nondeposition	Lag on silt	Very pale brown to light gray gravelly shelly sandy silt	Gravel, burrows, ripples	Lag deposit (gravel and shell) over silt	Poor to moderate penetration by SPI camera	30-A	12

Table G-1., continued

Summary Sediment Data Based on Analysis of Sediment Profile (SPI) and Plan-view Underwater Camera (PUC) Images

Sedimentary Environment	Facies	Surface Sediment	Bedforms	Sediment texture	Camera penetration	Example station	Frequency
Erosion or non-deposition	Lag	Very pale brown medium to coarse gravelly sand	Gravel pavement, scattered gravel, and shells	Lag deposit; not enough penetration to see substrate	Poor penetration by SPI camera	46-A (SPI) 47-A (PUC)	19
Erosion or nondeposition	Reverse graded gravel	Very pale brown, firm, reverse-graded, gravelly very coarse sand	Gravel pavement, scattered gravel, and coarse sand	Reverse-graded gravel to fine gravel to coarse sand to medium sand	Poor penetration by SPI camera	60-C (SPI) 9-A (PUC)	13
Erosion or nondeposition	Shell windrow	Shells and Very pale brown poorly sorted medium to coarse sand	Large weathered oysters and quahogs in lines or rows separated by burrowed sand or silt	Poorly sorted to well-sorted coarse sand and shell hash over gray silt	Poor to moderate penetration by SPI camera	50-A 50-C	5
Erosion or nondeposition	Shell windrow and gravel	Shells and Very pale brown poorly sorted medium to coarse sand	Large weathered oysters, quahogs, and gravel in lines or rows separated by burrowed sand or silt	Poorly sorted to well-sorted coarse gravelly sand and shell hash over gray silt	Poor to moderate penetration by SPI camera	36-A	15

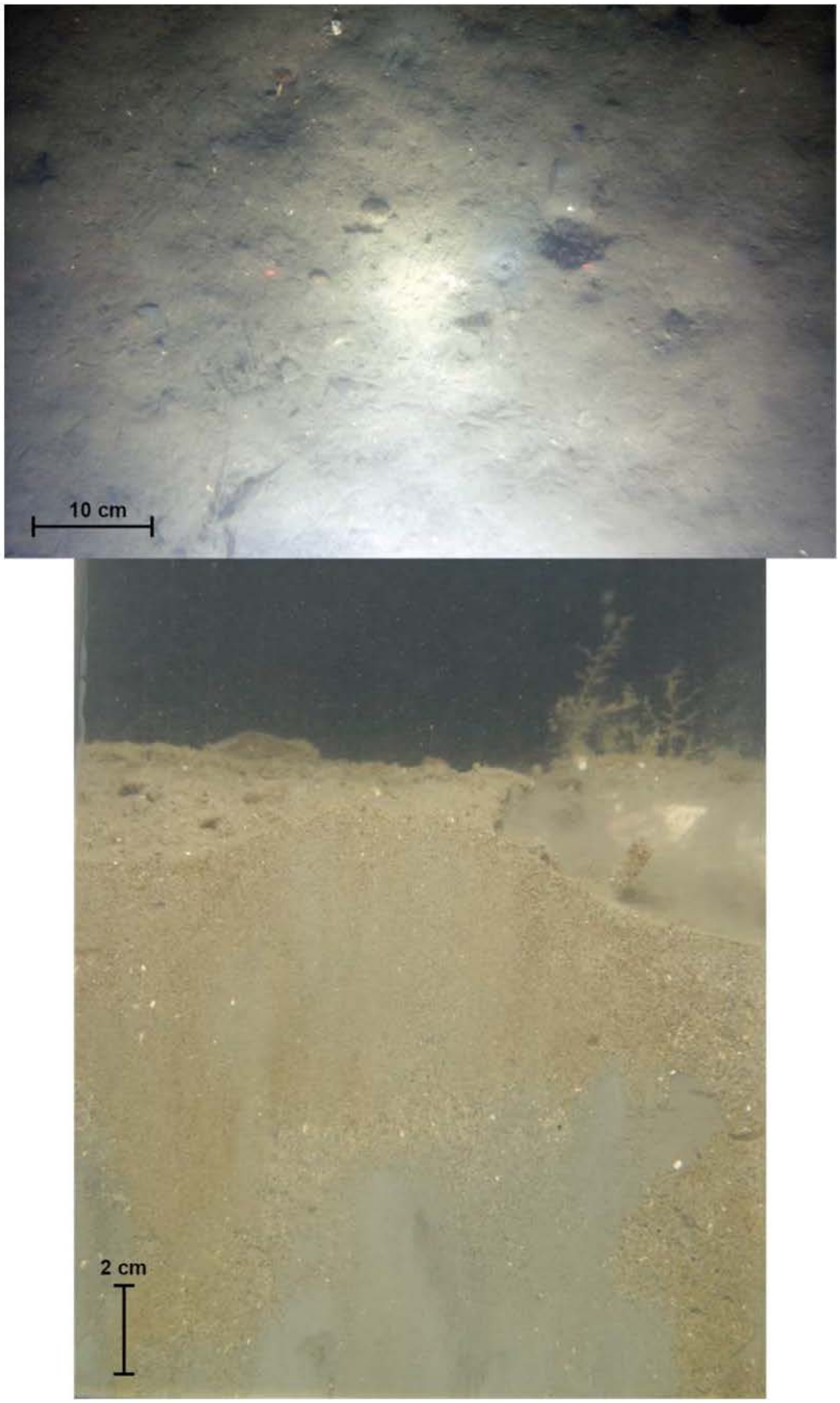

Figure G-1. Texture of surface features and subsurface sediment composition from Station 45 representative of a low backscatter region on a low rise on top of the disposal mound.

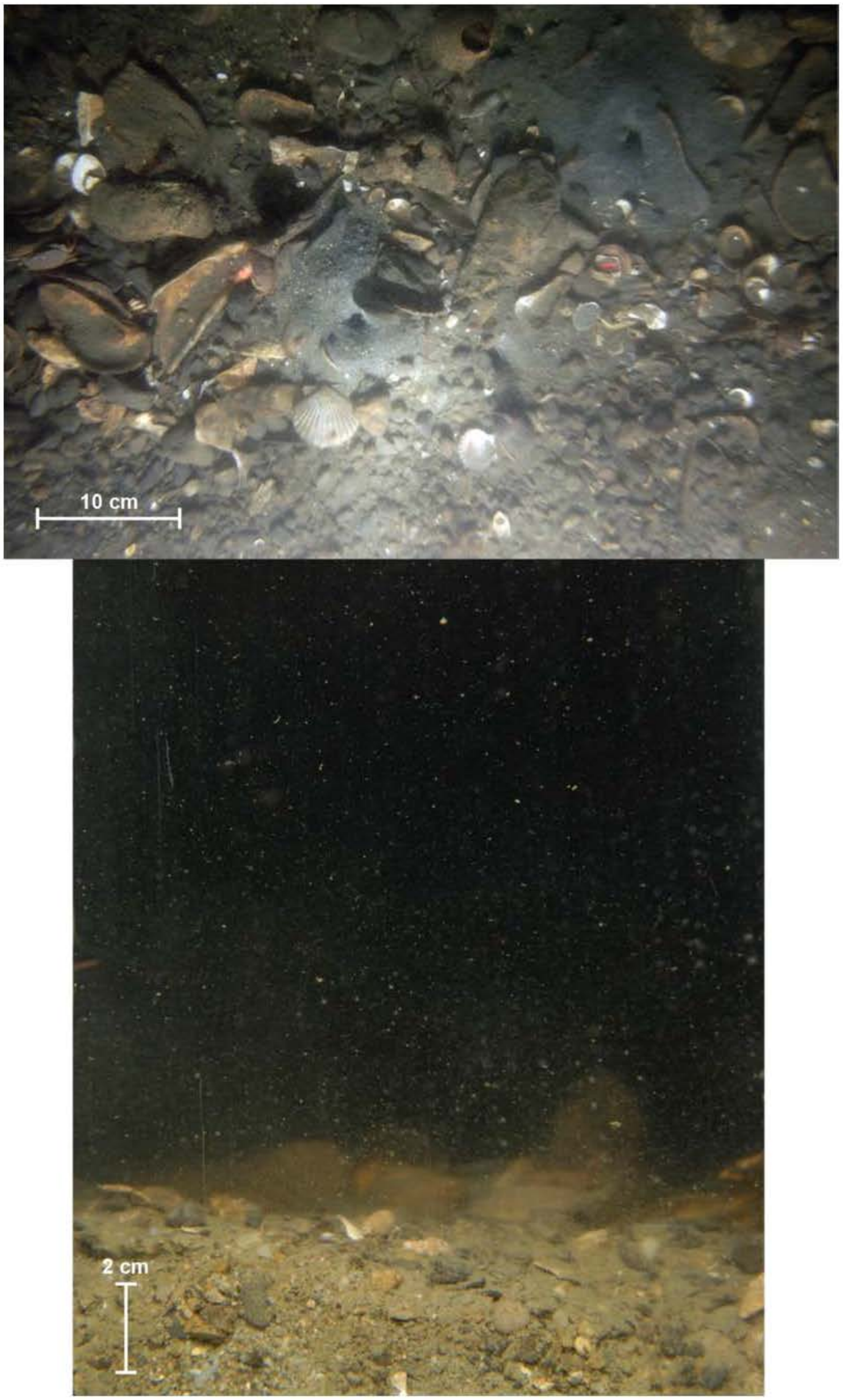

Figure G-2. Texture of surface features and subsurface sediment composition from Station 62 representative of a high backscatter region in a depression on top of the disposal mound.

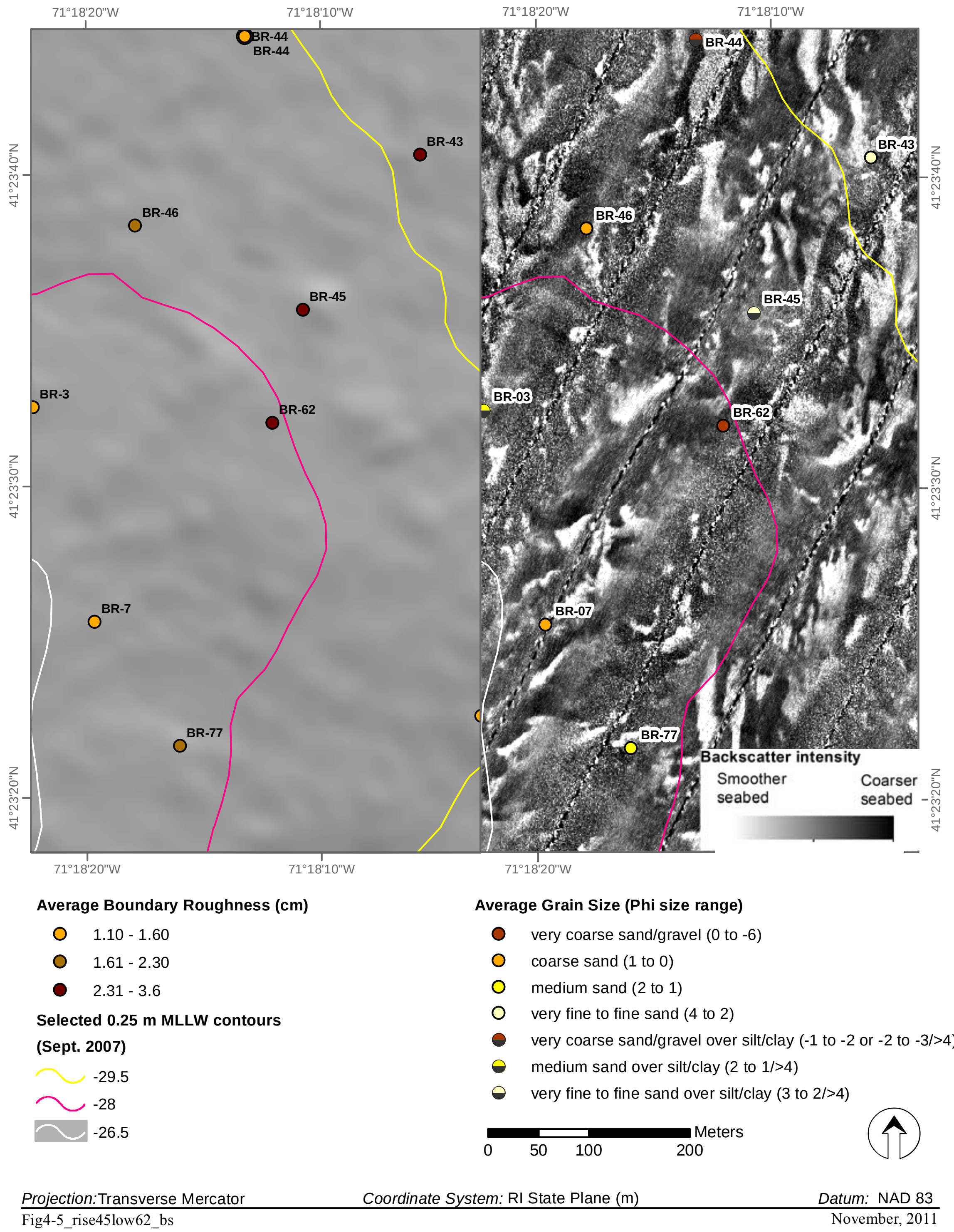

Figure G-3. Topography (left) and backscatter (right) over the top of the Brenton Reef Disposal Mound in the vicinity of Stations 45 and 62.

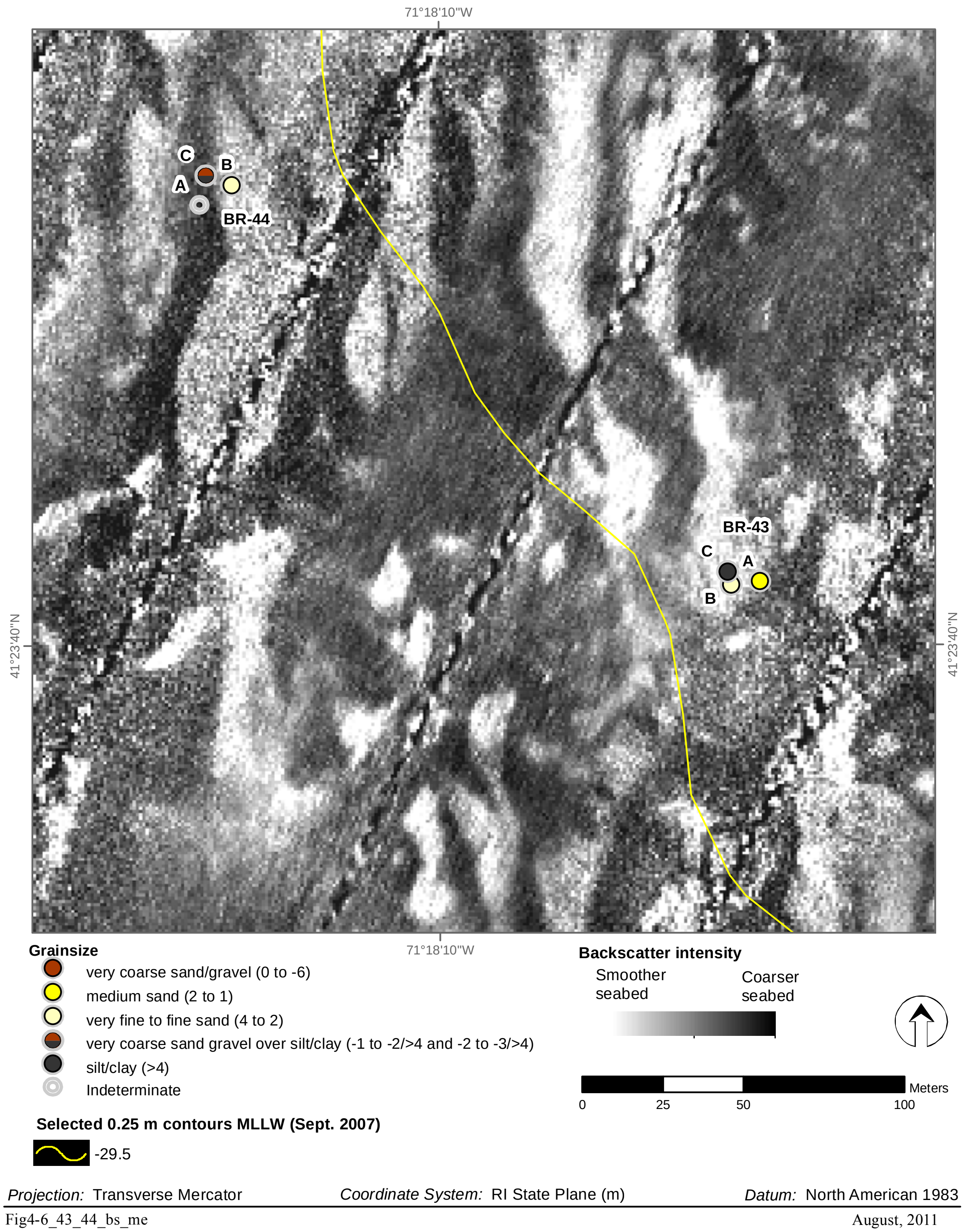

Figure G-4. Grain size results for individual replicates compared to backscatter patterns on the historical disposal mound. Station 44 had two replicates in high backscatter and one in low patchy backscatter. Station 43 had two replicates in low backscatter and one in higher backscatter. Compare to Figure 3-18.

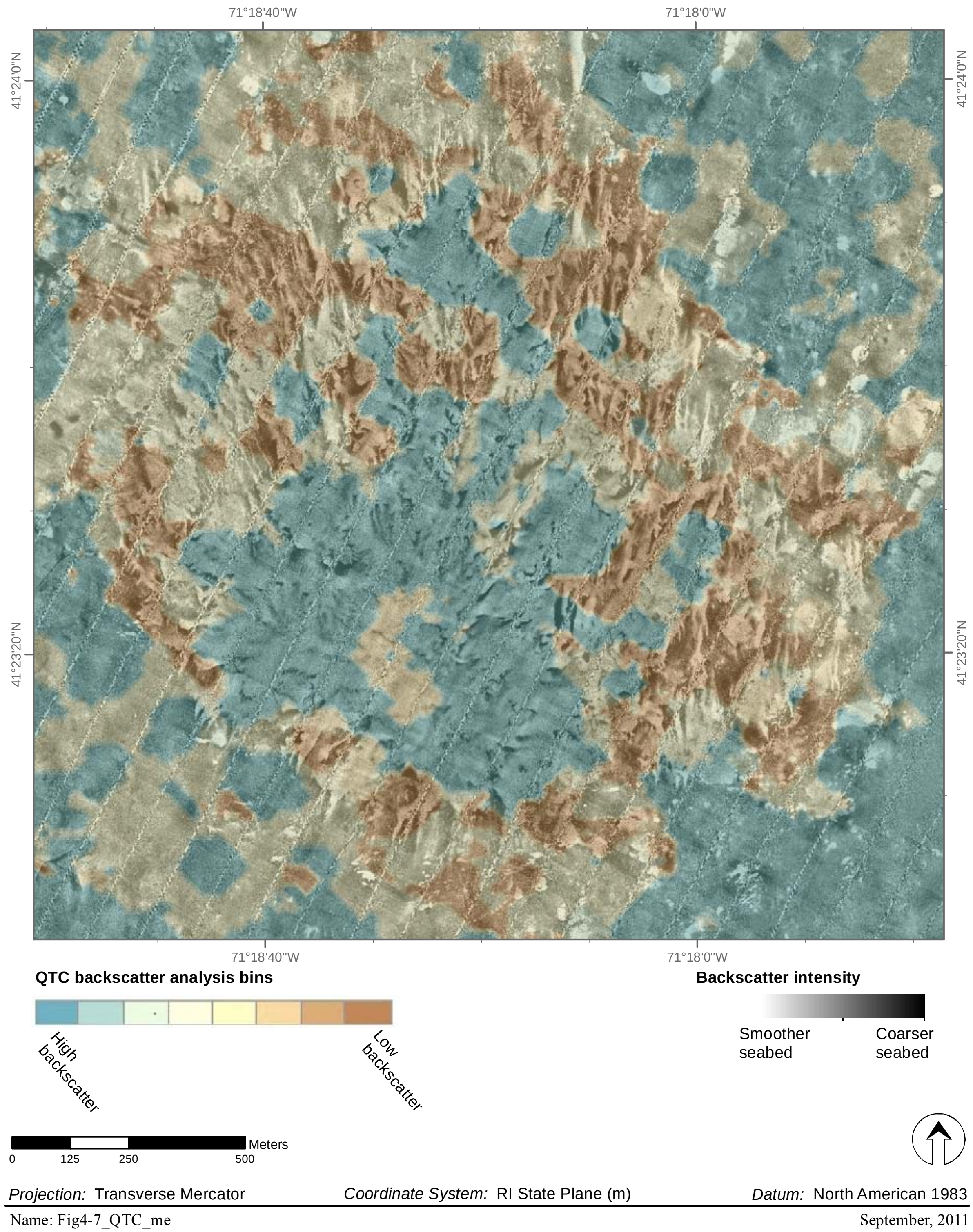

Figure G-5. QTC classification of backscatter at Brenton Reef Disposal Site draped over backscatter intensity.

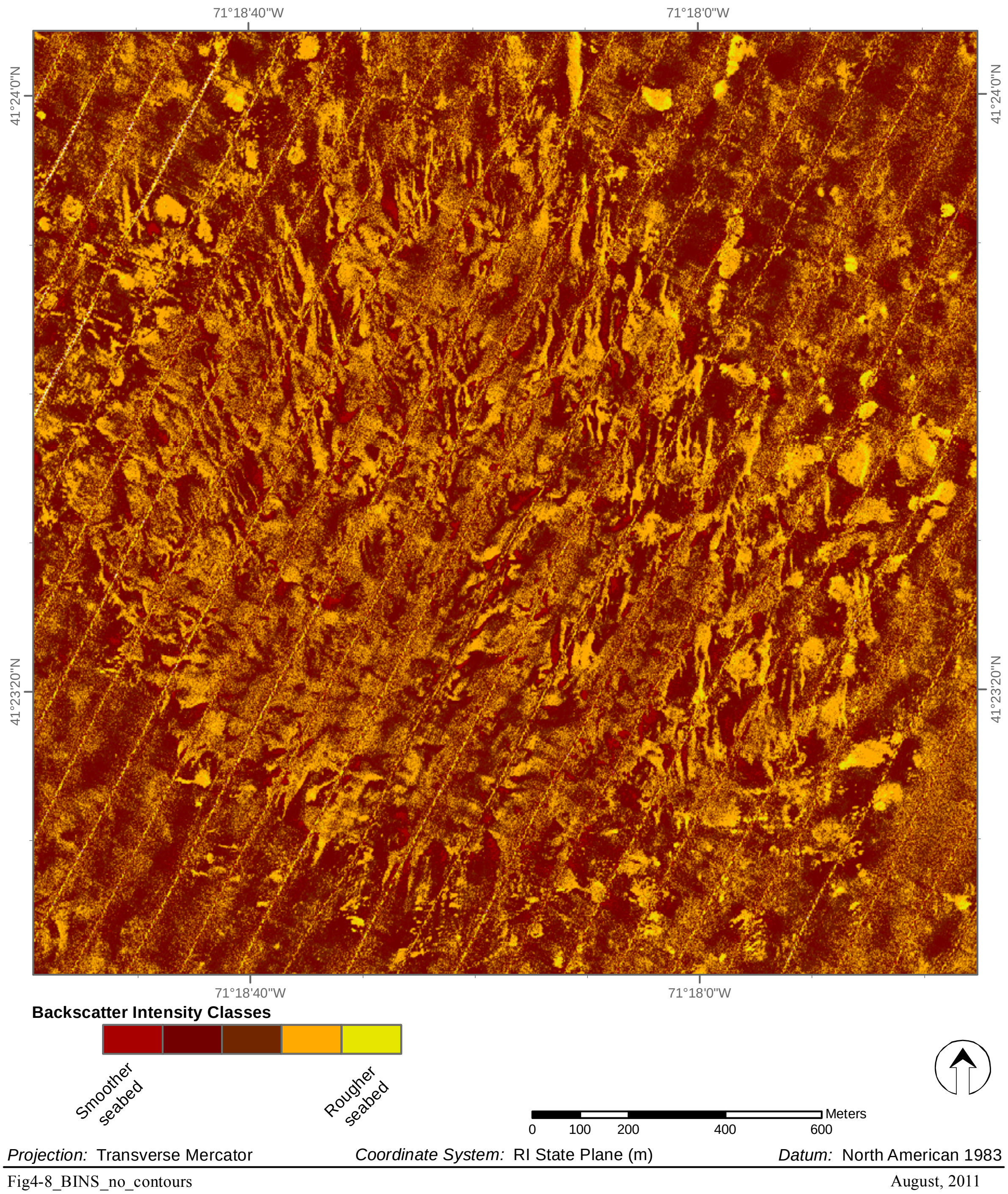

Figure G-6. Grouping of backscatter intensity at Brenton Reef Disposal Site into ranges.

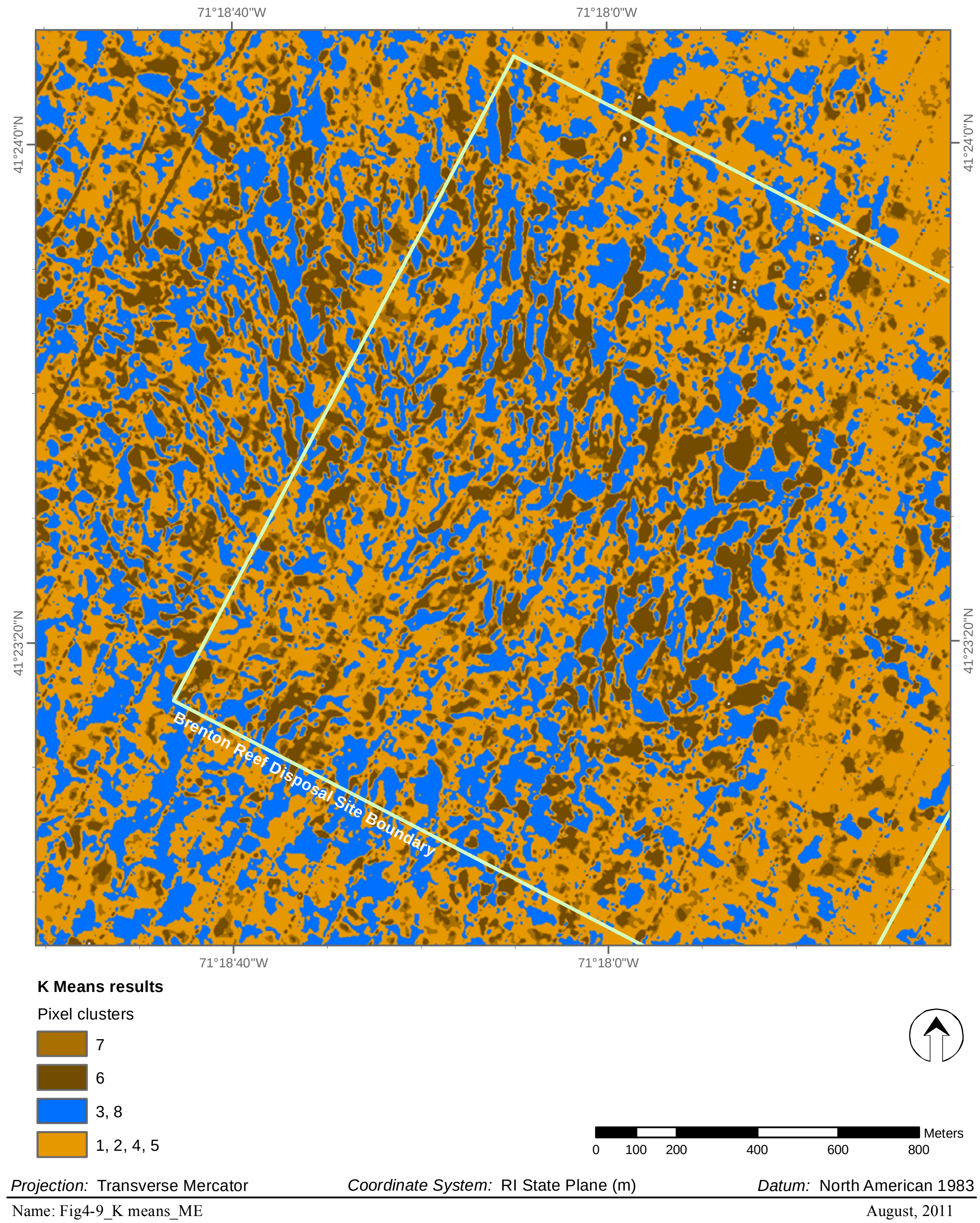

Figure G-7. K-means classification of backscatter intensity at Brenton Reef Disposal Site.

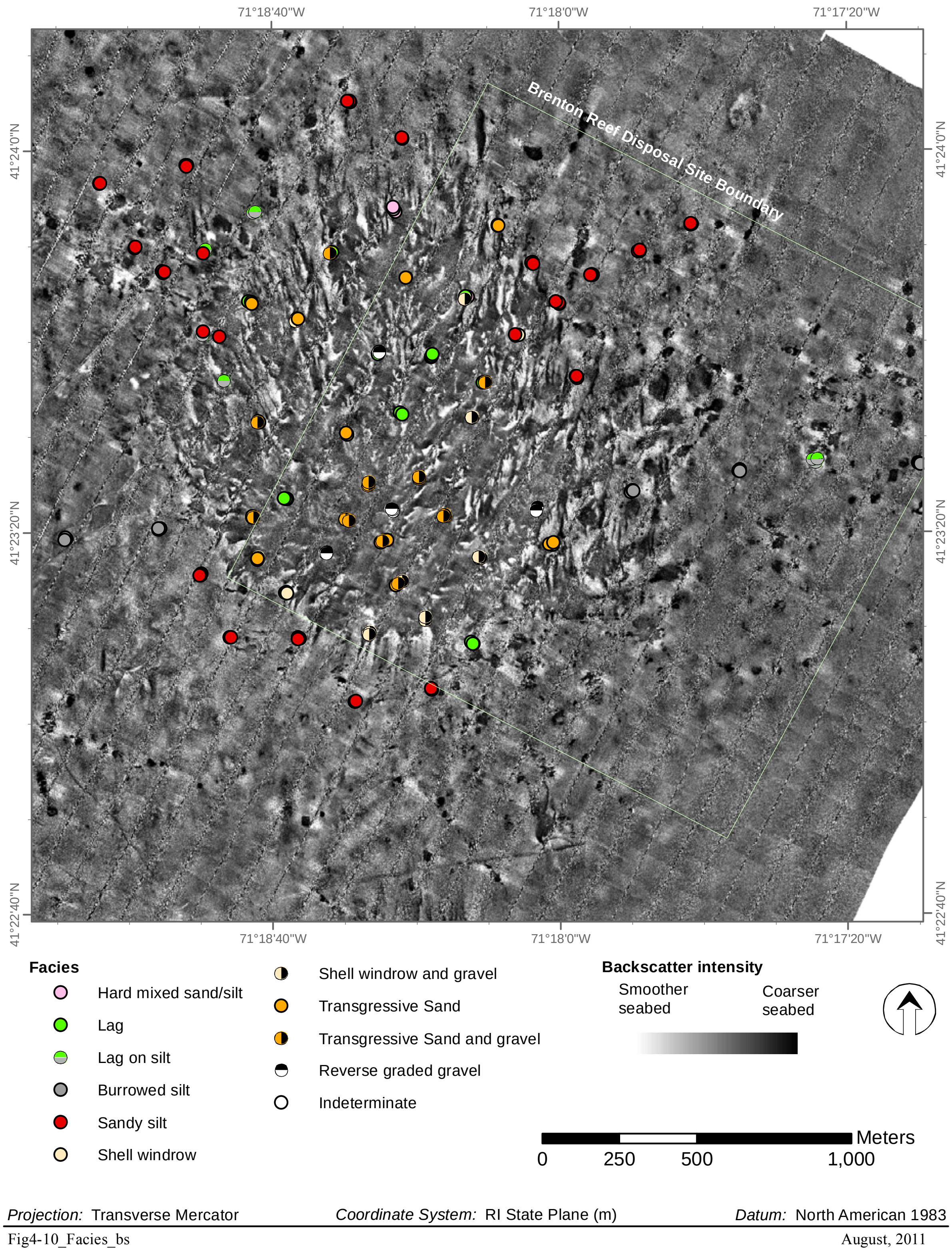

Figure G-8. K-means classification of backscatter intensity at Brenton Reef Disposal Site.

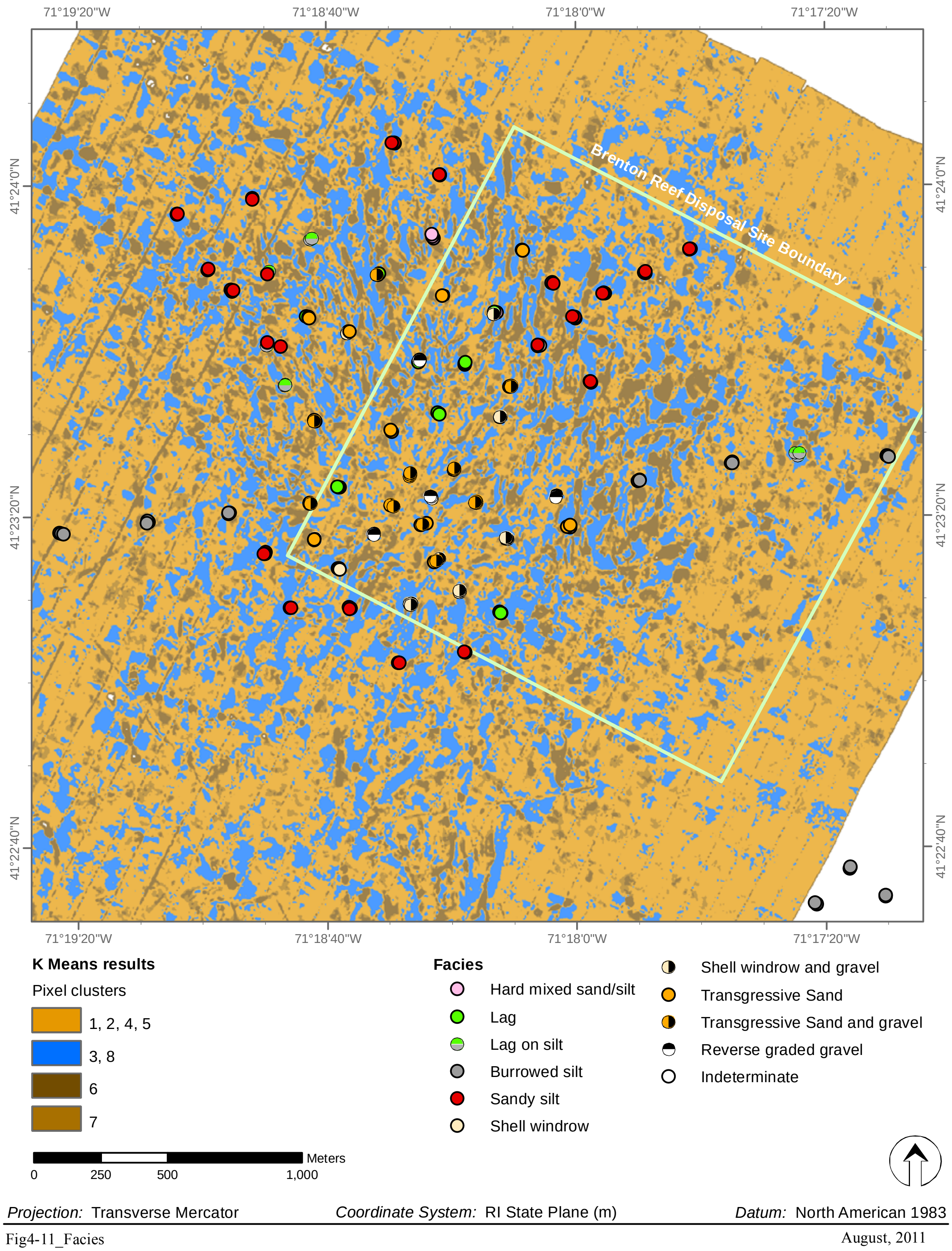

Figure G-9. Sediment facies distribution across the K-means-classified backscatter image of the Brenton Reef Disposal Site.

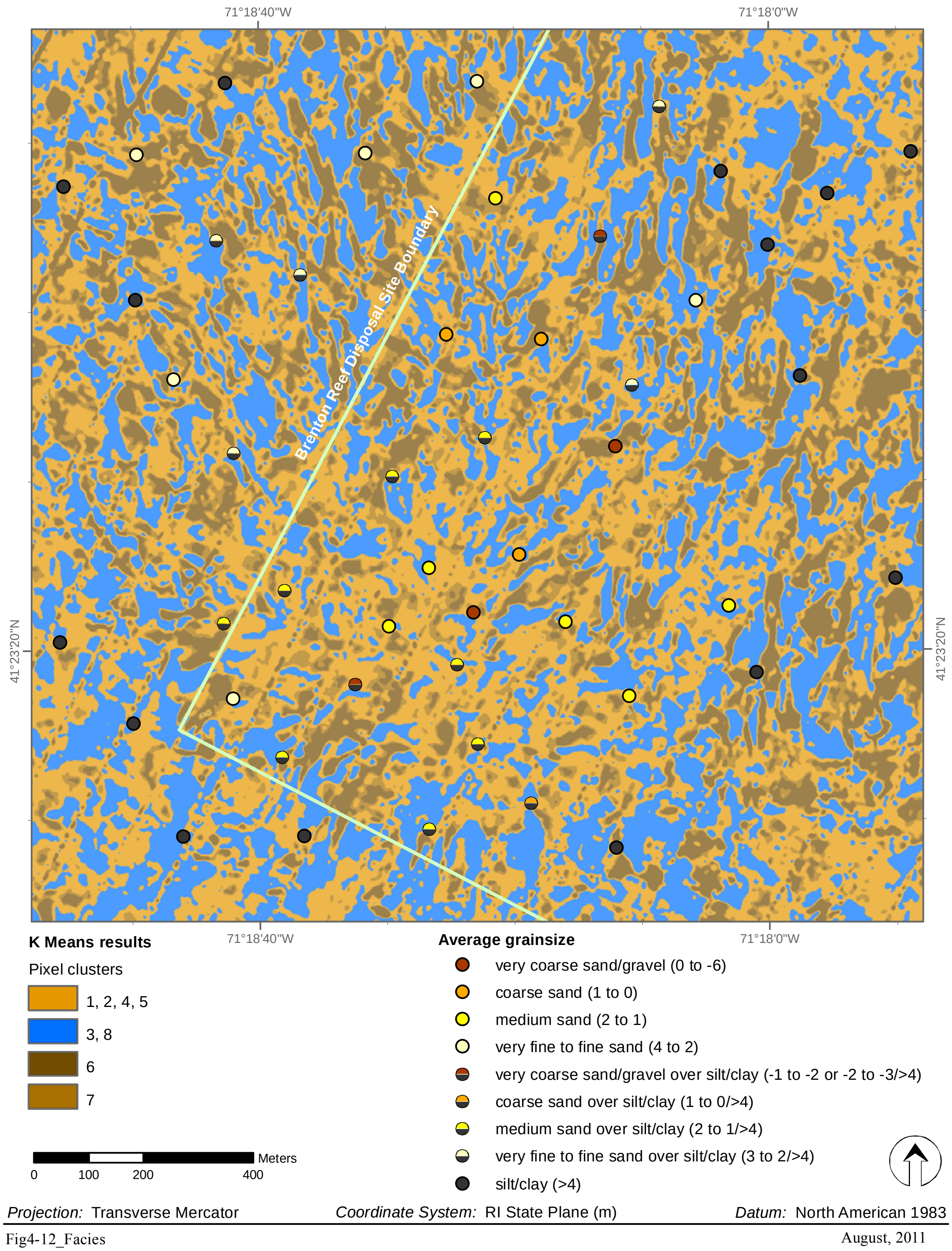

Figure G-10. Station-averaged grain size distribution across the K-means-classified backscatter image of the Brenton Reef Disposal Site.

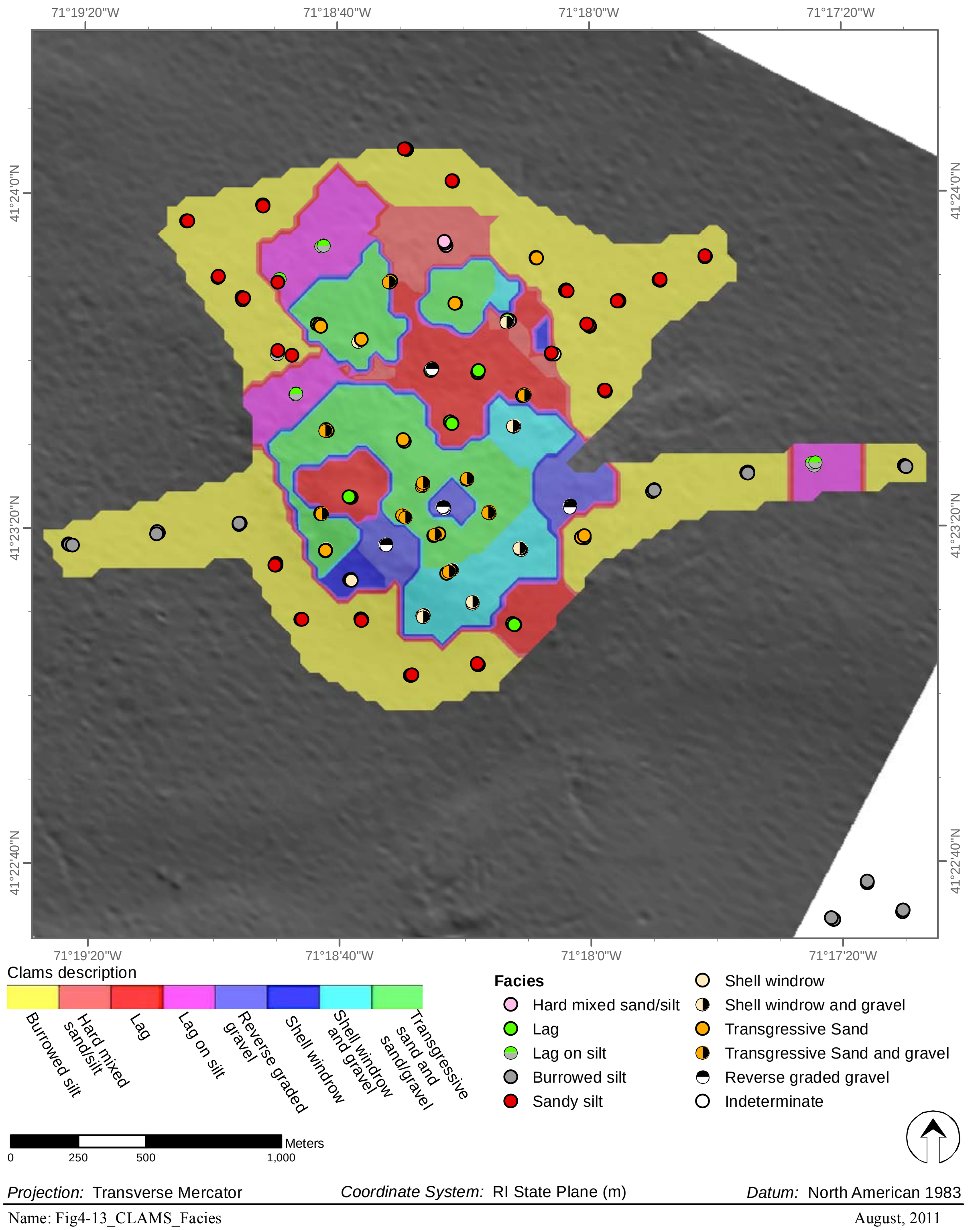

Figure G-11. Clustered distribution of facies classes across the historical Brenton Reef Disposal Mound Facies classes were clustered with CLAMS.

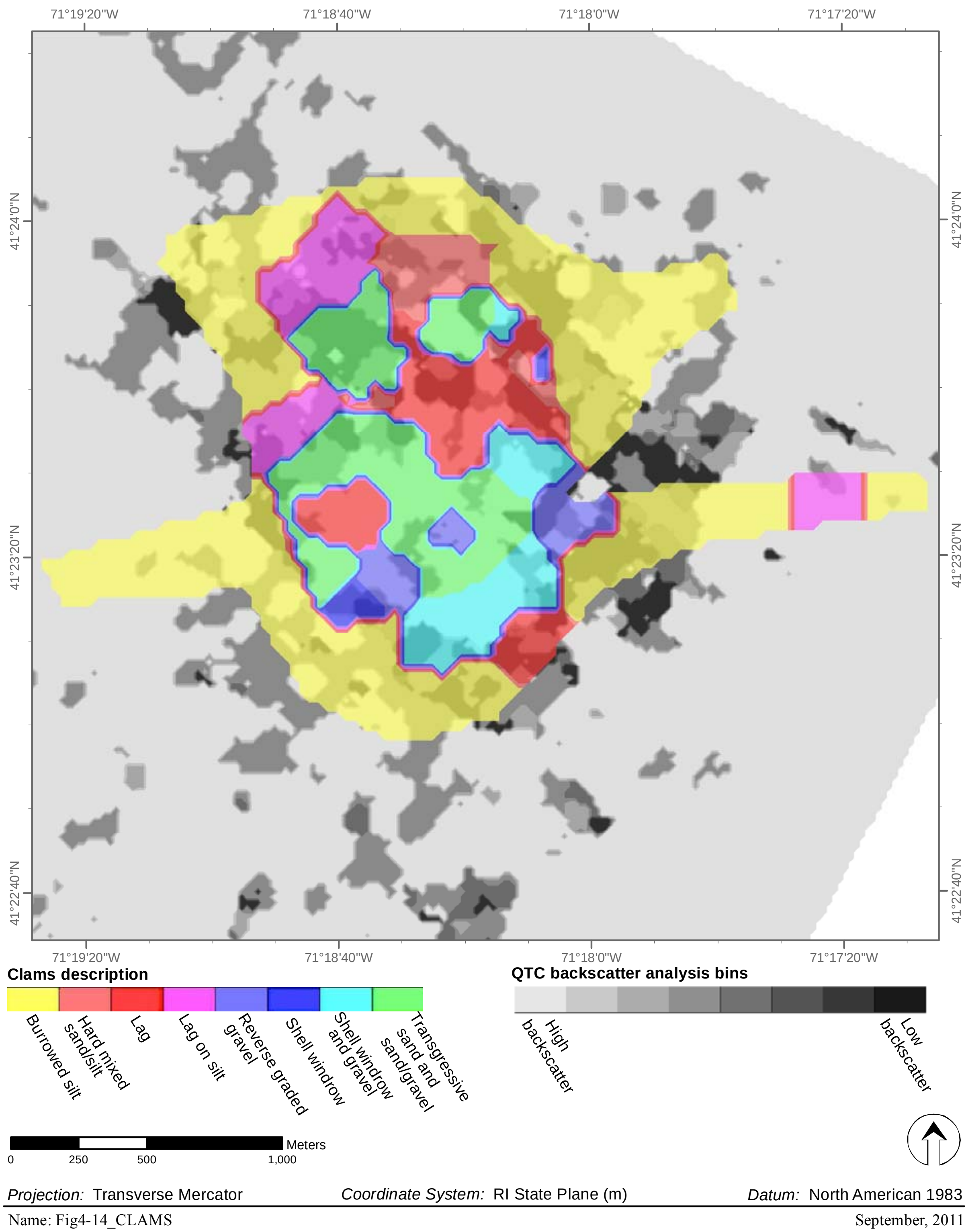

Figure G-12. Clustered distribution of facies classes across the historical Brenton Reef Disposal Mound compared to QTC classes of backscatter.

APPENDIX H

TABLE OF COMMON CONVERSIONS

APPENDIX H

Table of Common Conversions

Metric Unit Conversion to English Unit		English Unit Conversion to Metric Unit	
1 meter 1 m	3.2808399 ft	1 foot 1 ft	0.3048 m
1 square meter 1 m^2	10.7639104 ft^2	1 square foot 1 ft^2	0.09290304 m^2
1 kilometer 1 km	0.621371192 mi	1 mile 1 mi	1.609344 km
1 cubic meter 1 m^3	1.30795062 yd^3	1 cubic yard 1 yd^3	0.764554858 m^3
1 centimeter 1 cm	0.393700787 in	1 inch 1 in	2.54 cm